DOCTOR OF PHILOSOPHY

The Function Of SPO11 In Human Cancer Cells

Alahdal, Maryam

Award date:
2017

Awarding institution:
Bangor University

PRIFYSGOL

BANGOR

UNIVERSITY

The Function Of SPO11 In Human Cancer Cells

Ph.D. Thesis 2017

Maryam Abdulrahman Alahdal

Declaration and Consent

Details of the Work

I hereby agree to deposit the following item in the digital repository maintained by Bangor University and/or in any other repository authorized for use by Bangor University.

Author Name: Maryam abdulrahman Alahdal

Title: The Function of SPO11 in human cancer cells

Supervisor/Department: Dr. Ramsay James McFarlane / School of Biological Science.

Funding body (if any): Ummulqura University (Saudi Government)

Qualification/Degree obtained: PhD

This item is a product of my own research endeavours and is covered by the agreement below in which the item is referred to as "the Work". It is identical in content to that deposited in the Library, subject to point 4 below.

Non-exclusive Rights

Rights granted to the digital repository through this agreement are entirely non-exclusive. I am free to publish the Work in its present version or future versions elsewhere.

I agree that Bangor University may electronically store, copy or translate the Work to any approved medium or format for the purpose of future preservation and accessibility. Bangor University is not under any obligation to reproduce or display the Work in the same formats or resolutions in which it was originally deposited.

Bangor University Digital Repository

I understand that work deposited in the digital repository will be accessible to a wide variety of people and institutions, including automated agents and search engines via the World Wide Web. I understand that once the Work is deposited, the item and its metadata may be incorporated into public access catalogues or services, national databases of electronic theses and dissertations such as the British Library's EThOS or any service provided by the National Library of Wales.

I understand that the Work may be made available via the National Library of Wales Online Electronic Theses Service under the declared terms and conditions of use (http://www.llgc.org.uk/index.php?id=4676). I agree that as part of this service the National Library of Wales may electronically store, copy or convert the Work to any approved medium or format for the purpose of future preservation and accessibility. The National Library of Wales is not under any obligation to reproduce or display the Work in the same formats or resolutions in which it was originally deposited.

Statement 1:

This work has not previously been accepted in substance for any degree and is not being concurrently submitted in candidature for any degree unless as agreed by the University for approved dual awards.

Signed ……..

Date: ………..

Statement 2:

This thesis is the result of my own investigations, except where otherwise stated. Where correction services have been used, the extent and nature of the correction is clearly marked in a footnote(s).

All other sources are acknowledged by footnotes and/or a bibliography.

Signed …….

Date:…….

Statement 3:

I hereby give consent for my thesis, if accepted, to be available for photocopying, for inter-library loan and for electronic repositories, and for the title and summary to be made available to outside organisations.

Signed …….

Date: …….

NB: Candidates on whose behalf a bar on access has been approved by the Academic Registry should use the following version of Statement 3:

Statement 3 (bar):

I hereby give consent for my thesis, if accepted, to be available for photocopying, for inter-library loans and for electronic repositories after expiry of a bar on access.

Signed ……

Date: ……

Statement 4:

I agree to deposit an electronic copy of my thesis (the Work) in the Bangor University (BU) Institutional Digital Repository, the British Library ETHOS system, and/or in any other repository authorized for use by Bangor University and where necessary have gained the required permissions for the use of third party material.

In addition to the above I also agree to the following:

1. That I am the author or have the authority of the author(s) to make this agreement and do hereby give Bangor University the right to make available the Work in the way described above.
2. That the electronic copy of the Work deposited in the digital repository and covered by this agreement, is identical in content to the paper copy of the Work deposited in the Bangor University Library, subject to point 4 below.
3. That I have exercised reasonable care to ensure that the Work is original and, to the best of my knowledge, does not breach any laws – including those relating to defamation, libel and copyright.
4. That I have, in instances where the intellectual property of other authors or copyright holders is included in the Work, and where appropriate, gained explicit permission for the inclusion of that material in the Work, and in the electronic form of the Work as accessed through the open access digital repository, *or* that I have identified and removed that material for which adequate and appropriate permission has not been obtained and which will be inaccessible via the digital repository.
5. That Bangor University does not hold any obligation to take legal action on behalf of the Depositor, or other rights holders, in the event of a breach of intellectual property rights, or any other right, in the material deposited.
6. That I will indemnify and keep indemnified Bangor University and the National Library of Wales from and against any loss, liability, claim or damage, including without limitation any related legal fees and court costs (on a full indemnity bases), related to any breach by myself of any term of this agreement.

Signature: ……

Date : …….

Abstract

Cancer is currently the second most common disease resulting in high death rates globally (www.who.int accurate to 2015). A combination of various genetic and/or epigenetic modifications, which lead to distinct chromosomal abnormalities and/or mutations, cause somatic cell transformations leading to the formation of cancer cells. New strategy is emerging with the relatively recent identification and functional characterisation of cancer testis antigens (CTAs), which are antigens, encode by gene with expression normally restricted to the testis of adult males, which become activated in cancers. These (CTAs) can potentially serve as cancer-specific biomarkers, and could play a core role in cancer diagnosis and subsequent prognosis. This current study focuses on the human CTA gene, *SPO11* and the expression, protein localisation and function of this CTA in different cancer cells. In mice, infertility is observed when SPO11 is dysfunctional. Similarly, the homozygous null mutation of *Spo11* contributes to the arrest of meiotic division mid-prophase I. In several model organisms, including *S. pombe*, *Drosophila*, *Caenorhabditis elegans* and *Coprinus cinereus*, the loss of Spo11 function results in the production of defective gametes, ultimately indicating the failure of the meiotic process. Thus, Spo11 protein is necessary for accurate gamete formation. During this study SPO11 has been detected in testis, most cancer cells, but not found in the healthy normal tissues. SPO11 knockdown in different cancer cell lines results in reduced proliferation of these cells in an apoptosis-independent manner. SPO11 was also shown to co-localise with Bloom protein, a recQ-like-helicase involved in decatenation of dividing chromosomes. These results taken together suggest that the presence of SPO11 in non-meiotic cells changes the dynamics/timing of the cell cycle potentially by interfering with or modulating the chromosome structure during cell division. Instability within the chromosome structure and cell proliferation are two major factors considered to be involved in the development of human cancer. This study propose that the *SPO11* gene could be playing a critical role in controlling the genome stability of cancer cells, and thus necessary for stimulating and maintaining the oncogenic processes. SPO11 when present in cancer cells may also lead to aberrant initiation of DNA double-stranded breaks and/or altered DNA replication/chromosome segregation during mitosis resulting in chromosome changes. Future work was done in this study to purify SPO11 expressed in *E. coli* for use in crystal structure and *in vitro* assays to develop drugs to specifically target this protein in cancers where it has been detected.

Acknowledgments

In the name of Allah (God), the most Beneficent, the most Merciful All praise and thanks are only for Allah Almighty, the one through whom, by His blessing and favour, perfected goodness/good works are accomplished. The support and strength I have received from Allah are the secret behind the completion of my life project (Ph.D.). After Allah's support and help, I deeply appreciate the guidance and patience expressed by those whose names may not all be mentioned, allowing my dream to become possible.

First, I would like to sincerely express my appreciation for and gratefully acknowledge the assistance, guidance, encouragement and endless support of my supervisor, Dr Ramsay McFarlane, the leader of lab D7 group, during my laboratory work and write up. It was a pleasure working under his supervision, and I am proud to be one of his students.

In particular, it is my privilege to thank the kindest, warmest and most caring person in my life, my husband, Abdulqadir. You always supported, listened to my worries and gave me a shoulder to cry on. I would not be here if it were not for you; words alone cannot express the love and gratitude I owe to you. You always told me that I could do anything and I should not worry at all. Also, I am tremendously grateful to my loving and caring parents for their countless love and constant prayers. I also cannot forget to express my sincere gratitude to my lovely children, Thee yazan, Abduellah and Omran, for standing together and supporting me every step of the way throughout the most challenging time of my life.

Additionally, I would like to express my deep gratitude to Dr Ellen Vernon for her timely advice and for helping me with the laboratory techniques and her valuable guidance and keen interest at various stages of my project. I would also like to thank Dr Natalia Gomez for her guidance in the lab. Our lab environment was motivating, with smiling faces and respectful members.

List of Abbreviations

ACT	Beta Actin
AML	Acute myeloid leukemia
ATM	Ataxia-telangictasia mutated
ATP	Adenosine-5'-triphosphate
BCA	Bicinchoninic acid
BCR	Breakpoint cluster region.
bFGF	Basic fibroblast growth factor
BLAST	Basic local alignment search tool
BLM	Bloom syndrome protein
bp	Base pair
BRAF	B-Related Factor.
BRCA1	Breast cancer susceptibility gene 1
BRCA2	Breast cancer susceptibility gene 2
BSA	Bovine serum albumin
BTB	Blood-testis barrier
C-terminal	Carboxy-terminal domain
CDK	Cyclin-dependent kinase
cDNA	Complementary DNA
CE	Central element
CMV	Cytomegalovirus
CNS	Central nervous system
CO	Crossover
CpG	Cytosine-phosphate-guanine-
Cq	Quantification cycle
CRC	Colorectal cancer
CSCs	Cancer stem cells
CT	Cancer-testis
Ct	Threshold cycle
CTAG1B	Cancer/testis antigen 1B
CTAs	Cancer testis antigens
CTLs	Cytotoxic T lymphocytes

D-loop	Dissociation loop
Da	Dalton
DAPI	4’-6-diamidino-2-phylindole
DC	Dendritic cell
dH_2O	Distilled water
dHJ	Double-Holliday junction
DKKL	Dickkopf like acrosomal protein 1.
DMC1	Disrupted Meiotic cDNA 1
DMEM	Dulbecco's Modified Eagle Medium
DMSO	Dimethyl sulfoxide
DNA	Deoxyribonucleic acid
dNTPs	deoxynucleoside triphosphates
DPBS	Dulbecco’s phosphate-buffered
DSBs	Double-strand breaks
EB	Elution buffer
ECACC	European Collection of Cell Cultures
EDTA	Ethylenediaminetetraacetic acid
EGF	Epidermal growth factor
ELDA	Extreme limiting dilution analysis
esiRNA	Endo-ribonuclease prepared siRNA
EWSR1	Ewing sarcoma breakpoint region 1
FBS	Foetal bovine serum
GAGE-1	G antigen 1
GAPDH	Glyceraldehyde 3-phosphate dehydrogenase
GBM	Glioblastoma multiforme
gDNA	Genomic DNA
GFP	Green fluorescent protein
GST	Glutathione S-transferase tag
GTEx	Genotype-Tissue Expression
HBV	Hepatitis B
HCT116	Human colorectal carcinoma cell line
Hela	Henrietta Lacks
Her2	Hmg2p ER Remodeling.

HOP2	HOmologous Pairing.
HR	Homologous recombination
HRAS	Harvey rat sarcoma virus oncogene
IF	Immunofluorescent staining
IPTG	Isopropyl β-D-1-thiogalactopyranoside
kb	Kilobase
KDa	Kilodalton
KO	Knockout
KRAS	Kirsten rat sarcoma viral oncogene homolog
LB	Luria bertani
M-PER	Mammalian protein extraction reagent
MAGE-A	Melanoma antigen family A
MAGE-A1	Melanoma antigen, A1
MAGE-A2	Melanoma antigen, A2
MAGE-A3	Melanoma antigen, A3
MCS	Multiple cloning site
MDM2	Mouse double minute 2
Mer2	MEiotic Recombination.
MHC	Major histocompatibility complex
min	Minute
mL	Millilitre
mM	Millimolar
MND1	Meiotic nuclear divisions.
MRN	MRE11–RAD50–NBS1
mRNA	Messenger RNA
MRX	Mre11-Rad50-Xrs2
MW	Molecular weight
NBS1	Nijmegen breakage syndrome 1.
NCBI	National Centre for Biotechnology Information
NCO	Non-crossover
ng	Nanogram
NHEJ	Non-homologous DNA end-joining
NK	Natural killer

nM	Nanomolar
NRAS	Neuroblastoma ras oncogene
NRT	No reverse transcriptase
NTC	No template control
NUT	Nuclear protein in testis
NY-ESO-1	New York esophageal squamous cell carcinoma 1
ORF	Open reading frame
PBS	Phosphate buffered saline
PBST	Phosphate buffered salin-tween-20
PCR	Polymerase chain reaction
PFA	Paraformaldehyde
pH	Power of hydrogen
PIWIL2	Piwi like RNA-mediated gene silencing 2
pmol	Picomole
PRDM9	PR domain zinc finger protein 9
PSA	Prostate-specific antigen
PVDF	polyvinylidene difluoride
qRT-PCR	Quantitative, reverse transcription polymerase chain reaction
r.p.m	Revolution per minute
RAD2	RADiation sensitivity2.
REC8	RECombination8.
RFP	Red fluorescent protein
RM11	Ribosomal protein 11 mitochondrial large ribosomal subunit
RM12	Ribosomal protein 12 mitochondrial large ribosomal subunit
RNA	Ribonucleic acid
RNAi	RNA interference
RT	Room temperature
RT-PCR	Reverse transcription polymerase chin reaction
S	Synthesis-phase
SC	Synaptonemal complex
SCC	Sister chromatid cohesion
SCCs	Squamous cell carcinomas
SCM	Stem cell medium

SCP1	Sarcoplasmic calcium-binding protein 1.
SCS3	Suppressor of Choline Sensitivity.
SD	Standard deviation
SDS	Sodium dodecyl sulphate
SDS-PAGE	Sodium dodecyl sulphate polyacrylamide gel electrophoresis
SDSA	Synthesis-dependent strand annealing
SEM	Standard error of the mean
SEREX	Serological analysis of recombinant cDNA expression libraries
SFM	Serum-free medium
shRNA	Short hairpin RNA
SIC	Synapsis initiation complex
siRNA	Small interfering RNA
Ski8	SuperKIller.
SMC1	Structural maintenance of chromosomes
SPO11	SPOrulation
ssDNA	Single strand DNA
SSX	Sister-of-Sex-lethal
SW480	Colon Adenocarcinoma Cells
SYCP1	Synaptonemal complex protein
SYCP3	Synaptonemal complex protein 3.
TAAs	Tumour associated antigens
TAE	Tris-acetate-EDTA
TBE	Tris-borate-EDTA
TBS	Tris buffered saline
TCGA	The Cancer Genomic Atlas
TEX19	Testis Expressed 19
TM	Temperature of melting
TP53	Tumor protein 53
Tris	Tris (hydroxymethyl) aminomethane
TSGA10	Testis specific 10
TSGs	Tumor susceptibility gene
TSSK1	Testis-specific serine/threonine kinase 1
V	Volt

WB	Western blot
WCE	Whole cell extract
WHO	World Health Organization
X-CT	X- chromosome cancer testis genes
XAGE-2	X antigen family member 2.
µg	Microgram
µL	Microliter

List of Contents

List of Figures

List of Tables

1. Introduction

1.1 Cancer

1.1.1 Cancer overview

Although treatment and/or vaccination has eliminated several deadly diseases, cancer, which has been detected in human remains from over 3,000 years ago, is still considered to be one of the most lethal diseases in the world (Kelland, 2014). Cancer is one of the leading causes of death worldwide, especially in economically advantaged and developed countries (Jemal *et al.,* 2011). In spite of the substantial progress made in fighting against cancer, mortality rates from this disease are still high (Siegel *et al.,* 2013). According to the World Health Organisation (WHO), it is estimated there are more deaths caused by cancer than by heart disease and stroke (Ferlay *et al.,* 2015). Similarly, data indicates that cancer is 25% more harmful to men than women; in particular, lung cancer occurs more frequently than stomach, liver, colorectal cancer, prostate, breast and other cancers. Breast cancer was diagnosed as the second killer and tops the list in women (Ferlay *et al.,* 2015).

Cancer can initiate from any cell type or organ in the body and is characterised by uncontrolled cell division. In a number of cases, distant organs and normal tissues can also be invaded by cancerous cells in a process known as metastasis. DNA mutations and epigenetic modifications can also be responsible for the initiation of tumours by driving the cancerous cell proliferation (Stratton *et al.,* 2009; Sharma *et al.,* 2010; Brabek *et al.,* 2010; Tomasetti *et al.,* 2013; Wodarz & Zauber, 2015; Flavahan *et al.,* 2017).

1.1.2 Causes and types of cancer

Determining the causes of cancer is complicated, although several factors which include smoking (Washio *et al.,* 2016), radiation, chemicals (Burger *et al.,* 2013) and viruses (Parka *et al.,* 2016) have been implicated. Obesity, lifestyle, occupational factors, environmental factors and genetic factors also have a strong association with cancer occurrence (Martin-Moreno *et al.,* 2008; Song & Giovannucci, 2015; Negri Jr *et al.,* 2016). Another contributory factor is age. Men over 40 are susceptible to prostate and bowel cancer. While women may develop breast cancer starting at age 40, it most often occurs after age 50 (Autier, 2016). UK data shows that half of diagnosed cancer patients are approximately 70 years old, while 52 %

encounter death at the age of 75 years or more suggesting a relationship between age and cancer morbidity and mortality (Moller *et al.,* 2011). Tumours can be categorised as benign growths or malignant cancers. Non-cancerous benign tumours are characterised by their slow growth rate and they typically do not transfer to other tissues. Malignant tumours, on the other hand, are cancerous and often migrate to other places in the body during metastasis. Malignant tumours are usually deadly, especially when they spread to the vital organs (Souhami & Tobias, 2005; Valastyan & Weinberg, 2011). Cancerous diseases are divided into different classes based on cell type or the organ of origin. For instance, leukaemia is cancer of the blood cells (Park *et al.,* 2016) while a cancer type known as sarcoma has its origin in mesenchymal connective tissues and occurs in blood vessels, cartilage and muscles (Kisiel *et al.,* 2015). Another type of cancer is blastoma, which derives from immature tissues (Story & Johnston, 2016).

1.1.3 Hallmarks of cancer

The features of cancer involve the factors recognisable as necessary for the formation of malignant tumours. These factors are specific to cancers and enable them to proliferate, disseminate and survive. Generally, cancer cells are characterised by six hallmarks or traits. Self-sufficiency has been one of them in terms of growth signals, this means that the cancer cell division occurs in the absence of growth signals. Contrastingly, external growth signals control the normal cells playing a critical role in regulating cell division. The anti-growth signal insensitivity is another hallmark of cancer, as is the evasion of apoptosis, by which cancer cells avoid programmed cell death, which is essential for the removal of damaged cells. Another trait of cancer is the potential of cellular immortality. Tumour cells escape death, which normally occurs after a certain number of cell divisions; normal cells can undergo only a limited number of divisions. Another hallmark of cancer is sustaining angiogenesis, which is a process by which new blood vessels deliver nutrients and oxygen to cancer cells. Metastasis makes up the sixth of the originally proposed cancer hallmarks. (Hanahan & Weinberg, 2000; Sonnenschein & Soto, 2013). Hanahan and Weinberg (2011) later asserted that cancer has four more traits. These involve genome instability, which is liable to produce inflammation and genetic variety fostering a number of hallmark functions. Evading the metabolic pathway and immune system abnormalities are considered additions to the cancer hallmark list (See Figure 1.1).

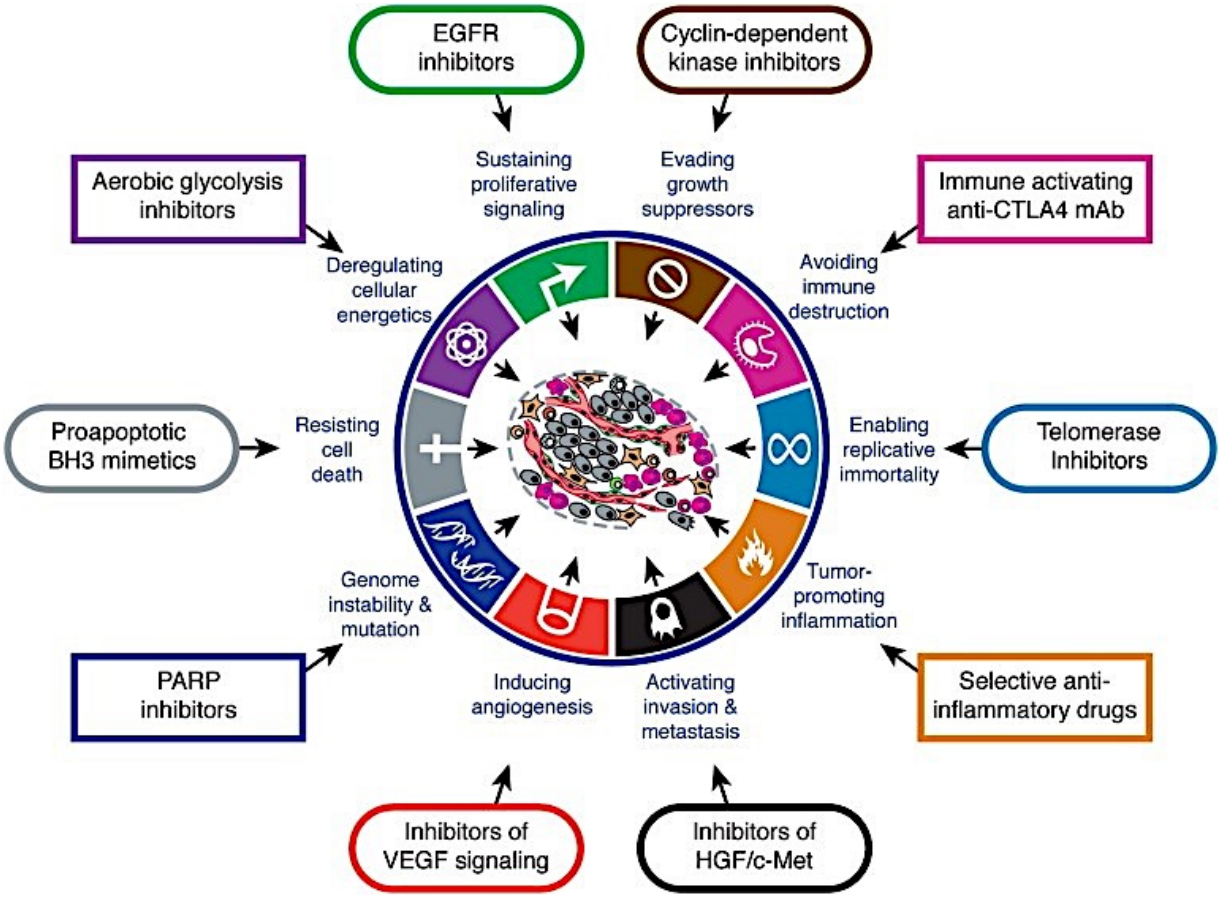

Figure 1.1: A schematic diagram of cancer hallmarks and their therapeutic agents. The figure summarises the ten features of cancer cells that contribute to the immortality of cancer cells (Hanahan & Weinberg, 2011). As a consequence of these strategies, cancer cells are able to contribute to inflammatory responses, bypass the immune system and contribute to differential energy use in spite of their mutation and genetic instability. It is possible for health care professionals and researchers to create pharmaceuticals that specifically interfere with these processes, thereby minimising the spread of cancer cells, as well as their impact on tissue and organ functionality (Adapted from Hanahan & Weinberg, 2011

1.2 Influence of genomic stability on cancer

In-depth studies of tumorigenesis formation show the involvement of three types of genes. The genomic stability genes, oncogenes and tumour suppressor genes are able to regulate the process of DNA repair and chromosome segregation. However, there is precise regulation of the proliferation of cells and contributions of these three types of genes to the hallmarks of cancer. An alteration in oncogene and tumour suppressor gene expression is the foremost causes of interruption in the division of cells and the consequent cancer formation. The promotion of cell growth by the oncogenes has the potential to cause cancer. The tumour suppressor genes, on the other hand, inhibit cell growth and promote apoptosis. The conjunction of oncogene expression and mutation or the dysfunction of tumour suppressor genes can trigger oncogenesis (Vogelstein & Kinzler, 2004; Negrini *et al.,* 2010a; Hanahan & Weinberg, 2011; Ferguson, *et al.* 2015; Kim, 2015; Morris & Chan, 2015).

1.2.1 Tumour suppressor genes in tumorigenesis

Tumour suppressor genes (TSGs) are capable of protecting cells from cancer. TSGs play a significant role in maintaining apoptosis and are responsible for cell cycle control. When TSGs mutate or are otherwise dysfunctional, the cell cycle does not stop, leading to uncontrolled cell division and, potentially, cancer (Thoma *et al.,* 2011; Weinberg, 2013). One of the key tumour suppressor genes is *TP53*; genetic alterations in *TP53* are detectable in half of cancer cases. *TP53* plays a critical role in commencing cell cycle inhibition, the processes of antiangiogenesis and the maintenance of the programmed death of the cells. A functional reduction has also been linked to metastasis (Surget *et al.,* 2014; Zhang *et al.,* 2015). The deactivation of *TP53* has been detected frequently in a wide range of cancers such as acute myeloid leukaemia (AML) (Seipel *et al.,* 2016) and colon cancer (Prabhu *et al.,* 2016). *TP53* is able to differentiate between progenitor cells and stem cells through regulated differentiation and specific pathways. The absence of it can result in the replication of stem cells, leading to the activation or maintenance of oncogenic epigenetic pathways (Levine *et al.,* 2016).

1.2.2 Oncogenes and cancer initiation

Oncogenes prevent the activation of apoptosis facilitate the continuation of uncontrolled cell proliferation. Oncogenes are commonly mutated genes, and they can be expressed at a high level in tumours (Croce, 2008; Bagci & Kurtgöz, 2015). Other oncogenes, such as cancer testis antigen (CTA) genes, are not mutated genes but derive an immunogenic expression in cancer patients (Whitehurst, 2014; Yang et al., 2015). Moreover, the proto-oncogene is a gene that has ability to change in to oncogenes under specific conditions, such as mutation. Many factors activate oncogenes, including gene amplification, chromosomal translocation, mutations in the gene and epigenetic dysregulation (Croce, 2008; Bagci & Kurtgöz, 2015).
An oncogene mutation alters the encoded proteins structure in such a way that modifies and alters their activity. The *Ras* oncogenes family, which includes *NRAS, HRAS* and *KRAS* genes, is an example of oncogenes (Croce, 2008; Fernandez-Medarde & Santos, 2011). In different oncogenes, mutations lead to carcinoma of different types. For instance, the *KRAS* oncogene mutation is found in lung, pancreatic and bowel cancer (Rodenhuis, 1992), whereas acute myelogenous leukaemia and myelodysplastic syndrome have *NRAS* mutations (Beaupre & Kurzrock, 1999). Additionally, the *BRAF* gene is an example of a proto-oncogene that activated in 14% of liver carcinomas, 18% of bowel cancers and 59% of melanomas (Davies *et al.,* 2002; Solit *et al*., 2006; Bagci & Kurtgöz, 2015).

Abnormalities and mutations in hereditary material are generated by agents that damage DNA, influencing the formation of cancer. The translocation of chromosomes is one genetic abnormality that has been linked to certain cancer types, such as chronic myeloid leukaemia (CML) arising from a mutual translocation between chromosomes 9 and 22. This is also called Philadelphia translocation (Stratton *et al*., 2009b). Chromosomal translocation can produce a mutation in the *EWSR1* gene that causes it to become an oncogene, leading to Ewing sarcoma in children (Slotkin *et al*., 2016). Chromosome instability (CIN) can also play a role in suppression or promoting of tumour progression (Pfau & Amon, 2012).

1.2.3 Genome stability genes

Genome stability genes play a role in correcting/repairing DNA errors, maintaining genetic modifications and segregating chromosomes. However, genetic changes or alterations in these genes have been shown to initiate tumours in the body (Negrini *et al.,* 2010). For example,

the *NBS1* gene is required to repair DNA double-strand breaks (DSBs)(Sharma *et al.,* 2015) and mutation of *NBS1* is associated with Nijmegen breakage syndrome (NBS), a congenital disorder (Tauchi, 2000). Furthermore, overexpression of *NBS1* is linked to liver cancer (Wang *et al.,* 2014), oesophageal carcinoma (Kuo *et al.,* 2012) and prostate cancer (Berlin *et al.,* 2014). Moreover, *BRCA1* and *BRCA2* tumour suppressor genes sustain genome stability and DNA repair, and their inactivation is linked to ovarian and breast cancer; mutation of these genes serves as a risk indicator (Yoshida & Miki, 2004; Trego *et al.,* 2016). A reduction in the function of the mouse double minute 2 (MDM2) homolog which encodes protein in humans through the *MDM2* gene, has been linked to inhibiting DSB DNA repair. The overexpression of the *MDM2* gene in certain cancer types has been found to be an oncogenic factor, while in other tumours, MDM2 is down regulated. This suggests that the behaviour of the *MDM2* gene is similar to oncogenes and tumour suppressor genes, which depend on the relevant cellular setting (Maluszek, 2015).

1.3 Tumour-Associated Antigens (TAAs)

Tumour markers consist of an array of different biomacromolecules produced in excess concentration by a wide variety of neoplastic cells. These markers are either endogenous product of highly active metabolic tumour cells, the products of newly active genes that normally remain inactive or newly acquired antigens (e.g. formed by mutation) at cellular and sub-cellular levels. The antigens produced by tumour cells indicate the presence of a tumour and might be present on the surface of the tumour cells, within the tumour cells, in bodily fluids, within the lymph nodes or inside the bone marrow**.**

Most of these antigens are proteins, some are novel genes and a few are RNAs, such as messenger RNA (mRNA) or microRNAs. Some markers are specific to the cancer type, while others are non-specific and found in many different types of tumours. Example of commonly used tumour markers are the Her2/neu-antigen found only in breast cancers, PSA, found only in prostate cancers and the BCR-ABL translocation responsible for the Philadelphia chromosome found in CML (for review, see Duffy, 2013).

Tumour markers or antigens have wide applications to disease prognosis, management and prevention. They are commonly used for screening and identification of malignant tumours, in the diagnosis of asymptomatic cancers, as prognostic indicators in some cancer types and

in determining the effectiveness of cancer therapy (for review, see Malati, 2007). Tumour antigens are classified into the following main categories:

- Viral antigens: these antigens are produced in cells infected by a virus. For example, cervical cancer is caused by the human papillomavirus (HPV) (Mirkovic, 2015).
- Differentiation antigens: these antigens are expressed in both normal and malignant cells. The antigens gp100, Melan-A/MART, TRP-1 and TRP-2 are all observed in melanoma (Roy, 2015).
- Overexpressed antigens: some antigens, such as PSA and epidermal growth factor receptor (EGFR), are overexpressed in the prostate and the breast, respectively (Apostolopoulos, 2015).
- Cancer testis antigens (CTAs): this family of genes is expressed only in human germ cells and malignant tumours (Gjerstorff, 2015).
- Neo antigens: generated by mutation of a pre-existing gene.

Cancer specific antigens that can serve as targets/biomarkers, called tumour-associated antigens (TAAs), are thought to be a necessary part of immunotherapy and other therapies targeting cancer. They are also useful in cancer diagnosis and prognosis (Luborsky, 2001).

The antigens present on the surface of the cancer cells are usually targeted by the immune system. However, several antigens can be present in small amounts on somatic cells, and thus are not cancer specific. TAAs trigger the immune system via a single epitope generation that the immune system recognises, which leads to the destruction of cancer cells (Krishnadas *et al.,* 2013). While TAAs may be used for cancer immunotherapy, they must possess essential features, including status as $CD8^+$ cytotoxic T cells (CTLs) target, a consistent presence in most tumours, and, in the cancer cells.

For many decades, human tumour antigens have been studied as potential immunotherapeutic targets, either for cancer vaccines or for therapy. For a tumour antigen to become a potential immunotherapeutic target there must either be high restriction in the expression of the antigen or it should be devoid of expression in the normal tissue so as to prevent autoimmunity. Over the years, many categories of antigens have been found to fulfil this requirement, including differentiation antigens (for example, in B-cell lymphoma, CD20), viral antigens (in cervical cancer, human papillomavirus antigens), and uniquely mutated antigens. In more recent times,

a new category known as CTAs has emerged with the potential to be cancer immunotherapy antigen targets (Lajmi *et al.,* 2015; Maxfield *et al.,* 2015; Wang *et al.,* 2016b).

1.3.1 Cancer testis antigen genes

CTAs are a group of proteins encoded by genes whose expression remains silent in normal somatic tissue and whose expression is restricted to tissues of the testis. These genes are generally found to be expressed in a large number of tumour cells and stem-like cells (Whitehurst, 2014; Yang *et al.,* 2015). The term 'cancer testis antigen genes' was first used by Chen *et al.* (1997); they are also known as cancer germline antigen genes. This is a broad and diverse family of cancer antigens named because of their unique expression pattern. Cancer testis antigens (CTAs) are seen in many cancers, but are otherwise expressed only in germ cells of the testis (Yang, 2015). CTAs do not show expression in any other normal tissue. They have variable expression levels for different cancer types. For example, CTAs are strongly expressed in malignant tumours, such as bladder, liver, melanoma and non-small cell lung carcinomas, as well as certain types of sarcomas and multiple myelomas (Scanlan, 2004).

These antigens are moderately expressed in malignant prostate and breast cancers and are weakly expressed in colon cancers, kidney cancers, and haematological malignancies (Lin , 2014) and (Sammut, 2014). The testis has an immune privilege thanks to the existence of the blood-testis barrier and lack of human leukocyte antibody (HLA) class I expression. This means that the immune system does not come into contact with these cancer testis antigens and thus, has no self-recognition. Due to the specific expression pattern of CTAs, they can be used for immunotherapy, diagnosis and treatment of cancers. They have even been used for the development of CTA-based vaccine therapy (Feichtinger, 2012). More than 100 CTA families have been identified and divided into two classes (Almeida, 2009):

Testis and/or CNS restrictive: Gene expression is restricted to the testis and some CNS tissue and cancer tissue.

Testis and/or CNS selective: Gene expression is found in the testis and CNS as well as one or more normal tissues and in cancers.

The normal function of several CT genes, including Spo11, in spermatogenesis, is the generation of double-strand breaks (Kalejs, 2006).

In a variety of cancers, CT antigens are suspected to play an important role in maintaining cell survival, promoting resistance to various forms of chemo- and radio-therapy and contributing to oncogenesis by downregulating p53 and p21 tumour suppressor genes (Kular, 2009; Nylund, 2012; Zeng, 2011; Cilensek, 2002; Duan, 2003; Zhu, 2008; Caballero, 2009).

It is hypothesized that CTAs are regulated by means of epigenetic mechanisms such as histone post-translational modifications and DNA methylation (Videtic & Hudler, 2015). It is demethylation that activates CTA during spermatogenesis. Numerous CTAs are targeted by humoral and cell-mediated immune reactions. The best example of this is the NY-ESO-1 antigen, which is positive in a majority of malignant cancers. A number of clinical trials which use CTAs specifically NY-ESO-1 and MAGE-A3 for vaccinating patients with melanoma, prostate, ovarian and lung cancers are underway (Whitehurst, 2014,). CTA genes represent potential targets for immunotherapy because they may play an important role in carcinogenesis and contribute to treatment resistance by malignant tumors (Litvinov, 2014).
In 1991, the first CTA gene family member, known as melanoma antigen-1 (*MAGE-A1*), was discovered in melanoma patients with the help of the T-cell epitope cloning technique (van der Bruggen *et al.,* 1991). In the following years, using the same techniques, other CTA genes like *MAGE-A2*, *MAGE-A3* and *GAGE-1* were discovered and identified (Gaugler *et al.,* 1994; De Backer *et al.,* 1999; Chomez *et al.,* 2001). The SEREX (serological analysis of recombinant cDNA expression libraries) technique was also used to discover further CTA genes. This system allows for the screening and identification of human tumours and the analysis of the immune response to the tumour-affected antigens. The same can be done with the help of autologous sera taken from cancer-affected patients (Sahin *et al.,* 1997). This method has helped in classifying different types of CTA genes, including *NY-ESO-1* (Chen *et al.,* 1997), *SSX* and *SCP1* (Tureci *et al.,* 1998). Bioinformatics can help identify relevant meiosis-specific CT antigen genes (meiCT) (Feichtinger *et al.,* 2012; Sammut *et al.,* 2014). Moreover, cooperative schemes like The Cancer Genome Atlas (TCGA) have been used to identify hundreds of CTA genes extracted from a large number of cancer patients (Kandoth *et al.,* 2013; Vogelstein *et al.,* 2013; Lawrence *et al.,* 2014; Wang *et al.,* 2016).

1.3.2 CTA gene classification

Multiple advanced strategies have identified more than 70 CTA gene families (Fratta *et al.,* 2011). These can be classified into two types, X-CTA and non-X-CTA genes (Simpson *et al.,*

2005). X-CTA genes are localised on the X chromosome, making up around 10% of its total gene configuration, and they are organised in well-defined clusters. X-CTA genes include *MAGE-A*, *MAGE-8*, *XAGE-2*, *MAGE-A3* and *NY-ESO-1* (Simpson *et al.,* 2005; Stevenson *et al.,* 2007; Caballero & Chen, 2009). Non-X-CTA genes are localised in the autosomal chromosomes. Non-X-CTA genes are generally present in single copies, unlike the paralogous cluster form found with X-CTA genes (Simpson *et al.,* 2005). *SCP-1* and *HORMD1* are examples of non-X-CTA genes (Tureci *et al.,* 1998; Chen *et al.,* 2005). The different position of these two types of genes suggests that they perform different functions (Caballero & Chen, 2009). CTA genes have been subdivided into four major groups depending on the expression profile found in normal and malignant tissues:

i. *Testis-restricted CTA genes* exhibit highly restricted expressions in cancers, adult testis and the placenta. Meiosis cohesin genes tested, RAD21L and SMC1beta, exhibited a tight testis-specific expression profile (Hofmann *et al.,* 2008).
ii. Testis- central nervous system (CNS) restricted genes show expression in cancers, the testis and the central nervous system of adult patients. These were the meiotic recombination hotspot activator genes such as PRDM9, TSSK1, SYCP1(Hofmann *et al.,* 2008).
iii. Testis selective genes show expression in cancers and the adult testis; however the expression is round in up to two normal somatic tissues also. TEX19, exhibited a testis-selective expression profile as it was expressed in the testis and the thymus (Hofmann *et al.,* 2008).
iv. *CNS selective genes* show expression in CNS tissues, adult testis and cancers and expression is found in up to two other normal somatic tissues (Hofmann *et al.,* 2008).

1.3.3 CTA gene functions

There is a lack of clarity regarding the role and function of some of the identified CTA genes. Different studies have highlighted the possible functions of these genes in tumorigenesis (Caballero & Chen, 2009; Fratta *et al.,* 2011; Sulek *et al.,* 2016). It has been identified that CT genes contribute to the cellular processes in the germ line (Cronwright *et al*., 2005; Gedye *et al.,* 2009), including their functional role in normal tissues and cell division (Jungbluth *et al.,* 2005). For instance, synaptonemal complex protein 1 (SYCP1) initiates chromosome synapses during meiosis 1, and meiotic crossover formation and SYCP1 deletion result in sterility (Tureci *et al.,* 1998; de Vries *et al.,* 2005; Schramm *et al.,* 2011). Meanwhile,

RAD21L and SMC1β generally assist in the regulation of meiotic recombination and meiotic sister chromatid cohesion (Ishiguro *et al.,* 2011; Lee & Hirano, 2011; Ward *et al*., 2016), but are reported as CTA genes (Feichtinger *et al*., 2012).

SPO11, another CTA gene, encodes a meiosis-specific protein with the ability to create meiosis-specific DNA double-strand breaks that initiate meiotic homologue recombination (Yamada & Ohta, 2013) (see section 1.5). The MAGE group of proteins can regulate the ubiquitination of proteins, and their abnormal production in cancer cells results in an altering of the signalling pathway and cellular progression through the process of ubiquitination (Weon & Potts, 2015). Additionally, MAGE-A1 controls cellular signalling pathways (Ghafouri-Fard & Modarressi, 2009). Furthermore, it has been found that, with the aid of other CTAs such as the transcription factor BORIS, which has an essential role in the regulation of the promoter methylation process via spermatogenesis during meiosis II of male germline cells (Klenova *et al*., 2002), the expression of the *MAGE* gene group can also be regulated (Vatolin *et al.,* 2005; Schwarzenbach *et al.,* 2014). The depletion of *MAGE-A* expression stimulates the recruitment of tumour suppressors such as P53 to target promoters (Marcar *et al.,* 2010a).

Oncogenesis is caused by a variety of factors, and recent research has demonstrated that cancer cells share some characteristics with germ cells (McFarlane, 2014; Feichtinger, 2014). For example; germ line genes have been shown to be important for tumour development in *Drosophila melanogaster*. The activation of the same pattern of germ line genes occurs in human tumours, indicating that germ line genes are oncogenic (Feichtinger *et al.,* 2014). CT genes are thought to be a main cohort of the germ line group. CT protein functions are poorly understood in the testis, whereas some roles in oncogenic processes have been verified (Gjerstorff *et al.,* 2015; Whitehurst, 2014).

CT genes are being studied by researchers due to their potential role in immunotherapy; these genes carry cancer-specific antigens (Gjerstorff, 2015). A recent study demonstrates that gene-encoding factors regulating meiotic chromosomes have functions controlling oncogenic genome dynamics; for example, REC8 meiosis' specific cohesion function in oncogenics drives ploidy changes and reductional chromosome segregation in mitotically proliferating cells (Folco *et al.,* 2017; Erenpreisa *et al.,* 2009). In addition, SYCP3, the meiotic synaptonemal complex protein, has been detected to disrupt recombination-mediated repair

and initiate ploidy changes in cancer cells (Hosoya *et al.,* 2011). The inter-homologue recombination regulator HOP2-MND1 has been demonstrated to be essential for oncogenic alternative lengthening of telomeres via an inter-non-homologue break-induced replication (BIR)-mediated pathway (Cho *et al.,* 2014). Moreover, certain CTA genes, like PIWIL2, help in cell proliferation and act as proto-oncogenes (Cheng *et al.,* 2011). In human melanoma, the up regulation of the CTA gene CAGE helps to stimulate the apoptotic evasion that allows the tumour to develop (Kim *et al.,* 2010).

Correspondingly, the up regulate expression of *TSGA10* disturbs the hypoxia-inducible factor (HIF)-1α and drives the development of angiogenesis (Mansouri *et al.,* 2016). The expression of CTA genes is mainly found in germ cells, and they are found in a range of cancer cell categories based on their histological features. These genes may have a postulated function in cancer cells that are used as valuable biomarkers and drug targets.

1.3.4 CTA gene expression

Before the process of spermatogenesis begins, the expression of X-CTA genes occurs in the spermatogonia cells present in the testis of male humans. However, the expressions of X-CTA genes have also been noticed in placenta cells. The expression of non-X-CTA genes is also seen in the last phase of germ cell differentiation (Simpson *et al.,* 2005; Stevenson *et al.,* 2007). In line with these studies, the expression of CTA genes is not found in somatic tissues. The assessment of mRNA for numerous CTA genes has elucidated their limited expression in non-germ line tissues such as those of the liver, pancreas and spleen. However, these genes are also classified as CTA genes, considering that their expression level is lower than 1% in comparison to the expression level found in normal testes (Caballero & Chen, 2009). Experiments have shown that CTA genes are co-expressed in the same positive tumour and that this behaviour increases in the later developmental stages of the tumour (Caballero & Chen, 2009). Studies on CTAs have demonstrated that genes like DKKL, PLU-1 and MAGEA3 are overexpressed in colorectal cancer cells and induce disease progression (Tarnowski *et al.,* 2016). With the help of immunohistochemistry, it has been found that CTA genes are regularly expressed in foetal ovarian tissues (Nelson *et al.,* 2007).

1.3.5 The Function of Cancer Testis/Antigens in Normal and Malignant Tumour

CTAs play an important role in cancer immunology because they have the potential to contribute to the development of high-specificity tests (Jungbluth *et al.*, 2005). Binding specificity is particularly relevant to cancer pharmaceutical development because it is necessary for drug targets to have sustained interactions to enable the immune system to target tumour cells for destruction (Jungbluth *et al.*, 2005). There is a need to better characterise the role of human cancer testis/antigens (CTAs) in germ tissue and tumour cells because their expression mechanism is not well elucidated, although researchers have providing increasing evidence of their role in tumour formation (Jungbluth *et al.*, 2005). Studying the role of CTAs in cell division in normal cells is a technique that researchers are utilising to gain a better understanding of CTA genes (Cronwright *et al.,* 2005; Gedye *et al.,* 2009). For example, *SPO11* is vital to the formation of DNA double-strand breaks.

In order to initiate meiotic homologous recombination, the synaptonemal complex protein 1 initiates chromosome synapsis during meiosis 1 (Schramm *et al.*, 2011; Tureci *et al.,* 1998; Yamada & Ohta, 2013). Likewise, BORIS plays an essential role in regulating the promoter methylation process via spermatogenesis during meiosis II of male germline cells (Klenova *et al.,* 2002). During oncogenesis, the germline genes are influential in tumour development (Janic *et al.,* 2010). For example, germ line genes have been shown to be essential in the development of brain tumours in *Drosophila melanogaster* (Janic *et al.*, 2010; Sumiyoshi *et al*., 2016).

The activation of the same pattern of germline genes occurs in human tumours, suggesting that certain human germ line genes or modifications of these genes are oncogenic (Feichtinger *et al.,* 2014). CTA genes are considered to be a major cohort of this germ line group. Although the functions of CT proteins are poorly understood in the testis, some involvement in the oncogenic process has been demonstrated (Gjerstorff *et al.,* 2015; Whitehurst, 2014).
The role of the CTA genes during normal development may contribute to the tumourigenic effect that they have on cancer cells. There is limited evidence regarding the function of CTA genes in cancer cells, although it has been hypothesised that they contribute to cell growth, transcriptional regulation, putative proto-oncogenes and genetic instability (Cheng *et al.*, 2011; Scanlan *et al.*, 2002). CTAs may also be significantly involved in the control of complex genes and the activation of abnormal genes during cancer progression (Mirandola *et*

al., 2011; Scanlan *et al.,* 2004; Whitehurst, 2014). Cancer progression is thought to be due to soma-to-germline transformation (Feichtinger *et al*., 2014; McFarlane *et al*., 2014).

Since genomic instability is a primary contributory factor to cancer development, the aberrant expression of CTA genes may be due to the dysfunction of proteins that are typically necessary for human development (Lindsey *et al.,* 2013). This relationship may arise owing to conflict between the meiotic germ cell pathways and the normal mitotic cell cycle. In human somatic cells, shortening of the ends of linear chromosomes (telomeres) after each round of DNA replication, regulates and limits cell growth through multiple mechanisms, such as induction of P53 and checkpoints in response to DNA damag (Harley *et al.*, 1990). Therefore, the alteration of normal human cells to cancerous ones requires maintenance of their telomeres through a fundamental mechanism, known as alternative lengthening of telomeres (ALT) (Henson *et al.,* 2002). The activity of ALT is dependent on several meiotic genes, such as *HOP2-MND1*, which are thought to be involved in the formation of intra-telomeric homologous recombination. Interestingly, these genes are considered a potential tool in cancer diagnosis and therapy owing to the significant role played by ALT in cancer cells (Cho *et al*., 2014; Cesare & Reddel, 2010).

1.4 *SPO11*

1.4.1 SPO11 function

SPO11 protein referred to as the initiator of meiotic double stranded breaks, is a necessary component of proper meiotic cell division (Keeney, 2008). Human Spo11 is located near the telomere of chromosome 20 at 20q13.31,which is a region that is amplified in certain breast and ovarian cancers. Chromosome 20 is known to amplify in breast cancer and associated with genomic instability in some tumour cell lines, which triggered an interest in the discovery of SPO11's mechanism in cancer (Nitiss, 2009). In addition, in the human cancer predisposition syndrome, Bloom's syndrome, one of the defining cytological features of cells is the high rate of sister chromatid exchange, which could be a consequence of errors in the double-strand break machinery, of which Spo11 is an essential component ((Wang, 2002).

According to annotation information reported by the United States National Centre for Biotechnology Information (NCBI), the gene has 15 exons and two major isoforms, referred to as SPO11α and SPO11β. SPO11α is a variant that skips exon 2, while SPO11β contains all 15 exons (Bellani *et al*., 2010). It is hypothesised that there are several additional variants of SPO11 present, but only two of them have been fully annotated. The protein that is encoded by the gene is a member of the TOP6A protein family (Hartung & Puchta, 2001).

SPO11 is involved in the meiotic recombination and chromosome segregation processes associated with DNA replication and cellular division. It initiates programmed meiotic DSBs Furthermore, this protein is necessary for the regulation of meiotic DNA replication, although the specific mechanisms that direct this practice are not currently well defined (Boateng *et al*., 2013; Cha *et al.,* 2000). The deletion of *SPO11* from *S. cerevisiae* has an adverse effect on the formation of mature recombination products, including Holliday junction formation (Keeney, 2001). Both of these processes involve the creation of double-strand breaks (DSBs) in the DNA of paired chromosomes.

Since SPO11 is necessary for cell division, it is well-conserved and has homologous forms in non-human organisms. For instance, in yeast, protein encoded by this gene is responsible for the formation of these DSBs. It accomplishes this by binding to the 5' end of the DSB and interacting with other proteins (NCBI). All eukaryotic SPO11 genes are similar in terms of their nucleotide sequence as well as the role of the Spo11 protein in supporting the formation of DSBs as a part of meiotic cell division. An additional suspected role of SPO11 is related to its ability to slow down the S phase of the cell cycle in a manner that is independent of its participation in the formation of DSBs (Loidl, 2013). Furthermore, SPO11 may play a role in the alignment of chromosomes during meiotic events. Researchers are interested in characterising the effects that SPO11 has on the cell cycle as well as cell division because this gene has many suspected roles. While there is genetic conservation and homology between SPO11 sequences in different organisms, some organisms do not require SPO11 to create DSBs in the DNA during meiosis.

As a part of this process, synaptonemal complexes associations with SPO11 for the creation of DSBs form. When the SPO11 gene is deleted from yeast cells, these synaptonemal complexes do not form (Bhuiyan & Schmekel, 2004). In some organisms, the creation of these complexes is independent of the formation of events related to meiotic recombination. As such, they do not require SPO11 for meiosis. For instance, *Drosophila melanogaste*r and *Caenorhabditis elegans* are able to form synaptonemal complexes when SPO11 is deleted.

Thus, while there is a high level of sequence conservation between SPO11 genes in different organisms, some organisms do not require SPO11 to complete meiotic recombination to the same extent as others. Features of the gene in different organisms may therefore be variable.

In mice, infertility is observed when SPO11 is dysfunctional (Romanienko & Camerini-Otero, 2000). Similarly, the homozygous null mutation of *Spo11* contributes to the arrest of meiotic division mid-prophase I (Romanienko & Camerini-Otero, 2000). In several model organisms, including *S. pombe*, *Drosophila*, *Caenorhabditis elegans* and *Coprinus cinereus*, the loss of Spo11 function results in the production of defective gametes, ultimately indicating the failure of the meiotic process (Celerin *et al.,* 2000; Cervantes *et al.,* 2000). Thus, Spo11 protein is necessary for accurate gamete formation. *Spo11* has been found to be present in all sequenced eukaryotic genomes, and the *Spo11* sequence is highly conserved across different species. This suggests the mechanism of the initiation of recombination through the formation of DSBs is highly conserved. Spo11 function has been shown in *S. pombe* (Rec12), *S. cerevisiae* (SPO11), nematodes (Spo11), *Drosophila* (MEI-W68), mice (Spo11) and humans (*SPO11*) (Hartung *et al.,* 2007). SPO11 homologs have also been identified in plants, such as *Arabidopsis thaliana*, but in a genetically more complex arrangement than in many other organisms.

A. thaliana has three *Spo11* genes, two of which (*Spo11*-1 and *Spo11*-2) are expressed during meiosis and are essential for meiotic recombination to occur (Hartung *et al.,* 2007). A comparison of the predicted SPO11 proteins from mouse and human subjects revealed an overall amino acid identity of 82% between common portions. The human protein is 396 amino acids long and contains an additional stretch of 38 amino acids near the N-terminus that is not present in mouse Spo11 (Boateng *et al.,* 2013). Mammalian proteins share a 25% identity with other members of the SPO11 family (Boateng *et al.,* 2013).

Although the two mammalian proteins share only a 20–30% identity with other members of the SPO11 family, there are three regions of a higher homology present within the related proteins (Boateng *et al.,* 2013). One region contains a catalytic tyrosine that is present in all functional homologs (Bergerat *et al.,* 1994). A second region shares a homology with the topoisomerase-primase (Toprim) domain common to topoisomerase VIA (TopoVIA), which may participate in cleavage and/or rejoining reactions by coordinating magnesium ions.
A third region of a higher homology is located near the C-terminal end of SPO11, but it is not similar to any previously described motif and it has no known function (Boateng *et al.,* 2013). In *S. cerevisiae*, the *SPO11* gene has no introns, whereas in mice, it spans 13 exons and can generate two major *Spo11* isoforms through alternative splicing (Romanienko & Camerini-Otero, 2000). Mouse *Spo11* is localised to chromosome 2H4 and human *SPO11* to chromosome 20q13.2-q13.3. The longer transcript, including all 13 exons, is translated into the SPO11β isoform (44.5 kDa), while skipping exon 2 generates a 12-exon transcript that is translated into the SPO11α isoform (40.3 kDa) (Bergerat *et al.*, 1997). Both transcripts have the catalytic tyrosine, which is encoded by exon-5 (Bergerat *et al.,* 1997).

The alternative splicing that gives rise to two isoforms in mice also takes places in humans (Boateng *et al.,* 2013). The additional 38 amino acids in the N terminus of SPO11β are involved in the binding of the heterodimer subunits of SPO11 (Corbett *et al.,* 2007; Graille *et al.*, 2008). An analysis of mice producing only SPO11β showed that this isoform is proficient in meiotic DSB formation, suggesting the role of SPO11β in generating the breaks that initiate meiotic recombination in early spermatocytes (Kauppi *et al*., 2011) (Figure 1.2).

These observations are consistent with the patterns of SPO11β, which peaks in early prophase, while DSBs are made at the leptoneme and zygoneme stages (Bellani *et al.*, 2010). *SPO11β* transcripts reach maximum levels in early spermatocytes and remain relatively constant throughout prophase. In male mice, *SPO11α* transcripts become prevalent in pachytene spermatocytes and peak in diplotene spermatocytes over a period of nine days (Bellani *et al.,* 2010). In females, on the other hand, *SPO11α* transcripts peak in zygoneme and decline as prophase I progresses, over a period of three days (Bellani *et al.,* 2010).

The fact that *SPO11α* transcripts are the prevalent from at the beginning of prophase I in females but not until mid-prophase I in males could be related to the difference in the lengths of prophase I in male and female meiocytes (Bellani *et al.,* 2010). Spermatocytes in a testis take 12 days to complete prophase, eight of which are spent in the pachynema stage (Bellani *et al.*, 2010).

Oocytes, on the other hand, undergo prophase in five days, spending about a day in each prophase substage and a day in the arrested diplotene stage, dictyate (Bellani *et al.,* 2010). This suggests SPO11α has a role in mid- to late prophase I that is conserved in male and female meiocytes (Bellani *et al.*, 2010).

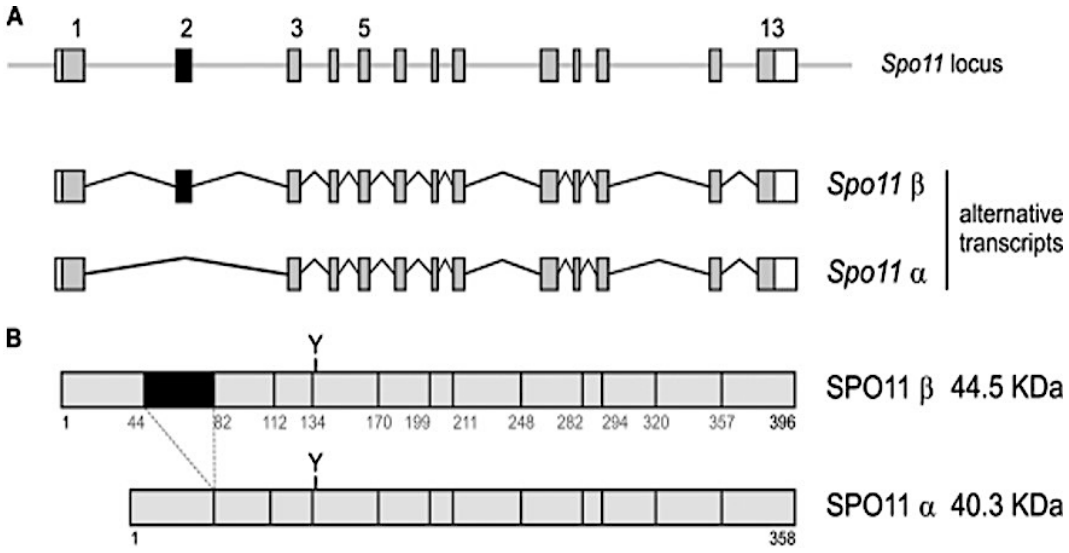

Figure 1.2: Genomic organisation, splicing pattern and polypeptides of mouse Spo11. (A) The *SPO11α* transcript does not contain exon 2, while the *SPO11β* transcript includes exon 2. (B) The polypeptides of SPO11α and SPO11β. The black square indicates the part encoded by exon 2. Y refers to the catalytic tyrosine encoded within exon 5 (Adapted from Boateng *et al.,* 2013).

Mammalian *SPO11*genes were found expressed at high levels only in the testes, while the mouse *Spo11* transcript is restricted primarily to meiotic germ cells and is maximally expressed at mid-pachynema. Surprisingly, it is observed in certain asexual species too, which leads to speculation that it may have additional functions that differ from meiotic recombination. In addition, this could be involved in chromosome paring or the pre-meiosis S-phase (Cha *et al.,* 2000; Boateng *et al.,* 2013; Loidl, 2013).

The mouse isoforms were presented due to a lack of available gene expression information for the human variant of Spo11. Genetic studies in model organisms have been responsible for the knowledge that scientists currently have regarding the functionality of SPO11 and its role in the formation of meiotic DSB formation. Studies of SPO11 functionality in several organisms have demonstrated that in *S. cerevisiae*, *S. pombe*, and *M. musculus*, the Spo11 protein becomes associated with the 5' end of broken DNA, which prompts topoisomerase functionality (Yeh *et al*., 2017). Furthermore, when mutations to SPO11 are made in these organisms, this function is disrupted, and meiotic recombination may be prevented. In some organisms that use SPO11 to stabilise recombination structures, Topo VIB-like subunits are implicated in this process. These subunits have been detected in plant and animal cells, demonstrating the prevalence of the SPO11 protein among different kingdoms.

To characterise the physiological role of *SPO11*, researchers have identified the genes that interact with *SPO11* during typical cellular activities. In particular, Ataxia-telangictasia mutated Ataxia-telangictasia mutated (ATM) kinase is a protein associated with *SPO11* because ATM is responsible for regulating the formation of DSBs through its control over the protein (Loidl, 2013; Lange *et al.,* 2011). Lange *et al*. (2011) suggested that in budding yeast and in mammals, DSBs might be responsible for activating ATM, which contributes to a negative feedback loop that regulates SPO11 activity (Loidl, 2013). The negative feedback loop contributes to the phosphorylation of either SPO11 or its accessory proteins, and this level of control determines the number of DSBs that can be generated by SPO11 (Lange *et al.,* 2016; Garcia *et al*., 2015).

In *S. cerevisiae*, the Ski8 protein is an observed component of this process, and it serves as a direct partner of SPO11, because both proteins are associated with meiotic chromosomes. It is thought that Ski8 plays a critical role along with SPO11 in the formation of DSBs.

In addition, the localisation of Ski8 in the cytoplasm or in the nucleus affects how it interacts with SPO11 (Keeney & Neale, 2006). In the absence of SPO11 or Ski8, SCs are not formed, and the recognition of homologous chromosomes is minimised (Keeney & Neale, 2006).

Recently, Robert *et al*. (2016) and Vrielynck *et al.* (2016) reported that the SPO11 protein has a partner known as the TopoVIB-like (TopoVIBL) protein, which is required for meiotic DSBs formation. This protein is present in both plants and animals, and it plays a role in generating meiotic DSBs (Robert *et al.,* 2016). In mice, TopoVIBL is associated with TopoVIA, which corresponds to the Spo11 splice variant β (Spo11β). It is hypothesised that Spo11β is responsible for the initiation of meiotic DSBs, due to the formation of a complex between Spo11β and TopoVIBL (Robert *et al*., 2016; Vrielynck *et al.,* 2016). The SPO11 genes are present in fungi and plants as well. SPO11 sequence is well-conserved in plants, fungi and humans. The strength of the conservation could be attributed to the need for these three types of organisms to undergo meiotic division.
Furthermore, these species are able to use sexual reproduction to create offspring (Sprink & Hartung, 2014). The presence of the SPO11 gene in plants, fungi, and animals demonstrates the importance of this gene to reproductive processes. Since SPO11 allows for reproductive success in these organisms, it is well-conserved in terms of its sequence as well as its function. Overall, SPO11 is genetically and functionally conserved across animal, plant and fungal species. Some organisms have evolved adaptations that allow them to form synaptonemal complexes in the absence of Spo11, but most organisms rely on the presence of Spo11 for the formation of stable DSBs. A majority of the information that has been collected regarding the mechanism of Spo11 was due to experiments performed in biological models, which means that knowledge about the role of SPO11 in humans is not yet fully understood. The high rate of conservation of SPO11 among organisms demonstrates that Spo11 plays an important role in reproductive success, due to the prevalence of this gene in many modern organisms.

1.4.2 DNA Topoisomerases and Spo11

Topoisomerases are essential for survival as they solve the topological problems (tangles and knots) inherent to chromosome metabolism by regulating the number of superhelical turns, or coils in a DNA molecule (Seoul & Neuman, 2016). They can be divided into two families depending on how many strands of DNA they are capable of breaking. Type I topoisomerase

catalyze single-strand break reactions while type II topoisomerases catalyze DSB reactions (Seoul & Neuman, 2016). Type II DNA topoisomerases are ubiquitous proteins that catalyze the ATP-dependent transport of one DNA duplex through another (Seoul & Neuman, 2016). All type II topoisomerases introduce both negative and positive supercoils into DNA molecules through the same mechanism. First, they cleave the phosphodiester backbone of the substrate DNA duplex. The topoisomerase then captures a second DNA duplex and passes the unbroken DNA through the break to repair the broken DNA and produce an intact molecule. These reactions are carried out in the presence of ATP, which is hydrolyzed to generate the energy consumed in the reaction (James & Wang 2002). Topoisomerase VI belongs to the IIB family of topoisomerases and its activity promotes relaxation of negative and positive supercoiled DNA and DNA decatenation through cleavage and ligation cycles (Gadelle *et al*., 2014). Structurally, Topoisomerase VI is composed of two subunits (A and B) that form a heterotetramer (Corbett *et al.*, 2007; Graille *et al.,* 2008).

Subunit A (TopoVIA) is the catalytic core of the enzyme as it carries the catalytically active tyrosine residues. Subunit B (TopoVIB) is dedicated to ATP hydrolysis. It contains an adenosine triphosphate (ATP) binding domain and a transducer domain that communicates with the ATP binding site and interacts with TopoVIA (Corbett *et al*., 2007; Graille *et al.,* 2008). DNA cleavage by TopoVI requires both subunits and ATP binding (Korbett, 2003) (Figure 1.3).

Structural studies of Topoisomerase VI have shown that it is related to the type IIA topoisomerases (Corbett, 2003). Topoisomerase VI carries out the same functions as type IIA topoisomerases and even shares several functional domains (Boateng *et al.,* 2013). The TopoVIB subunit is equivalent to the ATPase domain of type II topoisomerases, both structurally and functionally (Corbett, 2003). The TopoVIA catalytic subunit shares some functional domains with the topoisomerase IIA family, but is also structurally homologous to Spo11. Topoisomerases are responsible for catalysing the breakage of DNA strands and relevant repair reactions to rectify replication errors that occur during cell division (Vrielynck *et al.,* 2016). Some roles of topoisomerases in the DNA repair process include relaxing supercoiled DNA, supercoiling DNA and linking or unlinking single- and double-stranded DNA molecules (Vrielynck *et al.,* 2016).

The mechanism of action in topoisomerases occurs when a tyrosine residue encounters a phosphorus molecule in the DNA, thereby generating a tyrosyl phosphodiester link to the DNA and cutting the backbone of the DNA (Vrielynck *et al*., 2016). This allows other DNA strands to pass (Vrielynck *et al*., 2016). SPO11 plays a similar role as topoisomerases, but it remains covalently associated with the DNA after break formation (Vrielynck *et al*., 2016).

Studies on *S. cerevisiae* strongly suggest that meiotic recombination is initiated by the formation of DSBs and that this process is mediated by the SPO11 protein (Keeney *et al*., 1997; Keeney, 2001). SPO11was purified from DNA-protein complexes in mutant yeast strains where DSBs were initiated but not resected. Furthermore, chromatin immunoprecipitation (ChIP) assay experiments showed that SPO11 binds to chromatin in *S. cerevisiae*. These experiments also indicated that SPO11 is selectively associated with DNA hotspots, where DSBs occur more frequently. In the absence of SPO11, yeast does not form neither meiotic DSBs, nor does it form Holliday junctions or mature recombination products (Keeney, 2001).
Furthermore, without SPO11, homologous chromosomes in *S. cerevisiae* do not synapse (Keeney, 2001). Conversely, targeting of SPO11 to a specific DNA region in yeast (by virtue of its fusion with a DNA-binding domain) is sufficient to increase the amount of meiotic recombination that takes place at that site (Pecina *et al.,* 2002).

In mice, a disruption of SPO11 leads to male and female infertility (Baudat *et al.,* 2000; Romanienko & Camerini-Otero, 2000). SPO11-deficient mice spermatocytes are unable to generate DSBs or a synaptonemal complex; their homologous chromosomes fail to recombine and synapse, and even though some recombination between non-homologous chromosomes takes place, spermatocytes undergo massive apoptosis in mid-prophase I (Bellani *et al*., 2010). Some oocytes were able to progress through meiosis, but these were eliminated within the first few postnatal days (Romanienko & Camerini-Otero, 2000; Baudat *et al*., 2000). Furthermore, a point mutation in the mouse *SPO11* gene that results in the replacement of the catalytic Tyr138 with Phe leads to the absence of detectable meiotic DSBs in oocytes and spermatocytes (Carofiglio *et al.,* 2013). SPO11 expression patterns in humans, mice and fungi are consistent with its role in meiosis (Romanienko, 2000).

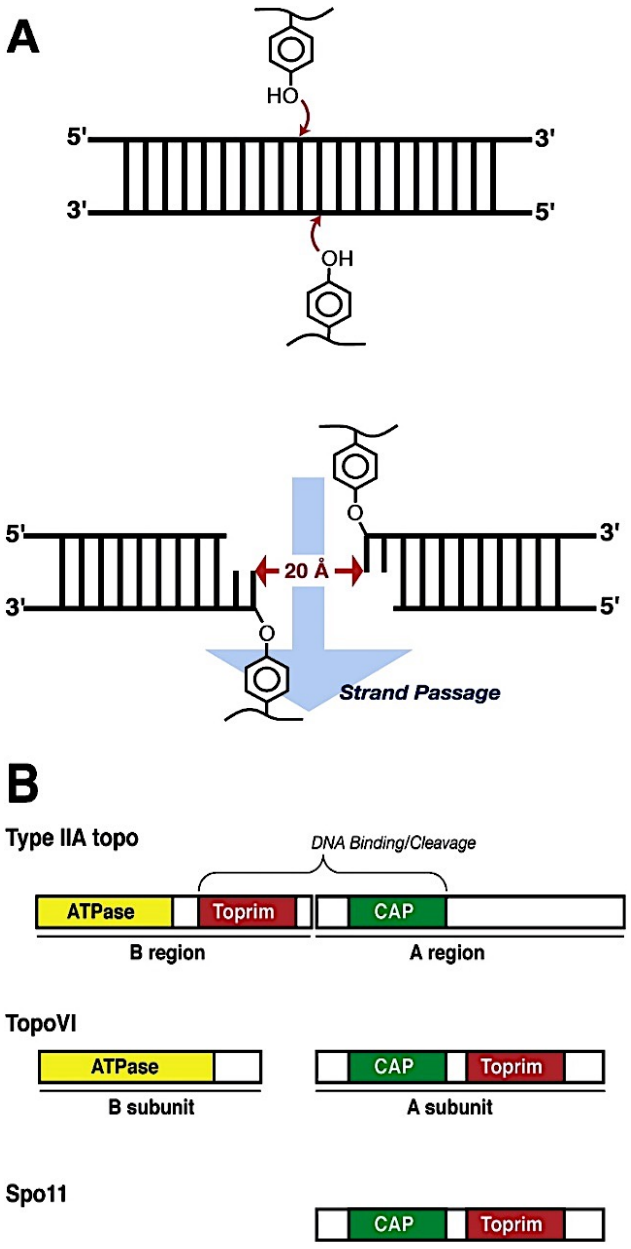

Figure 1.3: (A) Overview of double-strand break formation by type II topoisomerases (Source: Korbett, 2003). Each half of the topoisomerase cleaves one strand of DNA at the phosphodiester backbone. After cleavage, the two ends are separated (to allow the passage of the second DNA duplex) and then religated. (B) The structural organisation of type II topoisomerases, topoisomerase VI and SPO11. Type IIA topoisomerases are assembled as homodimers, each containing an ATPase domain (yellow), two helix-turn-helix CAP domains responsible for DNA binding and cleavage (green) and a metal-binding topoisomerase-primase (Toprim) domain (all type II topoisomerases require metal for full activity) (red). TopoVI is assembled as a heterotetramer and shares the three major domains present in type IIA topoisomerases, but not the organisation. SPO11 is homologous to the TopoVIA subunit of TopoVI.

1.4.3 Bloom's Syndrome and Topoisomerases

Bloom syndrome is a hereditary disorder characterised by immunodeficiency, proportional dwarfism, male infertility, light sensitivity and high incidence of different kinds of cancer (Karow *et al.,* 2000). The cells derived from Bloom syndrome patients show a high degree of chromosomal instability. This is marked by a dramatically increased frequency of sister chromatid exchange arising from the crossing over of chromatid arms during homologous recombination (HR) intermediate resolution (Karow *et al.,* 2000). The key function of the BLM protein is indicated by the suppression of HR-mediated crossover events due to the mutated *BLM* gene in Bloom syndrome.

In humans, BLM is one of five RecQ-like DNA helicases (Cheok *et al.,* 2005). BLM has the ability to dissociate varied DNA structures in a manner consistent with an HR regulatory role. These DNA structures bear a resemblance to HR intermediates, such as Holliday junctions (HJ) and D-loops (Karow *et al.,* 2000). BLM cooperates with Topo IIIα, a type IA topoisomerase, to catalyse double Holliday junction (dHJ) intermediate dissolution and generate exclusively non-crossover recombinants in a process known as dHJ dissolution (Wu & Hickson, 2003).

Topoisomerases are ubiquitous enzymes conserved to humans from bacteria. They play a key role in modulating DNA topology in transcription, replication and other cellular processes (Champoux, 2001; Wang, 2002), making them indispensible to the viability of the cell. There are four subfamilies of topoisomerases: IA, IB, IIA and IIB. The topoisomerases of type IA change the topological states of DNA in discrete steps via an enzyme bridging mechanism (Champoux, 2001; Wang, 2002). The initiation of the catalytic tyrosine residue creates a transesterification reaction in a single-stranded region, generating a transient DNA break that allows for the intact strand's passage through the break. After the broken strand's relegation by the reaction's reversal, the enzyme is free to engage in another round of catalysis (Champoux, 2001; Wang, 2002). Type IA topoisomerase family members include yeast topoisomerase III (Top3), *Escherichia coli* topoisomerase III (*Ec*Top3) and I (*Ec*Top1), and two isoforms of topoisomerase III, β (Topo IIIβ) and α (Topo IIIα), in higher eukaryotes. These enzymes exhibit the ability to negatively relax supercoiled DNA, while *Ec*Top1 can catalyse interlinking, unknotting and knotting DNA substrates that have been exposed to single-stranded regions (Champoux, 2001).

The common traits at DNA replication forks are single-stranded DNA gaps, replication termination sites and replication and repair sites, making it plausible that the main function of type IA topoisomerases is unlinking DNA catenanes. Type IA topoisomerases act in concert with RecQ helicases to control recombination events (Mankouri & Hickson, 2007). RecQ helicases are a family of highly conserved DNA helicases required for the maintenance of genome integrity (Hickson, 2003). The human topoisomerase IIIα (hTopo IIIα) interacts physically with BLM (Wu *et al.,* 2000; Johnson *et al.,* 2000).

The hTopo IIIα domain that interacts with the BLM has the requirement of suppressing SCE in BS cells (Hu *et al.,* 2001). This indicates that hTopo IIIα plays an anti-recombination role with BLM. Indeed, biochemical data *in vitro* have shown that hTopo IIIα and BLM catalyse the dissolution of dHJs, a DNA structure that arises as an intermediate during homologous recombination (Wu & Hickson 2003). The dissolution takes place via a strand passage mechanism preventing genetic exchanges between flank sequences. This has the effect of mimicking BLM-hTopo IIIα's *in vivo* role in suppressing SCE (Wu & Hickson 2003). The dissolution reaction, in the simplest case, is believed to have two components: the helicase activity of BLM catalyses the Holliday junctions' branch migration toward each other, resulting in the collapse of the Holliday junctions and subsequently generating two duplex DNAs interlinked through catenated single strands. This structure is known as hemicatenane, which is then decatenated by hTopo IIIα to complete the DHJs' dissolution (Plank *et al.,* 2006).

In every case, the failure of Topo III decatenate to resolve the replication fork convergence could lead to sister chromatids being interlinked after replication and incorrect sister chromatid disjunction in mitosis. In eukaryotes, Topo III functions in concert with RecQ-Mediated genomic Instability (RMI) proteins (Singh *et al.,* 2008; Xu *et al.,* 2008). The deletion of the gene encoding RMI1 in *Saccharomyces cerevisiae* results in phenotypes with a similarity to *top3*Δ, which includes sensitivity to DNA-damaging agents along with hyper-recombination, consistent with Top3 functioning along with RMI1 in the same pathway (Chang *et al*., 2005; Mullen *et al.,* 2005). RMI1 in humans binds to hTopo IIIα through its N-terminal domain, which is conserved (Wu et al., 2006), and this interaction apparently has importance *in vivo* for hTopo IIIα stability (Yin *et al.,* 2005). RMI1 has been shown to stimulate dHJ dissolution, *in vitro*, by BLM and hTopo IIIα (Raynard *et al.,* 2006; Wu *et al*., 2006).

Although topoisomerase's other type, IA, may play a role in the dissolution of dHJ *in vitro*, the stimulation of dissolution by RMI1 specifically requires hTopo IIIα (Wu *et al.,* 2006). The association of RMI1 with RMI2 (the second RMI protein) through the OB-fold domain at the C terminus forms heterodimeric RMI complex (Xu *et al.,* 2008). This RMI complex requires BLM phosphorylation in mitotic cells, as well as the recruitment of BLM to nuclear foci in response to DNA damage (Singh *et al.,* 2008; Yin *et al.,* 2005; Xu *et al.,* 2008). Further, the depletion of the RMI complex has been shown to cause an elevated level of SCE (Yin *et al.,* 2005; Xu *et al.,* 2008), the characteristic of BS cells that indicates the criticality of the RMI complex with respect to the function of BLM. Therefore, the BLM-hTopo IIIα-RMI1-RMI2 complex represents the functional unit in higher eukaryotes known as the BLM core complex (Liu & West 2008).

Remarkably, the action of BLM can disrupt the Rad51 presynaptic filament as well as stimulate DNA repair synthesis by DNA polymerase η (Bugreev *et al.,* 2007). These HR-related functions of BLM are strictly dependent on its ATPase activity (Wu & Hickson, 2003). BLM's ability to unwind HR intermediates while mediating the dismantling of the Rad51 presynaptic filament and catalysing Topo IIIα–dependent dHJ dissolution is important in regulating HR, limiting the formation of crossovers and preventing genome rearrangements by HR crossover (Hickson, 2003; Sung & Klein, 2006). On the other hand, the DNA repair synthesis activity of BLM may promote the non-crossover–producing synthesis-dependent strand annealing mechanism in HR (Bugreev *et al*., 2007).

The BLM–Topo IIIα complex is bound stably to a third protein, BLAP75 (Meetei *et al*., 2003). This enhances the BLM–Topo IIIα pair's ability to branch-migrate HJs or dissolve the structure of dHJs, yielding non-crossover HR recombinants. When DNA replicates in mitosis, it is necessary for topoisomerase to decatenate DNA. This is particulary critical at centromeres, as these structures play an important role in the assembly of kinetochores, which are necessary component of the spindle apparatus required for segregation of sister chromatids (Carroll & Straight, 2006). During this process, errors in chromosome attachment become apparent, and the involvement of the spindle assembly checkpoint (SAC) becomes active to present the segregation of chromosomes from occurring. Once this checkpoint is passed, however, the segregation of the chromosomes may move forward, which involves the recruitment and activation of a range of proteins, including topoisomerases (Yanagida, 2005) (Figure 1.4).

In 2012, Rouzeau and his colleagues determined that the proteins BLM and Plk-1 interact with the checkpoint helicase PICH. Specifically, these proteins colocalise at the centromeres during anaphase. Interestingly, these proteins are responsible for recruiting Topo IIα to the centromeres (Figure 1.5). Studies have also shown that when BLM and PICH are deleted, in Topo IIα recruitment does not occur effectively, indicating that it is a necessary component of chromosome segregation. As such, it is apparent that topoisomerases and helicases play a potentially important role in the recruitment of proteins during the DSB process. Their mutations may lead to genetic abnormalities that result in cancer.

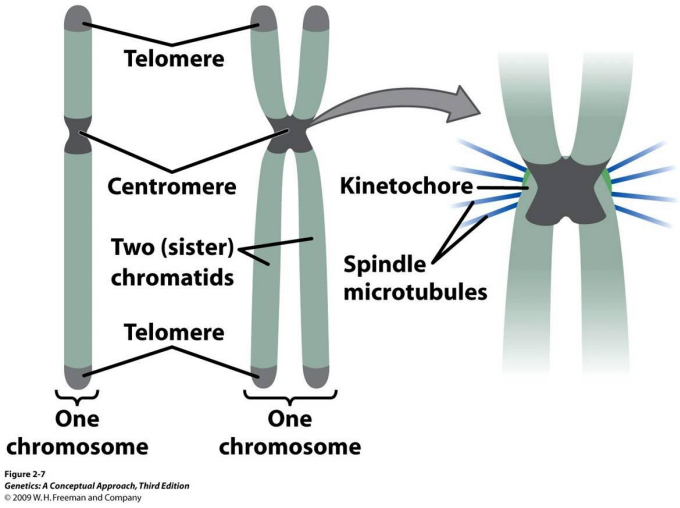

Figure 1.4: Diagram showing the location of the centromere (Pierce, 2012). During replication, microtubules attach to the kinetochore in each sister chromatid. This allows for equal segregation.

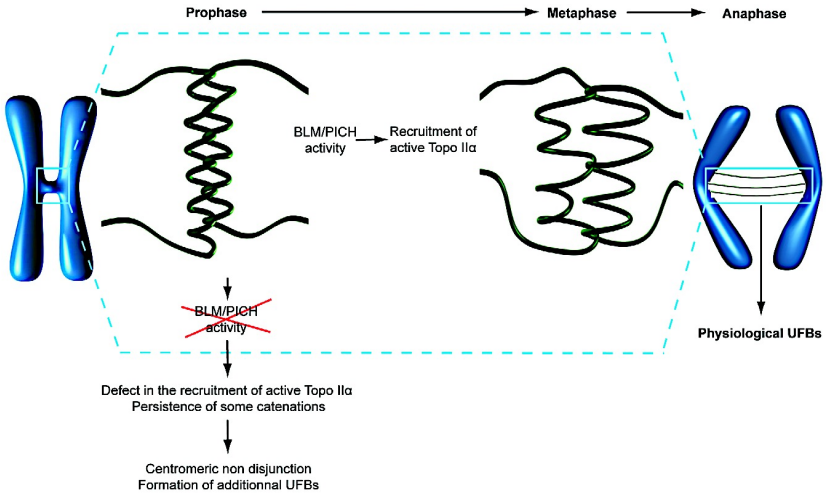

Figure 1.5: Model of PICH/BLM-dependant decatenation of centromeric DNA (Source: Rouzeau *et al.*, 2012). BLM and PICH work alongside one another to organise chromatin. This allows Topo II to access centromeric catenates. When BLM or PICH are not available, catenations result in centromeric non-disjunction formation of additional ultrafine anaphase bridges (UFBs).

1.5 Cell cycle

1.5.1 Overview of the mitotic cell cycle

Cell division occurs in all living organisms. The process of cell division in eukaryotes involves cell growth, replication of DNA and, subsequently, the production of new daughter cells. There are two kinds of cell division in eukaryotic cells: meiosis and mitosis. Accurate cell division is needed to maintain tissue and cellular homeostasis (Marston & Amon, 2004). After mitosis, two daughter cells, which are genetically identical, are produced. Mitotic cell division contributes to the repair and growth of tissues. Meiosis, on the other hand, is a form of cell division that is germ line specific and results in the production of haploid gametes.

The mitotic cell cycle is comprised mainly of two principal phases: interphase which includes Gap-1 (G1), S and Gap-2 (G2) and mitosis (M phase) (Figure 1.6). Mitosis is comprised of four subphases: prophase, metaphase, anaphase and telophase (Figure 1.7). During interphase, the preparation for cell division, which includes protein and RNA production, DNA replication and growth in size, takes place. Cytokinesis follows mitosis (M phase) in generating two daughter cells. The enzyme complexes that copy DNA have the highest access to chromosomal DNA during interphase. Interphase is also the period when the majority of gene transcription occurs (Raven *et al.,* 2014). Chromosomal DNA is duplicated during a part of interphase called the synthesis, or S, phase. As the strands of the two daughters DNA duplexes are produced, histones are recruited to form the structures called sister chromatids (Raven *et al.,* 2014).

In turn, the sister chromatids are held together by the cohesion complex. Cohesin contain four proteins, two of which are members of the structural maintenance of chromosomes (SMC) family of proteins. SMC proteins are the proteins that bind DNA, affecting the architectures of chromosomes. The cells, which lack SMC proteins, exhibit various defects in chromosome behaviour and chromosome stability (Blow & Tanaka, 2005). The available data suggests that cohesin complexes can form circles encompassing the two sister chromatids (Hagstrom & Meyer, 2003). Towards the end of S-phase, checkpoint mechanisms sense whether the DNA has been successfully copied. If the DNA has been successfully copied, cells will proceed into mitosis (Hagstrom & Meyer, 2003).

The quiescent state, or G0, is an additional phase or state that occurs when cells exit the cell cycle; yet retain viability (Singh & Dalton, 2014; Kronja *et al.,* 2014). The strict regulation of cell cycle progression in eukaryotic cells plays an important role in maintaining the integrity of the genome. Cell-division control is enabled by cyclin-dependent kinase (CDK) and checkpoints and their associated cyclins or specific activators. For instance, a checkpoint can be activated by any cell-division error, resulting in the slowing down, speeding up, and/or arrest of the cell cycle (Nurse, 1990; Sorensen & Syljuasen, 2012; Williams & Stoeber, 2012). It is important to note that checkpoint mechanisms and defective cell-cycle regulators are considered hallmarks of cancer and may affect cancer treatment and detection (Aarts *et al.,* 2013).

Prophase: Prophase represents over half of the process of mitosis. The nuclear membrane breaks down in higher eukaryotes to form a number of small vesicles and the nucleolus disintegrates. A structure called the centrosome duplicates itself by forming two daughter centrosomes that migrate to the opposite ends of the cell. The organisation is performed by the centrosomes to produce microtubules, which form the spindle fibres constituting the mitotic spindle (Lloyd & Chan, 2006). The chromosomes condense into compact structures.

Prometaphase: The centromeres of the chromosomes lead spindle-mediated migrate to the mid-line of the equatorial plane of the cell. This region of the mitotic spindle is called the **metaphase plate**. The spindle fibres bind to the kinetochore, a structure associated with each chromosome centromere (Raven *et al*., 2005). The individual spindle fibres bind to the **kinetochore** on opposing sides of sister centromeres. The condensation of the chromosomes continues.

Metaphase: The chromosomes align along the metaphase plate of the spindle apparatus. Chromosomes assume their most compacted state during metaphase. During this phase, the centromeres line up at the spindle's equator. Metaphase is particularly useful in cytogenetics, because it is at this stage that chromosomes can be visualised most easily. Moreover, the cells can be arrested experimentally with mitotic poisons like colchicines (Lloyd & Chan, 2006). Video microscopy reveals that during metaphase, there are temporary stoppages of the movement of the chromosomes. A complex checkpoint mechanism, the mitotic checkpoint, determines whether there is proper assembly of the spindle, and only the correctly assembled spindles enter anaphase (Lloyd & Chan, 2006).

Anaphase: This is the shortest phase of mitosis. The centromeres divide, and sister chromatids are pulled apart with a high decree of synchrony. The spindle fibres attach to regions of the kinetochore. The sister chromatids, which are separated, are now known as daughter chromosomes (Raikov, 1994). It is the synchronised separation and alignment in anaphase and metaphase that ensure that each daughter cell receives a copy of every chromosome.

Telophase: Upon reaching the poles of the cell during telophase, the chromatids decondense and a nuclear membrane forms around them. This nuclear division is followed by cytoplasmic division, also known as cytokinesis, where the cytoplasm separates in to two distinct daughter cells (Chan, 2006).

1.5.2 Overview of meiotic cell division

Meiosis can be described as the form of cell division responsible for generating gametes (egg cells and sperm cells in advanced eukaryotes) during the sexual reproduction of eukaryotes. In mammals, meiosis takes place in the female ovary and the male testis. Although meiosis is critical to the creation of genetic diversity, it also maintains precision in the number of chromosomes (Longhese *et al.,* 2008). In meiosis one round of DNA replication is followed by two successive rounds of chromosomes segregations to create haploid gametes.

Meiosis I, or the first round of chromosome segregation, reduces the number of chromosomes by reductionaly segregating homologous chromosomes. However, meiosis II, or the second psegregation resorts to the equation of the chromosomes when the separation of sister chromatids takes place (Clift & Marston, 2011; Marston & Amon, 2004). A distinguishing feature of meiosis is programmed recombination, which plays a significant role in homologue alignment and generates genetic diversity (Marston & Amon, 2004). Chromosomes replicate during the extended period of the premeiotic S-phase. This takes place before the interhomologous interactions, which plays an important role in the separation of homologous chromosomes and in meiotic recombination. Four stages or phases are involved in both divisions of the meiotic cell: includes prophase, metaphase, anaphase and telophase for each division Figure 1.8 (Zickler, 2006). .

Because the reduction of the number of chromosomes during meiosis I is a fundamental event, a number of essential events must occur. First, homologous chromosomes undergo meiotic recombination (Clift & Marston, 2011). Second, the attachment of microtubules derived from the identical spindle pole should be established between the kinetochores of each homologue's sister, this is known as centromere monopolarity. Subsequently, the homologous pairs are attached between them through chiasmata. Lastly, chiasmata are resolved and chromosome arm cohesin is removed, resulting in the dispersal of chromatid cohesin (Clift & Marston, 2011; Maston & Amon, 2004).

Most of the key events pertaining to meiosis I in prophase I, which is subdivided into five cytologically distinct phases: leptotene, zygotene, pachytene, diplotene and diakinesis (Figure 1.9; Table 1.1; (Baudat *et al*., 2013). During prophase I, homologous pairs are tangled together and move in the direction of the equatorial plate. In this phase, crossing over can occur. During prophase I the visibility of the chromosomes arises, the crossing over of the chromosomes takes place, the disappearance of the nucleolus occurs. The meiotic spindle is formed, and the nuclear envelope disappears (Freeman, 2011*)*.

During prophase I, chromosomes have become thicker, shorter and coiled. Crossing over and the pairing of duplicated homologous chromosomes occur. The process of genetic recombination gives rise to crossing over (Allers & Lichten, 2001). At this point, each pair of homologous chromosomes termed a bivalent. This is the tight grouping of the two chromosomes. The longest phase of meiosis is prophase I, which typically consumes 90% of the time with respect to the two divisions (Jones & Franklin, 2006).

Table 1.1: The substages of prophase I ((Baudat *et al*., 2013).

Substages	Features
Leptotene	Chromosomes undergo obvious individualisation (thin and thread-like) as they condense. The pairing of homologous chromosomes is also initiated programmed recombination (Baudat *et al*., 2013).
Zygotene	Homologous chromosomes come closer together, which results in synaptonemal complex (SC) generation. Which assembles between homologues. The telomeres have been clustering at the nuclear envelope (Qiao *et al*., 2012)
Pachytene	Chromosomes are thick and short. SC formation comes to completion. Crossing over occurs. At this stage, activity is found in the pachytene checkpoints, which arrest meiosis in the event of recombination and/or errors in chromosome synapsis that leads to promotion of apoptosis or repairing of process (Pellestor *et al.*, 2011).
Diplotene	SC release begins, although the linkage of homologous chromosomes remains as a result of unity between sister's chromatins (Buonomo *et al.,* 2000).
Diakinesis	Complete SC release occurs, and the condensation of homologous chromosomes occurs prior to the beginning of metaphase I. The beginning of spindle formation and the breaking down of the nuclease membrane take place (Ollinger *et al.*, 2008).

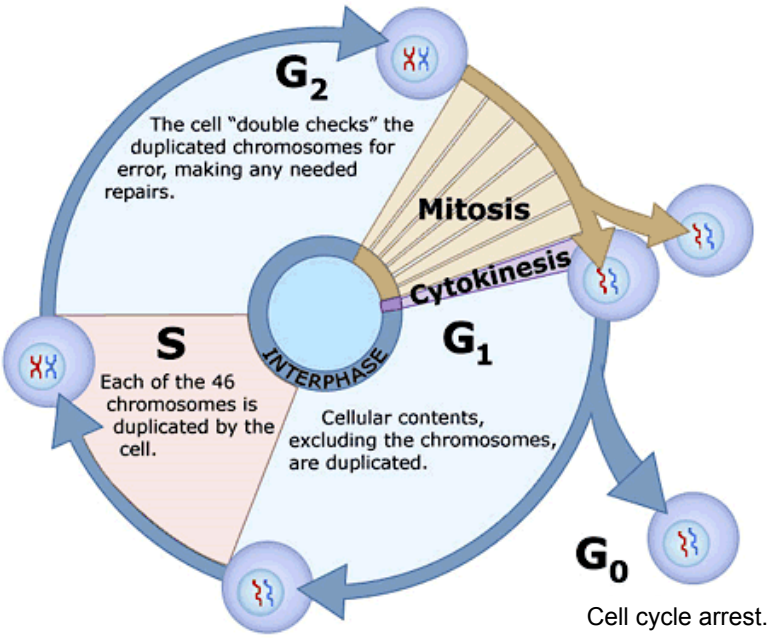

Figure 1.6: Schematic diagram of the eukaryotic cell cycle (adapted from Virtual Genetics Education Centre).

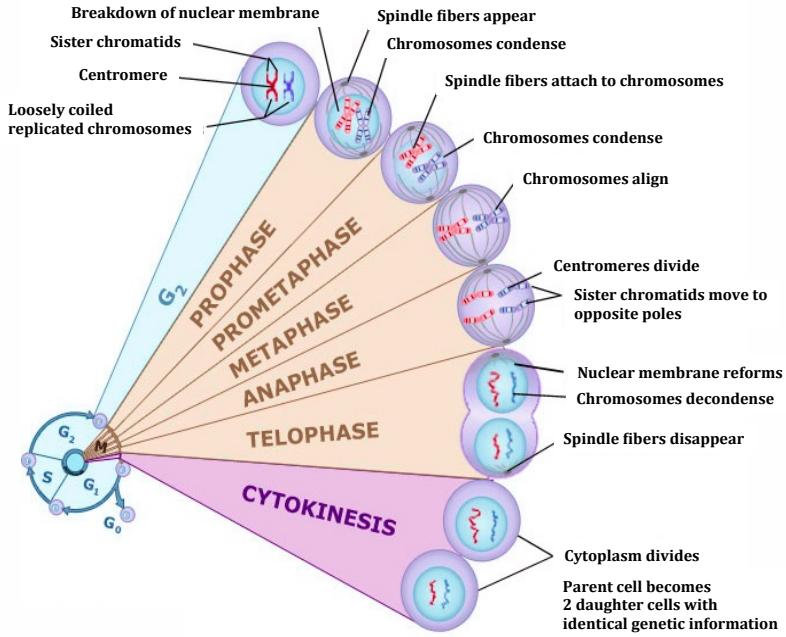

Figure 1.7: The stages of mitotic cell division (adapted from Virtual Genetics Education Centre).

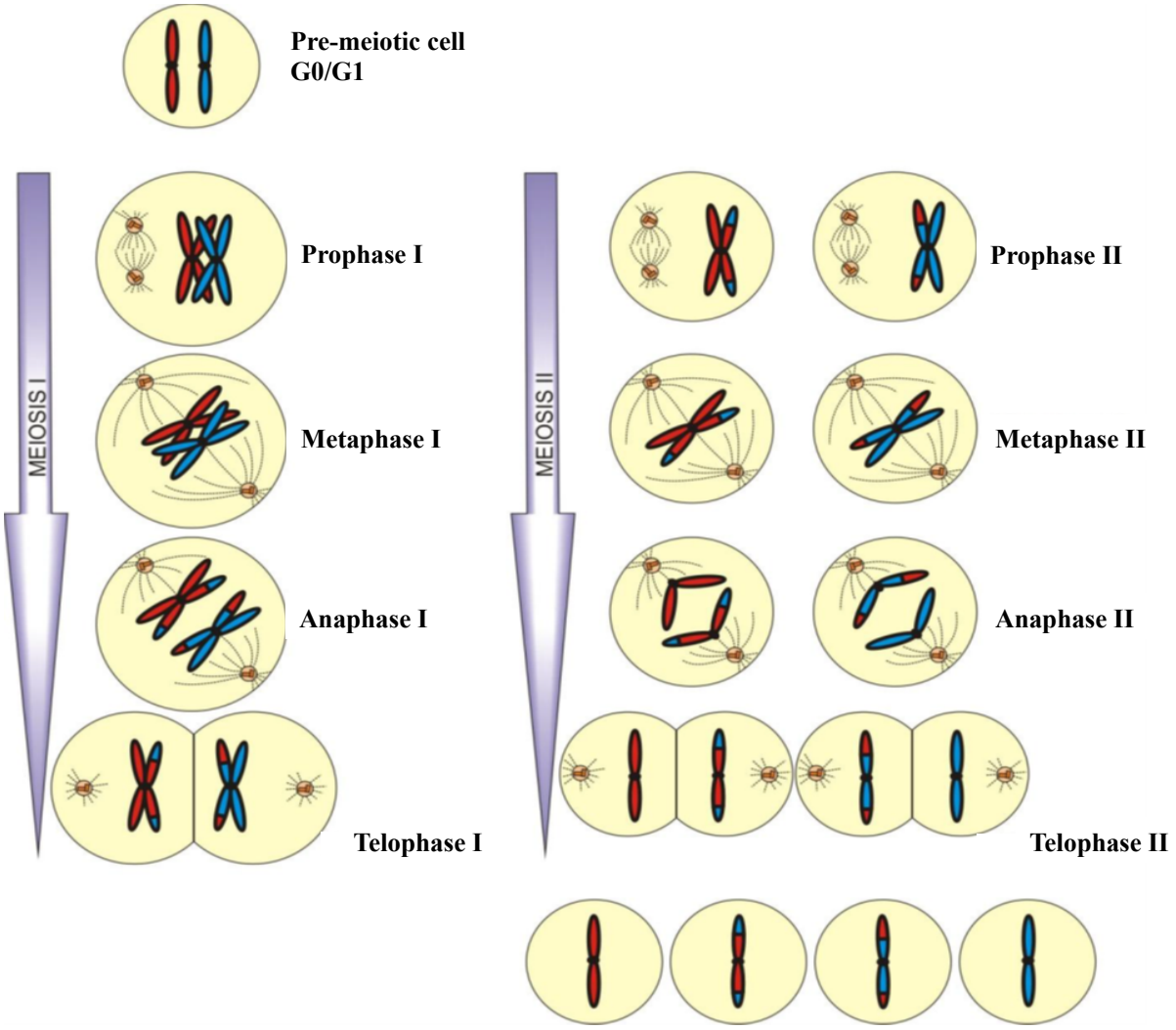

Figure 1.8: The stages of meiotic cell division. Two rounds of chromosomal segregation occur in meiosis. Meiosis I represents reduction of segregation and meiosis II represents segregation. In the figure, paternal chromosomes are represented by blue and maternal chromosomes are represented by red. First, there are four sub sections of meiosis I into separate phases: telophase I, anaphase I, metaphase I and prophase I. The chromosomes become visible and thick, and the generation of a spindle takes place during prophase. Further, during this phase, homologous chromosomes pair up, which results in crossing over, forming a unique combination of alleles on each chromatid. During metaphase I, the homologous pairs align on the cell's equator. During anaphase I, the homologous chromosomes are segregated and move to the opposite ends of the cell. During telophase I, two fresh haploid nuclei are produced. Meiosis II follows meiosis I and consists of four phases: telophase II, anaphase II, metaphase II and prophase II. During prophase II, after the nuclear envelope is broken down, the spindle is created. During metaphase II, the chromosomes are pulled to the centre of the cell and then randomly aligned at the metaphase plate. During anaphase II, each chromosome's centromere is split, which leads to the separation of the sister chromatids. Lastly, at the end of meiosis II, the four haploid daughter cells are produced (Zickler 2006).

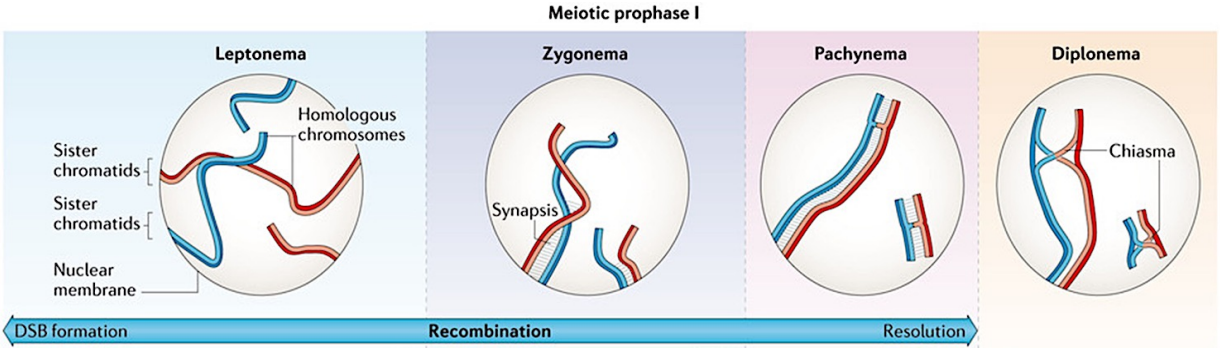

Figure 1.9: Chromosome organisation during meiotic prophase I. During meiotic prophase I, chromosomes are paired, and the pairs consist of homologous chromosomes. Each chromosome contains two sister chromatids. At leptonema, chromosomes are identified and associated with their partners as soon as the recombination appears through the initiation of DNA double-strand breaks (DNA-DSBs), which are introduced by SPO11. Meiotic recombination is completed before the end of pachynema. Paired chromosomes are linked to each other, forming homologs by virtue of the highly structured protein known as synaptonemal complex (SC) at zygonema. During crossover repair, the homologs are used as a template rather than the sister chromatin, leading to the initiation of chiasmata linkages between homologs at diplonema. The clustering of telomeres from one pole of the nuclear envelope is known as the bouquet stage, which indicates the transition state from leptonema to zygonema (Baudat *et al*., 2013).

1.5.3 Meiotic Recombination

Meiotic recombination is initiated by the introduction of programmed DNA double-strand breaks (DSBs) throughout the genome and subsequent repair. It is a mechanism used by most eukaryotes to enable the continuing of homologues to mediate the precise segregation of homologous chromosomes. The process enables multiple (often hundreds) of DSBs to be introduced throughout the genome by the topoisomerase type IIB-like complex, which contains SPO11 protein (Keeney *et al.,* 1997; Robert *et al.,* 2016; Vrielynck *et al.,* 2016). Subsequently, these DSBs are repaired to form either noncrossovers or crossovers. The crossover resolutions result in new chromosomes that are genetically distinct from both parental molecules. Contrastingly, the arising of noncrossovers takes place when the DSB from either homologous chromosomes or sister chromatids undergoes repair via relatively short tracts of DNA known as gene conversion. This also takes place near the initiation of the DSB, but fails to result in a physical link among the homologs, as intermediates do not mature to more stable structures needed for crossover. Therefore, the DNA sequence flanking the noncrossover site, refrain from varying from the original parental sequence (see Figure 1.10).

The induction of meiotic DSBs in *Saccharomyces cerevisiae* is mechanistically and temporally linked with DNA replication completion. This ensures that one event is not preceded by the other (Murakami & Keeney *et al.,* 2014). The formation of meiotic DSBs in *S. cerevisiae* requires multiple proteins (Keeney *et al.,* 2014). However, Mer2 is one component that cell-cycle kinases DDK (Cdc7-Dbf4 complex) and CDK (Cdc28 with either Clb6 or Clb5) target for phosphorylation. Mer2 phosphorylation is a key for initiating the formation of DSBs. There has been no equivalent phosphorylation event for initiating DSBs found in other organisms, although, a homolog of Mer2, Rec15, is found in Schizosaccharomyces pombe, (Doll et al., 2005).

DSB formation does not occur throughout the genome uniformly (Baudat & Nicolas, 1997). Instead, some regions are more favourable for the formation of DSB. These regions are known as hot spots, which have the tendency of being promoter and/or intergenic regions, where there is a wider dispersion of the nucleosomes (Petes, 2001). ChIPseq has obtained high-resolution DSB maps with the use of antibodies raised against known repair SPO11 proteins of the DSB (Buhler *et al.,* 2007).

Additionally, after the formation of DSB, the repair stage initially produces SPO11-bound oligonucleotide, which is a protein-DNA complex that marks the specific location of DSBs. The SPO11-oligonucleotides can be sequenced and provide a high-resolution DSB map. Mapping DSB hot spots via the ChIPseq results in extremely good correlation with SPO11-oligo maps, attesting to the utility and specificity of both approaches (Buhler *et al.,* 2007).

1.5.4 Mechanicm of the repair and formation of DNA double-strand breaks

Much of the knowledge regarding DSB repair and formation is based on organisms that can be easily modified genetically in assaying for observing repair intermediates. Nonetheless, studies of organisms, such as mice, have the ability to confirm the repair and formation of DSB in relation to pathways, whereas the identification of critical differences in DSBs is conducted in cross-species studies (Cole *et al.,* 2010). Keeney *et al.,* 2014, identified Spo11 as the protein that creates DSBs in *S. cerevisiae* during meiotic prophase I. Homologous proteins have been discovered in mice (*Spo11*β and *Spo11*α), flies (*mei-w68*), worms (*SPO-11*) and plants (*SPO11*-1,2,3) (Hartung & Puchta, 2000). The proteins, which are like topoisomerase II, are similar to the subunit of the Archaeal TopoVI A. Archaeal TopoVI requires both A and B subunits for function as a heterotetramer.

Recent investigations of the functions of the subunits of A and B and recent investigations in mice and plants have revealed the subunits which are equivalent working with SPO11β during meiosis, known as TOPVIBL and MTOPVIB, respectively (Robert *et al.,* 2016; Vrielynck *et al.,* 2016). Two Spo11 monomers are required to induce a single DSB (Figure 1.10a), with one DNA strand being broken by each protein (Keeney *et al*., 1997). As the process of DSB formation continues, there is covalent attachment of the Spo11 with DNA, and therefore, during subsequent processing it should be removed. Additional proteins are required for Spo11 action, most notably in *S. cerevisiae*, in which at least nine proteins are required: Xrs2, Rad50, Mre11, Rec114, Rec104, Rec102, Mei4, Mer2 and Ski8 (Keeney *et al.*, 2001).

1.5.5 Initial double-strand break repair

After the induction of the DSB in *S. pombe* and *S. cerevisiae*, the Nbs1/Mre11-Rad50-Xrs2 (MRN) complex, in combination with the Ctp1/endonuclease Sae2, cleaves the DNA strand

Attached to Spo11, liberating the Spo11-oligonucleotide complex (Hartsuiker *et al.,* 2009; Neal & Keeney, 2006). Spo11 refrains from cleaving the DNA on each strand at the identical nucleotide position. This results in the overhanging of the two-nucleotide and therefore prevents the filling up of the simple gap from the strand opposite to it (Liu *et al.*, 1995). The DNA molecule is double-stranded, and what results from it at this point is a short single-stranded DNA (ssDNA) tail, which is extendable by 5′–3′ exonuclease Exo1 (Zakharyevich *et al.,* 2010). The initial coating of the 3′ ended ssDNA takes place by the replication protein A (RPA) (Ribeiro *et al.,* 2015). This protects the potentially fragile ssDNA molecule and impairing secondary structure formation. The RecA family members Dmc1 and Rad51, gradually replaces the RPA. The Rad51/Dmc1-DNA complexes, in combination with the factors of chromatin remodelling, invade DNA templates in homologues chromosomes in search of homology; this is called single-end invasion (Hunter & Kleckner, 2001). The ssDNA invasion of an opposing DNA helix has the ultimate result of the complementary DNA strand displacement and the displacement loop (D-loop), which represent the last intermediate stage that is common to all outcomes of the repair (Zakharyevich *et al.,* 2010) (Figure 1.10).

1.5.6 Noncrossover/crossover designation

After the formation of the D-loop, DNA polymerases can undertake the synthesis of DNA using the invading 3′ end as a substrate, which extends the single-stranded molecule with the use of strands that are invaded as a template. If the invading strand, at this point, is displaced and disrupted, it can reanneal with the DSB other side of the DSB ends. After more DNA ligation and synthesis, DSB repair takes place. The repair pathway, known as synthesis-dependent strand annealing (SDSA), leads to a noncrossover events only with a gene conversion (Figure 1.10b; Allers & Lichten, 2001).

If there is no utilisation of SDSA, the extended D-loop is captured by the DSB's other side called second-end capture, this process creates a joint molecule (JM) between chromatids of two opposing sides (Szostak *et al*., 1983). At this stage, the endonucleases can cleave the junctions, which allows for further ligation and elongation in creating a crossover (Figure 1.10f; Martini *et al.,* 2011). Formation of a double Holliday junction (dHJ) occurs if nucleases do not act on the joint molecule (JM)(Figure 1.10c). These appear to be the D-loop extension's main product during meiosis (Bzymek *et al.*, 2010).

The dHJs can be repaired in two ways: (a) by dissolution (Figure 1.10d), or (b) by resolution (Figure 1.10e). The latter results in either a crossover or a noncrossover event. The repair of the dHJ is biased heavily in favour of the forming of a crossover in meiosis (Allers & Lichten, 2001). Alternatively, dHJs undergo dissolution via the action of topoisomerases and helicases to result in a noncrossover (Bizard & Hickson, 2014).

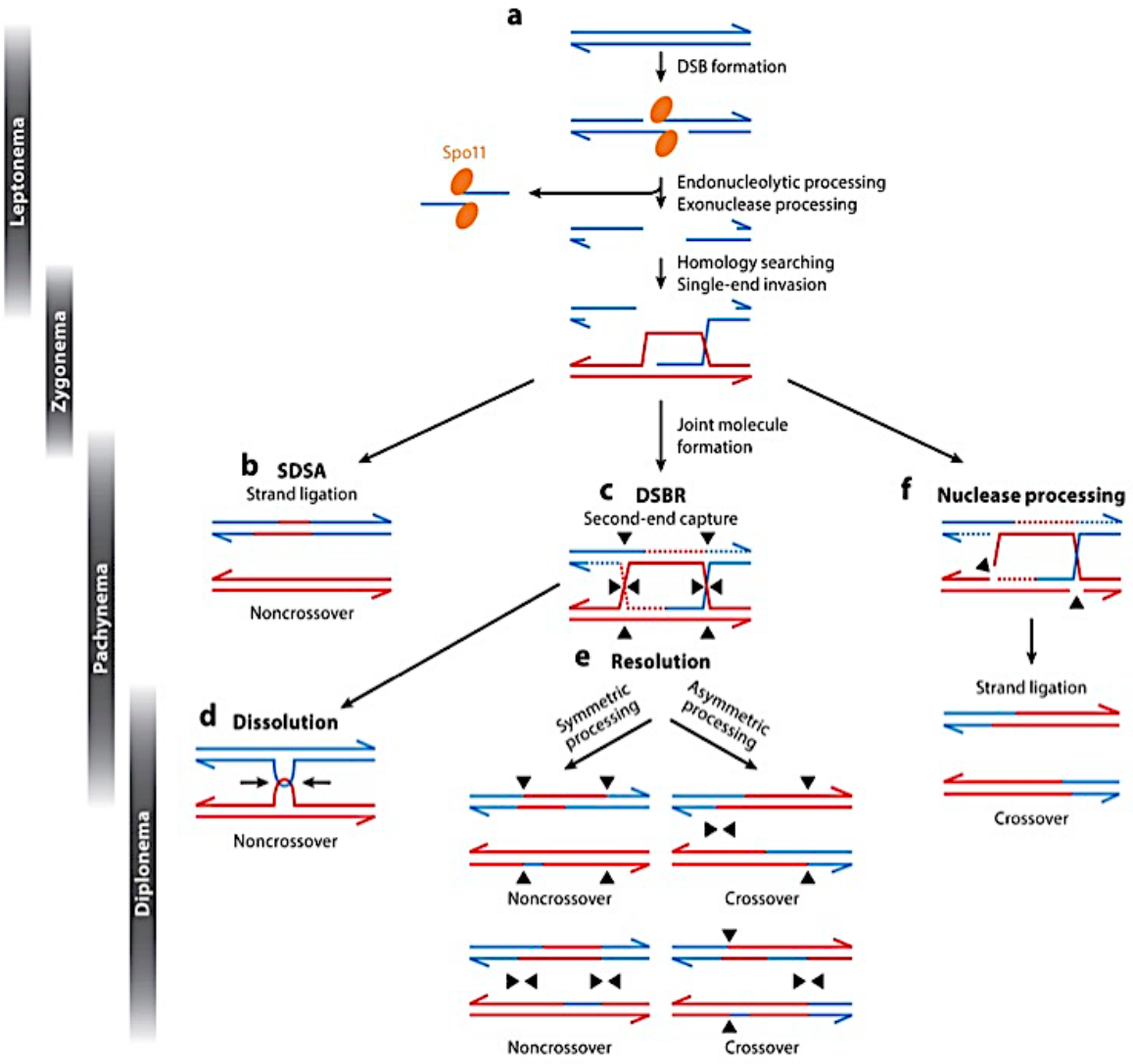

Figure 1.10: Diagram of meiotic recombination. The presence of DNA intermediates has been shown to be a required component of this process. DNA synthesis is represented in red. An accessory protein of Spo11 is needed for this process (adapted from Hunter, 2015). The figure illustrates the process of meiotic recombination as it occurs in *Saccharomyces cerevisiae*. Part (a) represents the meiotic recombination that results from the intervention of Spo11. Spo11 creates the double-strand breaks that establish which pieces of DNA can recombine. After the DNA is cleaved, Spo11 is freed and becomes involved in a Spo11-oligonucleotide complex. Part (b) shows that as the DNA is being extended, the strand itself can become displaced. This may prompt it to reanneal with the incorrect side of the DNA, resulting in an unsuccessful crossover event. However, the invading strand may continue to extend its length in nucleotides and create a larger D-loop. Part (c) shows that after the second-end capture of the fragmented DNA and after a period of growth of the complementary strand, a double Holliday junction is created. Part (d) illustrates the actions of two enzymes: helicases and topoisomerases. During this process, the Holliday junctions move towards one another and become dissolved into a noncrossover event. Part (e) indicates that the symmetry of the Holliday junctions determines whether they will participate in crossover or noncrossover events. Part (f) shows that after the strand invasion processes, nucleases are able to contribute to the development of crossovers by modifying molecules in their intermediate forms.

1.6 Aims of the project

The aims of this project will be to investigate the potential role of *SPO11* in cancer cells and to identify any oncological function. The *SPO11* gene will be studied because it has a restricted expression in almost all cancer cells but is not expressed in healthy somatic tissue. This resulted in the hypothesis that cancer cells might have an obligate requirement for SPO11. The approach will be to examine the mechanisms of action of *SPO11* via depletion and/or overexpression in the cancer cell lines in order to determine its contribution to cancer cell proliferation. Finally, an attempt will be made in this study to purify *SPO11* after expression in *Escherichia coli* for use in crystal structure development and *in vitro* assays. The objectives will be to confirm the hypothesis that *SPO11* is required for cancer cell proliferation and to elucidate the functional role of *SPO11* in cancer cells, which might help to identify *SPO11* as a cancer-specific drug target.

2. Material and Methods

2.1. Routine cell culture (parental cells)

The cells were grown in a humidified incubator at 37°C in 5% CO_2. The colon cancer cell line (SW480)[European Collection of Cell Cultures (ECACC), cell line authentication report number 710236782] were cultured in a Dulbecco's Modified Eagle Medium (DMEM) medium (Life Technologies, #61965) supplemented with 10% fetal bovine serum (FBS) from GIBCO, Life Technologies (#10270). Both the H460 cells (ATCC, # HTB-177) and A2780 cells (ECACC, # 93112519) were grown in a RPMI medium (Life Technologies, #61870) supplemented with 10% FBS from GIBCO, Life Technologies (#10270). The HCT116 cells (ECACC, cell line authentication report number 710236782) were grown in a McCoy's 5A medium (Life Technologies, #36600) supplemented with 10% FBS from GIBCO, Life Technologies (#10270). The stably transfected cell line HeLa Tet-On® 3G with pCMV-Tet3G was purchased from Clontech. The HeLa Tet-On® 3G cells were grown in a DMEM medium (Life Technologies, #61965) supplemented with 10% fetal bovine serum (FBS) from Tet System Approved FBS (Clontech, 631106) in the presence of 100 µl/ml Geneticin G418 antibiotic. The embryonal carcinoma cell line (NTERA-2 clone D1cells) was a gift from Prof. P.W. Andrews (University of Sheffield). The liver cancer cell line (HepG2) was a gift from Dr. J. Muller (University of Warwick). The ovarian cell lines (PEO14, TO14 and A2780), breast cell lines (MCF7 and MDA-MB-453), colon cell lines (HT29, T84, LoVo), astrocytoma cell line (1321N1) and melanoma cell lines (G361, MM127, COLO800 and COLO857) were obtained from European Collection of Cell Cultures (ECACC) https;//www.phe-culturecollection.org.uk/collection/ecacc.aspx). All cells used in this study were sent for short tandem repeat (STR) authentication by LGC standards UK on a yearly basis, the authentication report numbers in the thesis refer to the most recent report (SOJ20094; March 2016). The cell seeding density was 2-3x10,000 cells/cm, the medium was replaced every 4-5 days and the cells were passaged using 0.05% of Trypsin–EDTA (Sigma, 59417C) at a ratio of 1:6. A cryopreservation was performed in 1 ml of freezing medium containing 10% DMSO and FBS. All cell lines were routinely checked for mycoplasma contamination using the LookOut Mycoplasma PCR Detection kit (Sigma Aldrich, MP0035) as per the manufacturer's instruction and have undergone a16 loci short tandem repeat (STR) authentication (LGC Standards, UK). Table 2.1. shows the type of cell lines.

Table 2.1. List of the type of cell lines, refered to ECACC general cell collection:10112001 COCA culture.

Cell Line Name	Cell type	Growth Mode	Keywords	Cell Line Description
HeLa	**Epithelial**	**Adherent**	**Human cervix epitheloid carcinoma**	**Adherent human cervix epitheliod carcinoma cancer cell line with abnormal ploidy Derived from a cervical carcinoma from a 31-year-old female.**
HCT116	**Epithelial-like**	**Adherent**	**Human colon carcinoma**	**Adherent human colon carcinoma one of 3 strains of malignant cells isolated from a male with colonic carcinoma.**
SW480	**Epithelial**	**Adherent**	**Human colon adenocarcinoma**	**Derived from a grade 3-4-colon adenocarcinoma.**
TO14	**Epithelial**	**Adherent**	**Human ovarian cancer**	**TO14 is an adherent cell line derived from a metastasis to the omentum obtained at hysterectomy from a patient with a well differentiated serous adenocarcinoma.**
NTERA-2	**Epithelial**	**Adherent**	**Human Caucasian pluripotent embryonal carcinoma**	**The pluripotent human embryonal carcinoma cell line NTERA-2 clone D1**
HT29	**Epithelial**	**Adherent**	**Human Caucasian colon adenocarcinoma**	**Isolated from a primary tumour in a 44-year-old Caucasian female. Forms a well-differentiated adenocarcinoma consistent with colony primary, grade I.**
T84	**Epithelial**	**Adherent**	**Human colon carcinoma**	**Derived from a lung metastasis of colon carcinoma in a 72-year-old male.**
LoVo	**Epithelial**	**Adherent**	**Human colon adenocarcinoma**	**Derived from a metastatic tumour in the left supraclavicular region of a 56-year-old male with adenocarcinoma of the colon.**
Hep G2	**Epithelial**	**Adherent**	**Human Caucasian hepatocyte carcinoma**	**The Hep G2 cell line has been isolated from a liver biopsy of a male Caucasian aged 15 years, with a well-differentiated hepatocellular carcinoma.**
MCF7	**Epithelial-like**	**Adherent**	**Human Caucasian breast adenocarcinoma**	**Established from the pleural effusion from a 69-year female caucasian suffering from a breast adenocarcinoma.**
A2780	**Epithelial**	**Adherent**	**Human ovarian carcinoma**	**The A2780 human ovarian cancer cell line was established from tumour tissue from an untreated patient.**
PEO14	**Epithelial**	**Adherent**	**Human ovarian cancer; oestrogen receptor negative**	**PEO14 is an adherent cell line derived from a malignant effusion from the peritoneal ascites of a patient with a well-differentiated serous adenocarcinoma.**
G-361	**Epithelial**	**Adherent**	**Human Caucasian malignant melanoma**	**Established from a malignant melanoma of a 31 year old male Caucasian.**
COLO 857	**Epithelial**	**Adherent**	**Human melanoma**	**Derived from a right axilla lymph node of a 43 year old male with melanoma.**

2.2. Thawing of Frozen cancer cell lines

The cell vials were carefully and quickly removed from the liquid N_2 and transferred to a 37°C water bath. The thawed cell suspension was quickly transferred into 5 ml of pre-warmed medium to dilute out the DMSO. This cell suspension was immediately centrifuged at 100 xg for 5 minutes. Subsequently, the cell pellet was resuspended in 10 ml of growth medium. The cells were divided into two T25 flasks then transferred to 1XT75 for expansion of the culture and incubated there for 24 hours in a humidified incubator at 37°C with 5% CO_2.

2.3. Colonosphere Formation Assay

For in Vitro Assessment and Expansion of Stem Cells in Colon Cancer. The primary colonospheres were generated as previously described by Kanwar et al. 2010. The non-adherent sphere assay is a technique used for isolating and enriching CSCs. In this assay, the ability of the cells to undergo growth proliferation as floating spheres is evaluated under non-adherent and non-differentiating conditions (Sukach & Ivanov, 2007). Briefly, a single cell suspension of parental SW480 cells was plated onto 10 cm diameter ultra-low attachment culture dishes (Corning, Costar, 3474) at a concentration of $1x10^5$ cells in 10 ml of serum-free stem cell medium (SCM) containing: DMEM/F12 (1:1) (Life technologies, 31331) supplemented with: 1 ml of 50x serum-free B27 (Life Technologies, 17504-044), 10 ng/ml of basic fibroblast growth factor (bFGF; Life Technologies, PHG0264), 20 ng/ml of epidermal growth factor (EGF; Life Technologies, PHG0314) and 50 units of penicillin and 50 µg of streptomycin (Life Technologies, 15140122). The incubation was carried out at 37°C, 5% CO_2 and the medium was changed every other day. After 5-7 days, the colonospheres were centrifuged (400 x g) and washed with DPBS (Invitrogen, GIBCO 14190094) followed by dissociation with StemPro Accutase (Invitrogen, A11105-01). The single cell suspension was prepared by repeated pipetting using a 1000 µl pipette, and it was either sub-cultured using a 1:10 split ratio, used for further experiments, or frozen down. Cryopreservation was performed in 1 ml of the Cryomaxx II freezing medium (PAA, J05-012). The cryopreservation vials (1 ml cryotubes, Nunc, 343958) containing the cells were labelled with the name of the cells, passage number and date, frozen in a −80°C isopropanol cryo-freezing container and then transferred for long-term storage in liquid nitrogen.

The passage numbers were recorded as follows: the first number represented the number of passages of the parental culture in the DMEM/FBS medium; the second number refers to the number of passages in the SCM. For example, P44.7 cells were passaged 44 times in the DMEM/FBS and 7 times in the SCM.

2.4. Extreme limiting dilution analysis

An extreme limiting dilution analysis (ELDA) is a software application for limiting dilution analysis (LDA), with particular attention to the needs of stem cell assays as described in (Hu and Smyth, 2009) also, to determine the frequency of cells having a particular function that are present in a mixed population of cells. In brief, the colonosphere-derived cells were collected and diluted to form single-cell suspensions. These were plated in 96-well ultra-low attachment plates (Costar, Corning, 3474) at 1000, 100, 10 cells and 1 cell per 100 µl of Stem Cell Medium (SCM), see Section 2.3. This procedure was repeated for the untreated, Hiperfect treated, negative control siRNA and the *SPO11* siRNA treated cells. The transfection mixture for each condition contained 12.5 ng of siRNA, 0.3 µl of HiPerFect Reagent (Qiagen, 301705) and 4.7 µl of serum-free media. As in Section 2.3, the complexes were allowed to form for 15 minutes before being added to each well, and the cells were incubated at 37°C in a 5% CO_2 for 10 days. The cells were supplemented with 50 µl of SCM. The transfection complexes were re-applied after 4 and 8 days of incubation. At the end of 10 days of cell culture, the number of wells with colonospheres, which contained more than 20 cells, was counted using light microscopy. The frequencies of the colonosphere forming cells were determined using the ELDA webtool (http://bioinf.wehi.edu.au/software/elda).

2.5. Transfection (RNA interference)

The *SPO11* siRNA and a negative control siRNA were obtained from the Qiagen and used at a final concentration of 5 nM. The names and sequences of the siRNA are as listed in Table 2.2. HiPerFect reagent (Qiagen, 301705) was used to perform the transfection, according to the manufacturer's instructions. Prior to the transfection, 150 ng of siRNA (0.6 µl of 20 µM siRNA stock) and 6 µl of HiPerFect Reagent (Qiagen, 301705) were mixed with 100 µl of serum-free media (OptiMEM, Life Technologies, 11058-021) and incubated for 15 mints at room temperature (RT) to allow the formation of transfection complexes. $1.5x10^6$ SW480 cells were plated per well of a 6-well plate.

The transfection complexes were then added drop-wise with a gentle swirling of the plates to ensure uniform distribution. The transfected cells were subsequently "spiked" 24 hours later (siRNA/HiPerFect complexes added again to the attached cells). Approximately 48 hours after cell seeding, the whole cell protein lysates and RNA were extracted. The efficiency of the knockdown of the targeted mRNA was determined using the qRT-PCR and protein levels assessed by western blotting.

Table 2.2. List of siRNAs used in this study.

Gene	**Name**	**Qiagen Cat.no**	**Concentration**	**siRNA sequence**
SPO11	siRNA_1	SI00100366	20 μM	5'-CAGAGTGTACTTACCTAACAA-3'
SPO11	siRNA _2	SI00100373	20 μM	5'-ACAACTAATGTTAACGCATAA-3'
SPO11	siRNA _4	SI00100387	20 μM	5'-TACCTTCTACGATACAACTAA-3'
SPO11	siRNA _6	SI03024049	20 μM	5'-TTGCATCATGATTACGGGAAA-3'
Negative control	AllStarsNegativeControl siRNA	1027280	20 μM	Proprietary

2.6. Preparation of cancer cell line stocks

Once the cells were confluent, they were washed twice with 1X PBS before performing a trypsinization with 1x trypsin–EDTA (GIBCO, 1370163). 10 μl of the cells were transferred to 1.5 ml of Eppendorf containing 10 μl of trypan blue solution (Cat. No: T8154-20ML) and counted using either a hemocytometer or an automated cell counter (BioRad). The remaining cell suspension was centrifuged at 100xg for 5 minutes to obtain a cell pellet, which was aspirated and resuspended gently in 1 ml of freezing medium Dimethyl sulphoxide (DMSO) (1:9 DMSO: FBS) before transferred to a labelled Cryotube and then to the CoolCell^{R}LX at -80^{o}C.

2.7. Cloning of *SPO11* gene into pGEX_2T and pGEX-6p-1 vectors

The *SPO11* ORF was cloned into pGEX-2T and pGEX-6p-1 vectors in order to activate its expression and produce a high amount of protein *in vitro* for future structure analysis (Table 2.3). These vectors include a *tac* promoter, which is chemically inducible with IPTG,

A *lacI* gene for use in *E. coli* and also contained a glutathione S-transferase (GST) tag upstream of multiple cloning sites for protein functional analysis. pGEX-2T (Figure 2.1) has a specific thrombin site for cleaving the protein of interest from the fusion product with thrombin cleavage. pGEX-6p-1(Figure 2.2) has a specific protease site for cleaving the protein of interest from the fusion product with preScission protease.

1 µg of pGEX-2T vector and pGEX-6p-1 pGEX-6p-1 vector were digested independently with 10 units of *Bam*HI restriction enzyme and was ligated with full length *SPO11* cDNA. As described in Section 2.10.6, the ligation mix was first transformed and then positive colonies were selected as described in Section 2.10.7. The positive colonies were confirmed using sequence analysis to ensure *SPO11* cDNA was integrated in frame with the tag. Finally, plasmid isolation and transformation was performed using competent cells *E. coli* BL21 (DE3) for protein expression.

Table 2.3. List of Plasmids and their Universal Primers.

Vector		**Source**		
pGEX-2T vector		(GE Healthcare; 28-54653)		
pGEX-6P-1 vector		(GE Healthcare; 28-9546-48)		
Universal primers				
Vector	**Name**	**Primer Sequence**	**Melting Temperature (°C)**	**Product size (bp)**
pGEX2T	pGex F pGex R	5'-ATAGCATGGCCTTTGCAGG-3' 5'-GAGCTGCATGTGTCAGAGG-3'	55	4948
pGEX6p-1	pGex F pGex R	5'-ATAGCATGGCCTTTGCAGG-3' 5'-GAGCTGCATGTGTCAGAGG-3'	55	4948

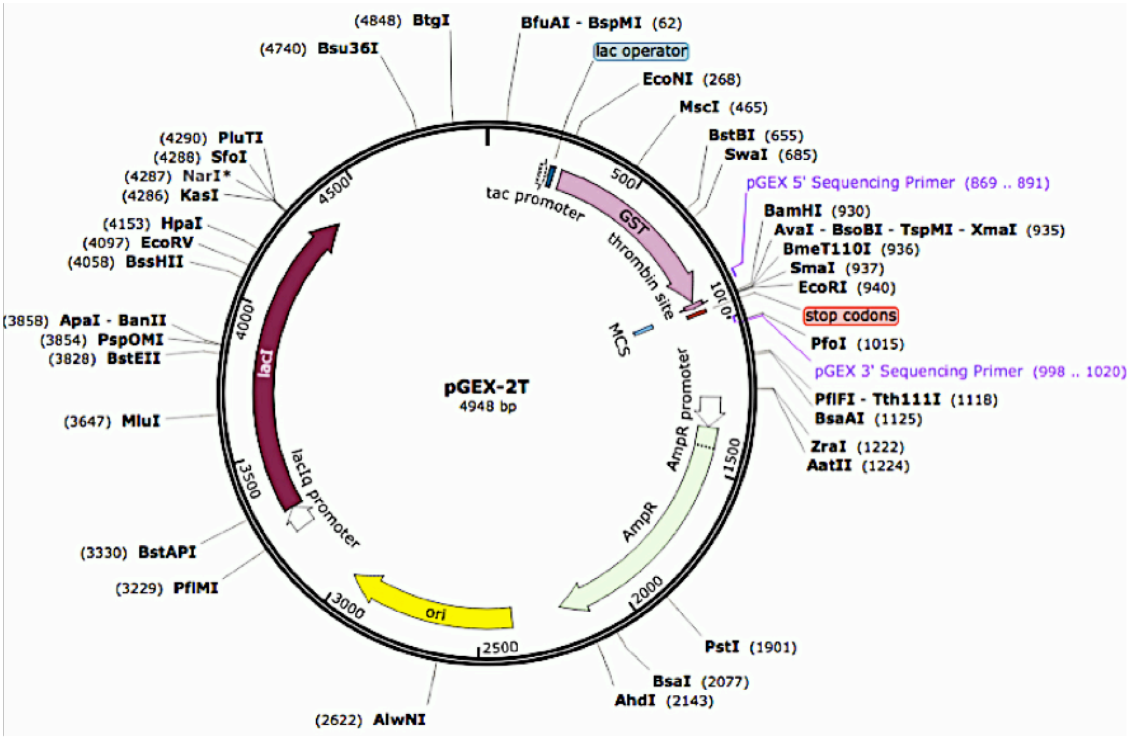

Figure 2.1: The diagram shows vector maps of pGEX-2T (figures adapted from Snap gene web).

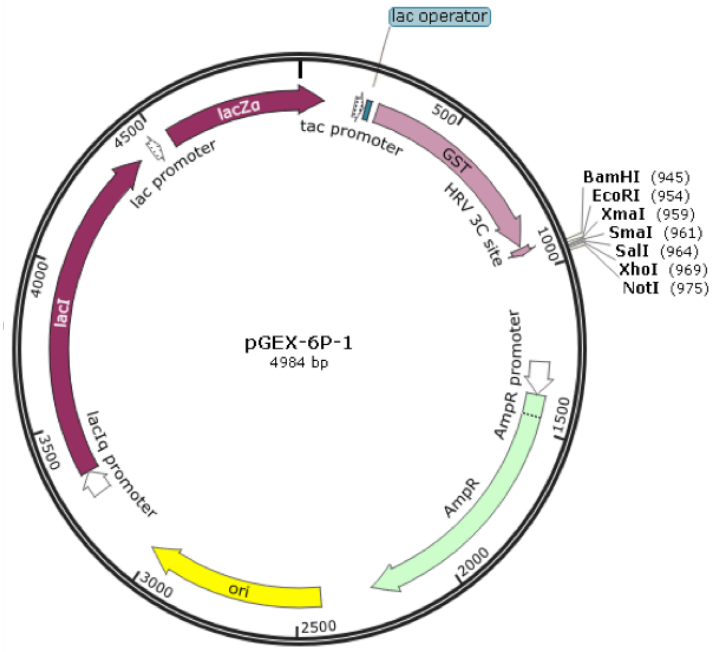

Figure 2.2: The diagram shows vector maps of pGEX-6p-1(figures adapted from Snap gene web).

2.8. The Tet-On 3G inducible gene expression system

To control the expression of a specific gene of interest (GOI) (in this study *SPO11*) within a specific cancer cell line the Tet-On 3G inducible system was selected from Clontech. This system relies on the presence of two plasmids pCMV-Tet3G and pTRE3G (Figure 2.3.

The pCMV-Tet3G plasmid constitutively expresses a transactivator, which binds to the promoter of pTRE3G only in the presence of doxycycline, to activate transcription from that promoter. The pTRE3G plasmid also contains the GOI under the control of this promoter. In this way, in the presence of doxycycline, the GOI is expressed. This system was used in both the HeLa and HCT116 cells. Table 2.4. shows the Plasmids used in this study.

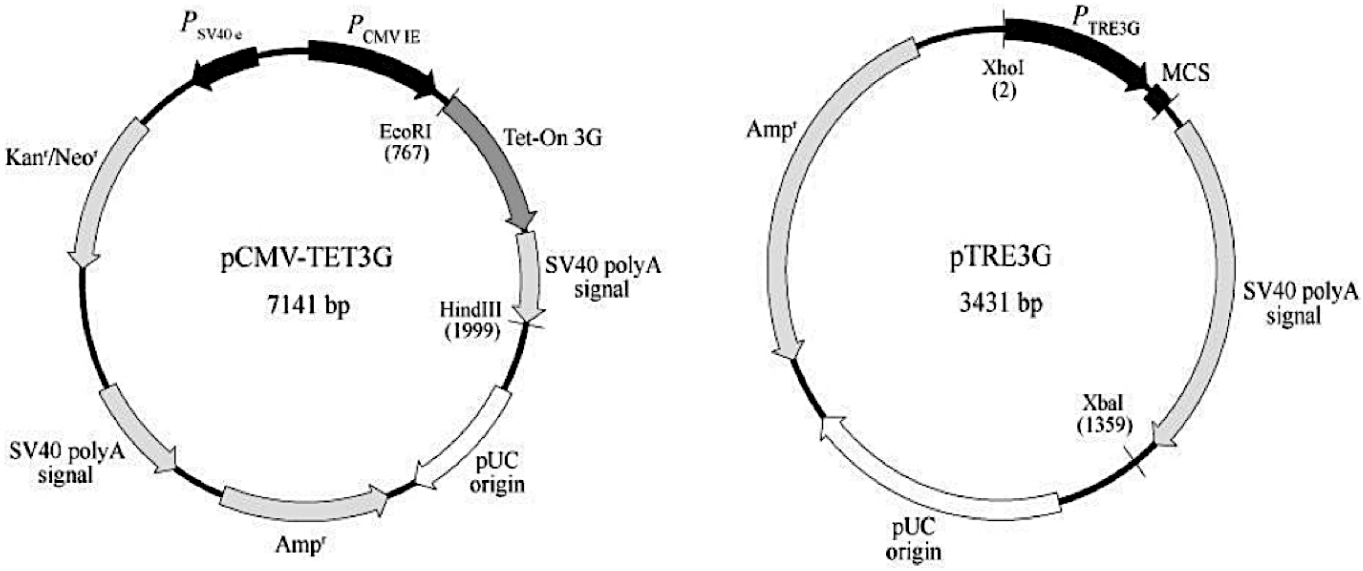

Figure 2.3. The figure is taken from Clontech's manual illustrating the Tet-On 3G system and modifications.

Table 2.4. List of Plasmids and plasmid primers used in this study.

Vector			Source	
pCMV -Tet3G – **regulator plasmid**			(Clontech #631168)	
pTRE3G – **response plasmid**			(Clontech #631168)	
pTRE3G-Luc – **response plasmid**			(Clontech #631168)	
Vector	**Name**	**Universal primers**	**Melting Temperature (°C)**	**Product size (bp)**
pTRE3G	F R	5'-ATTCCACAACACTTTTGTCT-3' 5'-GGTTCCTTCACAAAGATCCTC-3'	55	3431

a) Establishment of Stably integrated Tet-On 3G HCT116 clones

The first step in the system required making a stable cell line with the pCMV-Tet3G vector. This vector has a G418 (Selective Antibiotic) selectable resistance gene (neomycin). Before transfecting the cells with this vector, Genetecin "kill curves" for the HCT116 cells were carried out. The HCT116 cells were then cultured in 6 well plates and were transfected with the pCMV-Tet3G vector using Xfect reagent, following the manufacturer's instructions. The cells were split and the antibiotic G418 (optimum concentration chosen 500 µg/ml) was added to the media to select positive colonies. Post 15 days, single colonies were isolated and grown independently.

i) Genetecin selection

HCT116 Tet-On 3G was seeded on 6-well plates in McCoy's 5A medium + GLUTAMAXTM^{TM} supplemented with 10% Tet system Approved FBS (631106), and HeLa Tet-On 3G cell line was seeded in to 6-well plates in Dulbecco's Modified Eagle medium (DMEM) supplemented with 10% Tet system Approved FBS. The cells were incubated in a humidified incubator at 37^{o}C and 5% CO_2 until the cell density reach the confluent stage. Seven doses of Genetecin, from 100 - 500 µg together with untreated cells, were tested to optimise the minimum dose of Genetecin required to kill all cells after 3-5 days. The lowest optimum dose chosen for single colony selection was 400-500 µg/ml.

ii) Transfection of pCMV-Tet3G into HCT116

$1x10^5$ HCT116 cells were cultured in 6-well plates and were transfected with the pCMV-Tet3G vector using Xfect reagent (Clontech, 631317), following the manufacturer's instructions. The cells were split and the antibiotic G418 (optimum concentration chosen 500 µg/ml) was added to the media to select positive colonies. Post 15 days, single colonies were isolated and grown independently.

iii) Independent Tet-On HCT116 clone assessment using the luciferase assay system

Doxycycline-dependent transactivator induction was achieved using the luciferase assay system (Promega) in conjunction with the pTRE3G-luc vector. This vector contains the firefly luciferase gene under the control of the pTRE3G promoter. As mentioned above, the pTRE3G promoter is responsive to the transactivator only in the presence of doxycycline. The luciferase assay system converts the chemical energy of luciferin oxidation through an electron transition, forming the product molecule oxyluciferin, which produces light. The firefly luciferase, a monomeric 61 kDa protein, catalyses the luciferin oxidation using ATP/Mg_2. A flash of light is produced that decays quickly after the substrates and enzyme are combined.

$$\text{Luciferin} + O_2 + \text{ATP} \xrightarrow[\text{Luciferase}]{} \text{Oxyluciferin} + CO_2 + \text{AMP} + \text{PPi} + \text{LIGHT}$$

b) Luciferase Assay System

After 24 hours, the cells were harvested, and the luciferase activity was checked in samples using the Luciferase Assay System (Promega, E1500), by following the manufacturer's instructions. A 1420 VICTOR^2 Multilabel counter (Wallac, 1420-018) was used to record the Luminescence. The clones with the highest fold induction were selected. These clones were subsequently expanded and stored frozen as HCT116-Tet-On15 cells. Having obtained Relative Light Unit (RLU) readings for each clone, it was necessary to standardize the readings using the protein concentration of each lysate. The concentration of protein was determined using a BCA protein Assay kit (thermo Scientific, 23227), following the manufacturer's instructions, and an equal amount of each fraction were loaded for a western blot analysis. The values obtained were subsequently normalised to the un-induced controls.

RLU per µg protein = RLU of sample / protein concentration (µg/µl)

The amount of light is proportional to the amount of luciferase present, and this in turn is dependent on the activity of the transactivator within each of Tet-On 3G clones in the presence of doxycycline. Independent clones were initially seeded into 2 wells of a 6-well plate and transfected as described in Section 2.7.a (ii) with the pTRE3G-Luc vector. 4 hours after transfection, the media was replaced with +/- 1 μg/ml dox, and the clones were harvested 24 hours later.

c) Puromycin selection

The HCT116 Tet-On 3G was seeded into 6-well plates in McCoy's 5A medium + GLUTAMAXTM^{TM} supplemented with 10% Tet system Approved FBS, and the HeLa Tet-On 3G cell line was seeded into 6-well plates in Dulbecco's Modified Eagle medium DMEM supplemented with 10% Tet system Approved FBS and 100 μg/ml G418. The cells were incubated in a humidified incubator at 37^{o}C and 5% CO_2 until the cell density reach the confluent stage. Seven doses of Puromycin (Life Technologies, A1113803), from 0.8 to 10 μg together with untreated cells, were tested to optimise the minimum dose of Puromycin required to kill all cells after 3-5 days. The lowest optimum dose chosen for single colony selection was 1 μg/ml.

d) Establishment of Stably integrated pTRE3G: *SPO11* Tet-On 3G HCT116 and HeLa clones

The HCT116 Tet-On 3G and HeLa Tet-On 3G clones isolated needed to be transfected with the next vector of the Tet-On system: pTRE3G:*SPO11* (see Section 2.10). This was achieved essentially as described in the Clontech's manual accompanying the Tet-On 3G system and modification to this protocol. Before this vector could be transfected into the cells, Puromycin "kill curves" were established for the HCT116 Tet-On 3G and HeLa Tet-On 3G cells. The clones [(HCT116 cells (1x 10^5)] to be transfected were seeded into 6 well plates and incubated for 24 hours before transfection. The plasmid DNA, pTRE3:*SPO11,* does not have a selectable resistance marker and the Clontech protocol recommended co-transfection with a linear Puromycin selection marker (Clonotech, 631626) at a ratio of 20:1 (vector: linear marker) using Xfect transfection reagent. After two weeks, visible single colonies appeared, and large colonies were picked using cloning cylinders and were each transferred into a separate well of a 24-well plate and then grown independently in a 6 well plate in a maintenance concentration of G418 (100-200 μg/ml) and 1 μg/ml Puromycin. When confluent, cells were split from each well into three wells of 6 well plates for testing. 1 μg/ml

of Doxycycline (Sigma, D3072) was added to the medium, according to the manufacturer's protocol, to induce the expression of *SPO11*. The levels of *SPO11* expression were checked by qRT-PCR, and the SPO11 protein levels monitored by western blot.

2.9. Cell Imaging Methods

2.9.1 Indirect Immunofluorescence

Autoclaved coverslips (GPE Scientific CLS-1760-012) were transferred to each well of a 24-well plate. (1x 10^5) The SW480 cells were seeded into each well and grown until they were 70-80% confluent. The cells were washed in warm 1xPBS before fixing in freshly made 4% paraformaldehyde (PFA in 1xPBS) for 10 minutes at room temperature. The cells were washed 3x10 minutes in 1xPBS. To block the non-specific binding of antibodies and to permeabilize the membranes, the cells were incubated in 5% FBS/0.3% Triton™ X-100/1x PBS for an hour at room temperature. Subsequently, the cells were treated overnight with primary antibodies (see Table 2.5.) diluted in 1% BSA/0.3% Triton™ X-100/1x PBS.
This was followed by three washes with 1X PBS of 5 minutes each. The cells were incubated with Alexa Fluor secondary antibodies (see Table 2.6.), which were diluted in 1% BSA/0.3% Triton™ X-100/1x PBS for 2 hours in the dark at room temperature. This was followed by three washes with 1X PBS for 5 minutes each. Prolong® Gold Antifade Reagent with DAPI (Cell Signalling, #8961) was used for mounting the coverslips. A Zeiss LSM 710 confocal microscope and ZEN software (Zeiss) were used to detect immunofluorescence.

Table 2.5. List of Primary antibodies for indirect immunofluorescence (IF).

Antibody	Clone	Host	Dilution	Source	Cat.no.
Anti-SPO11	Monoclonal	Rabbit	1:3000	Abcam	ab81695
Anti-α-Tubulin	Monoclonal	Mouse	1:500	Abcam	ab80779
Anti-PICH (anti-ERCC6L)	Monoclonal	Mouse	1:200	Abcam	ab57434
Anti-BLOOM	Polyclonal	Goat	1:150	Santacruz	130314
Anti-Pericentrin	Mouse	Monoclonal	1:1000	Abcam	ab28144
Anti-Phopho-Histone H2A-X	Monoclonal	Rabbit	1:400	Sigma	9718

Table 2.6. Secondary antibodies for IF and their dilutions and sources.

Antibody	Host	Species Reactivity	Dye/Label	Excitation/ Emision	Dilution	Source	Cat. Number
Anti-rabbit IgG (H+L)	Goat	Rabbit	Alexa Fluor® 488	495/519	1:1000	Life Technologies	A11011
Anti-rabbit IgG (H+L)	Goat	Rabbit	Alexa Fluor® 568	578/603	1:1000	Life Technologies	A11034
Anti-goat IgG (H+L)	Donkey	Goat	Alexa Fluor® 488	495/519	1:1000	Life Technologies	A11055
Anti-goat IgG (H+L)	Donkey	Goat	Alexa Fluor® 568	578/603	1:1000	Life Technologies	A11057
Anti-mouse IgG (H+L)	Goat	Mouse	Alexa Fluor® 488	495/519	1:1000	Life Technologies	A11029
Anti-mouse IgG(H+L)	Goat	Mouse	Alexa Fluor® 568	578/603	1:1000	Life Technologies	A11031

2.10 Molecular Biology: Cloning and Gene editing

2.10.1 PCR primer design

The PCR primers were designed using a software Oligonucleotide properties calculator that also calculated the melting temperature (Tm) and C+G content (50-55%), relative to the length of primers (~20 bp). Preference was given to the primers, which possessed a C or G nucleotide. Human testis tissue RNA (1 µg) was converted to cDNA using a Phusion high-fidelity PCR master mix with a GC buffer (New England BioLabs), the full length *SPO11* cDNA was amplified from this cDNA. The PCR conditions were as follows: 1x cycle 98°C for 30 seconds, 35 cycles of denaturing at 98°C for 10 seconds, annealing 55°C for 30 seconds and extension at 72°C for 30 seconds/per 1 kb followed by a final extension at 72°C for 10 minutes. A 5 µl sample of the PCR product was electrophoresed using 1% agarose gel.

2.10.2 Purification of PCR products

The QIAquick PCR Purification kit was used to purify the PCR products. If multiple bands were identified in the PCR reaction after electrophoresis, bands of the correct size were excised from the agarose gel before purification, according to the manufacturer's instructions. The PCR product was purified for ligation into plasmid vectors or for sequencing purposes.

2.10.3 DNA sequencing

Prior to sequencing, the DNA samples were adjusted to a concentration of 5 ng/µl (300 bp -1 Kb fragments), 1 ng/µl in a total volume of 15 µl mixed with 10 pmol of the forward or reverse primer and sent to MWG Eurofins in bar coded tubes for automated sequencing. The sequencing results were identified using the NCBI Nucleotide BLAST search (Website: http://blast.ncbi.nlm.nih.gov/Blast.cgi).

2.10.4 Digestion of DNA

The PCR reaction products were mixed with loading dye (6x) run on 1% agarose gels. The specific bands were extracted, and purification was performed using a QIAquick PCR Purification kit as per the manufacturer's instructions. The purified PCR product was digested, with 10 units of *Bam*HI restriction enzyme, and the manufacturer's protocol was followed. Post digestion, the samples were incubated at 37°C for 2 hours and then electrophoresed on 1% agarose gel. Appropriate bands were selected and excised from the gel and purified as per the manufacturer's protocol (QIAquick Gel Extraction kit).

2.10.5 De-phosphorylation of plasmid

The plasmid and universal primer details are as shown in Table 2.2. 2.5 µg of plasmid was digested with 10 units of *Bam*HI restriction enzyme, mixed in 10 µl of *Bam*HI buffer E and 86.5 µl of ddH_2O in a total volume of 100 µl. This mixture was incubated at 37°C for 2 hours by addition of 11 µl Antarctic phosphatase buffer (NEB; B0289S) and 1 µl of Antarctic phosphatase enzyme. This mixture was incubated at 37°C for 15 minutes and was heat inactivated for 5 minutes at 65°C. The reaction was electrophoresed on 1% agarose gel and further purified using a QIAquick Gel Extraction kit, and the DNA concentration was determined using a NanoDrop spectrometer.

2.10.6 Gene ligation and transformation

The pTRE3G plasmid was digested and the *SPO11* gene was ligated into it as per the manufacturer's protocol. 50 nanograms of linearized plasmid was ligated with a 1-9 fold molar excess of the insert and mixed with a total of 10 µl sterile water and then 2x Quick ligase reaction buffer (5 µl) and 1 µl of Quick T4 DNA ligase were added, mixed and incubated at RT for 5 minutes and then incubated on ice. 5 µl of ligation product pTRE-3G*:SPO11* and 1 µl of control (de-phosphorylated cut and uncut vectors) were added to 50 µl of DH5X-alpha competent Escherichia coli (*E. coli*) cells + DNA were incubated on ice for 30 minutes followed by heat shock at 42°C for 30 seconds and then again chilled on ice for 5 minutes. 950 µl of Super Optimal broth with Catabolite repression (SOC) media was added to the mixture and incubated at 37°C with vigorous shaking (250 r.p.m) for an hour. The samples were plated onto LB agar plates containing 100 µg/ml of ampicillin antibiotic. Table 2.7. shows the lists of media used for the amounts, and Table 2.8. shows the bacterial strains.

Table 2.7. Medium recipe for *E. coli* growth.

Media	**Amount**
Luria Broth (LB)	
Tryptone	10 g
Yeast extract	5 g
NaCl	10 g
Water	Up to 1 Lt
For LB agar plates add:	
Agar	14 g
Water	Up to 1 Lt

Table 2.8. The *E. coli strains* used.

Bacteria	**Source**
DH5X-alpha competent *E. coli*	NEB; C2987I
BL21 (DE3) competent *E. coli*	NEB; C2527I

2.10.7 Screening of colonies

The selected colonies were grown in 10 ml of LB broth and 2 µl of this was used for PCR amplification using an internal primer for the external *SPO11* + universal pTRE3G (see Table 2.2.) in order to confirm if these were the correct colonies. The remaining medium with PCR positive colonies was inoculated in 5 ml of LB medium containing 100 mg/ml ampicillin and incubated overnight at 37°C with vigorous shaking at 250 r.p.m.

2.10.8 Plasmid extraction from *E. coli*

A 5 ml of overnight *E. coli* culture containing the positive clone of interest was used for plasmid mini preparation. Plasmids were isolated from bacterial culture using a QIAprep Spin Miniprep Kit (Qiagen, 27106) and protocol was followed as given by the manufacturer. The cell pellet was obtained by centrifuging the culture at 4,000 x g for 10 minutes at 4°C and the glycerol stock was kept in -80°C. The cell pellet was resuspended in a P1 buffer and transferred to an Eppendorf tube. To this, 250 µl of P2 lysis buffer was added then incubated at room temperature for 5 minutes followed by the addition of 350 µl of N3 buffer. The tube was gently inverted and subjected to centrifugation at 13,000 x g for 10 minutes. The supernatant obtained was transferred to a spin column and centrifuged at 10,000 xg for 1 minute.

750 µl of PE washing buffer was added and the columns were centrifuged at 13,000 x g for 1 minute. The columns were subjected to centrifugation to remove residual ethanol from the washing buffer. 50 µl of Elution buffer (EB) was used to elute samples from the columns. Plasmids used for transfection were extracted using a HiSpeed plasmid Midi kit (Qiagen, 12643) as per kit protocol. All plasmid were checked by restriction enzyme digestion with appropriate restriction enzyme. Sequencing was performed to confirm correct orientation of *SPO11* cDNA and to detect any gene mutations caused during PCR amplification. Only samples with the correct gene sequence orientation were used for further experiments.

2.11.1. Induction of protein production

24 hours before induction, BL21 (DE3) cells were transformed with *SPO11* and pGEX-2T or pGEX-6p-1 vectors. The expression of fusion proteins was first carried out on a small scale to confirm the ability of plasmid constructs to express the desired polypeptide. Four 1.5 ml cultures (1:10 dilution of overnight cultures) of the pGEX-2T recombinant were grown in LB broth/ampicillin (100 µg/ml) at 37°C in an orbital shaker. After 1 hour, isopropyl β-D-1-thiogalactopyranoside IPTG (Sigma-Aldrich) was added to three of the cultures (final concentration of 0.1 mM) to induce the production of fusion proteins, and the cultures were allowed to grow for 3, 5 and 7 hours, respectively. After incubation, the cells were taken from the induced and non-induced cultures, were pelleted by centrifugation (10 minutes 1,200 g) and resuspended in an equal volume of water. The fusion protein should be clearly detectable in the IPTG induced samples after electrophoresis on SDS-PAGE. To determine the efficiency of purification, fusion proteins were expressed in a 10 ml culture in response to IPTG. A single colony was selected and was resuspended in 10 ml of LB medium containing 100 µg/ml ampicillin. The Falcon tube was incubated overnight at 37°C at 180-200 r.p.m. For protein expression analysis; after overnight incubation, 2 ml of each SPO11 tube culture was transferred into a Falcon tube containing 18 ml of fresh LB medium, which contained 100 µg/ml ampicillin, and was incubated on a shaker at 37°C and 180-200 r.p.m. A spectrophotometer was used to measure the optical density (OD) at 600 nm until the culture reached a density of 0.6-0.8 OD units. IPTG to a final concentration of 0.1 mM was used to induce production of recombinant protein for 5 hours at 37°C.

2.11.2. Expression and purification of GST tagged *SPO11* using Triton-100X

Temperatures ranging from 15°C to 37°C and different concentrations of IPTG varying from 40 to 400 µM were used to check the optimal expression for the *SPO11* tagged gene; Samples were taken before and after induction and centrifuged for 20 minutes at 400 xg at 4°C, and cell pellets were collected. 500 µl of ice-cold 1X PBS or STE buffer containing protease inhibitor cocktail (Roche, 11836170001) was used to resuspend the pellets. The cell suspension was sonicated at low setting for 5 minutes on ice (30 seconds on and 30 seconds off). A 20 µl sample of sonicated cell lysate (whole cell lysis) was used to check whether the cells were fully lysed. To precipitate insoluble cell parts, 1% Triton was added to the entire solution and was centrifuged at 10,000 g at 4°C for 30 minutes. The supernatant was collected in Eppendorf tubes. The insoluble fraction (pellet) was resuspended in 300 µl of ice-cold 1X PBS solution. 10 µl samples each the soluble protein and the insoluble protein from the whole bacterial lysate and un-induced samples were subjected to the protein electrophoresis gel. These samples were mixed with an equal volume of 2x Laemmeli buffer and heated at 100°C for 10 minutes. The heated samples were electrophoresed using 4-12% SDS-PAGE gels 110 volts for an hour, and then the gel was stained with Coomassie blue (see Section 2.10.6).

2.11.3. Production of GST::SPO11 protein using Sodium Lauryl Sarcosinate (Sarkosyl)

This method was adopted from a published paper (Park *et al.,* 2011). In this method, the purification of insoluble fraction of GST-fusion protein was carried out exactly as described in the manufacturer's instructions of purification. The cell pellet was resuspended in 300 µl of ice-cold STE buffer containing 2% sarkosyl, 5 mM dithiothreitol (DTT) and 100 µg/ml lysozyme and incubated on ice for 15 minutes. The sample was sonicated on ice at a low setting for 5 minutes (30 seconds on and 30 seconds off). The samples were centrifuged at 18,000 g for 30 minutes and the supernatants were transferred to new Eppendorf tubes. 2% of Triton X-100 was added to the cell lysate and incubated for 30 minutes on ice and was centrifuged at 10,000 g at 4°C for 30 minutes. The supernatant was collected in new Eppendorf tubes. The insoluble fraction (pellet) was resuspended in 300 µl of ice-cold 1X PBS solution. 10 µl samples of each the soluble protein and the insoluble protein from the whole bacterial lysate and un-induced samples were subjected to the protein electrophoresis gel. These samples were mixed with an equal volume of 2x Laemmeli buffer and heated at 100°C for 10 minutes. The heated samples were electrophoresed using 4-12% SDS-PAGE

gels and 110 volts for an hour, and then the gel was stained with Coomassie blue (see Section 2.11.6).

2.11.4. Purification of soluble GST protein

Soluble GST Fusion protein isolation was performed using the Pierce GST Spin purification kit (Thermo Fisher Scientific, 16106), following the manufacture's protocol, and GST spin traps (GE Healthcare).

2.11.5. Thrombin and preScission protease cleavage of fusion protein

Protease cleavage was achieved by incubating 10 units/mg of Thrombin (GE Healthcare-SLBH8091V-1) with pGEX-2T::SPO11 and preScission protease (GE Healthcare-399393) with pGEX-6p-1::SPO11) in the GST columns, according to the manufacturer's guidelines. The Thrombin reaction mixture was prepared as follows: for each ml of Glutathione Sepharose bed volume, 50 µl (50 units) of thrombin was mixed with 950 µl PBS, the thrombin mix was then loaded to the column containing the purified fusion protein before the elution step, following the manufacture's protocol, for the Pierce GST Spin purification kit (see section 2.10.4) and incubated at room temperature (+22-25°C) for 1, 2, 6 hours.
Also different concentrations of Thrombin were used to determine the optimal length and condition of incubation required for complete digestion of the fusion protein. Following incubation, the column was washed with 3 beads volumes of PBS, and the suspension was centrifuged at 500 g for 5 minutes to pellet the Glutathione Sepharos. The elute was collected in different tubes and analysed by SDS-PAGE of both elute and beads. The elute will contain the SPO11 protein and thrombin, while the GST protein of the tagged protein should remain bound to the Gluthaione Sepharose (beads).

2.11.6. Coomassie Brilliant blue staining

Protein gels were immersed in 10-15 ml of Coomassie Instant Blue (Expendeon, ISBIL) for 1-2 hours with gentle shaking. The gel was washed several times with ultrapure water to remove any residual stain. A Bio-Rad image reader was used to visualize the gels.

2.12 RT-and qRT-PCR

2.12.1. Extraction of total RNA and cDNA synthesis

A RNeasy Plus Mini Kit (Qiagen, 74136) was used for the extraction of the total RNA from the cells, according to the manufacturer's instructions. Briefly, the cell pellet obtained after centrifugation (300 g for 5 minutes) was washed with 1X DPBS (invitrogen, GIBCO 14190094). The cells with a density of 5 x 10^6 cells or 5 x 10^6 - 1 x 10^7 were resuspended in 350,600 µl of lysis buffer RLT plus, respectively. A QIAshredder spin column (Qiagen, 97654) was used to homogenize the cell lysates. The flow-through was transferred immediately to gDNA Eliminator spin columns. The gDNA Eliminator spin columns were used to remove genomic DNA contamination; the RNA samples were treated with DNaseI to remove all traces of genomic DNA contamination. The DNaseI enzyme effectively targets only DNA for digestion, while leaving the RNA molecules intact. For each 40 µl of RNA sample, 2 units of DNaseI enzyme was used. The samples were then incubated at 37°C for 20-30 minutes. A NanoDrop ND-1000 spectrophotometer (NanoDrop Technologies) was used to determine the quantity and quality of the isolated RNA see (Section 2.11.3). A cDNA synthesis was performed using a Quantitect Reverse Transcription kit, by following the manufacturer's instructions. Briefly, 1 µg total of RNA was subjected to a reverse transcription to yield the first strand cDNA. The final cDNA product was diluted ten times with DNase/RNase-free water. The cDNA quality was estimated by RT-PCR using primers for β-Actin (Table 2.11.). Controls without reverse transcriptase for all samples were generated and showed no amplification in the subsequent PCRs.

2.12.2. PCR condition

Briefly, the PCR reaction was carried out in a 50 µl final volume using 1x MyTaq Red Mix (Bioline, BIO-25043), each primer at 10 pmoles concentration, diluted 2 µl cDNA template and DNase/RNase-free water. The following cycling conditions were used: initial denaturation at 95°C for 1 minute, 40 cycles with each cycle consisting of 95°C for 15 seconds, 55°C for 15 seconds and 72°C for 10 seconds and a final extension step of 72°C for 5 minutes. Table 2.11. Below shows the gene-specific primers used for the RT-PCR screening.

2.12.3 Quantitative Real-time PCR (qRT-PCR)

A total RNA extraction was performed using an RNeasy Plus Mini Kit (Qiagen, 74136), according to the manufacturer's instructions. The quantity and quality of the RNA was measured by a NanoDrop ND-1000 spectrophotometer. The integrity of the RNA was analysed using a denaturing agarose gel or Biorad's Experion™ Automated electrophoresis. To set up the reaction, an RNA concentration of below 1000 ng/µl was used; if it was more concentrated, then the RNA was diluted with nuclease free water and measured again to avoid pipetting errors due to low volumes. First, the reaction for the cDNA synthesis was set up in reverse transcriptase reactions using 1 µg of the total RNA: with a superscript III Quantitect Reverse Transcription kit (Qiagen, 205310), following the manufacturer's instructions.

The real-time PCR reactions were performed in triplication in a total volume of 20 µl on a CFX96 RealTime System C1000 Thermal Cycler (Bio-Rad) using a Life technologies Taqman Gene expression Master mix (usually 2x concentration #4369016 kept at 2-8 degrees out of light (for detail method please refer to following link: https://tools.lifetechnologies.com/content/sfs/manuals/cms_039284.pdf).

Amplify genes of interest using Taqman 20x primer assays (https://bioinfo.appliedbiosystems.com/genome-database/gene-expression.html). To normalise results, two endogenous reference genes were used (Table 2.9.)

Table 2.9. Taqman probe primer sets.

qRT-PCR Primers		
Gene	Name	Thermo Fisher
β-Actin	Hs99999903_ml	Thermo Fisher
GAPDH	Hs99999905	Thermo Fisher
SPO11	HS00173288	Thermo Fisher

2.12.4. RNA /DNA quantification

To determine the quantity and quality of the RNA, DNA samples, a NanoDrop 2000c UV-Vis Spectrophotometer was used. The concentration (in ng/µl) of the sample was calculated using the absorption value at 260nm multiplied by 40 (the constant for RNA), while the sample purity was determined by the ratio of absorption at 260nm to 280nm, with a value of 2.0 indicating a pure RNA/DNA sample.

2.13. Agarose gel electrophoresis

For the 1% gel, 1 g of agarose powder was melted in 100 ml of Trs-Borate-EDTA buffer (TBE x 1) by boiling in a microwave for 3 minutes. The Solution was allowed to cool before adding 5 µl of the peqGREEN DNA/RNA dye (Peqlab, 37-5000) to the melted agarose solution. The gel was poured into a casting tray containing plastic combs to create wells for sample loading. Usually, a comb forms 20 wells. Upon cooling, the gel polymerized and the combs were removed in order to place the gel in the electrophoresis tank containing the TBE buffer (1x). Before loading, the DNA samples were mixed with 6x loading dye alongside an appropriate size marker, either the Hyperladder I Kb or, for smaller products, the Hyperladder II, Hyper ladder IV (Thermo Scientific). The duration of the electrophoresis varied depending on the size and percentage of the gel, but typically, it lasted between 1 hour and 1.5 hours. Once migrated, the bands are then visualised using the Chemido up Imaging Systems (Biorad) machine and sizes are determined by comparing them against the DNA ladder Bio-Rad.

2.14 Sample preparation, extraction of cytoplasmic and nuclear protein

A 1:1 mixture of hypotonic buffer (50 mM Tris-HCl pH 7.4, 0.1 M sucrose, 1 mM AEBSF with one complete mini, EDTA-free protease inhibitor cocktail tablet/10 ml) and an equal volume of lysis buffer C (1% Triton, 10 mM magnesium chloride, 1 mM AEBSF with one complete mini, EDTA-free protease inhibitor cocktail tablet/10 ml) was used for cell lysis. Subsequent to the lysis, the mixture was incubated on ice for 30 minutes. Post centrifugation at 6000 g for 2 minutes, the supernatant that contained cytoplasm was transferred to a new tube. The lysis buffer N [(50 mM Tris-HCl pH 7.4, 100 mM potassium acetate (KAc), 1 mM AEBSF with one complete mini, EDTA-free protease inhibitor cocktail tablet/10 ml)] was used to resuspend the nucleus containing cell pellet. Using a Pierce® BCA Protein Assay Kit

(Thermo Scientific, 23227), the protein concentration was determined in both the cytoplasmic and nuclear fractions.To the cytoplasmic and nuclear extracts, an equal volume of sample buffer, Laemmli 2× Concentrate, was added and the lysates were boiled at 100°C for 5 minutes.

2.15 Western blotting

The whole cell-lysates were prepared from cells by using an M-PER lysis buffer (utilizes a proprietary detergent in 25 mM bicine buffer, pH 7.6; Thermo Scientific, 78503), supplemented with a Halt Protease Inhibitor Cocktail (Thermo Scientific, 87785) and a Halt Phosphatase Inhibitor Cocktail (Thermo Scientific, 78420) as per the manufacturer's instructions. A BCA Protein Assay Kit (Thermo Scientific, 23227) was used to determine the concentration of total proteins. Approximately 30 µg of the total protein extract was used.

Western blotting method was used to determine molecular weight and relative amounts of the specific protein in given sample of tissue homogenate. A 4x Bolt LDS Sample Buffer (Life Technologies, B0007) and a 10x Bolt Sample Reducing Agent (Life Technologies, B0009) were added to the 30 µg of protein and subsequently denatured at 70°C for 10 minutes before it was subjected to electrophoresis on the Bolt 4-12% Bis-Tris Plus Gel, 15 well (Life technologies, BG04125BOX) using a Bolt MES SDS Running Buffer (Life Technologies, B0002). A protein ladder (Precision Plus Protein Dual Color Standards, Biorad, 1610374) was also included on the gel to determine where the desired proteins migrated during the process at 100 V for 1 hour. The gels were electro-blotted onto a methanol-soaked PVDF membrane (Immobilon-P, Millipore, IPVH00010) at 500 mA for 2 hours in a 2x Towbin buffer (380mM Glycine, 50 mM Tris). After the PVDF transfer, the membranes were blocked with 5% milk in PBS/0.5% Tween 20 at 4°C for an hour. The blocked membranes were probed with the primary antibodies (see Table 2.10.) in 5% milk/PBS/0.5% Tween 20 at 4°C overnight. When the monoclonal antibodies were used, the membranes were washed three times each for 5 minutes with 5% milk/PBS/0.1% Tween 20. When the polyclonal antibodies were used, the membranes were washed with 5% milk PBS/0.5% Tween 20 at room temperature. After washing, the membranes were incubated with their corresponding secondary antibodies (see Table 2.11.), which were diluted appropriately at room temperature for 1 hour followed by a 10 minute wash in a milk solution and an additional three washes of 10 minutes each in PBS/0.1% Tween 20 (monoclonal antibodies) or PBS/0.5% Tween 20 (polyclonal antibodies)

at room temperature. A Pierce ECL Plus Western Blotting Substrate (Thermo Scientific, 32132) and CL-X Posure Film (Thermo Scientific, 34091), an enhanced chemiluminescence detection system, was used for antibody detection, by following the manufacturer's instructions.

Table 2.10. List of Primary Antibodies for WB.

Primary Antibody	**Cat.no.**	**Host**	**Dilution**	**Clonality**	**Source**
SPO11	Ab81695	Rabbit	1:1000	Monoclonal	Abcam
Anti-Tubulin	T6074	Mouse	1:8000	Monoclonal	Sigma
GAPDH	Sc365062	Mouse	1:3000	Monoclonal	Santa Cruz
BLOOM	130314	Goat	1:150	Polyclonal	Santa Cruz
Lamin B	Sc6217	Goat	1:1000	Polyclonal	Santa Cruz
MAGEC	Ab61404	Mouse	1:500	Monoclonal	Abcam
Cleaved-Caspase 3	9664	Rabbit	1:1000	Monoclonal	Cell signalling
GST (91G1)	54755	Rabbit	1:1000	Monoclonal	Cell signalling

Table 2.11. List of Secondary Antibodies for WB.

Secondary Antibody Cat.no.	**Source**	**Host**	**Species reactivity**	**Conjugate**	**Dilution**
7074	Cell Signalling	Goat	Rabbit	HRP	1:3000
7076	Cell Signalling	Hours	Mouse	HRP	1:3000
A5420	Sigma	Rabbit	Goat	HRP	1:3000

2.15.1 Source of human normal tissue lysates

Human normal lysates were provided from a different company as described in Table 2.12.

Table 2.12. Source of normal lysates used in western blot.

Normal tissues	**Source**	**Cat. No.**	**Protein amount**
Testis	Abcam	Ab30257	20 µg
Thymus	Abcam	Ab30146	20 µg
Skeletal muscle	Abcam	Ab29331	20 µg
Small intestine	Abcam	Ab29276	20 µg
Ovary	Abcam	Ab30222	20 µg
Colon	Abcam	Ab30051	20 µg
Breast	Abcam	Ab30090	20 µg
Testis	Novus Biological	NB820-59266	20 µg
Lung	Novus Biological	NBP2-27734	20 µg
Ovary	Novus Biological	NBP2-28454	20 µg
Liver	Novus Biological	NBP2-29220	20 µg
Colon	Novus Biological	NBP2-28208	20 µg

2.16 Senescence staining

A single cell suspension of SW480 colonosphere cells at a concentration of $1x10^5$ cells were grown in 10 ml of serum-free stem cell medium by plating cells onto 10 cm-diameter ultra-low culture dishes. The *SPO11* siRNA and negative control siRNA was used at a final concentration of 5 nM. Using HiPerFect Reagent, transfection was carried out, according to the manufacturer's instructions (see Section 2.3). Post 4 and 8 days of the incubation, the transfection complexes were reapplied. On day 10 of the incubation, the cells were stained and observed. The media was changed on days 4 and 8 of the incubation. Senescence staining was performed using a β-galactosidase staining kit (Cell Signaling, 9860), following the manufacturer's protocol.

2.17 Gene deletion experiment

Each of the wells of the 6-well plates were seeded with HCT116 TetOn3G cells at a density of $1X10^5$ cells per well. Post 24 hours, the cells were transiently transfected with a 1 µg pCas-Guid (gRNA 2 vector) (GE 100002) Origene (Sequences 3'-CGGGCTGCCTCCTAGTGTTG -5') in 250 µl of opti-MEM I. 1 µg of the donor DNA plasmid (Figure 2.4) was added into the same 250 µl of opti-MEM and then gently vortexed. The gRNA vectors and scramble control were taken in separate tubes and the transfection was done using the Xfect transfection reagent (Clontech, 631317) according to manufacturer's instructions. For the experiment, the cells were split and placed into 4x10 cm plates. The cells were subject to hygromycin selection (Clontech, 631309) for 10 days at a concentration of 600 µg/ml. After selection, the resistant colonies were selected using a cloning cylinder, and from that, the cultures were expanded. This was followed by a genomic DNA extraction using a DNeasy blood & tissue kit (Invitrogen, 69506), a protein extraction, freezing down the cells and storage. Each extracted genomic DNA sample was then analysed using PCR. In each sample, a targeted region was amplified using primers flanking the targeted regions (Table 2.13.). Wild type and truncated genomic fragments were resolved by gel electrophoresis and sequenced. Furthermore, an RT-PCR was performed for the quantification of copy numbers of targeting regions using primers across different targeting sites.

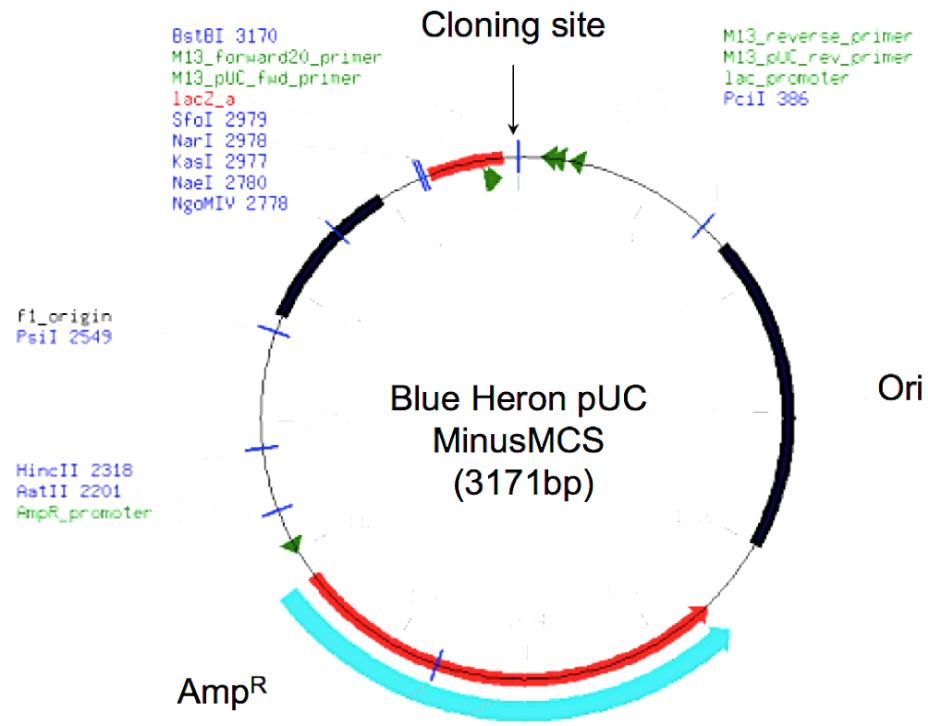

Figure 2.4: Donor vector Blu Heron pUC MinusMCS map. Adapted from BluHeron the Gene Synthesis Company.

Table 2.13. List of PCR Primers using for gene deletion experiment.

Gene	Primer	Primer Sequence	Melting Temperature (°C)	Product Size (bp)
SPO11	F (Exon 1) R (Exon 13)	5'-GACTGGATCCATGGCCTTTGCACCTAT-3' 5'-GACTGGATCCTTATATCCATCCTCCAA-3'	55	1191
	F (Exon 1) R (Exon 6)	5'-AAACGTCGAAGAACGAGGCC-3' 5'-GCA CCA CAG GTA CAA TTC AC-3'	55	625
	F (exon 3) R (Exon 12	5'-CAGAAAGATCAAAAGTGATT-3' 5'-CCC TTT TTG TCA GTG GAA TC-3'	55	728
	F: Exon (1) R: Intron (1)	5'-ATGGCCTTTGCACCTATGGG-3' 5'-GTGGTTGGTTTGGGCTTAAA-3'	58	863
	F: 5'UTR R: Exon (1)	5'-CGAGGGCTGGGATTTTAACC-3' 5'-AACGTCGAAGAACGAGGCC-3'	58	680
	F: 1693 R: 1820	5'-CGCAGCCACTCTGTAGAAA-3' 5'-ACGGGTACTCAGGAAGGAT-3'	58	100
	F: 5'UTR R: intron (1)	5'-CGAGGGCTGGGATTTTAACC-3' 5'-GTGGTTGGTTTGGGCTTAAA-3'	58	1500
	F: Hygr R: Intron (1)	5'-AGAAGTACTCGCCGATAGTG-3' 5'-GTGGTTGGTTTGGGCTTAAA-3'	58	1300
	F: 5'UTR R: Hygr	5'-CGAGGGCTGGGATTTTAACC-3' 5'-CTGAAAGCACGAGATTCTTC-3'	58	2100
	B-Actin F B-Actin R	5'-TGCTATCCCTGTACGCCTCT-3' 5'-CGTCATACTCCTGCTTGCTG-3'	58	553

2.17.1 Hygromycin selection

HCT116 was seeded into 6-well plates in McCoy's 5A medium + GLUTAMAXTM^{TM} supplemented with 10% Tet system. The cells were incubated in a humidified incubator at 37^{o}C and 5% CO_2 until the cell density reach the confluent stage. Seven doses of Hygromycin from 100 to 700 μg together with untreated cells were tested to optimise the minimum dose of Hygromycin required to kill all cells after 3-5 days. The lowest optimum dose chosen for single colony selection was 600 μg/ml.

2.17.2 Creating Standard Curves with Genomic DNA or Plasmid DNA Templates for Use in Quantitative PCR

Genomic DNA (gDNA) and plasmids containing cloned target sequences are commonly used as standards in quantitative PCR. This calculations that can be used for determining the mass of gDNA and plasmid templates that correspond to copy numbers of target nucleic acid sequences. For detail method refer to following link:
http://www6.appliedbiosystems.com/support/tutorials/pdf/quant_pcr.pdf

2.18 Use of inducible shRNA system to knockdown gene expression

This system is used for controllable and specific gene silencing with every cell being targeted. Knockdown is achieved by using a microRNA-adapted short hairpin RNA (shRNA) specifically designed by ThermoFisher to target the X region within the *SPO11* gene with pTRIPZ lentiviral inducible vectors. Since this vector is configured to be a Tet-On system, the shRNA sequence expression is regulated by the presence of doxycycline.

2.18.1. Transduction, colony selection and induction of shRNA-molecules

HCT116 cells were used to carry out the transduction. Cells were seeded in 96-well plates with 1000 cells/well. Different concentrations of the virus were then added to the cells and tested alongside different induction times. The optimum exposure time to the virus was established as 4 hours, and then finally, the virus addition was done. A polybrene of 8 μg/ml (Sigma, H9268) was added to the transduction reaction. After 72 hours, the cells were washed and incubated with a fresh medium containing 4 μg/ml puromycin. The process was repeated every 3 days. After 2-3 weeks, the resistant colonies were selected, picked and grown independently. shRNA molecules were induced by the addition of 1 μg/ml doxycycline. The efficiency of knockdown was tested by RT-PCR. Table 2.14 showes shRNA target sequences.

Table 2.14. shRNA target sequences.

shRNA	Clone ID	Target Sequence	Target area
SPO11 (1)	V3547699-227203523	5'-GTATCCCACAGTTTCTTGA-3'	EXON (9)
SPO11 (2)	V3547699-227769143	5'-ATGCACATTATTTCTATGC-3'	EXON (10)
SPO11 (3)	V3547699-228235763	5'-TGTCAGTGGAATCAAACTA-3'	EXON (12)
Negative control	VSC6571	Proprietary	

3. siRNA depletion of SPO11 on cancer cell proliferation

3.1 Introduction

One of the key features of cancer cells is their ability to divide in an uncontrollable manner. There are a number of factors that contribute to this cell division, including genetic changes, metabolic alteration and microenvironment interactions (Hirohashi *et al*., 2016). Some human meiosis-specific genes have been shown to be expressed in human cancer cells (Koslowski *et al.*, 2002). While germ-line genes can influence the regulation of meiotic cell division, their expression in human cancer cells can also reveal a potential role for CTAs in the progression of cancer (McFarlane *et al*., 2015). Thus, the activation of germ-line genes in mitotic cells might be one of the contributing factors governing genome instability in these cells, which is a hallmark of cancer (Hanaha & Weinberg, 2011).

Although the literature proposes that CTA gene expression may play a role in the formation of a tumour, the exact role that many of these proteins play in this process is yet to be fully elucidated (Whitehurst, 2014). To date the MAGE protein family has been the most extensively studied of the CTA proteins. It has been reported that MAGE proteins contribute to the survival of a cell, increase malignancy progression and promote its tumorigenic properties (Bai *et al.,* 2005; Doyle *et al*., 2010). Furthermore, in melanoma cells, siRNA depletion of some CTAs, such as GAGE, SSX4 and XAGE1, causes tumour cell viability decline (Caballero *et al.,* 2013). The effectiveness of XAGEI depletion was observed to be consistent in various cancer cells, including melanoma cell lines, lung adenocarcinoma and prostate cancer (Caballero *et al*., 2013).

Studies showing CTA gene overexpression has further supported the idea that these genes are oncogenic (Xu *et al.,* 2007; Zhou *et al.,* 2010). They indicate a relationship between tumour growth, cell proliferation and the overexpression of CTA genes in cancerous cells. Zhou *et al.* (2010) demonstrated that reducing the TSP50 levels in murine embryonal carcinoma stem cells by 70% using a shRNA technique had a negative effective on cell growth, and resulted in apoptosis of these carcinoma cells. Additionally, Maxfield *et al.* (2015) used of siRNA methodology in order to silence many CTA genes (over one hundred) which were expressed in a wide range of cancer cell lines (derived from prostate, breast, ovarian, skin, non-small cell lung cancer and bone tumours). To demonstrate many CTA genes are needed for cancer

cell viability. As previously mentioned the basic property of CTA genes is their restricted expression in human germ cell lines and malignant cells, with little or no expression in healthy somatic cells (Cheng *et al.,* 2011; Hofmann *et al.,* 2008; Simpson *et al.,* 2005; Whitehurst *et al*., 2014). Some CTAs are normally involved in spermatogenesis and in the testes, and different stages of spermatogenesis can be identified by observing the expression patterns of these CTAs. For example, SPO11 functions during early reduction division in meiosis and NY-ESO-1 or MAGE-A can be detected in spermatogonia having mitotic clonal prevalence (Simpson *et al.,* 2005).

In normal *SPO11* is a meiosis-specific gene, and the SPO11 protein initiates meiotic recombination by cleavage of double-strand DNA (see Section 1.2.3 in Chapter 1), which helps, mediate chromosome alignment during meiotic homologous synapsis (Lam & Keeney, 2014). The transcripts for mouse *Spo11* and human *SPO11* genes are only normally present in adult testes, but not in other somatic tissues (Koslowski *et al.,* 2002)). However, RT-PCR and northern blot techniques in addition to data-mining the NCBI GenBank for expression patterns in tumorous and somatic tissues have previously identified *SPO11* as a potential CTA gene (Koslowski *et al.,* 2002). Koslowski et al. Showed that the *SPO11* gene was not expressed in various non-testicular normal tissues, including liver, lung and ovary, but it was expressed in one melanoma cell line, two cervical cancer cell lines and two lung melanoma cell lines. Additionally, *SPO11* was found to be expressed in malignant cell lines of the prostate, colon and ovary in humans (Koslowski *et al.,* 2002).

It is hypothesized that the *SPO11* gene may play a critical role in controlling the genome stability of cancer cells and that it is necessary for stimulating and maintaining the oncogenic processes. The aim of the work described in this chapter was to assess SPO11 protein levels in both normal and cancer cells in order to confirm *SPO11* as a CTA gene. In addition, the study was investigated what happens to colorectal cancer cells when a level of SPO11 was reduced to address the question of whether SPO11 is required for cancer cell proliferation.

3.2 Results

3.2.1 Protein levels of SPO11 in normal tissue and cancer cells

The expression of the *SPO11* gene in the testes under normal conditions has been shown using data from a northern blot analysis (Romanienko & Camerini-Otero, 1999). *SPO11* was also identified as a possible CTA gene in normal and cancer cells on the basis of the results of a RT-PCR (Koslowski *et al.,* 2002). Here the aim to assess whether SPO11 is a CTA by analysing protein distribution in normal and cancer cells. This study used the anti-SPO11 antibody ab81695; validation of this antibody was achieved using three different techniques; SPO11 depletion by siRNA in this chapter (Section 3.2.4), gene deletion by the CRISPR system (see Chapter 5) and the production of recombinant SPO11 in *E. coli* (see Chapter 6).

Whole cell extract (WCE) were generated from 17 different cancer cell lines and 14 normal tissues, including the testis to detect the *SPO11* gene expretion (this was done collaboratively with Dr. F. Althobaiti and Dr. I. Aldeailej). For a CTA control, anti-MAGE-C1 antibodies were used, while anti-GAPDH was used as a loading control. Using the anti-SPO11 antibody, a band of 44 kDa was observed in whole cell extracts, which is consistent with the predicted size for SPO11β. However, SPO11 was not detectable in the normal tissues, except for the spinal cord for which there was a smear that was a smaller size than expected for SPO11β or α (Figure 3.1). Western blots of cancer cell lines, including lung, liver, colon, breast, ovary, astrocytoma, embryonal carcinoma and melanoma, had a band that showed the correct size for SPO11 β at high levels for all cell lines (Figure 3.2).

3.2.2 Subcellular localisation of SPO11 protein in cancer cell lines

Western blot was used to determine the localisation of the SPO11 protein in proliferating cancer cells. The fractionation of cells into cytoplasm and nuclear extracts was carried out for the cell lines NTERA2, HCT116, G361, A2780, LoVo, PE014 and TO14 (this was done collaboratively with Dr. I. Aldeailej). SPO11 protein was present at low levels in the cytoplasm, but was found at high levels in the nucleus for almost all cells (Figure 3.3). In HCT116 cells, no cytoplasmic SPO11 was detected, but a strong nuclear band was observed.

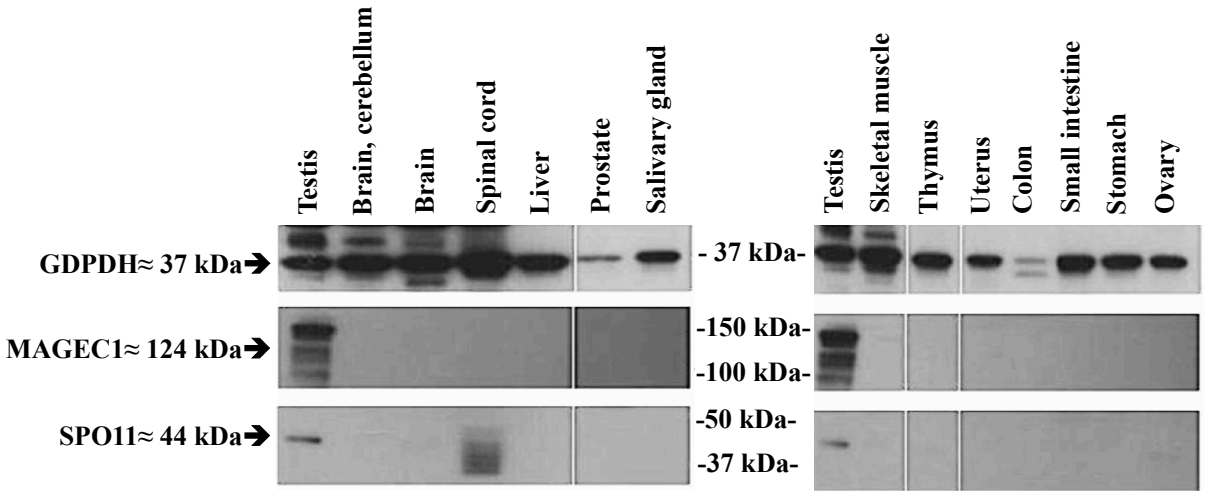

Figure 3.1: Western blot analysis of SPO11 in normal tissues(Testis, Brain cerebellum, Brain, Spinal cord, Liver, Prostate, Salivary gland, Skeletal muscle, Thymus, Uterus, Small intestine, Stomach, Ovary). Anti-MAGE-C1 was used as a CTA control and anti-GAPDH was used as a control for loading. Anti-SPO11 indicated a band consistent with SPO11β only in the testis extract. A low molecular weight band is seen in spinal cord extract.

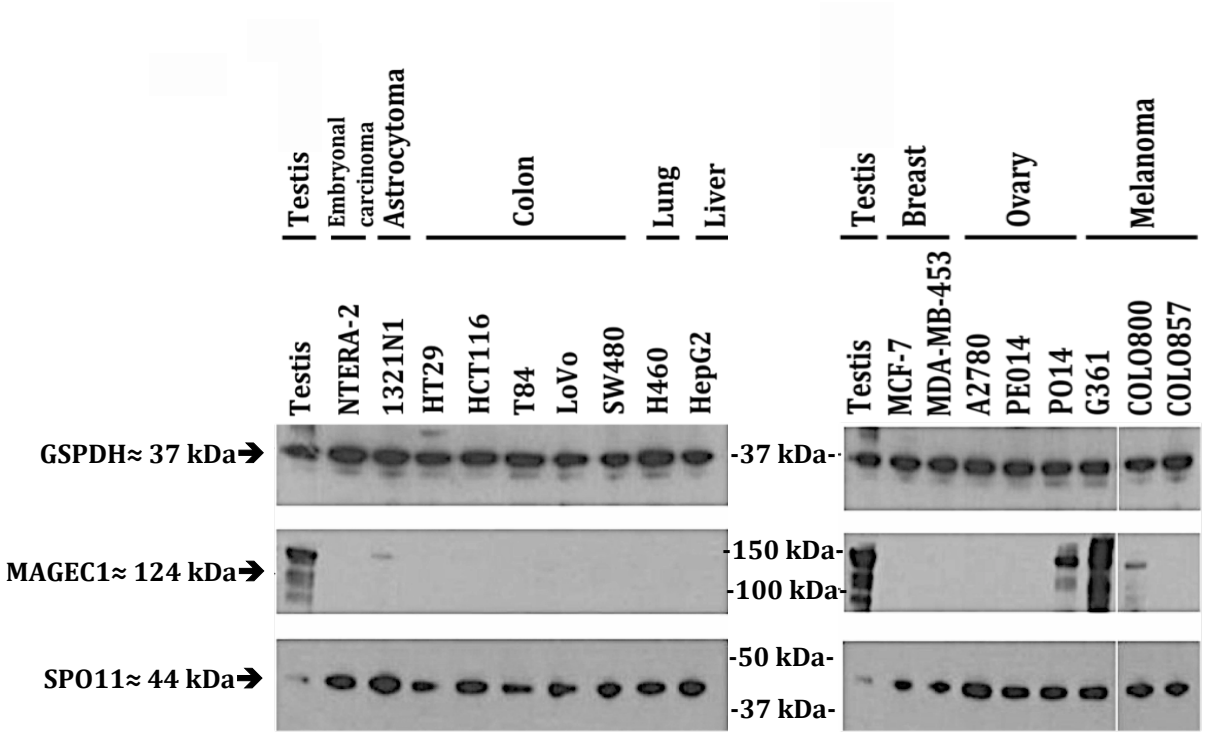

Figure 3.2: Western blot analysis of SPO11 in cancer cell lines(Embryonal carcinoma, Astrocytoma, colon, Lung, liver, Breast, Ovary, Melanoma). Anti-GAPDH was used as a control loading and MAGEC1 was used as a CTA control, present in melanoma and one of the ovarian cancer cell lines; A band consistent with SPO11β is present in all cell lines.

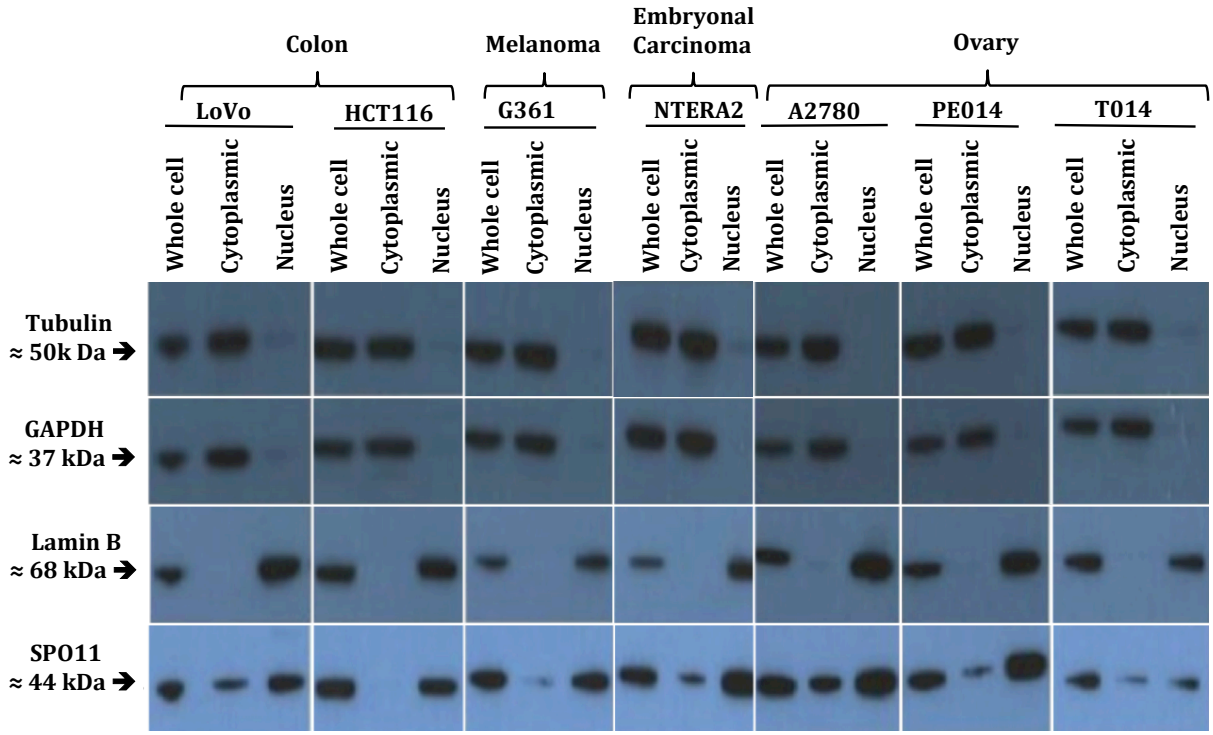

Figure 3.3: Western blots analysis of the intracellular localisation of SPO11 in different cell lines (LoVo, HCT116, Melanoma, Embryonal Carcinoma, Ovary (PE014, A2780 and T014). Anti-Tubulin and anti-Lamin B antibodies served as positive controls for checking the efficiency of the fractionation; anti-GAPDH was used as a loading control. A band consistent with SPO11β was present in the nucleus of all cells, and lower levels were observed in the cytoplasm in most cells, except HCT116 where SPO11 was only detected in the nucleus extract.

3.2.3 Immunofluorescence analysis of SPO11 in SW480 cells

To confirm the western blot analysis, and to identify any sub-nuclear structures that SPO11 might localise to, immunofluorescence (IF) analysis was carried out on SW480 cells. The SPO11 staining results showed that SPO11 is localised in the nucleus as discrete foci (Figures 3.4 and 3.5). A dispersed SPO11 nuclear localisation is seen in interphase cells (whilst this was weak in these figures colleagues in the team observed extensive nuclear stain). As cells progress in to mitosis SPO11 is seen as foci associated with areas surrounding the DNA (during metaphase), while appearing in the interchromosomal space between segregating chromosomes in anaphase. A preliminary literature search for proteins involved in segregating entangle chromosomes, that might localize to this inter-chromosome space in anaphase flagged up the Bloom (BLM) protein. BLM plays an important role in controlling homologous recombination (HR), repairing DSBs and dissolving double Holliday junctions (dHJs) (Kikuchi *et al.,* 2009; Wu & Hickson, 2003). BLM functions to dissolve chromosome catenations in conjunction with a topoisomerase activity (topoisomerase IIIα) (Leonard *et al.,* 2000). As SPO11 is a topoisomerase-like protein, and the fact that SPO11 localized to the interchromosomal space in anaphase led to the hypothesise that SPO11 could potentially act in conjunction with BLM in cancer cells, possibly in a topoisomerase-like fashion. Therefore, the SW480 cells were co-stained with antibodies against SPO11 and BLM. This revealed that SPO11 and BLM had and overlapping distribution pattern, and in fact appear to co-localise between segregating chromosomes in anaphase (Figures 3.4). Since SPO11 and BLM co-localize it could propose that SPO11 is co-operating with BLM to help disentangle abnormal chromosomal connections and help the cancer cells continue to divide. From this result, the hypothesis was that SPO11 depletion using siRNA might inhibit chromosomal segregation and prevent cell division (see Section 3.2.4).

During the SPO11/BLM co-localization studies, two strong SPO11-specific stained foci were observed where the centrosome was expected to localise, which did not co-localize with BLM (Figure 3.4). Based on this observation, SW480 cells were co-localized with SPO11 and various centrosome specific antibodies; Pericentrin (PCNT) and Plk1-interacting checkpoint helicase (PITCH), and SPO11/PCNT/Plk-1 co-localization is observed at the centrosomes (Figures 3.5 and 3.6).

(a)

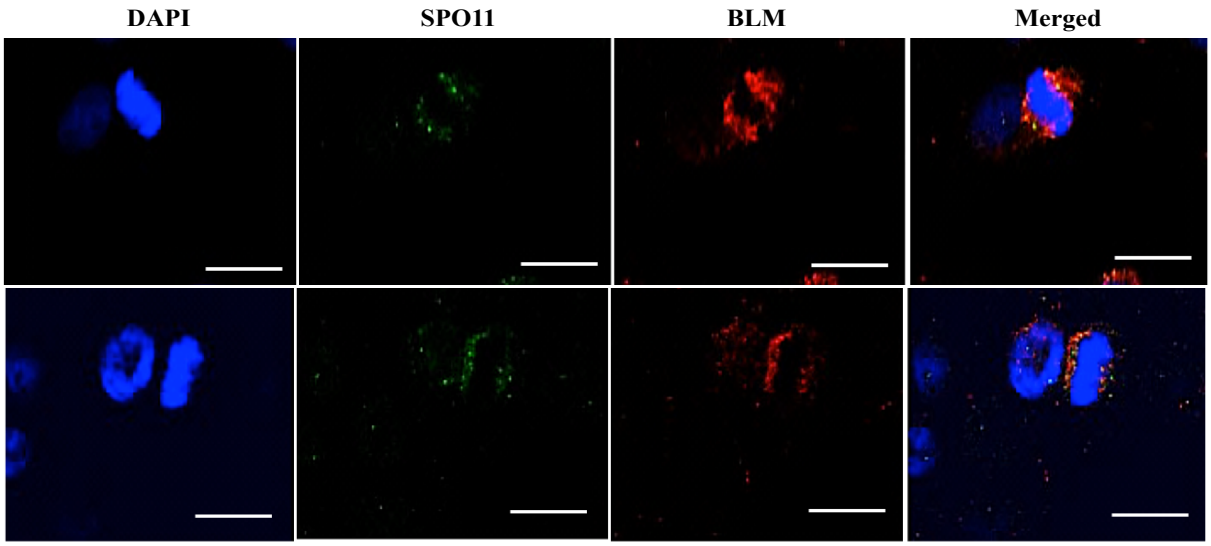

(b)

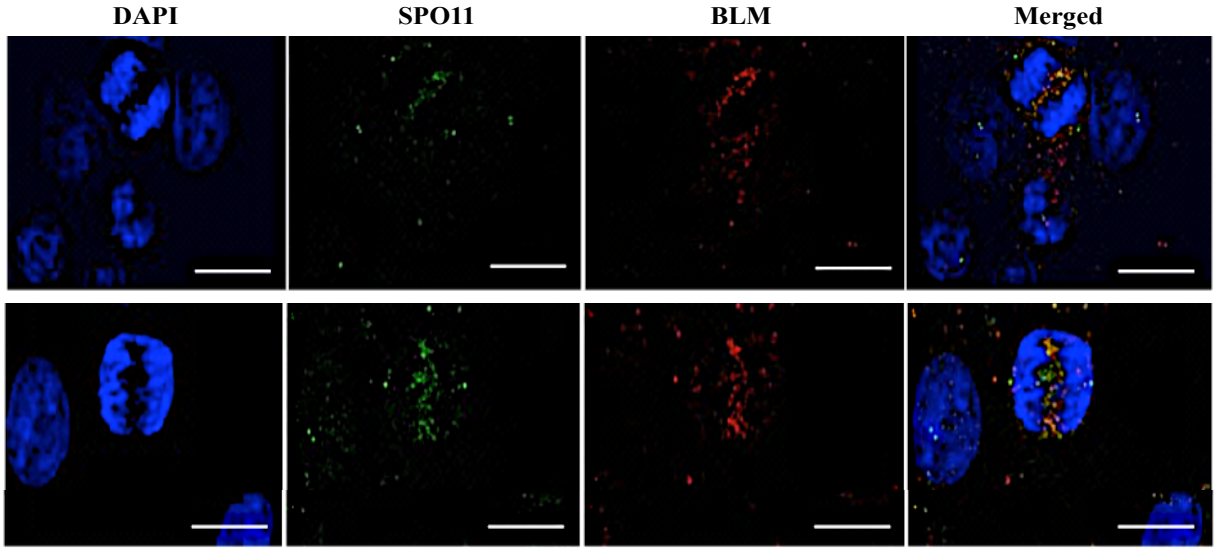

Figure 3.4: IF staining analysis of SW480 cells staining with anti-SPO11 and anti-BLM antibodies. IF analysis of fixed SW480 cells enabled visualisation of proteins during metaphase and anaphase. The anti-SPO11 antibody is stained green. The anti-Bloom is stained red. The DNA is stained with DAPI blue. A Zeiss LSM 710 confocal microscope with a 40 x oil objective was used to obtain the images. Scale bars represent 20 μm. (a) and (b) represent images taken in distinct experiments.

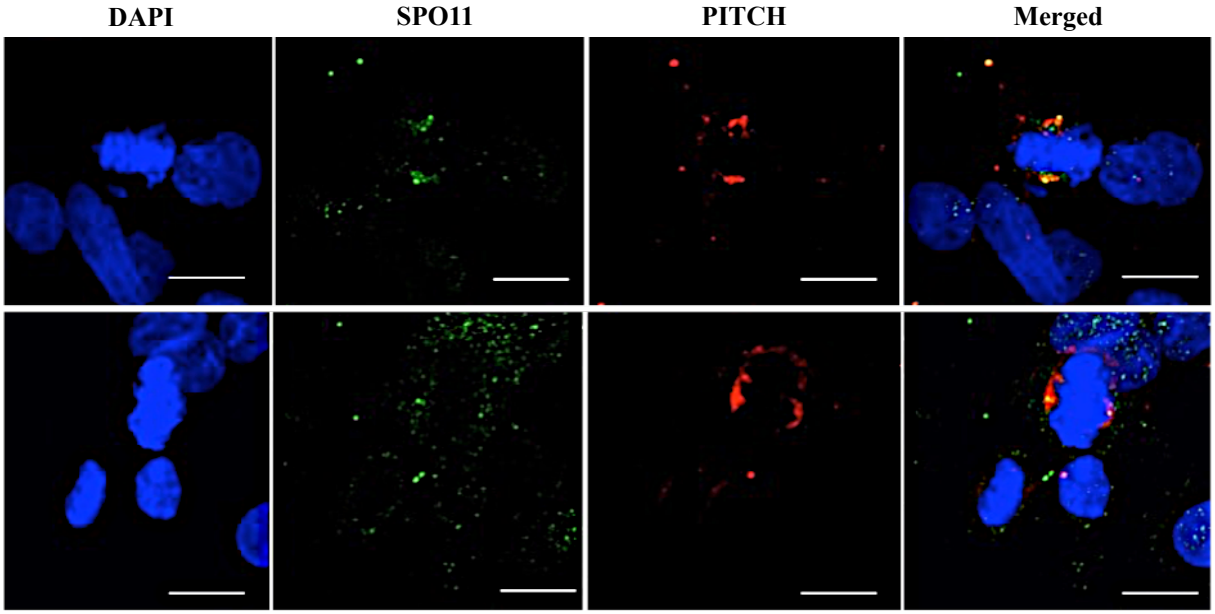

Figure 3.5: IF staining analysis of SW480 cells stained with anti-SPO11 and anti-PITCH antibodies. IF analysis of fixed SW480 cells enabled visualisation of proteins during anaphase. The anti-SPO11 antibody is stained green. The anti-PITCH is stained red. The DNA is stained with DAPI blue. A Zeiss LSM 710 confocal microscope with a 40 x oil objective was used to obtain the images. Scale bars represent 20 μm.

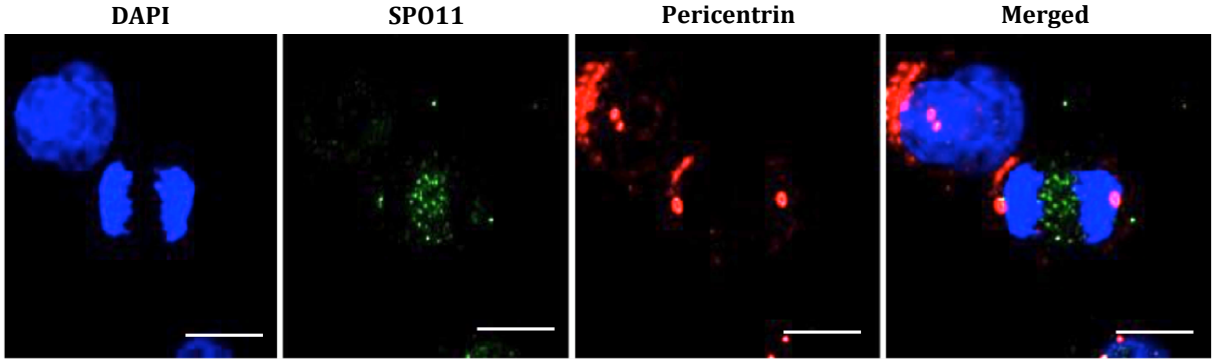

Figure 3.6: IF staining analysis of SW480 cells stained with anti-SPO11 and anti- pericentrin antibodies. IF analysis of fixed SW480 cells enabled visualisation of proteins during anaphase. The anti-SPO11 antibody is stained green. The anti- pericentrin is stained red. The DNA is stained with DAPI blue. A Zeiss LSM 710 confocal microscope with a 40 x oil objective was used to obtain the images. Scale bars represent 20 μm.

3.2.4 SPO11 controls the mitotic proliferative potential of cancer cells

To understand whether SPO11 can function in a non-meiotic context in cancer cells, siRNA was employed to deplete the *SPO11* mRNA. The objective of the knockdown technique is to analyse the impact that a decrease in a particular protein has on any cell line. This technique also helps in the validation process of the antibody used in the western blots and immunofluorescence (IF) techniques. Two primary siRNAs were utilised for this purpose: siRNA-2 and siRNA-4. This work was conducted in close collaboration with a lab colleague (Dr. F. Althobaiti) and all analyses were consistent. SW480 cancer cell line was used in this study and also a lab colleague used multiple other cell lines, which showed similar result, so the work presents here is further validated (unshown data generated by Dr. F. Althobaiti and Dr. Ellen Vernon).

Many attempts to reduce the level of SPO11 protein in various cancer cells using different concentrations of siRNA, were performed as well as different numbers of "hits" (number of times the cells are transfected with that particular siRNA), but all these conditions appeared to have no effect on the intensity of the SPO11 44 kDa band on a western blot (not shown). Therefore, it could be proposed that the siRNAs used in this study did not specifically target SPO11, or the anti-SPO11 antibody was not specific.

With this in mind it was decided to investigate these points further. Firstly, the study was used different cell seeding density for transfection with various siRNAs to determine whether this had an effect. At this point it was observed that treatment with SPO11-specific siRNA led to the detachment of many cells, and a large number of floating cells were obtained. Protein extracts were previously taken from the cells that were still attached (not the floating cells). Thus, it was hypothesise that the depletion of SPO11 using specific siRNA led to the detachment of the cells and the remaining attached cells retained SPO11 if they were unaffected by the siRNA treatment. This hypothesis was investigated further here. Different numbers of SW480 cells (25×10^3, 50×10^3, 75×10^3 and 100×10^3 cells per well) were placed in cultured wells before transfection with SPO11 siRNA. After 24 hours post-transfection, 7 hits of siRNA-2 and siRNA-4 were applied to knockdown SPO11. Attached and floating cells were collected separately.

The SPO11 protein level was assessed by western blot using the anti-SPO11 antibody and in these experiments the level of SPO11 protein was measurably decreased in attached cells when low cell seeding concentrations were used, especially at 25 x 10^3 cells per well (Figure 3.7). For the floating cells, significant SPO11 knockdown was observed with all seeding densities of SW480 cells (Figure 3.7).

Dead floating cells were generated by hydroxyurea (HU) treatment, in order to determine whether all detached cells (siRNA targeted or not) were depleted of SPO11. These HU treated floating cells were found to contain SPO11 protein (Figure 3.8), which indicated that detachment alone was not reducing SPO11 protein level; similar data were obtained by a colleague used distinct siRNAs.

To gain insight into whether SPO11 is requiring for cancer cell survival a cell proliferation analysis was carried out on SW480 treated with SPO11 siRNA. The cells were seeded in 6-well plates with 25 x 10^3 per well, after 24 hours, the cells were transfected every day for 8 days with the either siRNA-2 or siRNA-4; a non-interfering siRNA served as the negative control. The cells were harvested during 8 days and then counted and trypan blue was used to stain the membranes to count dead cells. The counting of the cells was done using a haemocytometer under an optical microscope. The cell count curves represent the total number of cells (Figure 3.9). The results indicate that the number of surviving cells transfected with siRNA-2 and siRNA-4 is less than the number of surviving cells in the untreated group and the group treated with non-interfering siRNA. Images taken of the cell line before harvesting are shown in (Figure 3.10) confirmed the effect of SPO11 decrease on cell proliferation, similar results were observed by colleague uses distinct siRNAs.

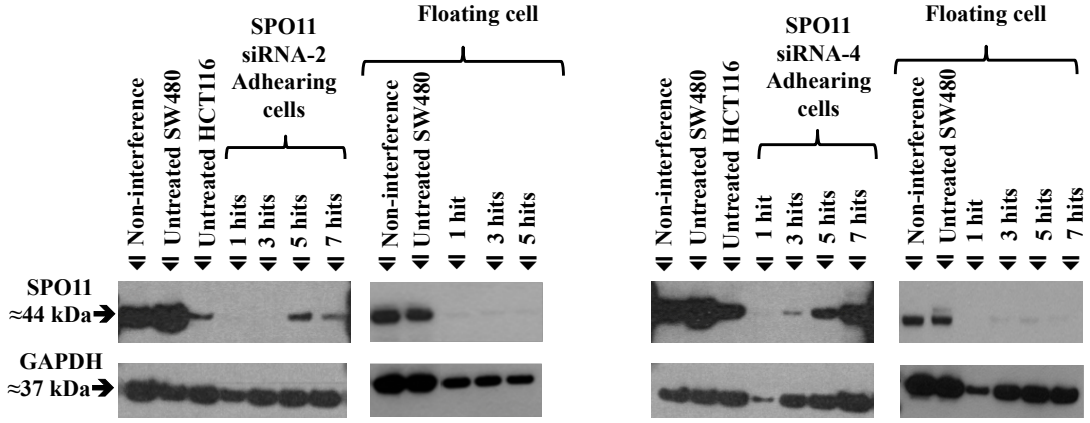

Figure 3.7 Western blot analysis showing siRNA SPO11 knockdown in attached and floating SW480 cells using siRNA-2 and siRNA-4. Untreated cells were positive controls, and cells treated with non-interfering siRNA were negative controls. GAPDH protein levels were used as the loading control (bottom). The experiment was performed on (25 x 10^3 cells) SW480 cells using HiPerFect transfection reagent (7 hits). (A) Knockdown of SPO11 was detected in attached SW480 cells compared with the negative or positive controls. Also, successful SPO11 knockdown was seen and full depletion of SPO11 was found when the protein was collected from the floating cells with the use of siRNA-2 and siRNA-4. (n=2) for the total number of cells.

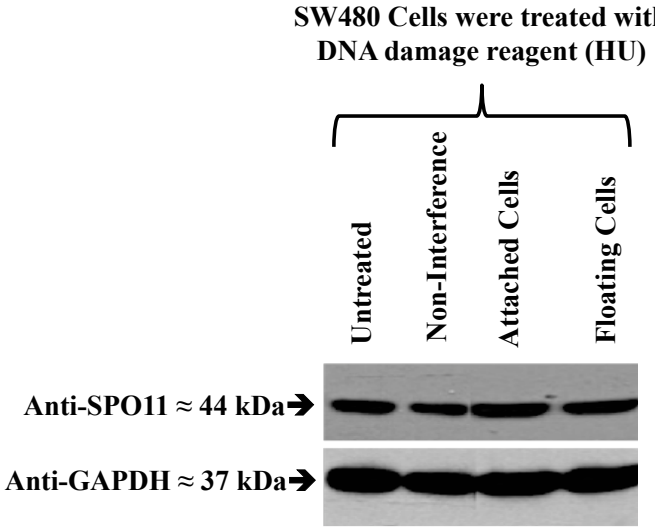

Figure 3.8 Western blot analysis showing Floating cells with hydroxyurea (HU). Floating cells were induced with hydroxyurea (HU) reagent and the level of SPO11 was compared with that of the attached cells (Dr. F. Althobaiti assisted with these western blots).

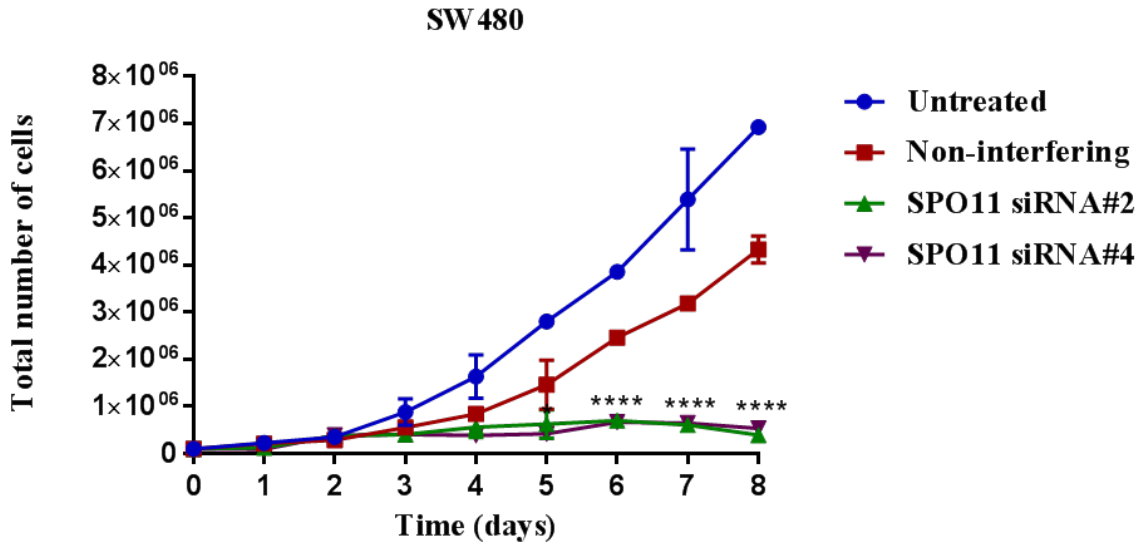

Figure 3.9. SPO11 is required for the proliferation of SW480 cells. The depletion of SPO11 mRNA caused by siRNA inhibits SW480 cell proliferation. Untreated SW480 cells served as positive controls and cells treated with non-interfering siRNA served as negative controls for SPO11 knockdown. The error bars represent the standard error for the total number of cells, as calculated for three repeats (****P < 0.0001). (n=2) for the total number of cells.

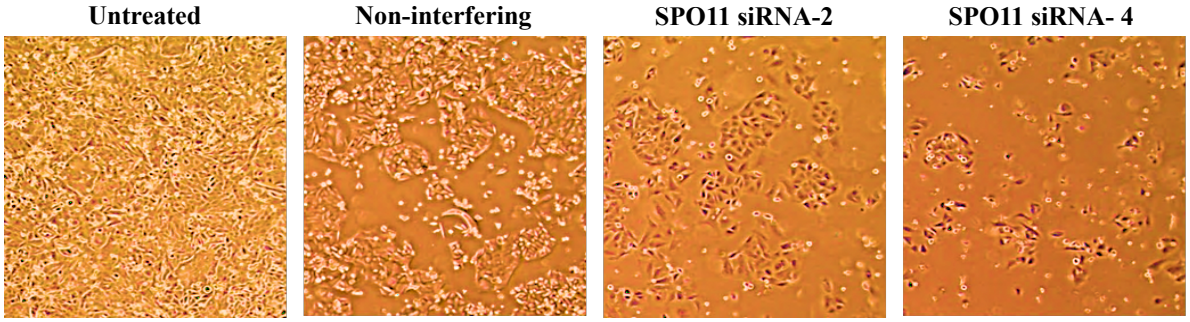

Figure 3.10. The proliferation of SW480 cells. Cell images taken before trypsinization to assess the cell density on day 8 using an Eclipse-inverted microscope (5 x lens). (n=2) for the total number of cells.

3.2.5 SPO11 knockdown does not induce apoptosis

Since reduced number of cells and reduced protein level were observed following SPO11 knockdown, it was necessary to examine whether cells undergo apoptosis in response to SPO11 depletion. Apoptosis is programmed cell death that is a controlled and regulated process that plays significant role in the healthy development of organisms. A number of changes are initiated in the cells undergoing apoptosis, including caspase activation. By evaluating the levels of these caspases, the degree of apoptosis can be assessed (Chudhury *et al.,* 2012). In this study, the assessment of the caspase-3 protein levels was done after SPO11 depletion using different siRNA. GAPDH protein was used as a control for testing the quality of whole cell extract loading. Assessment of the response to apoptosis was done through caspase-3 cleavage in the SW480 attached cells (Figure 3.11). No cleavage was identified after the SPO11 knockdown from siRNA-1, siRNA-2 and siRNA-4, so no measurable caspase dependent apoptosis was observed, also with untreated and non-interference cells. Uncleaved caspase bands were present in all cells.

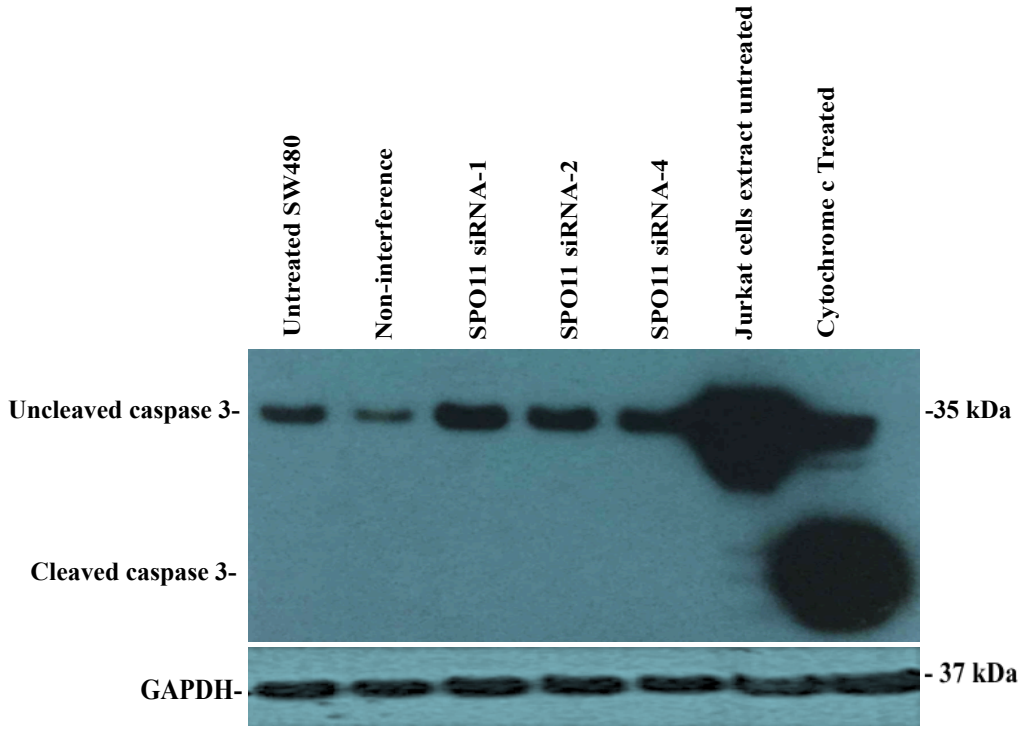

Figure 3.11: Western blot detection of cleaved caspase-3. Analysis of extracts from Jurkat cells untreated (negative controls); SW480 cells treated with siRNA-1, siRNA-2 and siRNA-4. GAPDH protein levels were used as a loading control (bottom) and Jurkat cells extract cytochrome c was used as a positive control. No apoptosis was observed as determined by the detection of cleaved caspase-3.

3.2.6 Colonosphere culture

Tumours are a mixture of different cell types. Because they are heterogeneous in nature, the cells are known to have different functions (reviewed in Meacham & Morrison, 2013). CSCs give rise to tumours, which are phenotypically heterogeneous population cells that called the tumour microenviroment (TME). These cells supported by an extracellular matrix (ECM) involve signaling molecules as cytokines, hormones and growth factors (Raggi *et al.,* 2015). If the cancer stem cell (CSC) model is followed, tumours are comprised of a subpopulation of cells resembling stem-like cells, which are capable of undergoing proliferation and differentiation into heterogeneous lineages of cancer cells (reviewed in Clevers, 2011; Magee *et al.,* 2012). CSCs have been detected in a wide range of tumours (O'Brien *et al.,* 2007; Ricci-Vitiani *et al*., 2007). The presence of CSCs might lead to the reappearance of tumors following radiotherapy or chemotherapy (Alison *et al.*, 2011; Beck & Blanpain, 2013; Stange & Clevers, 2013). The non-adherent sphere assay is a technique used for isolating and enriching CSCs. In this assay, the ability of the cells to undergo growth proliferation as floating spheres is evaluated under non-adherent and non-differentiating conditions (Sukach & Ivanov, 2007). There are a number of common properties between CSCs and sphere-forming cells: both express high level of stemness markers, both can self-renew, both have a strong resistance to radiation and chemotherapy compared with cells grown as adherent cell lines (Zhong *et al*., 2010). These properties make the assay useful for characterising CSCs and calculating their frequency (Kanwar *et al.,* 2010). Moreover, the cells that are cultured under conditions free of serum resemble the original tumours rather than the traditional cell lines cultured in serum (Lee *et al.,* 2016).

The SPO11-positive HCT 116 and SW480 cell lines were used to derive colonospheres. Colonospheres are enriched for cancer stem-like cells. The culture of the cells was first done in a growth medium in which the Fetal Bovine Serum (FBS) served as a monolayer of flat polygonal epithelial-like cells, and then in a stem cell medium (SCM) that was supplemented with growth factors, Basic fibroblast growth factor (bFGF) and Epidermal growth factor (EGF). The cells were found to retain a round morphology under serum-free culture conditions. The cells also remained unattached to the surface of the culture dishes and formed spheres after 6 days (Figure 3.12).

The colonospheres demonstrated the capacity for long-term self-renewal and could, therefore, generate secondary colonies. Recording the cell passage numbers was performed as follows: the first number represented the number of passages of the parental culture in the DMEM/FBS medium, while the second number represented the number of passages in the SCM. Western blot analysis was useful for confirming that both the parental cells and the spheres derived from this cell line produced a detectable level of SPO11 protein and HCT116 and SW480 cells grown as monolayers or spheres had the same levels of SPO11 (Figure 3.13).

3.2.7 Self-renewal potential of HCT116 colonosphere cell transfected with SPO11 siRNA-2 and siRNA-4

An extreme limiting dilution assay (ELDA) (Hu & Smyth, 2009) was undertaken to determine the ability of sphere derived HCT116 cells to undergo self- renewal and eventually form spheres under conditions of siRNA-induced SPO11 depletion or in the presence of SPO11.
HCT116 cells passage P13.20 was used for the analysis. The cells were cultured as clonospheres colonies then were seeded in dilutions of 10, 100 and 1000 cells per well using 96-well plates. After 24 hours, the cells treated with HiPerFect Transfection reagent and the non-interfering which used as a negative control for SPO11 siRNA2 and 4. Also, cells images were taken after 10 days using a light microscope to observed any changing in cell self-renewal and proliferation.

The renewal of HCT116 sphere cells treated with siRNA-2 and 4 were significantly reduced compared with the negative control (Figure 3.14/3.15 A; conducted collaboratively with Dr. F. Althobaiti). When comparing untreated HCT116 sphere cells to non-interfering or HiPerFect treated cells, no significant difference was detected ($P > 0.05$) in the self-renewal frequency. Conversely, significant differences were detected between the non-interfering and the SPO11siRNA2+4 transfected cells ($P < 0.05$) (Figure 3.15 A, B). The number of HCT116 sphere cells that survived after SPO11 depletion was much lower compared with the negative control and untreated (Figure 3.14 B).

3.2.8 Knockdown of SPO11 results in quiescent-like state

According to the ELDA assay, few spheres were formed after the SPO11 knockdown. This was the reason why it was important to determine whether senescence or apoptosis occurred. No apoptotic response was observed as measured by the induction of caspase-3 cleavage (Figure 3.16). The single cells plated in the proliferation assay remained present, and were morphologically unchanged throughout the experiment (Figure 3.17).

The cells did not undergo senescence following SPO11 knockdown as assessed by lysosomal senescence associated β-galactosidase activity (Figure 3.18). The inhibition of the proliferation of the cells after SPO11 knockdown was reversible. After SPO11 knockdown, single cells were transferred to fresh SCM; the cells showed signs of recovery and spheres were formed (Figure 3.19).

The results of a western blot analysis on the SPO11 protein levels in SW480 colonosphere cells that were transfected with different siRNAs demonstrated that the strongest reductions in SPO11 protein were achieved using siRNA-1, siRNA-4 and siRNA-6 compared with GAPDH (Figure 3.20). In addition, cells grown as spheres that transfected with siRNA were assessed by RT-qPCR, Results were normalised to a combination of two endogenous reference genes (*GAPDH*, and *ACTB*) the RT-qPCR analysis indicated that the SW480 cells that grew as spheres after transfection with siRNA-2, and siRNA-6 showed a reduced level of *SPO11* expression when compared with the negative control (Figure 3.21).

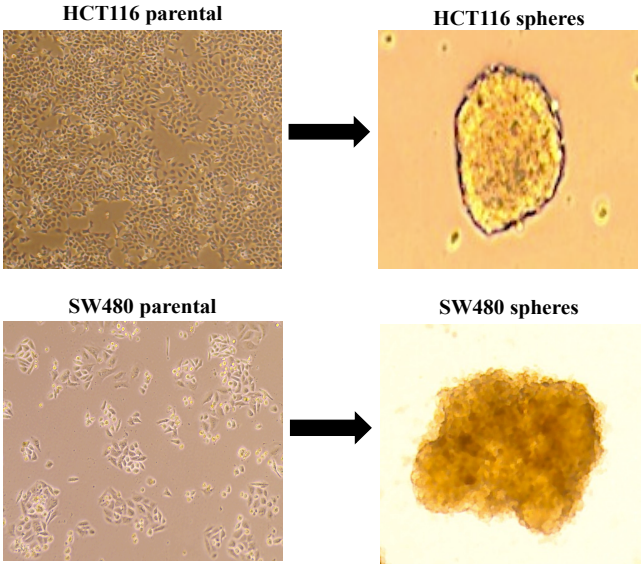

Figure 3.12.Characterization of colonospheres. The cells formed spheres after 6 days also remained unattached to the surface of the culture dishes

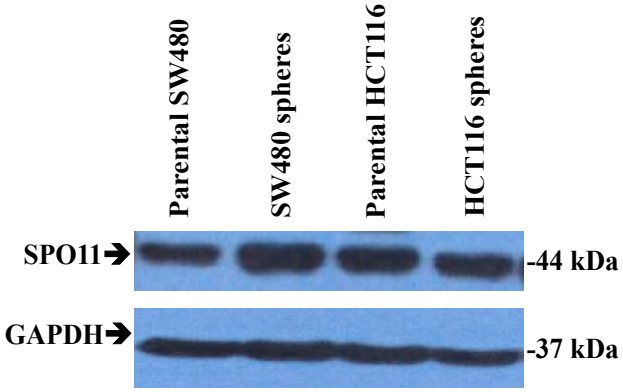

Figure 3.13: Western blot analysis of SPO11 in colonospheres. Western blot analysis derived from SW480 and HCT116 cells and their respective parental cells. Loading was controlled by GAPDH.

Table 3.1: The colonosphere HCT116 cells -forming frequency in each treatment conditions.

Number of cells per well	Number of wells plated	**Number of Wells Showing Colonospheres (HCT116 cells)**				
		SPO11 siRNA-2 transfected cells	SPO11 siRNA-4 transfected cells	Untreated cells	Negative control siRNA transfected cells	**HiPerFect-only treated cells**
Ultra-low Attachment Plate, HCT116 Cells, Passage Number P13.20						
1000	12	11	12	12	12	**12**
100	12	7	8	11	11	**11**
10	12	5	6	12	11	**11**
Sphere-forming frequency (95% CI)		1/157 1/33–1/75)	1/55 (1/105-1/29)	1/13 (1/38–1/6)	1/14 (1/32–1/7)	**1/14 (1/32–1/7)**
P value*	**4.15e-12**					

(B)

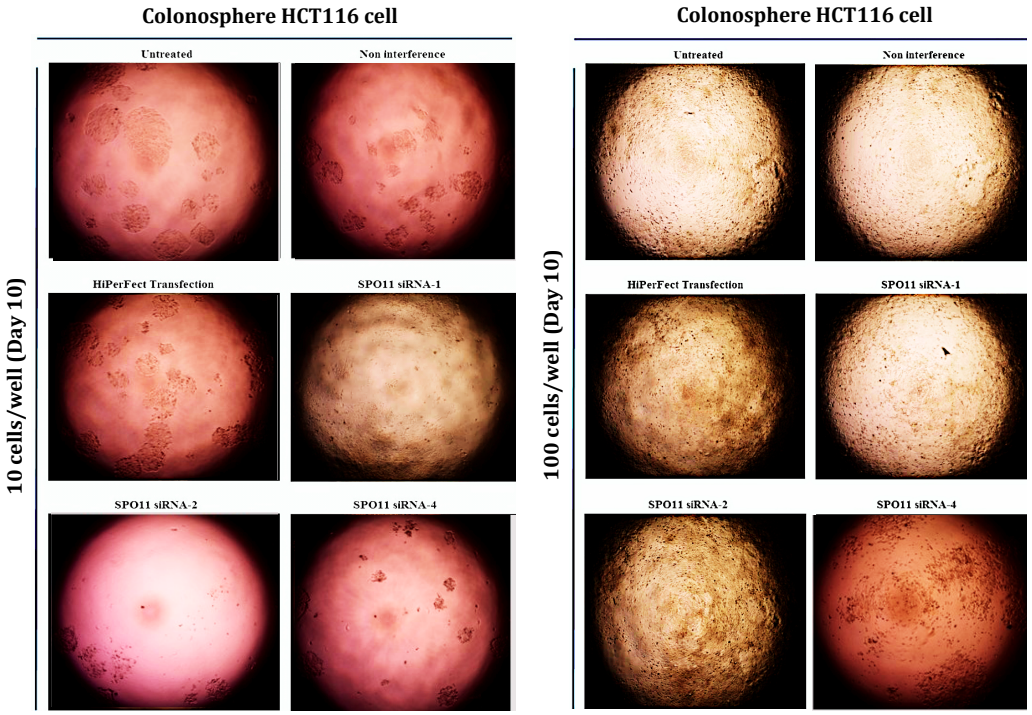

Figure 3. 14 Effects of SPO11 depletion on HCT116 cell self-renewal as determined by an extreme limiting dilution analysis. (A) ELDA assay showing the influence of SPO11 knockdown on the proliferation/ self-renewal (colony formaing ability) of HCT116 cells. cells transfected with siRNA 2 and 4 for 10 days with 100, 10 cells/ml seeded respectively. Non-interfering and HiPerFect transection served as negative control whereas untreated cells used as positive control. (B) The growth of cells transfected with SPO11 siRNA 2 and 4 is affected compared with the growth of untreated and non-interfering cells.

(A)

HCT116 cells / SPO11 siRNA 2 and 4				
Group1	Group 2	Chisq	DF	Pr(>Chisq)
Negative control	Untreated	0.0885	1	0.766
Negative control	SPO11 siRNA2	33.4	1	7.46e-09
Negative control	SPO11 siRNA4	10.4	1	0.00124
Untreated	SPO11 siRNA2	37.4	1	9.7e-10
Untreated	SPO11 siRNA4	12.6	1	0.000379 ←
SPO11 siRNA2	SPO11 siRNA4	6.54	1	0.0105 ←

(B)

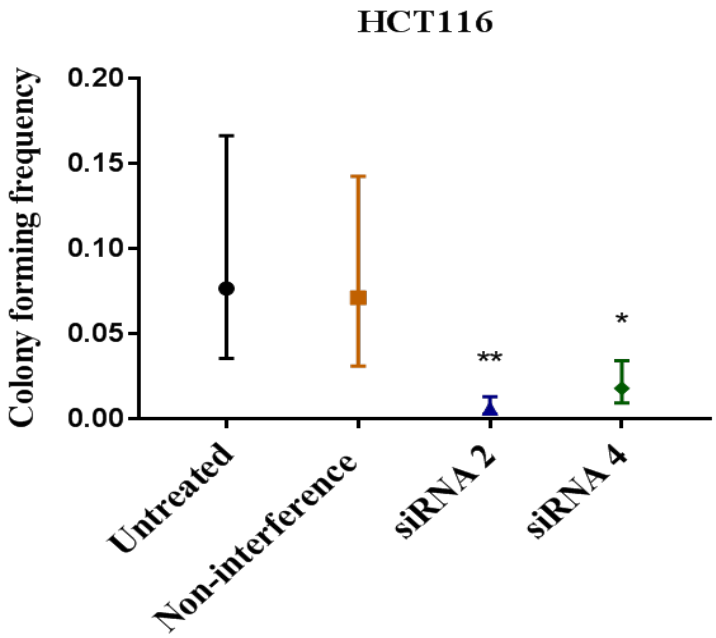

Figure 3.15 Effect of SPO11 self- renewal on HCT116 cells as determined by an extreme limiting dilution analysis. (A) Comparison of cells transfected with SPO11 siRNA 2 and 4 to untreated and non-interfering. Chisq indicates Chi-Square. DF refers to Degrees of Freedom. Pr(>Chisq) points probability value. Pr(>Chisq) < 0.05 means the differences are significant. The results show that transfected HCT116 cells with siRNA 2 and 4 result in significant affecte of self-renewal (B) Influence of siRNA 2 (**: $p<0.01$) and siRNA 4 (*: $p<0.01$) knockdown on HCT116 cells compared to non-interfering cells, which were used as a negative control.

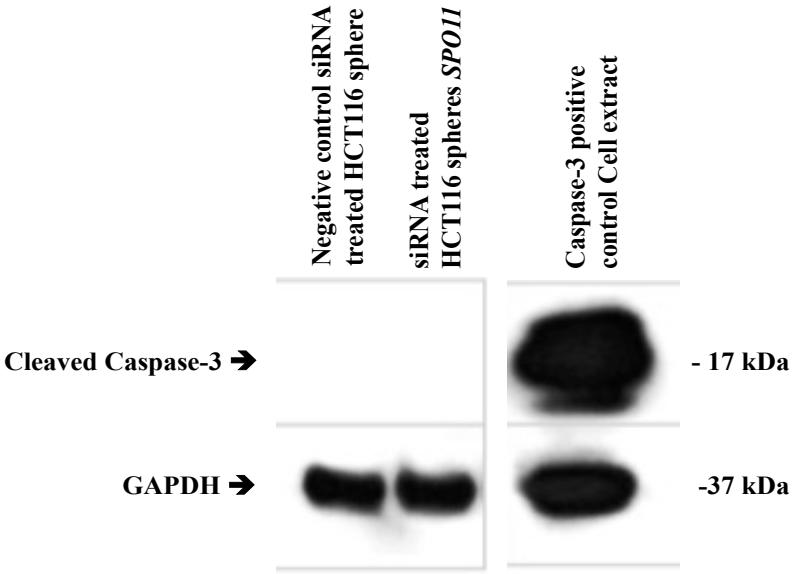

Figure 3.16: Western blot detection of cleaved caspase-3. No apoptosis was observed as determined by the detection of cleaved caspase-3. Cytochrome c-treated Jurkat cell extract was taken as a positive control.

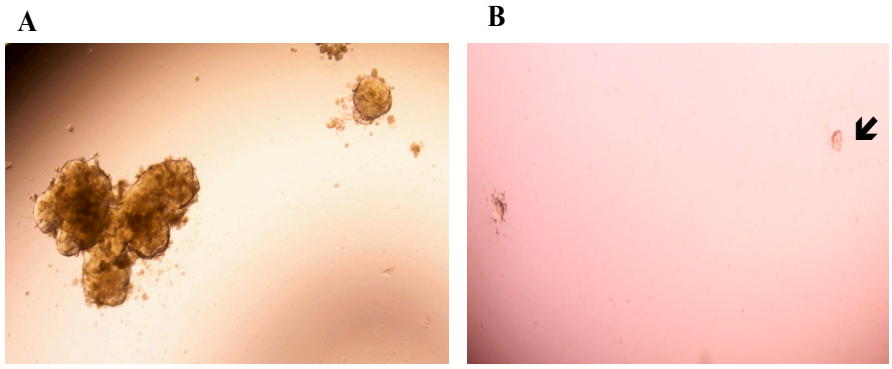

Figure 3.17. Clonospheres morphological after 10 days treatment. (A) a sphere formed from single HCT116 cells after 10 days treatment with non-interfering siRNA (control condition). (B) Single HCT116 cells that remain in culture after 10 days treatment with siRNA-4 the arrow points to a single cell (×10 magnification).

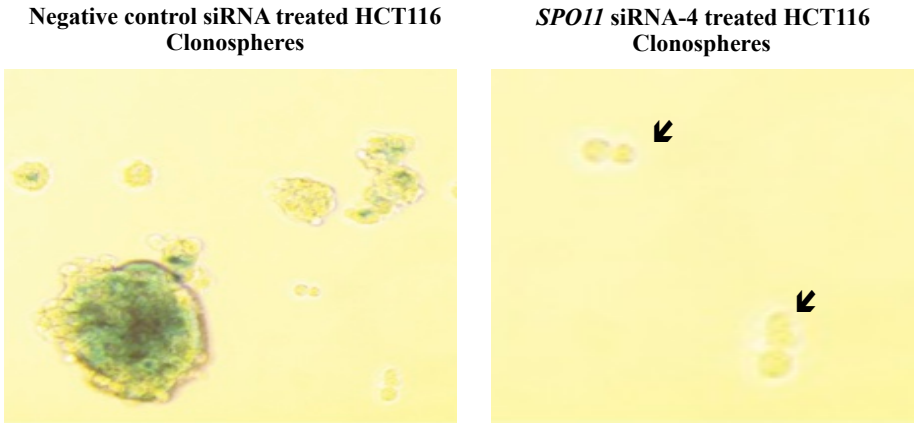

Figure 3.18 Senescence β-galactosidase staining of HCT116 colonospheres. There was a strong positive staining for lysosomal senescence-associated β-galactosidase activity in the central area of large spheres. However, the peripheral cell layer did not stain, nor did small spheres (the arrow show the small spheres did not stain). Moreover, no staining was detected in the HCT116 sphere precursors after the SPO11 knockdown.

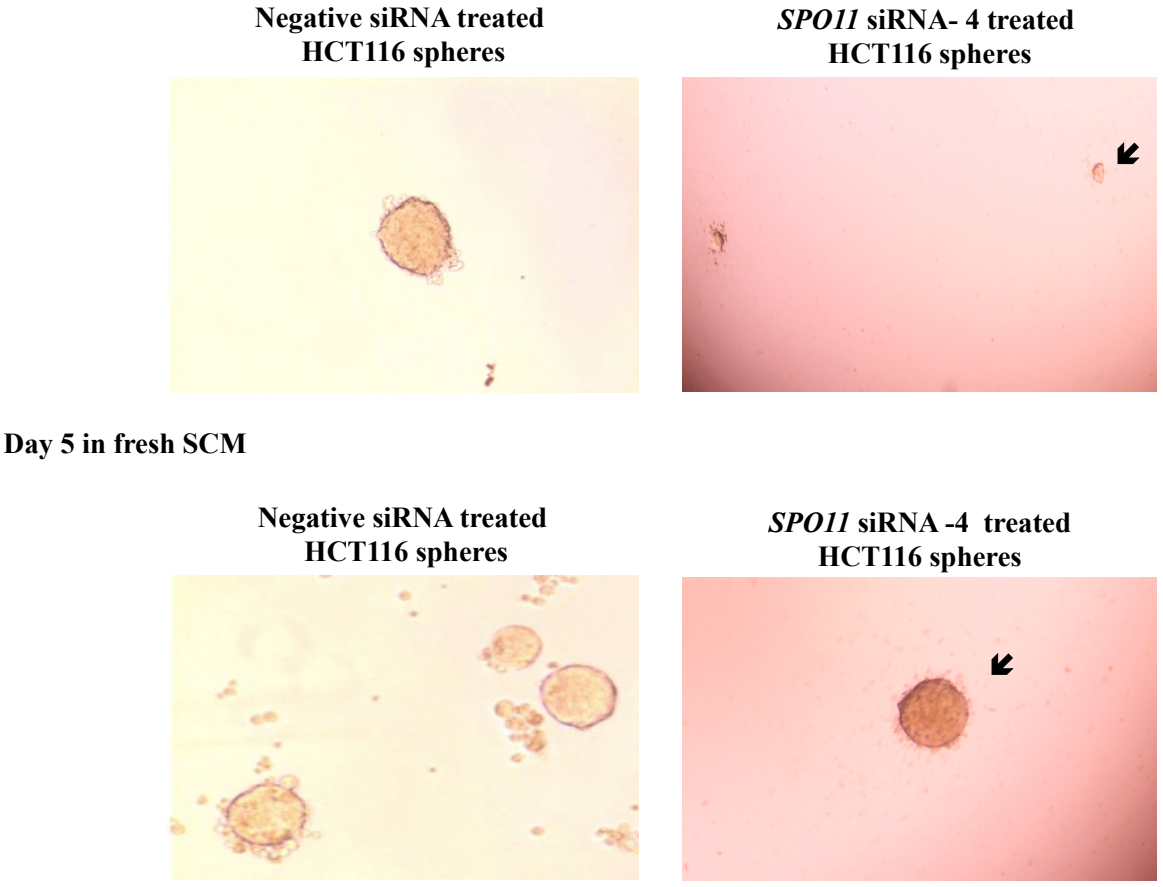

Figure 3.19: The cell growth inhibition induced by SPO11 knockdown is reversible. After *SPO11* knockdown, arrows show remaining single cells that were transferred to fresh SCM in the absence of siRNA recovered and formed spheres.

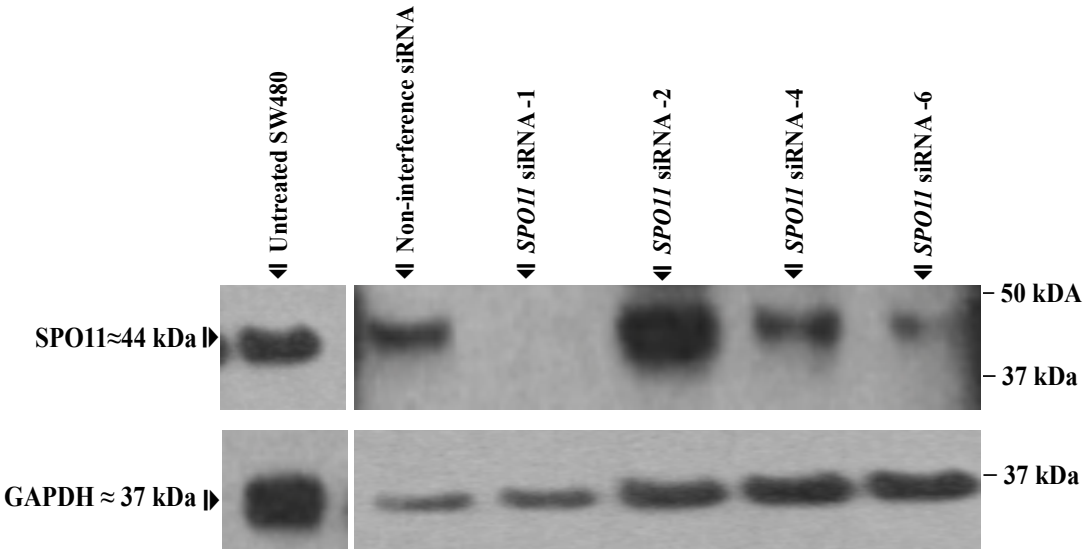

Figure 3.20. Western blots of SPO11 protein levels in SW480 colonosphere cells transfected with different siRNAs. The western blots of whole cell extract (WCE) using commercial anti-SPO11 antibody (ab81695) indicates a single band of the correct predicted size in SW480 colonosphere cells. When the SPO11 protein level was compared with GAPDH, the strongest reduction in SPO11 protein was seen after transfection with siRNA-1, siRNA-4 and siRNA-6.

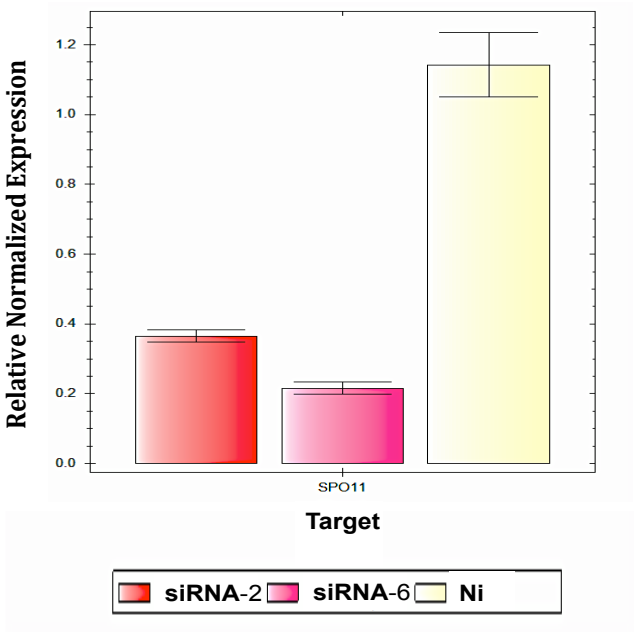

Figure 3.21. Gene expression data showing the level of SPO11 mRNA in SW480 colonosphere cells transfected with different siRNAs. qRT-PCR analysis indicates that CRC cells grown as spheres following transfection with negative siRNA, siRNA-2, and siRNA-6 showed a reduced level of SPO11 compared with the negative control. To analyse the data, the Bio-Rad CFX manager was used. The error bars indicate the standard error for the three replicates. Results were normalised to a combination of two endogenous reference genes (*GAPDH* and *ACTB*).

3.3 Discussion

CTA genes may have a crucial role in the progression of cancer, which might be involved in the control of cell proliferation and cell division (McFarlane *et al.,* 2014). Moreover, meiotic CTA genes may contribute to cancer formation/maintenance for example, the synaptonemal complex protein. SYCP3 has the ability to control cancer cells by forming a complex with BRCA2 that inhibits HR (Hosoya *et al.,* 2011). When these factors are targeted, the tumour cells might be affected and the symptoms might be minimised, which could produce a cancer specific treatment. Normal cell division is a highly regulated process and requires balance between the activities of all the genes responsible for the promotion of cell proliferation and suppression. Cancer occurs when there is a disruption in this balance and the cells divide in an uncontrollable manner. In this chapter, evidence is presented indicating SPO11 has positive effects on the proliferation of colorectal cancer (CRC) cells *in vitro.*

The objective of the work described in this chapter was to confirm that SPO11 is a CTA and to understand the impact that SPO11 knockdown has on the proliferation of cells in cancer cell lines. Moreover, the goal of this work was to have a clear insight in to the cellular localisation of SPO11 in cancer cells. SPO11 was present in all of the different types of cancer cells used in this study, including melanoma, lung, breast, colon, embryonic carcinoma and astrocytoma cancer samples. These findings are consistent with the results of a previously study that used northern blot analysis for exploring the gene expression of *SPO11* in cancers (Shannon *et al.,* 1999). The results of the present study, as well as the results from the study by Shannon *et al*. confirmed that SPO11 is a CTA. Gjerstorff (2016) and Hofmann *et al*. (2008) pointed out that SPO11 is not only found in male germ cells, but may also be a CTA Results of the present study proposed an oncogenic action of the SPO11 protein in cancer proliferation, which suggested that there is chance of using SPO11 as a cancer biomarker and treatment target.

In both cancer cells and normal cells, the balance between cell death and cell proliferation plays a significant role in the overall functioning of normal tissue homeostasis. Cancer is associated with an alteration in this balance and CTAs have been linked to this. For example, Zhou *et al.* (2010) identified that CTA TSP50 plays a major role in breast cancer development; moreover, a reduction in the expression of *TSP50* has a major impact on cell colony generation and migration, cell proliferation and cell apoptosis (Zhou *et al*., 2010). This exemplifies the importance of CTAs in oncogenes.

The cell fractions of cytoplasm and nucleus that were collected for the determination of the SPO11 localization indicated that all observed cell lines had a strong localisation of SPO11 in the nuclear fraction. However, the HCT116 cell line showed only nuclear localisation. This was also confirmed in IF of SW480. There might be some other characteristics of SPO11 that could explain the low levels of protein present in the cytoplasm. Existing studies indicate that DNA binding proteins that are multifunctional are found both in the cytoplasmic and nuclear compartment, with different functions to serve (Wilkinson & Shyu, 2001). From this analysis, it could be proposed that the SPO11 protein can serve as a multifunctional protein in cancer cells, but the known topoisomerase-like function of SPO11 in meiosis might suggest it has function restricted to the nucleus.

In order to further investigate the proposal that SPO11 plays a role in mitotic chromosome dynamics, co-staining with BLM protein provided evidence to suggest that SPO11 functions together with BLM. BLM has been shown to play an important role in controlling homologous recombination (HR), which aims to repair DSBs and dissolve double Holliday junctions (dHJs) (Kikuchi *et al.*, 2009; Wu & Hickson, 2003). SW480 cells co-stained with SPO11 and BLM revealed that SPO11 and BLM have an overlapping distribution pattern and SPO11 and BLM seem to co-localise in SW480 cells throughout anaphase and metaphase, and localizes between segregating chromosomes in anaphase.

Because SPO11 is expressed in cancer cells, the results suggest that it works with BLM to help dissociate lagging chromosomes at anaphase and helps cells continue to proliferate. Moreover, it has been reported that BLM localises and cooperates with PICH in centromeres and both proteins play important roles in the recruitment of active Topo IIIα in centromeres to eliminate DNA catenation before the onset of anaphase (Rouzeau *et al.,* 2012). SPO11 is ubiquitously expressed in all eukaryotes and mediates the initiation of meiosis through the formation of DSBs in a manner very similar to topoisomerase VI (Martini, 2002). Current study was suggested that SPO11 is a Topo-type protein and might function in a similar way to the Topo that interacts with BLM and PICH.

Two strong SPO11 stained foci were observed where the centrosome was expected to localise. Consequently, the results suggest that the foci might be the centrosomes. Pericentrin (PCNT) and Plk1-interacting checkpoint helicase (PITCH) specific antibodies were used to confirm this observation. PCNT and PITCH are known to localise in the centrosome region, and SPO11/PCNT/Plk-1co-localisation was observed in the centrosomes independently of BLM protein.

Since apoptosis resistance is considered a hallmark of various tumour cells, it has been noted that anti-apoptotic factors have the ability of providing various therapeutic strategies, which will help to treat cancer. Furthermore it is also found that actions of the common cancer treatment methods like chemotherapy and radiotherapy, is depended on the stimulation of apoptosis. Therefore, a common reason for therapeutic resistance is apoptosis deficiency (Teodoro *et al.,* 2012). The process of apoptosis can be assessed using the caspases or commonly known as cysteine protease that are usually present in cells in their inactive state. For triggering the apoptosis these enzymes are required to be activated and cleaved (Dash, 1994). Caspase-3 was used herein to examine whether SPO11 depletion induces apoptosis through this pathway. It was observed in parental SW480 cells that caspase-3 were not activated also uncleaved caspase bands were present in all cells thereby demonstrating that SPO11 knockdown did not induce apoptosis. However, although there was no apoptosis evidence in these attached cells, it is possible that apoptotic cells had detached and were not assessed here. Further into the study, the detection of the effect of SPO11 depletion on the survival of cancer cells was done with an ELDA assay. Reduction in the SPO11 protein level in HCT116 sphere cells resulted in a decrease in the proliferation frequency and siRNA 2 and 4 has a significant effect on SPO11 compared with the negative control. The colonosphere assay was done to assess the relationship of SPO11 with the self-renewal of HCT116 cells. Spheres can be formed by self-renewing, as well as by proliferating progenitors, and these spheres can retain their multipotency (Stingl, 2009; Pastrana *et al.,* 2011).

There was no standardised protocol for the production of spheres at that time and the procedure for the experiment used different parameters, such as cell seeding density, medium volume and composition, culture time and surface area of the culture dish (reviewed in Chaichana *et al.,* 2006). Spheres are known to be generated from a wide array of solid tumours and cancer cell lines, including HCT15, HT-29, HCT116, SW480, SW620, LoVo, LS174T, DLD1 and RKO (Kanwar *et al*., 2010; Chen *et al.,* 2011).

However, strong reduction in SPO11 protein was seen after transfection with siRNA-4 and 6 assed by western blot and qRT-PCR analysis compared with non-interference and untreated cells and that effect on cell proliferation.

The SPO11 depleted in HCT116 sphere cells did not appear to result in senescence or apoptosis as assessed by caspase-3 cleavage and β- galactosidase assays, respectively. The morphology does not change and remains normal for the duration of the experiment. However, suitable conditions for growth can lead to the recovery of the cells from proliferation arrest. This is consistent with SPO11- depleted cells being in a quiescent-like state. The quiescent state is adopted in steam cells for the preservation of the main functional features of the cells. Cells in this state remain poised and ready to be activated, rather than being inactive or dormant (Cheung & Rando, 2013). The recovery from *SPO11* deletion (Figure 3.16) supports this.

In summary, SPO11 was found to be expressed in all cancer cells studied. This suggests it is important as a feature of a wide range of cancer cells. In addition, IF and cell fractionation suggested that the SPO11 protein was located in the nuclei of the cancer cells where a topoisomerase activity might be expected. The interphase nuclear foci might also suggest a non-anaphase function (Cha *et al.,* 2000) previously suggested a role for SPO11 in pre-meiotic DNA replication (Cha *et al.,* 2000). Follow the siRNA depletion the protein level of SPO11 was significantly reduced in attached and floating cells and cell proliferation was inhibited. Moreover, the depletion of SPO11 protein in SW480 and HCT116 spheres cells restricted in inhibition of self-renewal. The overall results of the study indicate that SPO11 express in cancer cells which makes it require for cell survival and possible cancer specific drug target. The possible function of SPO11 in cancer cells remains unclear and that this will be addressed in the following chapters. However, the co-localization to BLM might suggest a topoisomerase like-function in anaphase.

4. Over expression of *SPO11*

4.1 Introduction

The results from Chapter 3 showed that SPO11 appeared to be required for cancer cell proliferation, as demonstrated by SPO11 siRNA depletion in HCT116 and SW480 cells. Chapter 3 results also showed that SPO11 is required for self-renewal of cancer stem-like cells. Furthermore, SW480 cells co-stained with SPO11 and BLM revealing that SPO11 and BLM have an overlapping distribution pattern throughout anaphase and metaphase, and these proteins localise between segregating chromosomes in anaphase. Because SPO11 is active in cancer, the results suggest that it cooperates with BLM to help dissociate catenated chromosomes at anaphase and this allow cells to continue to proliferate.

SPO11 orthologues are ubiquitously expressed in all eukaryotes in meiosis and they mediate the initiation of meiotic recombination through the formation of DSBs in a manner very similar to topoisomerase VI (Keeney, 1997; Martini, 2002). *SPO11* orthologs have been distinguished in numerous living organisms and demonstrate a four-constrained motif, which is strongly conserved (Keeney *et al*. 1997; Keeney, 2001). Loss of *SPO11* in *S. cerevisiae* prevents the meiotic synaptonemal complex forming correctly, meiotic S phase is accelerated, meiotic prophase is shortened, and there is a lack or absence of synapses between homologous chromosomes (Alani *et al.,* 1990; Cha *et al.,* 2000; Giroux *et al.,* 1989; Klapholz *et al.,* 1985; Loidl *et al.,* 1994; Menees *et al.,* 1992; Rockmill *et al.,* 1995; Weiner & Kleckner, 1994). *Spo11* null mice are infertile indicating an important role (Cole *et al.,* 2010). SPO11 is type IIB topoisomerase-like protein and might function in cancer a similar way to topoisomerase IIα that interacts with BLM and PICH. Whilst *SPO11* is meiosis-specific in most organisms, there are *SPO11* orthologs in plants and *Drosophila*, which have been suggested to have mitotic functions supporting a potential cancer functional role.

The aim of the work in this chapter was to further explore the function of *SPO11* in cancer cells by setting up a system where *SPO11* expression could be regulated to explore *SPO11* function by (a) over-expressing *SPO11* (in this chapter) and (b) making a *SPO11* deletion cell line containing an inducible *SPO11* which it could switch off (see Chapter 5). Also, to see whether deletion both copies of *SPO11* from HCT116 altered the characteristics of this cancer cell line in order to study the potential functional role of *SPO11*. So, it was first necessary to have a cell system in place where *SPO11* expression could be regulated. Therefore, the aim of the work in this chapter was to generate cells with an inducible *SPO11*. Once *SPO11* cDNA regulated HCT116 clones were generated which had genomic *SPO11* knocked-out, it could then investigate the concequences when *SPO11* expression was switched off (see Chapter 5).

4.2 Results

4.2.1 Tet-On 3G Inducible Expression System

The tetracycline-inducible gene expression system (Tet-On3G) is one of the most common inducible gene expression systems for mammalian cells (Gossen & Bujard, 1992; Vigna *et al.,* 2002; Loew *et al.,* 2010). Cells that express the Tet-On3G transactivator protein also have transgenes under the control of a TRE3G promoter (p_{TRE3G}), which expresses a high level of the gene of interest only when cultured in the presence of doxycycline (DOX). The Tet-On 3G transactivator protein undergoes a conformational alteration in the presence of doxycycline, this allows the protein to bind to the tet-operator (*tetO*) sequences located in P_{TRE3G} promoter and, in turn, induces the expression of the gene of interest, in this case *SPO11* (Figure 4.1). In this chapter, a doxycycline-responsive cell line was created that was able to induce expression of the *SPO11* gene by (a) cloning *SPO11* in to a pTRE3G vector to generate an inducible construct, (b) create a Tet-On 3G expressing stable cell line (c) create and screen for double-stable clone capable of high induction of *SPO11*.

4.2.1.1 Cloning the *SPO11* gene into the pTRE3G vector

To generate an inducible clone of *SPO11,* the full-length human *SPO11* open reading frame (NCBI, Gene ID NM_012444), which has size of 1191 bp, was amplified from the cDNA of ordinary human testis RNA using Phusion High-Fidelity PCR Master Mix with GC buffer (Figure 4.2). Amplification primers were designed with *Bam*HI restriction sites to facilitate cloning. The right *SPO11* band was extracted from the gel, purified, and then digested with *Bam*HI and purified. A *Bam*HI digested and purified pTRE3G vector (3431 bp) was used to clone the full length of *SPO11* (Figure 4.3). The ratios of the *SPO11* gene to the plasmid utilized were 6:1 and/or 9:1; insert: plasmid. Ampicillin resistance was utilized for selection after transformation into the DH5α strain of *E. coli*. A number of colonies were chosen and PCR analysis was performed utilizing internal primers for *SPO11* to confirm that the right colonies were selected (Figure 4.4). Colonies with positive PCR were selected for overnight culturing. The recombinant plasmids were further checked by restriction digestion of the purified plasmids using *Bam*HI to confirm accurate cloning. Analysis of the digestion pTRE3G::*SPO11* by agarose gel confirmed the presence and indicated successful cloning of *SPO11* (Figure 4.5). *SPO11* positive clones were sent for DNA sequencing to confirm the proper orientation and to check for mutations. The colonies chosen for further investigation

did not contain any mutations. The universal primers and internal primers utilized for these checks are recorded in Table 2.2 (Methods and Materials).

4.2.1.2 Creation of a Tet-On3G-expressing stable cell line

In the Tet-On system, two steps are required to generate a stable cell line that will expressing Tet-On 3G transactivator; this cell line serves as the host to permit the expression of *SPO11* gene. The two steps to generate this line are (a) expressing the Tet-On3G transactivator protein (integrated under G418 antibiotic selection) and (b) demonstrating a high level of induction from p_{TRE3G}. To obtain this, HCT116 cells were transfected with pCMV-Tet3G plasmid containing the transactivator gene using Xfect transfection reagent and selected with G418 (Figure 4.6; also see subsequent section). Before transfection a cell kill curve was carried out on the HCT116 cells using different concentrations of the antibiotic G418 to optimise the minimum dose that would kill all cells after 3-5 days in the absence of a resistance gene. Untreated cells were used to compare the effect of the antibiotic on the treated cells. The minimum antibiotic dose that killed all untransfected cells within 5 days was 400–500 μg/ml (Figure 4.7). Colonies transfected with pCMV-Tet3G were tested and twenty-four clones were isolated and analysed for induction. Figure 4.8 shows examples of G418 resistant colonies following pCMV-Tet3G transfection.

4.2.1.3 Testing Tet-On3G clones for induction of TetOn3G transactivator

To test level of induction in the HCT116 Tet-On3G cells, colonies were tested individually for induction clones and these were seeded into 6-well plates; for each colony one-third of the total amount was stock plates and two-thirds were used for the luciferase-screening assay. Three candidate colonies were chosen (12, 13 and 15) and were transfected with pTRE3G-Lus vector in which luciferase is under the control of the Tet-On system (see Section 2.7. a. iii in Materials and Methods) after 4 hours, 1 μg/ml doxycycline was added to one of the duplicate wells, while leaving the second well Dox-free. After 24 hours luciferase activity was calculated; the assay for luciferase activity was expressed as counts per second (CPS) and the fold induction was calculated for the relative light unit (RLU)/protein level (+Dox RLU/-Dox RLU) (Figure 4.9). Result showed Clone number 15 exhibited highest fold induction; which was stocked and labelled as HCT116-Tet-On3G.15 to be used in the next step for creating an inducible *SPO11* cell line.

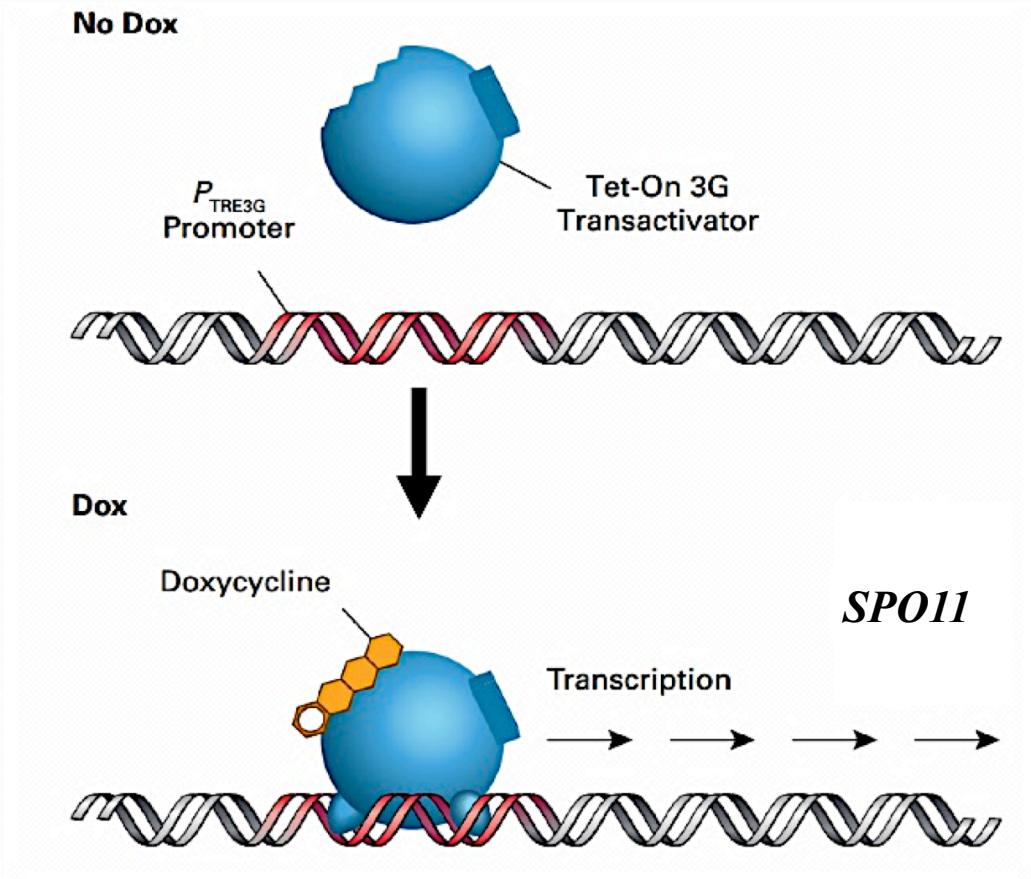

Figure 4.1 The Tet-On3G inducible system allows induction of the expression of *SPO11* only in the presence of doxycycline. Tet-On3G transactivator protein (blue) undergoes a conformational alteration in the presence of doxcyclin. This allows the protein to bind to the tet-operator (*tetO*) element (red) within the P_{TRE3G} promoter of the TRE3G plasmid and, in turn, induces the expression of *SPO11* cDNA.

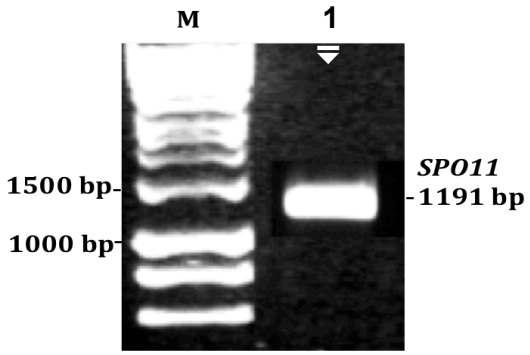

Figure 4.2 PCR amplification of the full open reading frame of *SPO11*. Lane 1: PeqGREEN DNA dye stained agarose gels show that the expected PCR product size of the *SPO11* fragment is1191 bp. cDNA was generated from the total RNA prepared from testes. HyperLadder 1 Kb (5 µl) was used as a marker.

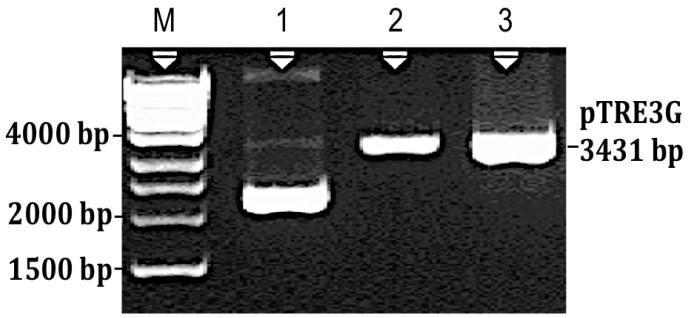

Figure 4.3 Digestion of pTRE3G plasmid with *Bam*HI restriction enzyme. Agarose gel (0.8%) stained with PeqGREEN DNA dye. Lane 1: uncut pTRE3G vector; Lane 2: *Bam*HI cut and purified pTRE3G vector; Lane 3: digested pTRE3G plasmid before purification. HyperLadder 1 Kb (5 µl) was used as a marker.

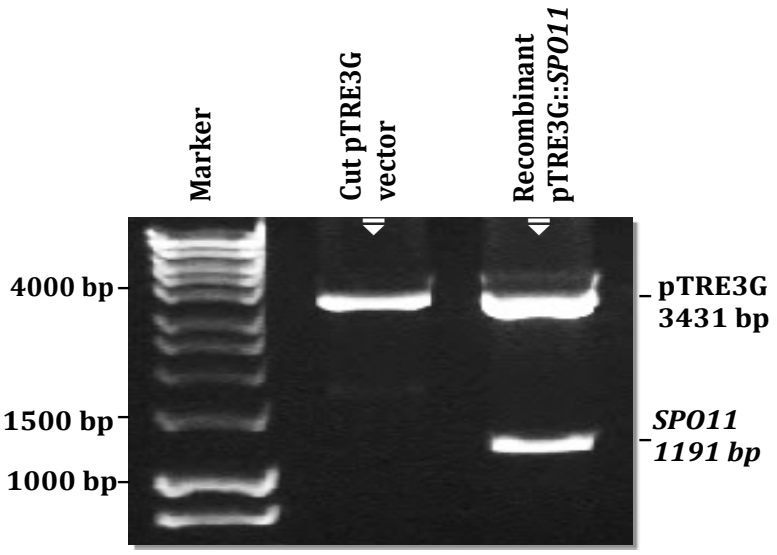

Figure 4.4 Digestion of pTRE3G::*SPO11* constructed plasmid with *Bam*HI restriction enzyme. Agarose gel (0.8%) was stained with PeqGREEN DNA dye. Middle lane: digested pTRE3G plasmid after purification; right hand line: digestion of pTRE3G::*SPO11* construct with *Bam*HI enzyme. Two bands were obtained; the upper band is the pTRE3G vector and the lower band is the *SPO11* gene (1191 bp). Left hand lain: HyperLadder 1 kb marker.

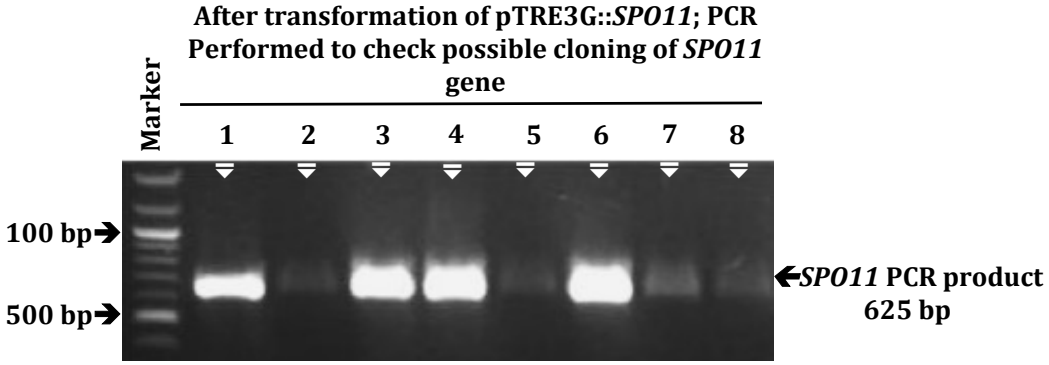

Figure 4.5 PCR profile analyses the *SPO11* positive clones after transformation into *E. coli.* *SPO11* was ligated at the *Bam*HI site of pTRE3G and transformed into the DH5α strain of *E. coli*. Random colonies were selected. PCR was performed to check the possibility of transformation using internal primers for *SPO11*. PCR products were fractionated on 1% agarose gels and stained with PeqGREEN DNA dye. HyperLadder II (5 µl) was used as a marker. Lane 1: positive testis control; Lanes 2-8: candidate colonies containing the *SPO11* gene.

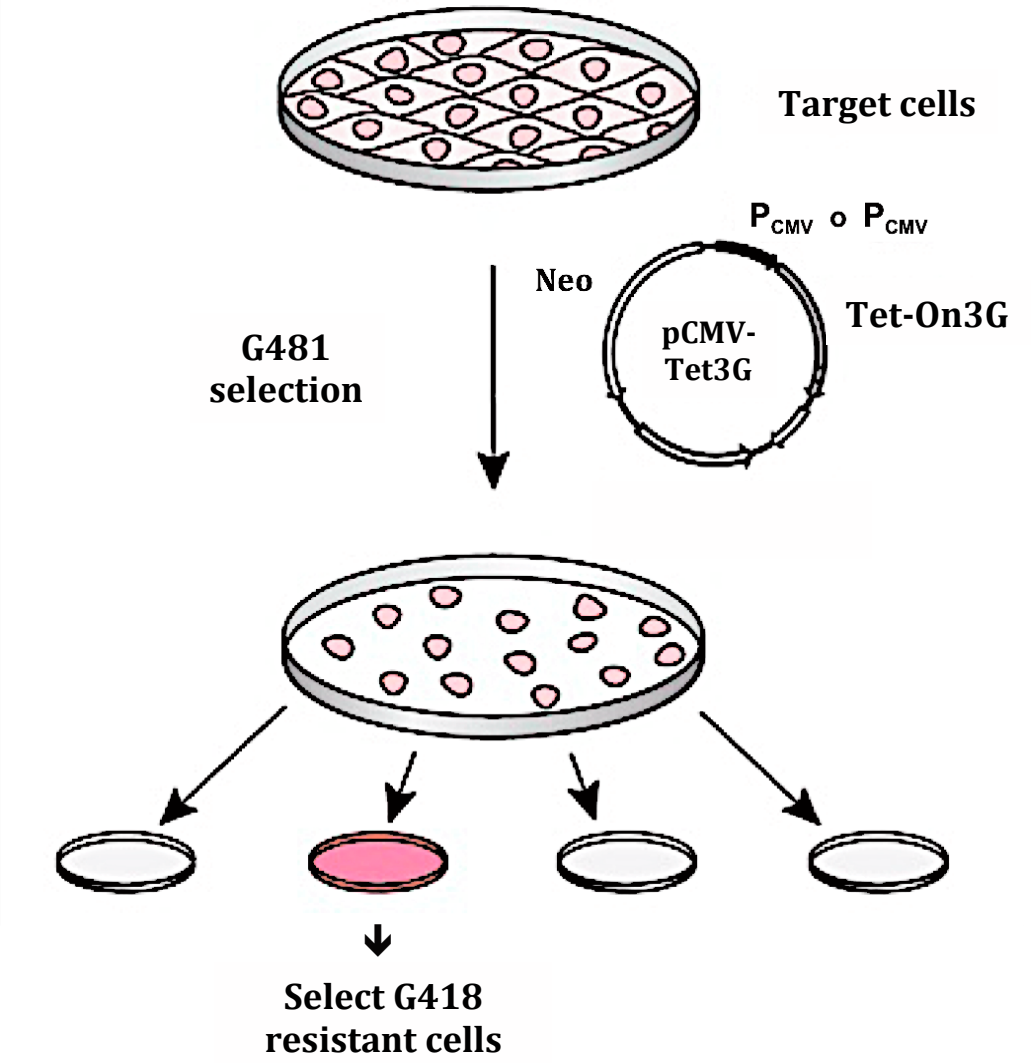

Figure 4.6 Establishing the Tet-On3G system in HCT116 cells. HCT116 was transfected with the pCMV-Tet-On3G plasmid and cells with G418 were selected to generate a stable Tet-On3G cell line constitutively expressing Tet-On3G transactivator. This cell line served as the host for a pTRE3G-based expression vector, which was transfected into the Tet-On3G cell line.

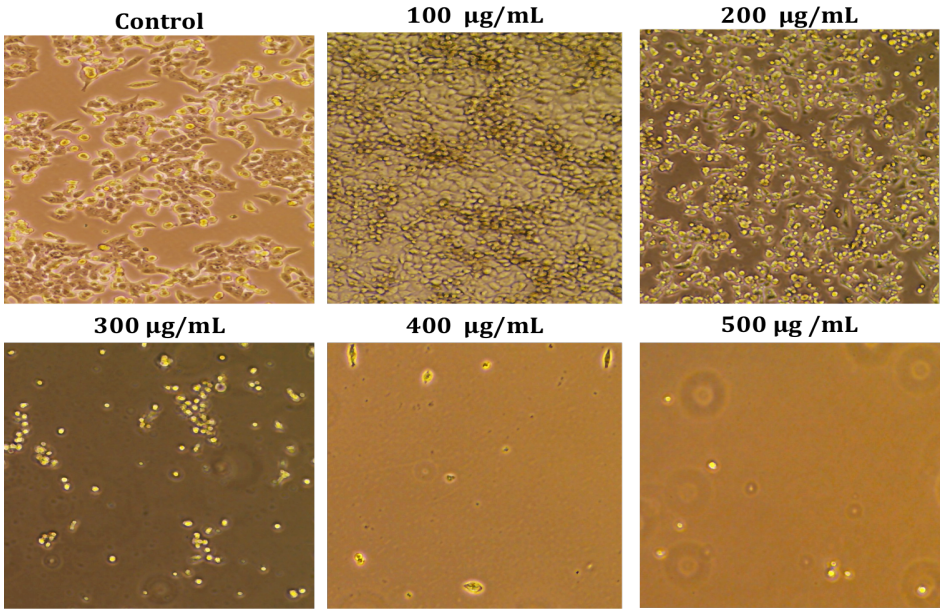

Figure 4.7. Geneticin (G418) kill curve. A cell kill curve was carried out on the HCT116 cells using different concentrations of the antibiotic G418. HCT116 cells were grown in media without antibiotic for 48 hours. Five doses of geneticin (100 to 500 µg) were then used to optimize the minimum dose that would kill all cells after 3–5 days. Untreated cells were used to compare the effect of the antibiotic on the treated cells. The antibiotic dose that killed all cells within 5 days was 400–500 µg/ml.

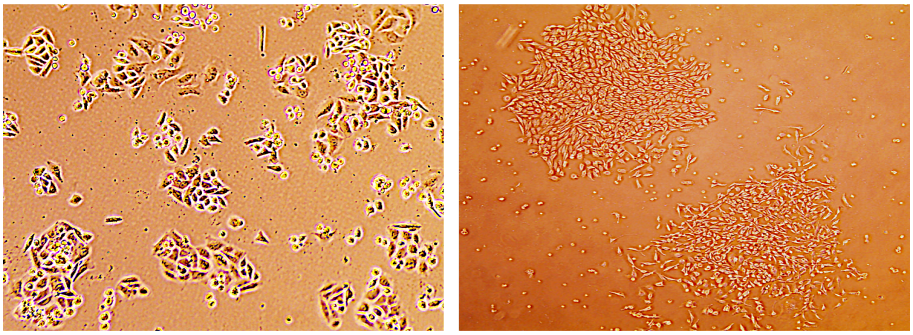

Figure 4.8 HCT116 cells transfected with pCMV-Tet3G plasmid. After 2 weeks, G418-resistant colonies appeared. colonies were transferred into separate wells of a 24-well plate using a cloning cylinder, then to a 10 cm plate and finally to T75 flasks.

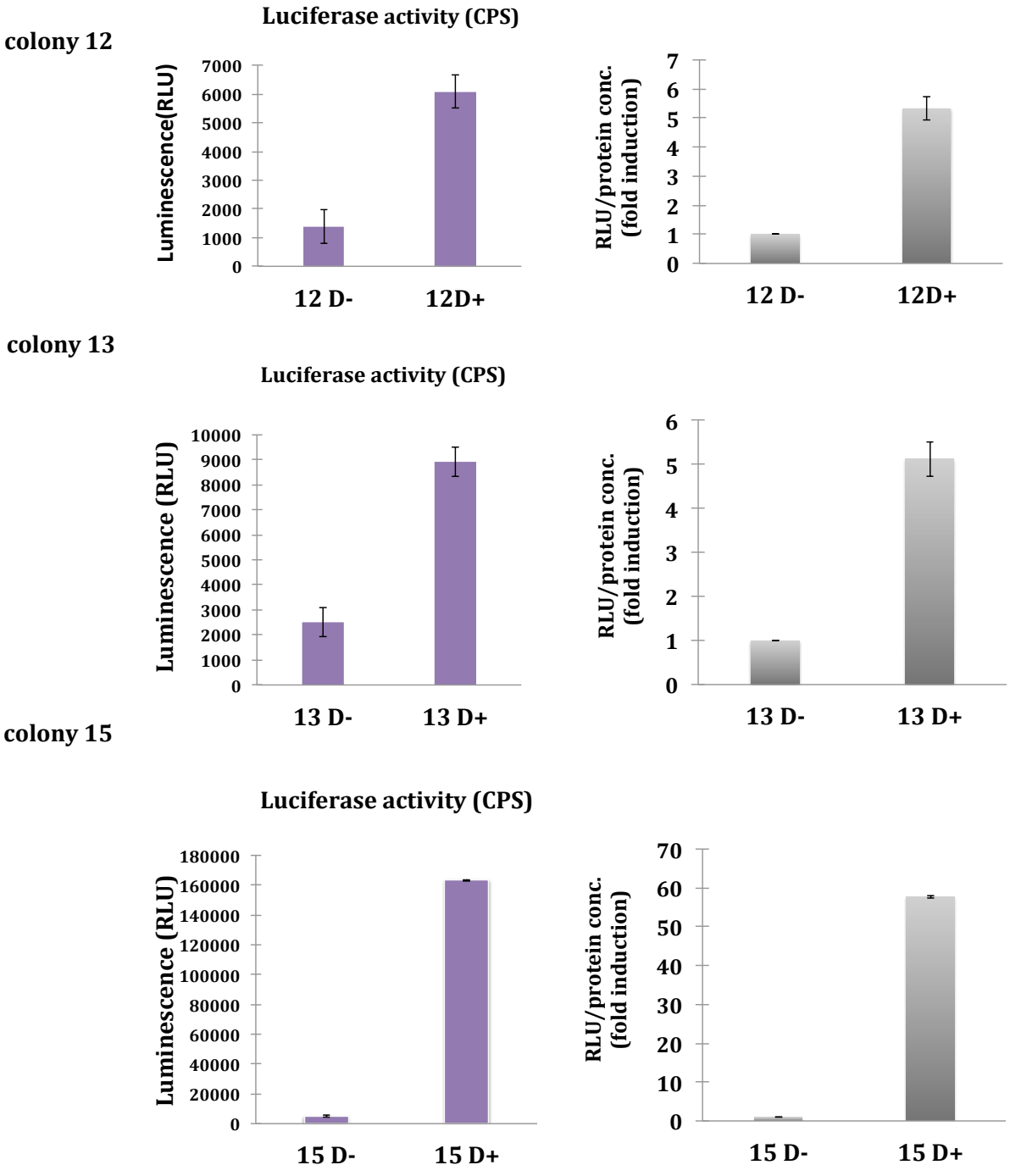

Figure 4.9 Luciferase assay for testing Tet-On3G colonies for induction. HCT116 Tet-On3G colonies were tested individually for induction. First, the three colonies (12, 13, 15) were transfected with pTRE3G-Lus vector using Xfect transfection reagent, then (Dox+) 1 µg/ml was added to one of the duplicate wells, while leaving the second well (Dox-) free. The assay for luciferase activity was expressed as counted per second (CPS) and the fold induction was calculated for the RLU/protein level (+Dox RLU/-Dox RLU); colony number 15 exhibit the highest fold induction.

4.2.2 Establishment of a double-stable HCT116 Tet-On and HeLa Tet-On3G cell line

The generation of a double stable Tet-On3G cell line inducing *SPO11* under control of a TRE3G promoter (P_{TRE3G}) was the goal. We aimed to create a system for regulatable (ON/OFF) overexpression of *SPO11* in human cancer cells to study the effect when genomic copies of the *SPO11* gene are deleted and inducible *SPO11* is turned off. We had created HCT116 cells with the inducible transactivator (see previous section) and a HeLa-Tet-On3G based system was obtained from a commercial source (Clontech). Double-stable cell lines with regulatable *SPO11* were generated by transfecting HCT116 Tet-On3G.15 and HeLa Tet-On3G cells with the pTRE3G::*SPO11* plasmid along with a linear selection marker for the puromycin antibiotic (Figure 4.10). This was followed by selection for double-stable transfected cells that were resistant to G418 and puromycin antibiotics.

4.2.2.1 Selection of double-stable HCT116 Tet-On3G.15 and HeLa Tet-On3G cells

Before cotransfection, different concentrations of puromycin were used to optimize a cell kill curve. HCT116 Tet-On3G.15 and HeLa Tet-On3G cells were grown in media without antibiotic for 48 hours and then seven doses of puromycin (0–2.5 μg/ml) were optimised as the minimum dose that would kill all cells after 3–5 days. Untreated cells were used as controls to compare the effect of puromycin on treated cells, and 1 μg/ml was the optimum dose based on colony selection (Figure 4.11). The minimum antibiotic dose that killed all untransfected cells in 5 days was 1.0 μg/ml. HCT116 Tet-On3G.15 and HeLa Tet-On3G cells were cotransfected with pTRE3G plasmid containing the *SPO11* gene or with empty pTRE3G plasmid (control) along with the puromycin linear selection marker, at a ratio of 20:1 (constructed plasmid: puromycin marker). After 4 days of cell growth in antibiotic-free media, 100 μg/ml G418 and 1 μg/ml puromycin were added. All untransfected cells died whilst single cells that appeared after 4–5 days of treatment and had possible transfection (Figure 4.12). After 2 weeks of cell culture in media under optimised antibiotic selection, resistant colonies begin to appear with possible gene cloning (Figure 4.13). Large colonies were selected using cloning cylinders, grown in separate 10 cm plates and then expanded in T75 flasks.

Each clone was then tested individually by comparing the expression of *SPO11* in the presence or absence of 1 μg/ml doxycycline. Cells were grown in this experiment in a high quality Tet free approved FBS which was functionally tested for this inducible system and free of tetracycline contamination.

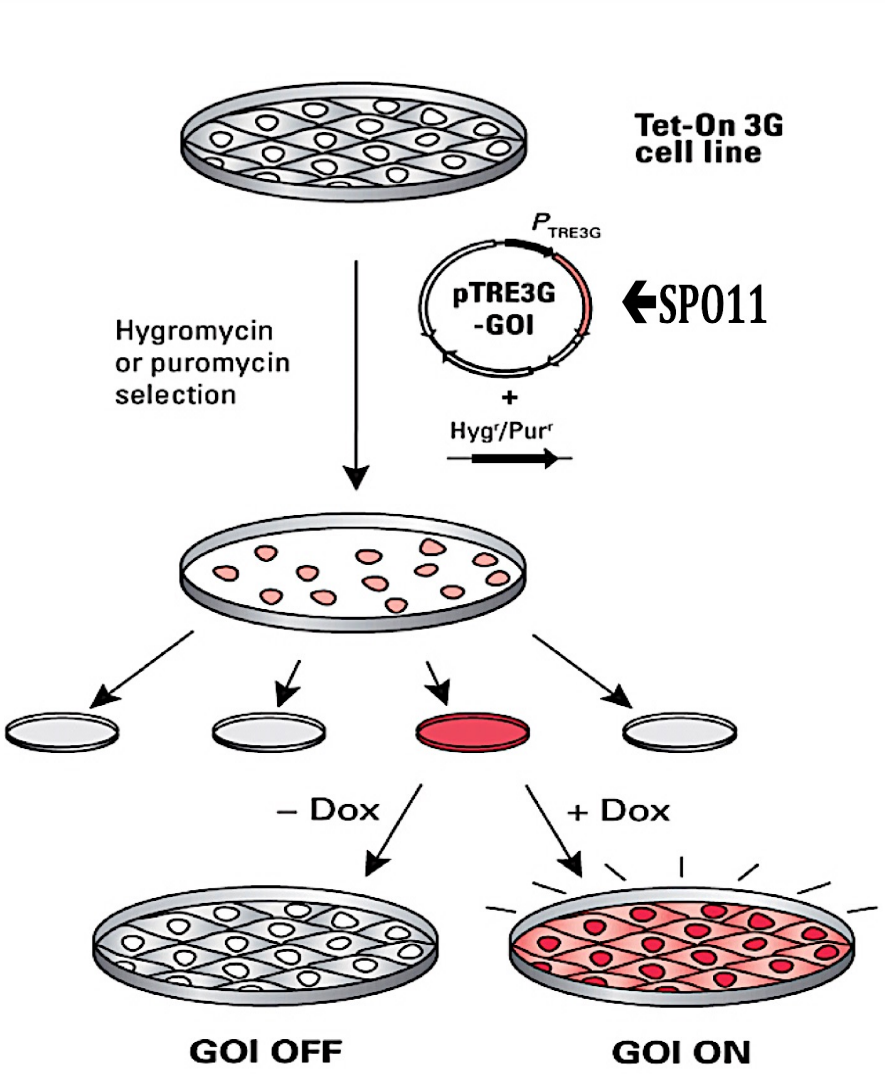

Figure 4.10 Creating a double Tet-On3G cell line. HeLa Tet-On3G and HCT116 Tet-On3G.15 cells that express the tetracycline (Tet) regulated transactivator protein were transfected with an expression plasmid containing *SPO11* cDNA (pTRE3G::*SPO11*) along with a puromycin linear marker to induce the expression of *SPO11* cDNA. Doxycycline (Dox) (1 μL/ml) was used for overexpression of *SPO11*.

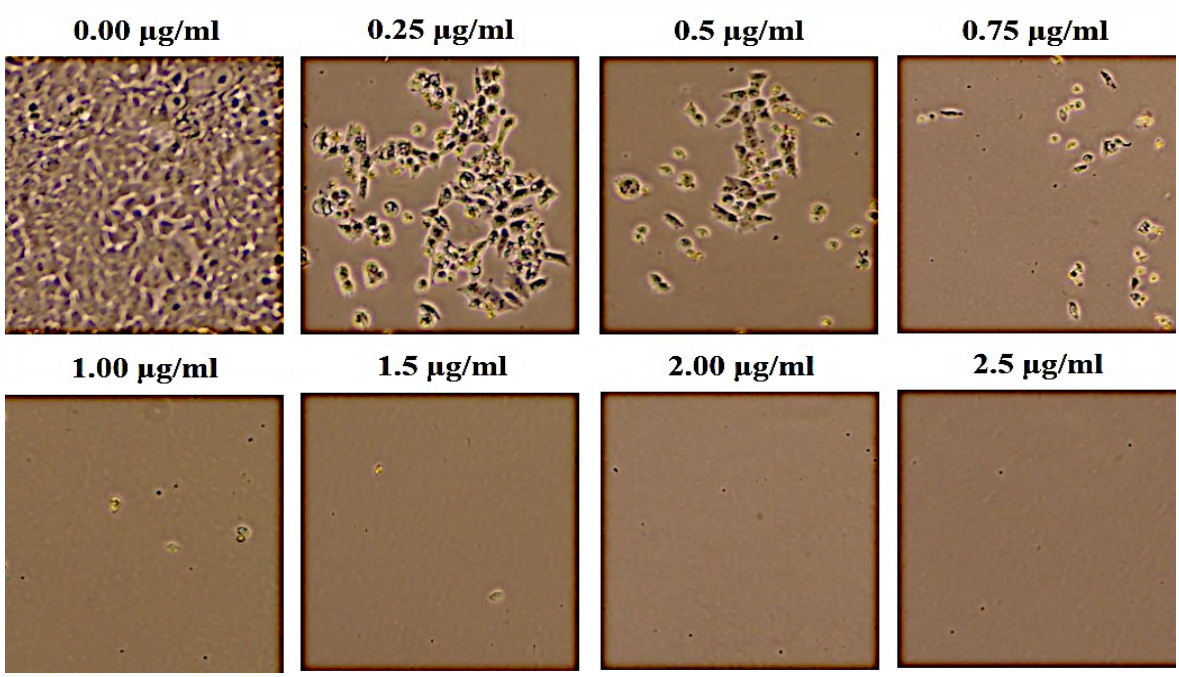

Figure 4.11 Puromycin kill curve. Untransfected HCT116 Tet-On3G.15 cell lines were exposed to different concentrations of puromycin and left to grow for 3–5 days. In both HCT116 Tet-On3G.15 and HeLa Tet-On3G cells, it was determined that a concentration of 1 µg/mL was sufficient to kill all cells.

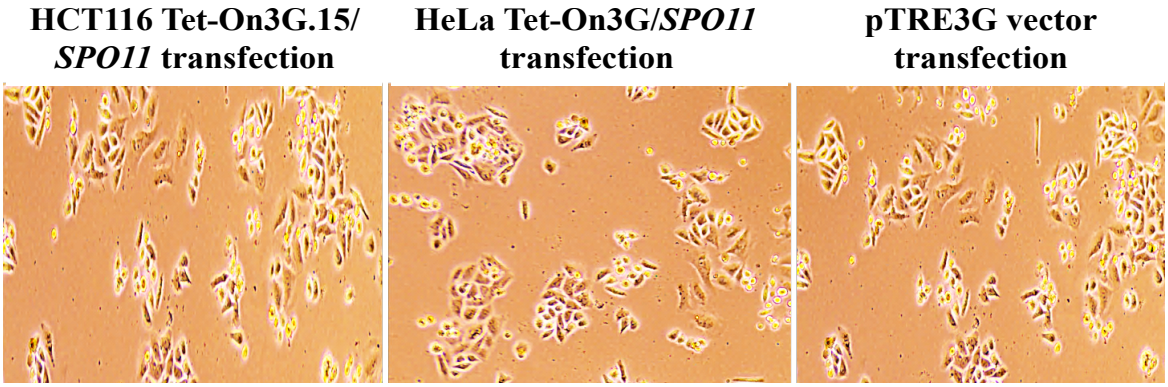

Figure 4.12 HCT116 Tet-On3G.15 and HeLa Tet-On3G cell lines transfected with the *SPO11* gene after 4 days of cell growth. Cells were transfected with pTRE3G plasmid containing *SPO11* with a puromycin linear selection marker at a ratio of 20:1 (construct:puromycin marker). Empty pTRE3G plasmid was transfected into the cells as a transfection control. After 4 days of growth, most of the cells had died except for cells containing the puromycin selection marker. Single cells started to appear 4 days after adding 1 µg/mL puromycin. Example images are shown for each cell line.

G418 and puromycin – resistant colonies

HeLa-Tet-On3G/SPO11

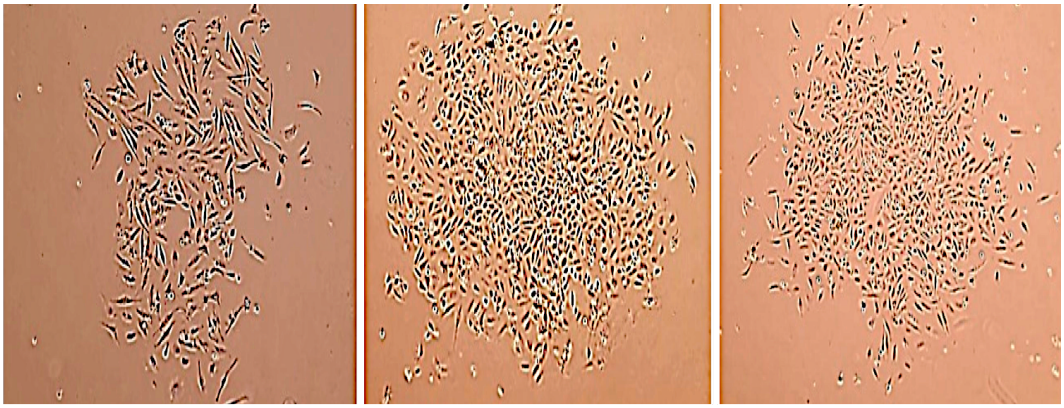

HCT116-Tet-On.15/*SPO11*

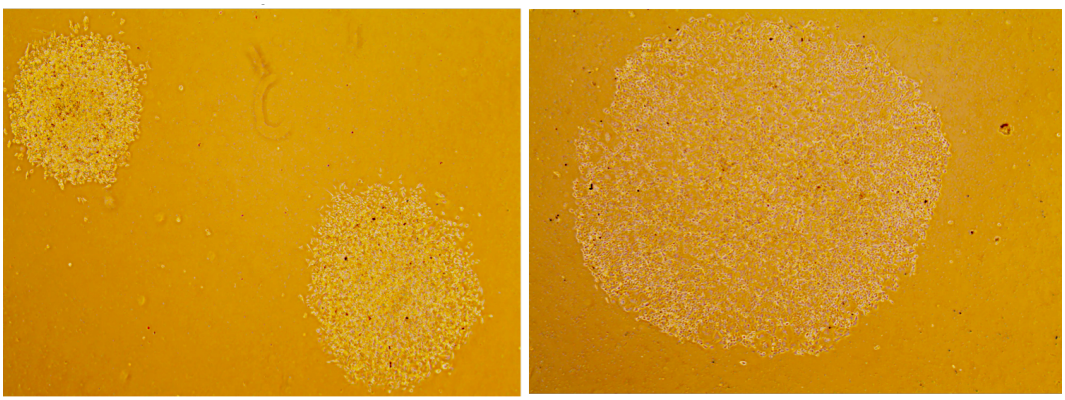

Figure 4.13 HCT116 Tet-On3G.15 and HeLa Tet-On3G cell lines transfected with the *SPO11* gene. Colonies were seen after 2 weeks of cell growth. Single cells started to appear and were cultured in 96-, 24-, then 6 well to expand the cultures in the presence of 1 μg/mL puromycin. Example images are shown for both cell lines (HeLa-Tet-On3G/*SPO11*-Top; HCT116-Tet-On3G.15/*SPO11*-bottom).

4.2.3 RT-PCR and qRT-PCR analysis of overexpressed *SPO11* in the double-stable HCT116 Tet-On3G.15 cell line

The integration of *SPO11* into the HCT116 Tet-On3G.15 cell line successfully created double stable cell lines. This was confirmed by inducing them with 1 μg/mL doxycycline for 24 hours; additionally, a portion of clones was collected without doxycycline. Total RNAs were extracted and cDNA was synthesized from each clone in either the absence or presence of doxycycline. Two primer sets were utilized to confirm the expression of the pTRE3G::*SPO11* construct and testis cDNA was utilized as the positive control. PCR products were not detected in the HCT116 and HeLa cells, or most of cancer cells used in this study, confirming *SPO11* expression with the use of Western blot analysis (figure not shown). However, the cancer cells did not appear to have induced high levels of the *SPO11* gene, leading to speculation that there were lower levels thereof. Subsequently, PCR was applied First, to analyse the expression of *SPO11* cDNA in the HCT116Tet-On3G.15 cells and the HeLaTet-On3G cells before transfected with the construct pTRE3G::SPO11 plasmid as control (Figure 4.14) result showed no measurable elevated *SPO11* expression in either although protein was detectable using western blot analysis in Figure 4.18. Second, PCR was applied on the four positive HCT116-Tet-On3G.15/*SPO11* clones to detect and analyse the expression of *SPO11* in the present or absent of doxycycline to confirm that doxycycline-responding cell line able to induce expression of the *SPO11*cDNA (Figure 4.15). Colonies number (3) and (4) demonstrated no elevated expression either in the presence or absence of doxycycline and these clones were excluded from this study because there were no obvious expression of *SPO11*cDNA. Colonies number (1) and (2) demonstrated elevated expression in the presence of doxycycline and these clones were used for further analysis because there were have obvious expressions of *SPO11*. Moreover, *SPO11* expression was examined in two independent colonies selected after integration of the pTRE3G vector only as control. No elevated *SPO11* expression was detected in HCT116Tet-On3G.15 transfected with pTRE3G plasmids either in the presence or absence of doxycycline after 24 hours (Figure 4.16).

For further quantitative analysis qRT-PCR was carried out to measure the level of *SPO11* induction in positive *SPO11* colonies (1) and (2) after induction with doxycycline. qRT-PCR reactions were carried out in triplicate in a total volume of 20 µl on a CFX96 Real-Time System C1000 Thermal Cycler (BioRad) using Life Technologies TaqMan Gene Expression Master Mix and primers for *SPO11*.
The result was normalized against the qRT-PCR results of two reference genes, *ACTB* and *GAPDH*; the results are shown in (Figure 4.17). The qRT-PCR results showed low expression of *SPO11* in the absence of doxycycline. In contrast, a high level of *SPO11* expression was observed in colonies (1) and (2) after doxycycline induction. However, qRT-PCR showed a moderate induction in colony (4). No quantification cycle (Cq) reading was shown in the negative controls NTC (no template control) or NRT (no reverse transcriptase).

Western blot analysis of cells overexpressing *SPO11* in the double-stable HCT116-Tet-On3G.15/*SPO11* cell lines showed relatively modest changes to levels of SPO11 protein after induction with 1 µg/mL doxycycline for 48 hours. Loading was controlled by GAPDH (Figure 4.18). An examination for *SPO11* overexpression was conducted to further study the effect of this gene on the proliferation of cancer cells. Growth curves of HCT116 Tet-On3G.15/*SPO11*cells untreated and doxycycline treated (Figure 4.19) showed the control (no Dox) gives poor levels of proliferation (as measured by cell number increase).

4.2.4 RT-PCR and qRT-PCR analysis of overexpressed *SPO11* in double-stable HeLa Tet-On3G inducible cells

The successful integration of *SPO11* into HeLa Tet-On3G cells was achieved by transfecting four independent colonies with pTRE3G::*SPO11* vector and inducing them with 1 µg/mL doxycycline for 24 hours. A small amount of each clone was cultured in the absence of doxycycline. Total RNA was isolated and cDNA was synthesized from each clone either in the presence or absence of doxycycline. *SPO11* primers were utilized to confirm the expression of the pTRE3G::*SPO11* construct and testis cDNA was utilized as the positive control, two clones (1) and (3) exhibit measurable elevated *SPO11* expression using qualitative RT-PCR (Figure 4.20). *SPO11* expression was assessed in two independent colonies selected after integration of the pTRE3G vector only. No *SPO11* expression was shown in HeLa Tet-On3G transfected with pTRE3G plasmids either in the presence or absence of doxycycline after 24 hours (Figure 4.21).

qRT-PCR was carried out to quantify the level of *SPO11* expression in colonies (1) and (3) after induction with doxycycline. qRT-PCR reactions were carried out in triplicate in a total volume of 20 µl on a CFX96 Real-Time System C1000 Thermal Cycler (BioRad) using Life Technologies TaqMan Gene Expression Master Mix and primers for *SPO11*. The result was normalized against the qRT-PCR results of two reference genes, *ACTB* and *GAPDH*; these results are shown in Figure 4.22. The qRT-PCR results showed low expression of *SPO11* in the absence of doxycycline. In contrast, elevated levels of *SPO11* expression was observed in colonies (1) and (3) after doxycycline induction. No quantification cycle (Cq) reading was shown in the negative controls NTC (no template control) or NRT (no reverse transcriptase)

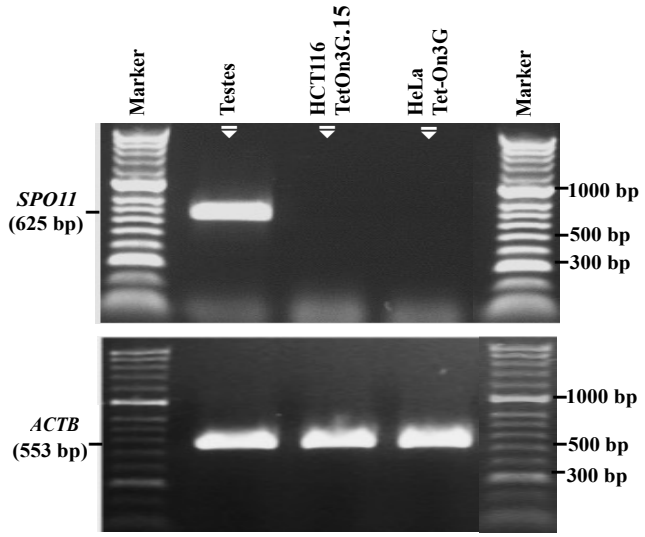

Figure 4.14 qualitative RT-PCR analysis of the expression of *SPO11* in HCT116 Tet-On3G.15 and HeLa Tet-On3G cell lines. Agarose gels of RT-PCR product stained with PeqGREEN DNA dye showed no excessive expression of *SPO11* in either the HCT116 Tet-On3G or HeLa Tet-On3G cells. A testis sample was included as a positive control. *ACTB* served as the positive control for the cDNA samples.

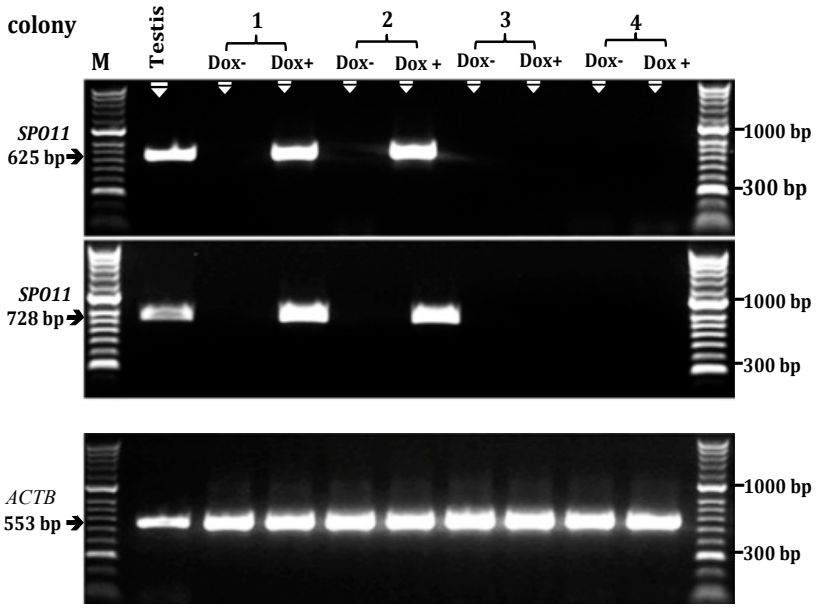

Figure 4.15. qualitative RT-PCR analysis confirming expression of the *SPO11* gene after induction in the HCT116 Tet-On3G system. Four colonies were induced with 1 µg/mL doxycycline for 24 hours. *ACTB* served as the positive control for the cDNA samples. Two pairs of primers were designed for the *SPO11* gene and it was expressed to higher level in colonies (1) and (2) in the presence of doxycycline and not expressed in the absence of doxycycline. Colonies (3) and (4) showed no expression elevation either in the absence or the presence of doxycycline. Lane T: positive testes control. Agarose gels (1%) stained with PeqGREEN DNA dye to visualize the PCR product; M is a HyperLadder II marker.

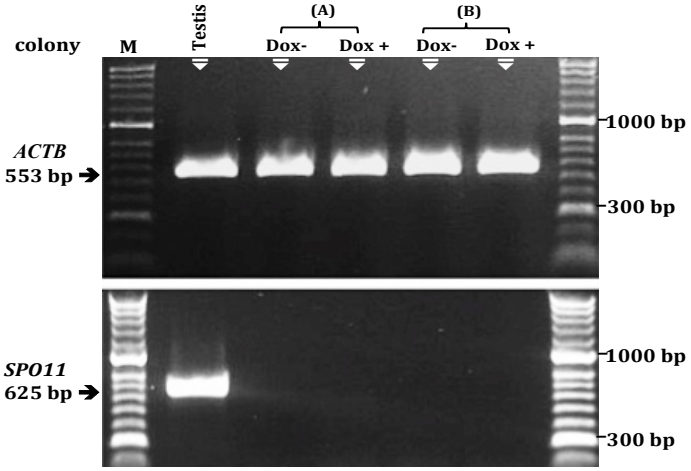

Figure 4.16 qualitative RT-PCR analysis of the *SPO11* gene in two independent colonies transfected with a pTRE3G empty vector only. (A) HCT116 Tet-On3G.15 cells and (B) HeLa Tet-On3G cells were transfected with pTRE3G plasmids and induced with 1 µg/mL doxycycline for 24 hours. *ACTB* served as the positive control for the cDNA samples. RT-PCR was performed to check the expression of the *SPO11* gene after induction with the pTRE3G vector only. No elevated expression was detected in the colonies, either with or without doxycycline. Lane T: positive testis control. Agarose gels (1%) stained with PeqGREEN DNA dye to visualize the PCR product.

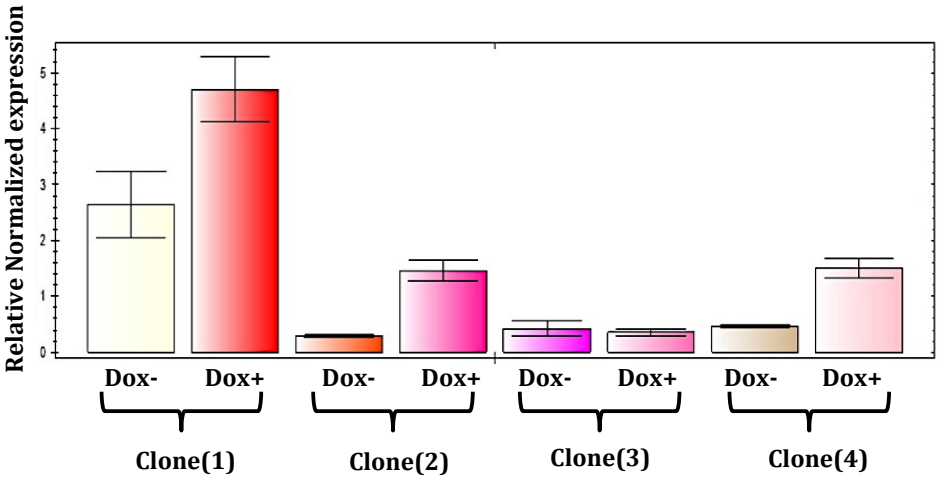

Figure 4.17 quantitative data showing the level of *SPO11* gene expression. qRT-PCR analysis showing the transcript levels for the *SPO11* gene in double-stable HCT116 Tet-On3G.15/*SPO11* cells after induction with doxycycline. Colonies (1), (2), (3) and (4) from double-stable HCT116 Tet-On3G.15/*SPO11* cells showing changing levels of *SPO11* expression. The Bio-Rad CFX Manager was used to analyse the data. The error bars show the standard error for three replicates. Results were normalized to a combination of two endogenous reference genes (*GAPDH* and *ACTB*). Error bars show the standard error of the mean.

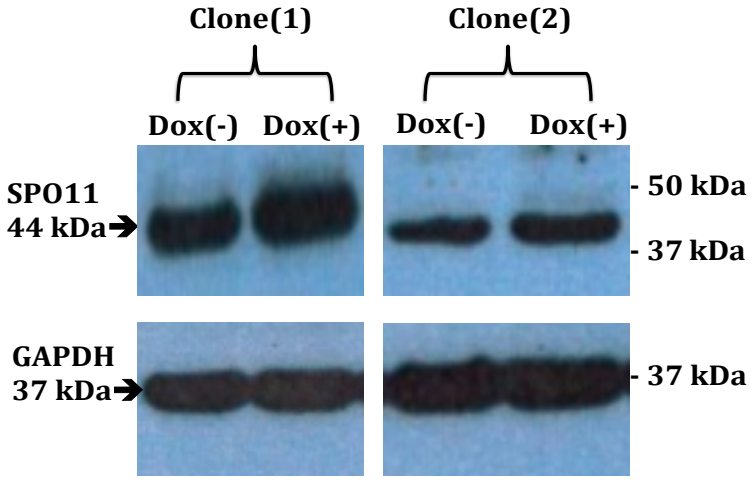

Figure 4.18 Western blot analysis confirmed an increased SPO11 protein level. Western blot images are representative of three replicates similar result were obtained for each. Colony (1) and clone (2) from double-stable HCT116 Tet-On3G.15/*SPO11* cells show changing levels of SPO11 protein after induction with 1 µg/mL doxycycline for 48 hours. Loading was controlled by GAPDH.

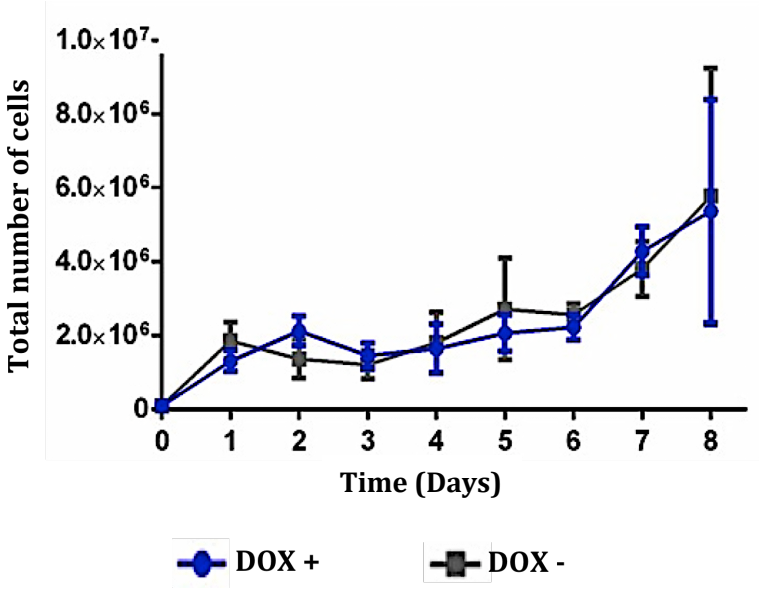

Figure 4.19 Proliferation levels for HCT116 Tet-On3G.15 with the *SPO11* clone (1) induced overexpression. Total cell count for untreated and doxycycline-treated HCT116 Tet-On3G.15/*SPO11* cells showing no significant differences. The error bars represent the standard deviation (n=2) for the total number of cells.

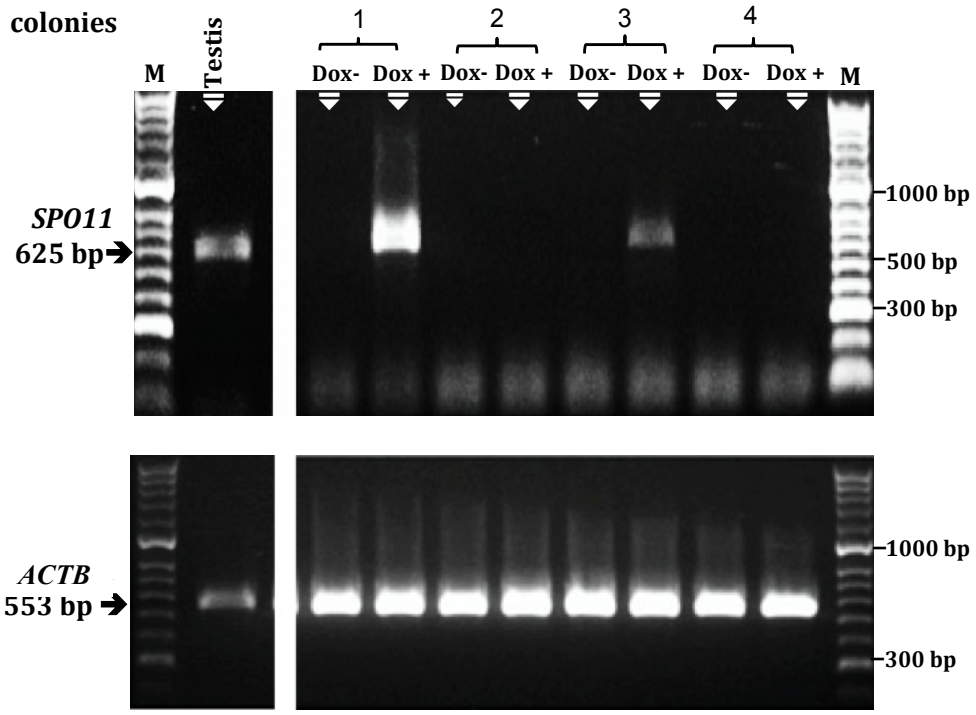

Figure 4.20 Qualitative RT-PCR analysis confirming expression of *SPO11* after induction in the HeLa Tet-On 3G/*SPO11* system. Four independent colonies of HeLa Tet-On3G cells transfected with a pTRE3G::*SPO11* construct were assessed. The cells were cultured in the absence or presence of 1 µg/mL doxycycline for 24 hours. *ACTB* served as the positive control for the cDNA samples. Internal primers were designed for the *SPO11* gene and expression was elevated in colonies (1) and (3) in the presence of doxycycline and not in the absence of doxycycline. Colonies (2) and (4) showed no measurable elevated expression either in the absence or presence of doxycycline and were not candidate colonies. Agarose gels (1%) stained with PeqGREEN DNA dye to visualize the PCR product; M is a HyperLadder II marker.

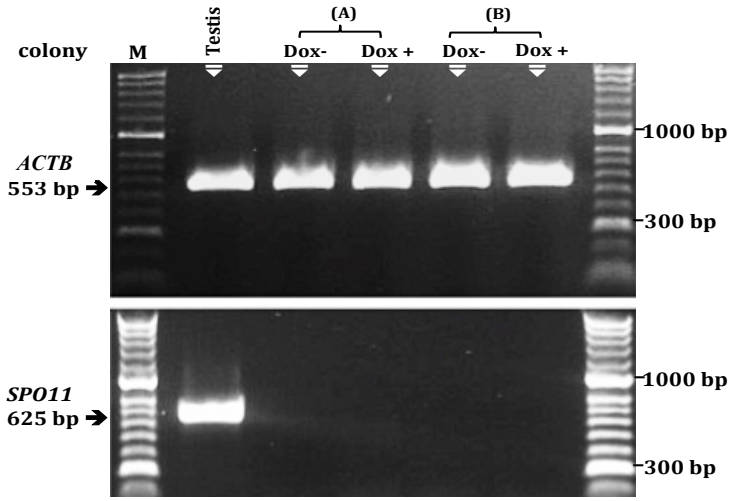

Figure 4.21 Qualitative RT-PCR analysis of *SPO11* gene expression in two independent colonies transfected with pTRE3G empty vector only. (A) HCT116 Tet-On3G.15 cells and (B) HeLa Tet-On3G cells were transfected with pTRE3G plasmids and induced with 1 µg/mL doxycycline for 24 hours. *ACTB* served as the positive control for the cDNA samples. RT-PCR was performed to check the expression of the *SPO11* gene after induction with 1 µg/mL doxycyclin for 48 hours. No elevated expression was observed in the colonies, either with or without doxycycline. Lane 1: positive testis control. Agarose gels (1%) stained with PeqGREEN DNA dye to visualize the PCR product.

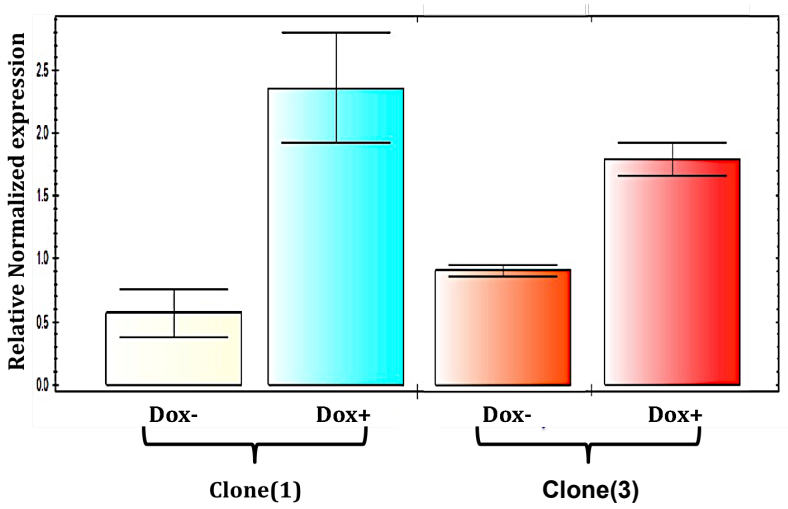

Figure 4.22 Quantitative qRT-PCR data showing the level of *SPO11* level expretion. qRT-PCR analysis showing the transcript levels of the *SPO11* gene in double-stable HeLa Tet-On3G cells after induction with 1 µg/mL doxycycline for 48 hours. The Bio-Rad CFX Manager was used to analyse the data. The error bars show the standard error for three replicates. Results were normalized to a combination of two endogenous reference genes (*GAPDH, ACTB*). Error bars show the standard error of the mean.

4.3 Discussion

The so-called hallmarks of cancer depict the various ways that malignant cells escape cell cycle control, creating nonstop tumour advancement and proliferation (Hanahan & Weinberg, 2000; 2011). Consequently, it is necessary to understand how this proliferation is driven and how it can be inhibited. The aim of this study was to determine whether *SPO11* overexpression affects the proliferation of a colorectal cancer cell line *in vivo*. In Figure 4.19 the control was not grown sufficiently therefore, the absence of sufficient growth in the control, as measured by the increase in the number of cells, meant that it was not possible to attain a definite conclusion. This could infer that the Tet system is leaking and *SPO11* expression was not switched off completely; this would explain the lack of growth in the control owing to the expression of *SPO11*cDNA, which might have negatively influenced cell proliferation. To advance this work, a control line should be developed which contains the Tet system without the SPO11 open reading frame. If the cells remained impaired in their proliferative potential, then the cause of the reduced proliferation is not due to SPO11, but more likely it is a simply technical issue.

In Chapter 3, *SPO11*-depleted SW480 and HCT116 cells demonstrated a significant decrease in cell doubling times, suggesting that *SPO11* depletion inhibits colorectal cancer cell proliferation. These results imply that *SPO11* expression offers a proliferative advantage, however, this suggests there may be a biological threshold at which a specific amount of SPO11 protein is sufficient to confer a proliferative advantage. Janic *et al.,* (2010) studied the ectopic expression of germ-line genes in *Drosophila* tumours and concluded that the initiation and activation of these genes provides a proliferative advantage in cancer cells. This supports the theory of soma-to-germline transformation realized to carcinogenic processes, which causes the activation of germ-line genes, which includes CTAs (McFarlane *et al*., 2014). In this specific situation, *SPO11* might be activated in both SW480 and HCT116 cells as part of this transformation, which might contribute to their acquisition of a proliferative advantage.
As mentioned in Chapter 3, SPO11 is homologous to the topoisomerase subunit TopoVI A in archaebacteria. This protein is structurally related to the Type IIB family of eukaryotic topoisomerases (Corbett *et al*., 2007). Rouzeau and Cordelières (2012) found that Topo IIα proteins are localised to the centromere to undertake normal decatenation during replication by BLM and PICH.

As a homolog of the TopoII B protein subunit, it is possible that the BLM protein will be able to recognise SPO11 in the same manner as the topoisomerase. It may be that in cancer cells, BLM is able to colocalize with the SPO11 protein, and use this mechanism to recruit SPO11 to the chromosomes.

The finding that further elevation in *SPO11* does not stimulate hyper proliferation suggests other factors might be rate limiting. This could be BLM level. However, a topoispmerase VIB-like partner protein for SPO11 in meiosis was recently identified, TOPOVIBL (Robert *et al*. 2016; Vrielynck *et al*. 2016) it could be that *SPO11* requires TopoVIBL as a partner to drive mitotic proliferation activity. TopoVIBL levels might be the limiting factors and so it could be worth studding this possibility further, this was not done as TopoVIBL was only identified as a *SPO11* binding partner late in this work. It would be interesting to determine if SPO11 and TopoVIBL co-purified in in human cancer cells and have Topoisomerase activity.

5. Generating a knockout SPO11 cell line

5.1 Introduction

CRISPR/Cas9 is an advanced gene editing system that is widely used in biotechnology for generating gene knockout (KO) cell lines and mutant models for mice and other organisms. It is derived from the immunological systems of archaea and bacteria (Riordan *et al*., 2015). CRISPR/Cas9 gene KO is achieved after transfection of the target cells with a plasmid that has two independent genes; one codes for a short CRISPR RNA molecule (crRNA), also called a guide RNA (gRNA) specific for the genomic region of interest (typically 20 nucleotides long; see Figure 5.1) and the other Cas9 nuclease. The Cas9 nuclease can then target the genomic DNA at these pre-determined gRNA sequences. This process requires a trans-activating crRNA (tracrRNA) that is responsible for recruiting the gRNA into the Cas9 complex (Deltcheva *et al*., 2011). The gRNA-DNA base pairing and a protospacer-adjacent motif (PAM) determine the recognition of the cleavage sites. The PAM is a three-nucleotide sequence (NGG) that is juxtaposed to the complementary DNA region (Marraffini & Sontheimer, 2010). It must be noted that a single gRNA has the potential to recruit Cas9 to targeted genomic sites; as a result, DNA DSBs can be generated in DNA at very specific locus (Jinek *et al*., 2012). The CRISPR/Cas9 system is currently in use for site-specific genome editing purposes in a wide range of organisms and cell types (Gratz *et al*., 2013; Mali *et al*., 2013).

Cas9 nucleases cleave both strands of genomic DNA, and the break can be corrected by both homology directed repair (HDR) pathways and non-homologous end joining (NHEJ) pathways. Modified Cas9, which is known as Cas9D10A, creates a single-strand nick, which inhibits the activation of NHEJ (Mou *et al*., 2015). The DSB is made further usable by the targeted integration of a homologous construct that contains both fluorescent and antibiotic marker cassettes. This leads to clonal selection and generation of stable cell lines. During homologous recombination, the homologous donor DNA permits the insertion of new sequence information into the break site.

The aim of the work described in this chapter is to knock out both the endogenous genomic *SPO11* genes in HCT116 cancer cells containing the Dox regulatable *SPO11* (see Chapter 4) (HCT116 has two alleles of *SPO11*), and to see whether knocking out both copies of *SPO11*

from HCT116 alters the characteristics of this cancer cell line when the exogenous regulatable *SPO11* is turned off (i.e. no Dox). Previous attempts to knock out *SPO11* from different cancer cells without an exogenous regulatable *SPO11* were unsuccessful (Aldeailej, PhD thesis, Bangor University, 2013) and resulted only in the generation of heterozygote clones. This in itself might suggest that *SPO11* is required for the proliferation of cancer cells, a theory supported by the siRNA depletion of *SPO11* seen in Chapter 3 where the lack of *SPO11* led to a dramatic reduction in cell growth. Having generated exogenously regulatable *SPO11* clones was the aim to generate clones without genomic *SPO11* copies.

Genomic copies of *SPO11* were targeted with a gRNA directed towards the intron 1 region in combination with a donor plasmid containing homologous sequences that flanked exon 1 in addition to a hygromycin-resistant cassette as described in Figure 5.2. In this manner, the CRISPR/Cas9 technology allowed for the site-specific targeting of genomic exon 1 without affecting the cDNA constructs present in the clones.

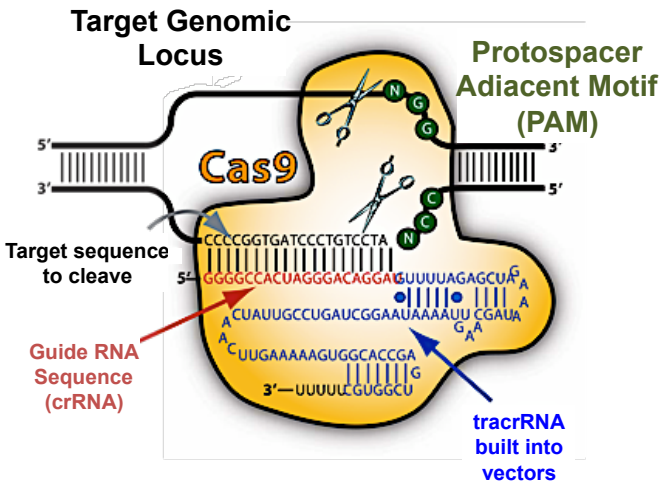

Figure 5.1 A schematic showing the mechanism of CRISPR/Cas9 genomic DNA cleavage. The guide RNA (gRNA) sequence (shown in red) that was bound to single gRNA (tracerRNA-crRNA chimera, shown in blue) binds to complementary bases at a specific locus and recruits the Cas9 nuclease (shown in orange), which cleaves the DNA at the gRNA-highlighted site, target loucus containing a protospacer adaptor motif (PAM) of sequence (NGG) (SBI system Biosciences).

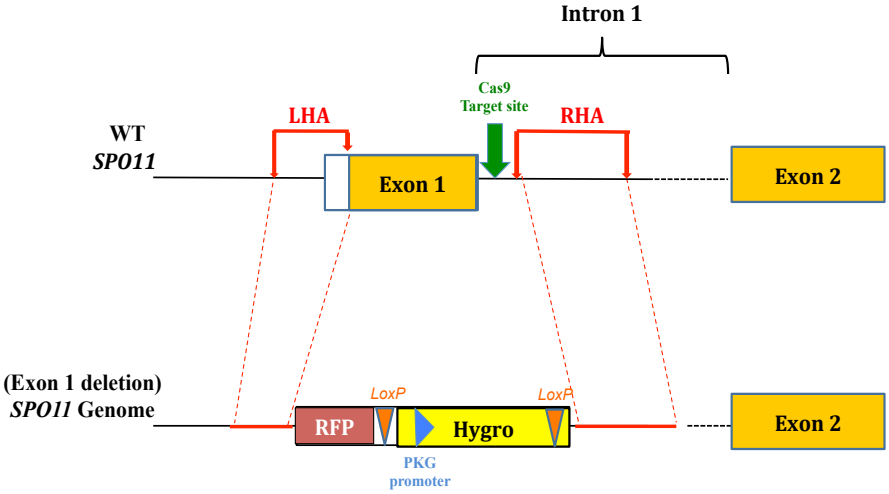

Figure 5.2 Schematic of CRISPR targeting of *SPO11* Exon 1. A region of the human (*SPO11* intron 1) locus is targeted by a gRNA+Cas9 (in green) in order to insert a RFP-hygromycin cassette that present in the Donor vector which contains homologous arms (LHA and RHA) at the 5' and 3' end of the expression cassette, each arm include sequence homologous to the genomic DNA surrounding the targeted locus. The homology arms were designed to be close to cut site for efficient recombination to occur.

5.2 *SPO11* gene disrupted using the CRISPR/Cas9 technique

The reagents and constructs for the CRISPR/Cas9 KO were used as described in Figure 5.1. The gRNA targeting sequence was directed towards intron 1 of *SPO11* (Figure 5.3) was cloned into a vector containing the expression cassette for the Cas9 protein. The CRISPR/Cas9 cuts the double-stranded DNA at the targeting site. A donor template DNA vector was created (www.Origene.com/Blue Heron) with a RFP-hygromycin cassette flanked by the homologous arms (see Figure 5.4) of the chosen cleavage site, which provided a template for the homologous repair. The functional cassette was incorporated into the genome when gRNA (1) and donor (2) DNA were co-transfected in to HCT116-Tet-On3G.15/*SPO11* cell line (see Figure 5.5; www.origene.com).

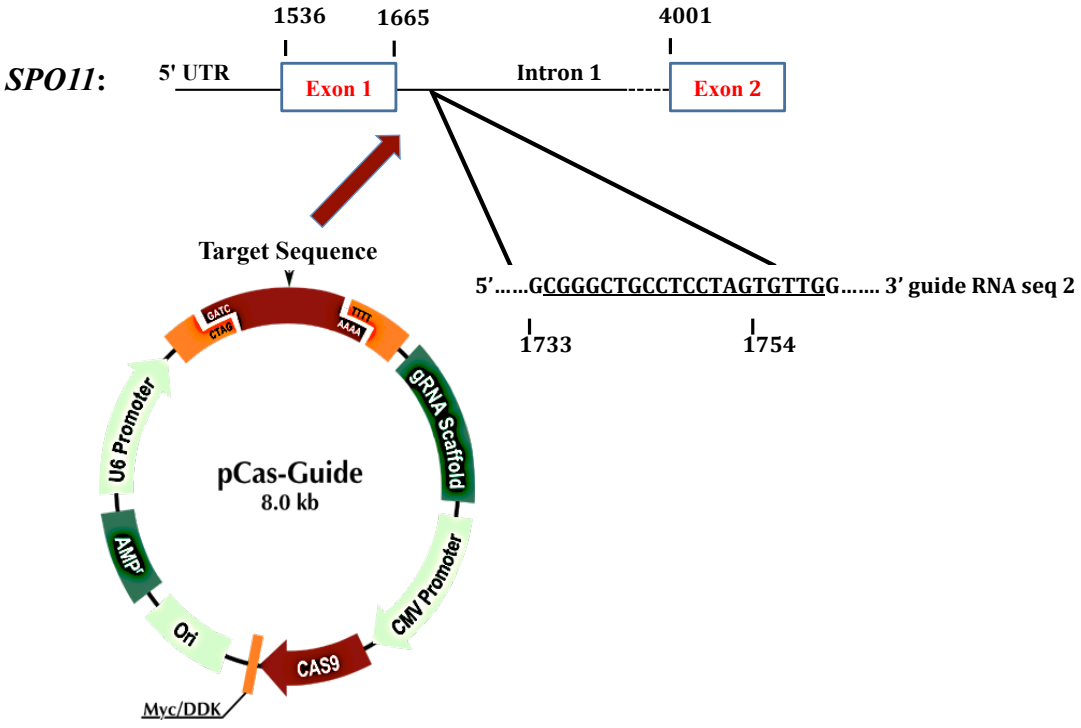

Figure 5.3 pCas-guide vector. The guide RNA (gRNA) sequence to be targeted within intron 1 of *SPO11* was cloned into a vector that also contained an expression cassette for Cas9 (indicated by a CAS9 brown arrow). The numbers denote the relative positions of *SPO11* exons, 5' untranslated region (5'UTR), intron 1 and the gRNA sequence (relative to NC_018931, region 55804500 to 55820180, and 1-15681 bp respectively).

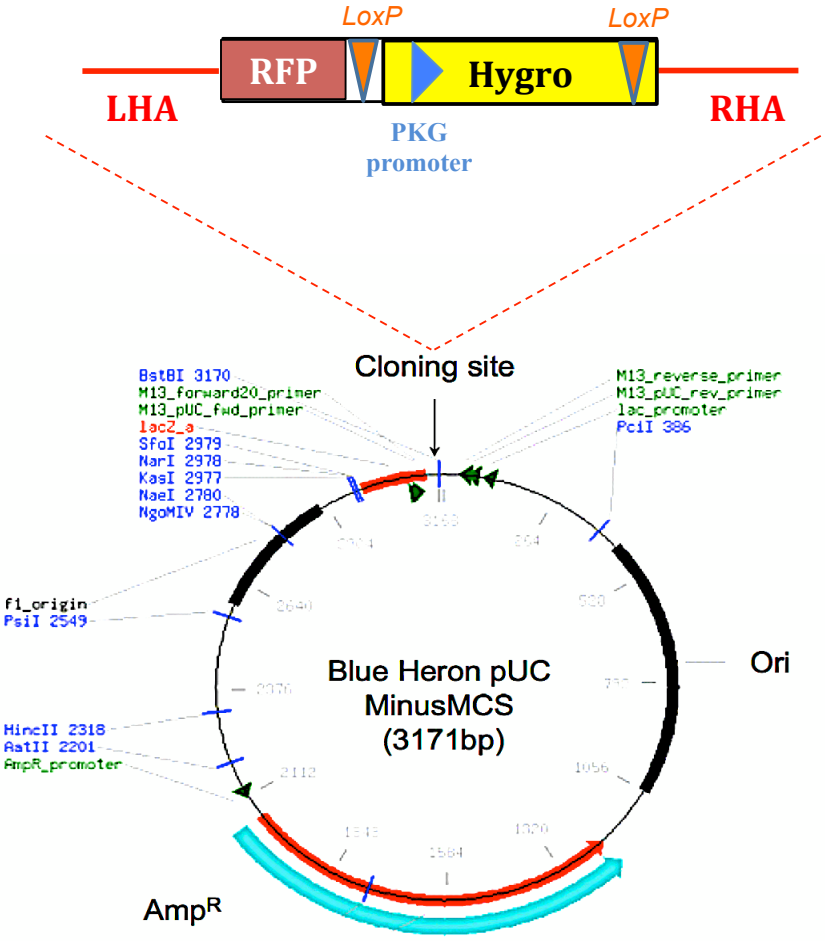

Figure 5.4 Donor vector map: Blue Heron pUC minusMCS. The plasmid containing both sequences flanking exon 1 and a RFP-hygromycin-resistant cassette, HR targeting vector serve as the donor template to induce HR in cells that have been targeted at a specific locus using CRISPR/Cas9. The 5' and 3' homologous sequences exactly homologous to the template (genomic sequence) with the DSB, and preferably directly adjacent to the actual DSB site. Left and right Homology arm design (LHR and RHR) is shown in red (Adapted from Blue Heron Biotechnology-the Gene Synthesis Company; origene.com).

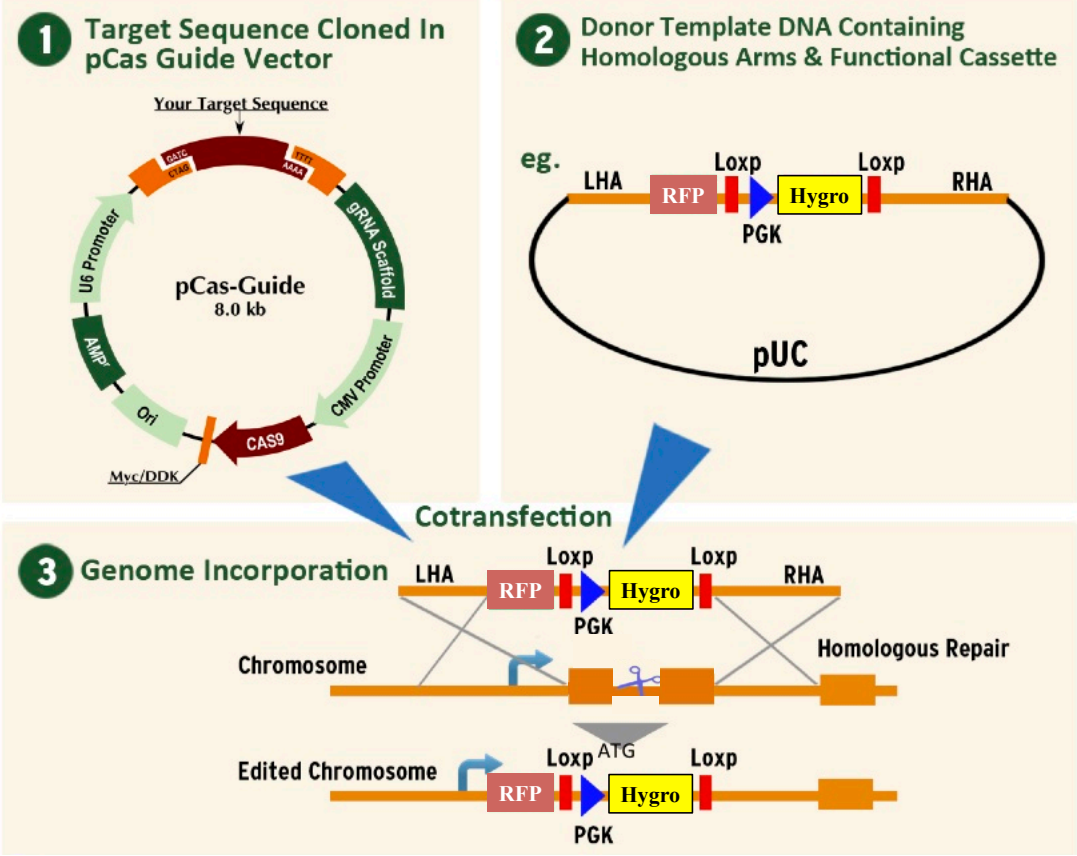

Figure 5.5 Example of Genome editing using Cas9/CRISPR. (1) A guide RNA (gRNA) vector targeting the coding sequence was cloned into a vector containing the expression cassette for the Cas9 protein. CRISPR/Cas9 cuts the double-stranded DNA at the target site. (2) A donor template DNA vector was created with a RFP-hygromycin cassette flanked by the homologous arms of the chosen cleavage site, which provided a template for homologous repair. (3) The functional cassette was incorporated into the genome when (1) + (2) were co-transfected. Adapted from the Origene product information website (www.origene.com).

5.3 Results

5.3.1 Genomic PCR analysis

A CRISPR/Cas9 system was adapted to knock out the *SPO11* gene in two cell lines HCT116-Tet-On 3G.15/*SPO11* and HeLa-Tet-On 3G/*SPO11*. The cells were transfected chemically using Xfect transfection reagent (see Section 2.10) with a specific gRNA construct and donor plasmid, as described above, which resulted in the selection of a number of hygromycin-resistant HCT116-Tet-On-3G.15/*SPO11* clones. However, the HeLa-Tet-On3G/*SPO11* clones did not survive for subsequent PCR analysis. These cells grew extremely slowly in comparison with the parental cells or the cells transfected with a scramble-control gRNA construct during the hygromycin selection period, so there was no way to expand the clones to make stocks. HCT116-TetOn3G.15/*SPO11* whole cell extracts (WCEs) from individual hygromycin-resistant clones were collected and subjected to western blot analysis as well as qRT-PCR and RT-PCR analysis. Genomic DNA was also extracted after transfection using Qiagen DNeasy blood and tissue kit. PCR analysis was conducted to verify the correct RFP-hygromycin integration in the genome and to amplify the targeted region using primers within the deletion region. The primer pair (2) R: exon-1/F: 5'UTR (Figure 5.6, 5.7) did not appear to amplify any product, even in the heterozygote clones. This was most likely due to technical issues (annealing temperature for example). R: Exon-1 primer is the complementary reverse sequence of F: Exon-1 primer, and this primer (F: Exon-1) has been successfully used together with R: Int-1 (primer pair -1) to amplify products in the heterozygote clones. In addition primer pair (3) F: 5'UTR/R: Int-1 is also sufficient as a PCR screen as the primers are situated outside both homology arms and can detect untargeted CRISPR/CAS9 events in the heterozygote clones. Primer pair (6) F: Exo1/R: Exon-13 was used to amplify the *SPO11* cDNA that is expressed from the transfected construct pTRE3G::*SPO11*(see Figure 5.6, 5.7) see also the primer sets in Table 2.13. Genomic DNA PCR analyses were performed on all the hygromycin-resistant clones obtained, and both wild-type and truncated genomic fragments were resolved by gel electrophoresis and each PCR product was sequenced. Of the 162-hygromycin positive clones obtained (Figure 5.8), all of which were screened with PCR primer pairs represented in Figure 5.6, 5.7 (sets 1-6). Of these clones only 4 were positively identified as *SPO11*$^{-/-}$ homozygote knockout clones (three independent genomic extractions of three of these clones and subsequent PCR analysis and confirmation by sequencing); KO 21, KO 31, KO 116. A fourth clone, clone KO 86 grew

extremely slowly and although further genomic extractions were eventually performed on these cells, due to the speed of growth it was difficult to use these cells for subsequent experimental analysis as well as their poor recovery from liquid nitrogen stocks. Of the heterozygote clones obtained, one was randomly selected and used for further analysis alongside the KO clones. Clone 114 only has one copy of wild-type *SPO11*, with the RFP-hygromycin cassette replacing the other copy of *SPO11* (see Figure 5.8). Targeted deletions were further verified, and fragments generated by PCR were isolated and sequenced to confirm proper integration. Sequencing showed that exon 1 of *SPO11* was replaced with the RFP-hygromycin cassette in clones KO 21, KO 31, KO 116.

5.3.2. qRT-PCR and western blot analysis of *SPO11* gene expression in HCT116-TetOn3G.15/*SPO11* cells after CRISPR/Cas9 targeting

Western blot and qRT-PCR analyses were carried out to assess the level of *SPO11* expression in the CRISPR cell lines (i.e. clones KO 21 and KO 31) after induction with doxycycline. qRT-PCR reactions were carried out in triplicate in a total volume of 20 µl using a CFX96 real-time detection system (Bio-Rad C1000 thermal cycler) with Life Technologies TaqMan Gene Expression Master Mix and primer/probe sets for *SPO11*. The results were normalised against the qRT-PCR results of two reference genes, *ACTB* and *GAPDH,* and the results are displayed in Figure 5.9. The qRT-PCR results showed an obvious difference when comparing HCT116-Tet-On3G.15/*SPO11* to clone number 31 in the presence or absence of doxycycline, but which showed no notable reductions at the SPO11 protein level in any of the clones (see Figure 5.10).

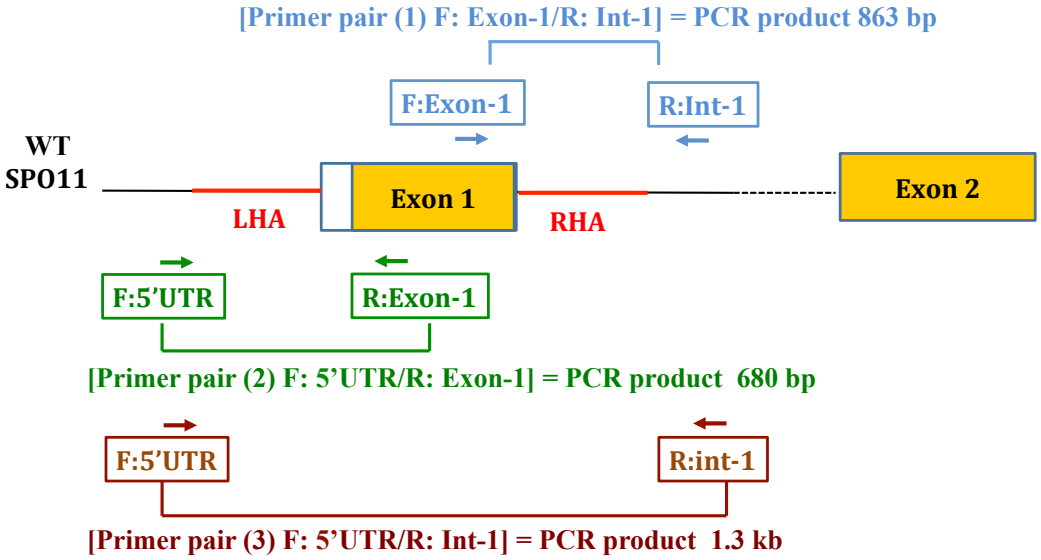

Figure 5.6 Schematic of potential PCR products obtained using these primer sets. Shows the WT *SPO11* genomic locus and PCR products obtained with primer set (1) (2) and (3).

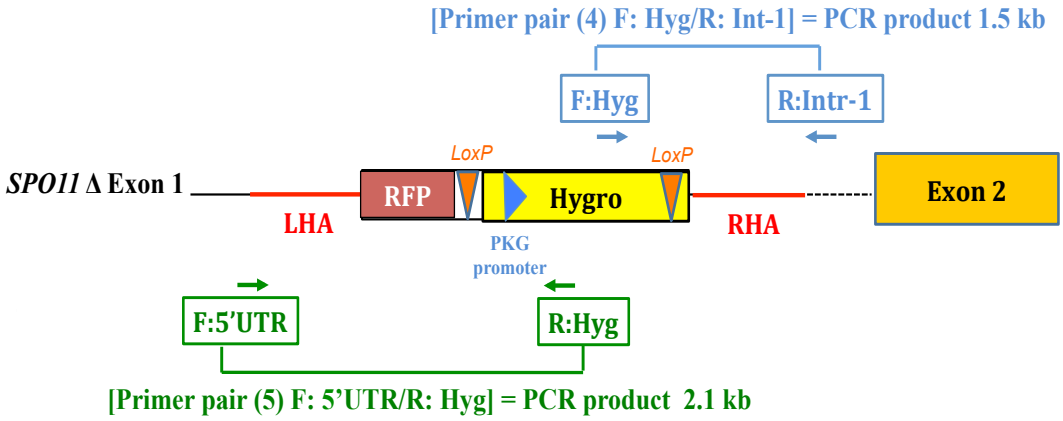

Figure 5.7 Schematic of potential PCR. Shows the integration of the RFP-hygromycin cassettes and the PCR products that should be obtained with primer sets (4) and (5).

(A)

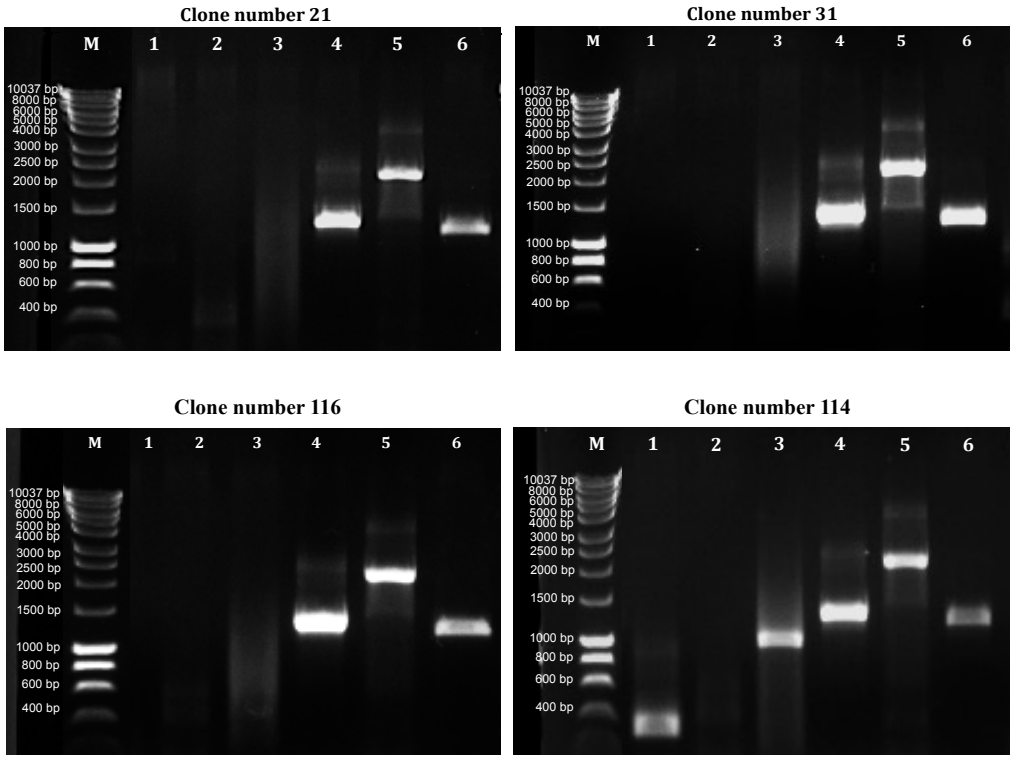

(B)

Total 162 clones	Number of Clones Obtained (% total)
Died before PCR stage and no stocks	20 (12.3%)
WT (F: Exo-1/R:Int1 = Exon 1 positive/correct size PCR product) no intronic DNA lost	95 (58.6%)
Targeted clone (F: Exo-1/R: Int-1 positive PCR product BUT smaller than expected) 500bp DNA lost/no cassette integrated	14 (8.6%)
Targeted clone (F: Exo-1/R:Int-1 positive = WT correct size + smaller band) 1 WT copy/1 500bp intron lost so no cassette integrated	14 (8.6%)
Potential KO (first round screening) Re-test, re extraction of genomic DNA twice more (and integrated cassette sequenced)	19 (11.72%) 4 clones KO (2.4%)

Figure 5.8 PCR analyses of potential *SPO11* knockout (KO) clones. (a) Agarose gels showing the PCR analysis of the genomic DNA extracted from a number of hygromycin-resistant clones (21, 31, 116 and 114). Different primer sets were used to detect the correct integration: (1) F: Exon-1/R: Int-1 = 863 bp, (2) R: exon-1/F: 5'UTR = 680 bp, (3) F: 5'UTR/R: Int-1= 1.5 kb, (4) F: Hyg-R: Int-1 = 1.3 kb, (5) R: Hyg/F: 5'UTR = 2.1 kb and (6) F: Exo1-R: Exon-13 = 1.2 kb, while M = 1 kb Hyper Ladder. (b) Table showing the total number of clones obtained and a summary of various PCR products identified in these clones, as well as percentage of these different clones obtained.

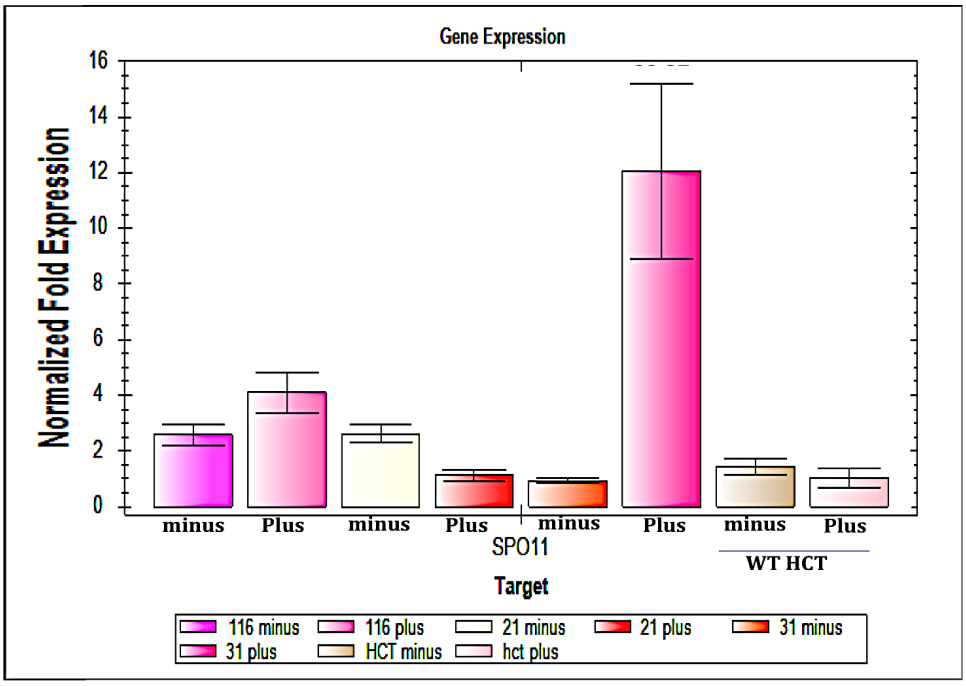

Figure 5.9 Quantitative RT-qPCR analyses of *SPO11* gene expression in HCT116-Tet-On3G.15/*SPO11* cells after CRISPR. Clone KO 21, clone KO 31 and KO 116 were compared with HCT116 (WT). The Bio-Rad CFX manager was used to analyse the data. The error bars show the standard error for three replicates. Results were normalised to a combination of two endogenous reference genes (*GAPDH, ACTB*). The error bars show the mean standard error.

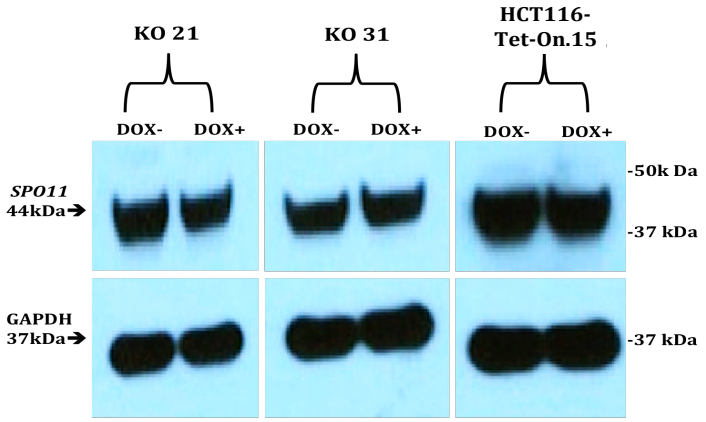

Figure 5.10 Western blot analyses of SPO11 proteins in HCT116-TetOn3G.15/*SPO11* cells after CRISPR/Cas9 targeting. The western blot analysis images are representative of three repeats. SPO11 protein levels are shown with and without doxycycline (48-hr induction) for clones KO 31, KO 21 comparing with HCT116-Tet-On.15 cell as control, showing no change in SPO11 protein levels. Loading control: GAPDH.

5.3.3. Growth curve analysis

HCT116-Tet-On3G.15/*SPO11* cells were grown in the presence of doxycycline unless otherwise stated. For growth curve analysis, the clones were seeded into 6-well plates with 50 x 10^3 cells. After 24 hours, half of the plates for each clone were induced with 1 μg/ml of doxycycline, while the other half were grown in tetracycline-free media. A sufficient number of 6-well plates were set up for each clone so that the samples with and without doxycycline could be analysed each day for the duration of the experiment. The cells were counted using trypan blue, a blue dye which is taken up only by dead cells. The cells were counted using either a hemocytometer or an automatic cell counter. Cell count curves represent the total number of cells +/- doxycycline over a 5-day period for clones KO 21, KO 31 and heterozygote 114. The number of cells in the absence of doxycycline appeared to be lower than that of cells grown in the presence of doxycycline. HCT116-TetOn3G.15 cell growth was unaffected by doxycycline (see Figure 5.11).

5.3.4 Analysis of the growth and protein levels of HCT116-TetOn3G/*SPO11* clones over two weeks

To determine the effects of the prolonged depletion of *SPO11* on the growth of cancer cells, a growth curve analysis was carried out on HCT116-TetOn3G.15/*SPO11* clones KO 21, KO 31 and heterozygote 114. The clones were cultured in tetracycline-free serum-containing media (also without doxycycline) for 2 weeks and were then seeded in 6-well plates with 75 x 10^3 cells concentration. The cells were harvested every day and counted (using the method described above) using trypan blue. The cell count curves (shown in Figure 5.12) represent the total number of cells each day throughout the experiment. The cell counts for KO 21, KO 31 and heterozygote 114 were much lower than the number of HCT116-TetOn3G.15 control cells. Images were taken of all clones just before the cells were harvested (see Figure 5.13). To determine SPO11 protein levels, western blot analysis was carried out on day 7 samples of all the clones tested and this result showed a significant decrease of SPO11 proteins when compared with the untreated HCT116-TetOn3G.15/*SPO11* cells (Figure 5.14).

5.3.5 Genomic DNA (gDNA) standard curve for HCT116

A genomic DNA standard curve, established using HCT116 gDNA, can be used to calculate *SPO11* copy numbers in the knockout clones generated during this project. HCT116 gDNA contains two copies of *SPO11*. Given that the mass of the gDNA per genome can be converted to picogram units using the formula (see Material and Methods 2.17.2), and the size of the haploid human genome is estimated to be 3.4 x 10^9 Celera [Celera Genomics estimate taken from the Applied Biosystems site which is approximately 3 billion bp (haploid)], therefore, after calculated It was know that 3.3 pg of gDNA should contain 1 copy of *SPO11*. A primer pair set flanking the CRISPR/Cas9 target site in intron 1 (Figure 5.16: purple) was designed, (forward primer [1693F] and Reverse Primer [1820R] = product 127 bp) and a standard curve was set up with HCT116 WT gDNA ranging from 100,000 to 0.1 copies of *SPO11* (Figure 5.15). This standard curve was used for comparison with a known concentration of CRISPR gDNA clones (300 ng of 21 "KO", 31 "KO" and 114 "heterozygote") in order to compare g*SPO11* intron 1 targeted regions between the different CRISPR/Cas9 targeted cell lines. The WT (*SPO11*+/+) HCT116 cells should contain 2 copies of the targeted region, the heterozygote should contain 1 copy (*SPO11*+/-) and the KO clones should have none (*SPO11*-/-). Figure 5.17 shows the Cq values for g*SPO11* intron 1 copy number of (a) HCT116 (WT) the Cq values was between 100,000 and 10,000 (between log 4-5) and (b) the heterozygote 114 clones the Cq values between 10,000 and 1,000 (between log 3 and 4). The result suggests that there is a log difference in the copy number of the g*SPO11* intron 1 region between HCT116 WT and the heterozygote 114 clones. On the other hand, the Cq values for the knockout (KO) *SPO11* cell lines (clones KO 21, KO 31 and KO 116) the Cq values that ranged between log 0 and 2; there is a two-log difference between the heterozygote and WT HCT116 cells and these clones (Figure 5.18).

KO 31

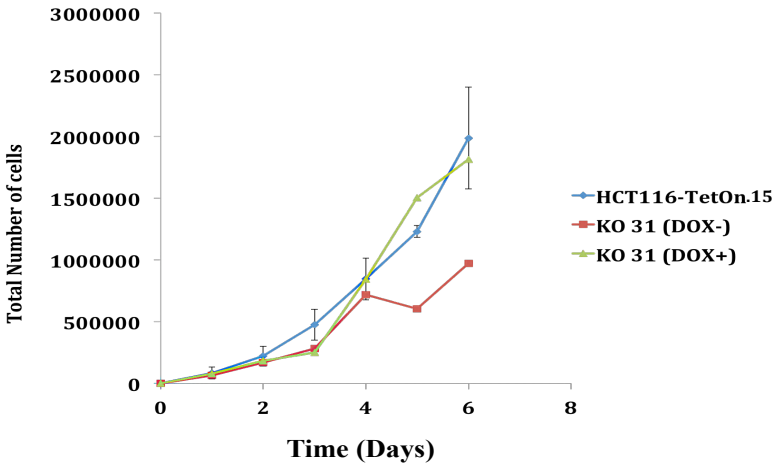

KO 21

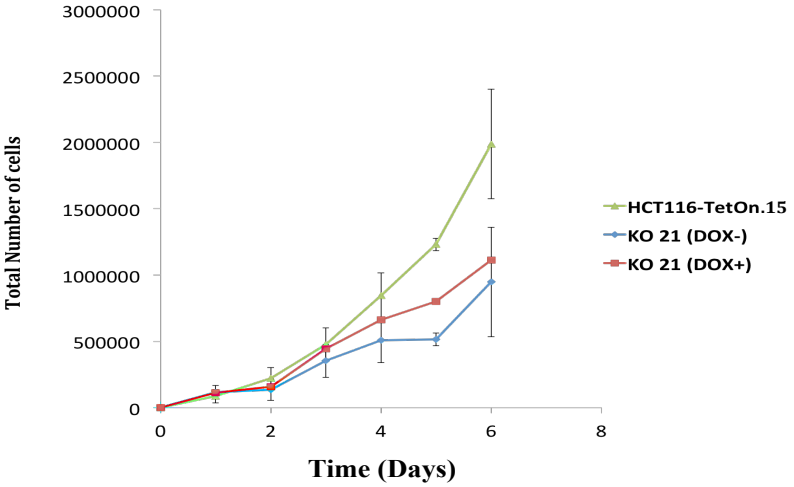

Heterozygote 114

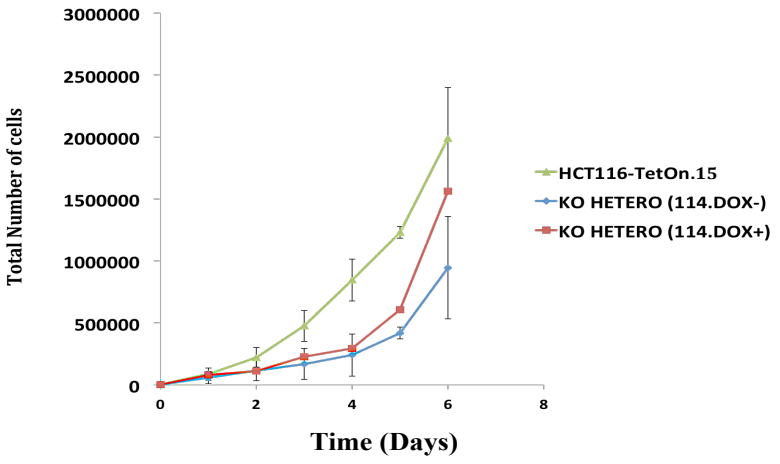

Figure 5.11 Growth analysis of HCT116-TetOn3G.15/*SPO11* KO clones. The growth and proliferation with and without doxycycline of HCT116-TetOn3G.15/*SPO11* clones KO 21, KO 31 and heterozygote 114 compared to HCT116-TetOn3G.15 parental cells. The error bars represent the standard deviation (n=3) for the total number of cells.

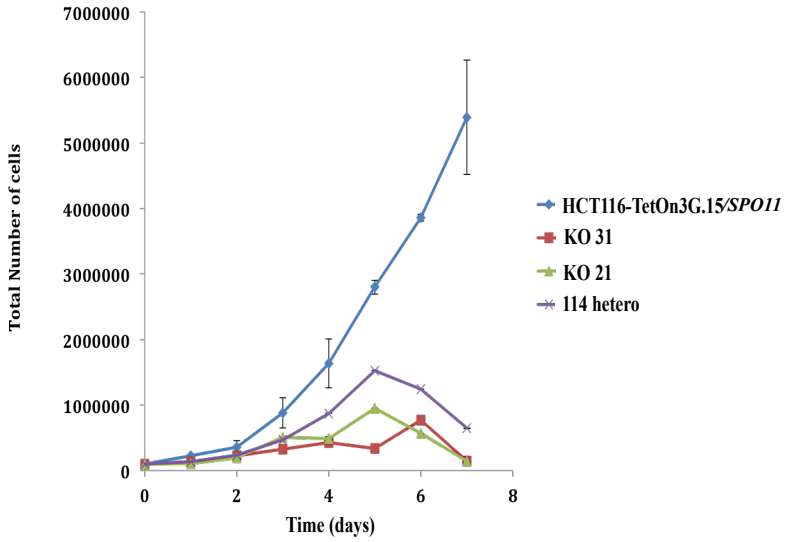

Figure 5.12 The growth and proliferation of HCT116-TetOn3G.15/*SPO11* knockout (KO) *SPO11* cells: KO 21, KO 31 and 114 heterozygote compared to controls. Knockout (KO) SPO11 cells: KO 21, KO 31 and heterozygote 114. The clones were cultured in tetracycline-free serum (no doxycycline) for 2 weeks and compared to the HCT116-TetOn3G.15/*SPO11* cells. The error bars represent the standard deviation (n=3) for the total number of cells.

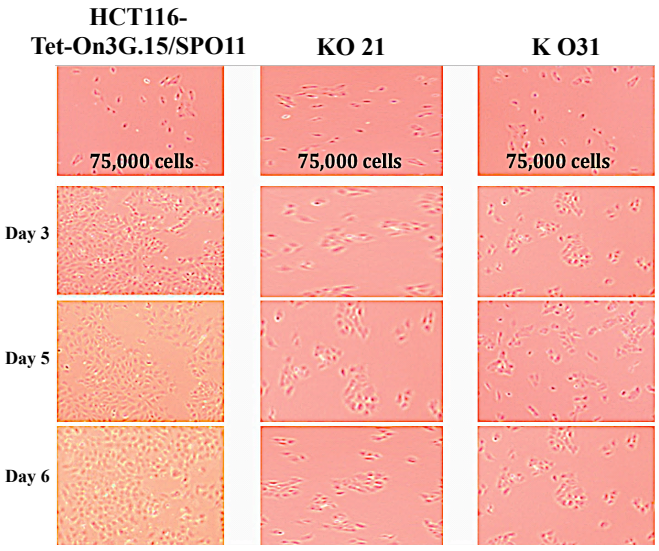

Figure 5.13 Growth of the HCT116-TetOn3G.15 cells compared to knockout (KO) *SPO11* cells: KO 21 and KO 31. Cells were grown in tetracycline-free serum media (no doxycycline) for 2 weeks then 75,000 cells were seeded to 6-well plates. For all cell lines, the images were taken over a period of 6 days just prior to harvesting. The proliferation of the *SPO11* KO cells was reduced compared to the HCT116-TetOn3G.15/SPO11 cells.

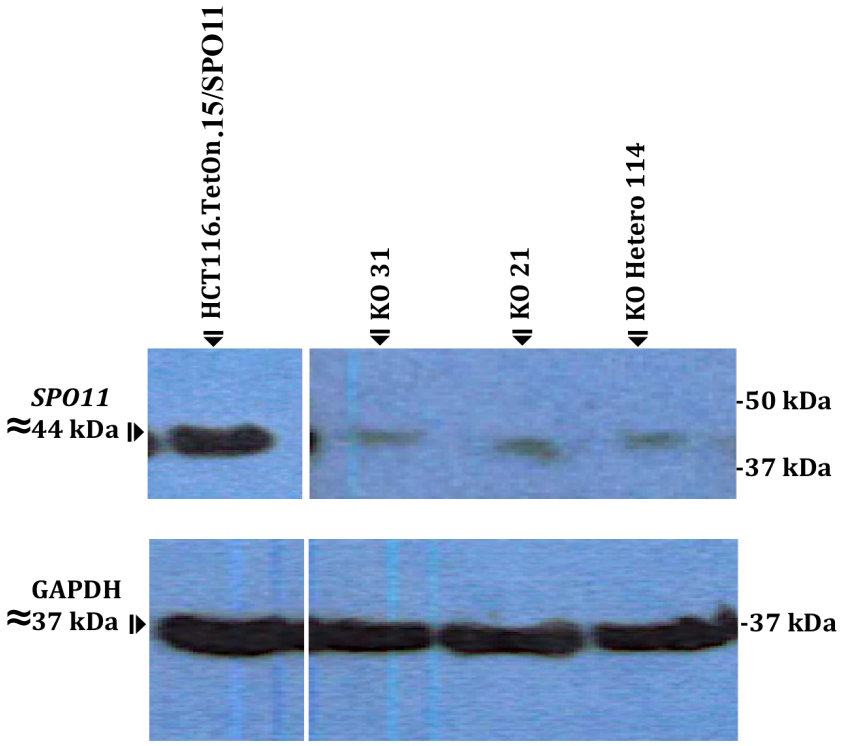

Figure 5.14 Western blot analysis of SPO11 protein in HCT116-TetOn3G.15/*SPO11* cells after CRISPR. KO 31, KO 21 and heterozygote 114 cells showed reduction in protein levels compared with control HCT116-TetOn3G.15/*SPO11* cells. The growth rate of these clones were assessed by culturing in tetracycline-free serum (no doxycycline) for 2 weeks after that the cells were lysed in day 7. Loading was controlled by GAPDH.

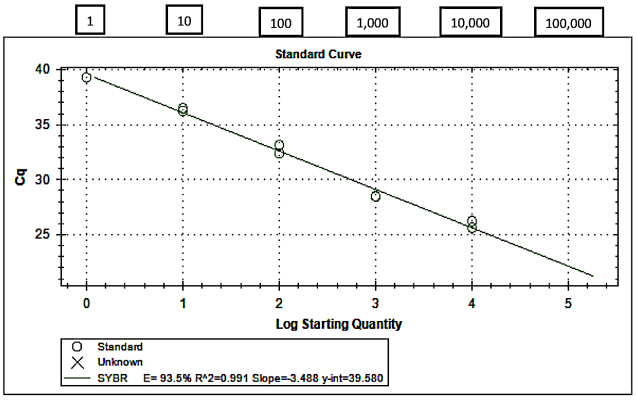

Figure 5.15 Samples from the qPCR standard curve for HCT116 gDNA. Cq values for the HCT116 gDNA standard curve. gDNA HCT116 was serially diluted five-fold to generate a template for the standard curve using the primer set illustrated in (b). Dilutions ranged from 5 = 100,000 copies of g*SPO11* equivalent to 330 ng gDNA, 4 = 10,000 copies, 3 = 1000 copies, 2 = 100 copies, 1 = 10 copies, 0 = 1 copy). The efficiency of the primer set was 93%. The standard curve amplifies a specific product (as determined by the sequencing the PCR product). This standard curve was used to compare the Cq values between knockout (KO) and heterozygote *SPO11* genomic DNA samples.

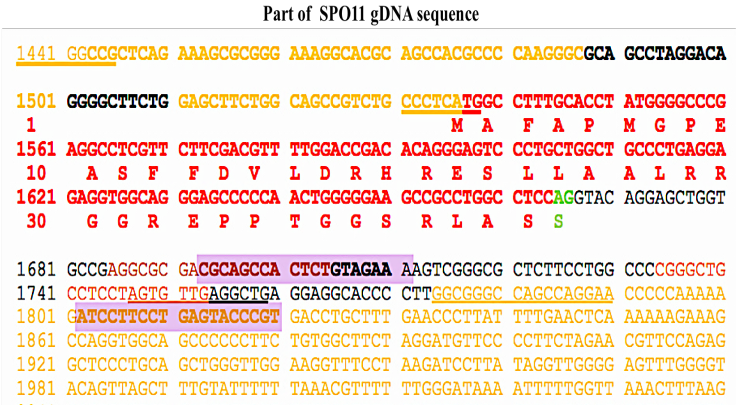

Figure 5.16. *SPO11 gDNA* sequence. Part of the SPO11 gDNA sequence illustrates the coding sequence (CDS) exon1 (red text) = 1536 bp to 1665 bp, yellow text = R/L homology arms (partial), forward primer (1693F) and reverse primer (1820R) (purple text) = product 127 bp, (1734-1753) = CRISPR/Cas9 targeted sequence cut at 1747 bp (+/-500 bp) missing in 1 copy of the heterozygote and both are missing in SPO11 KO clones.

(A)

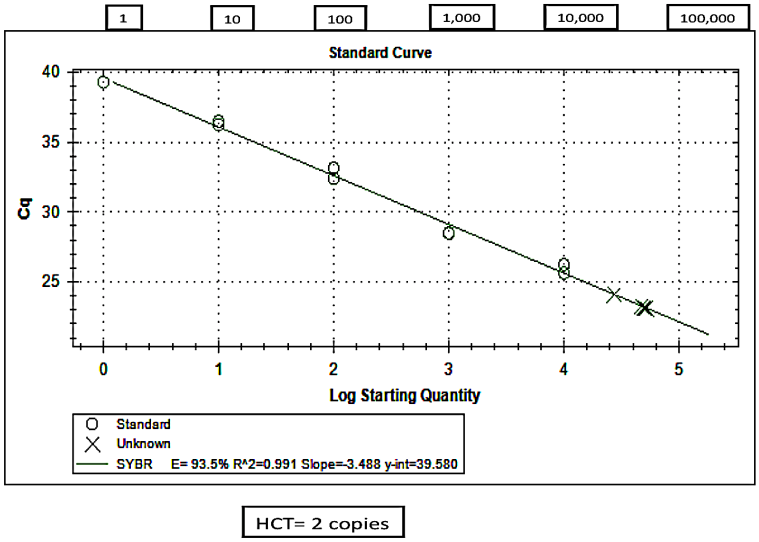

(B)

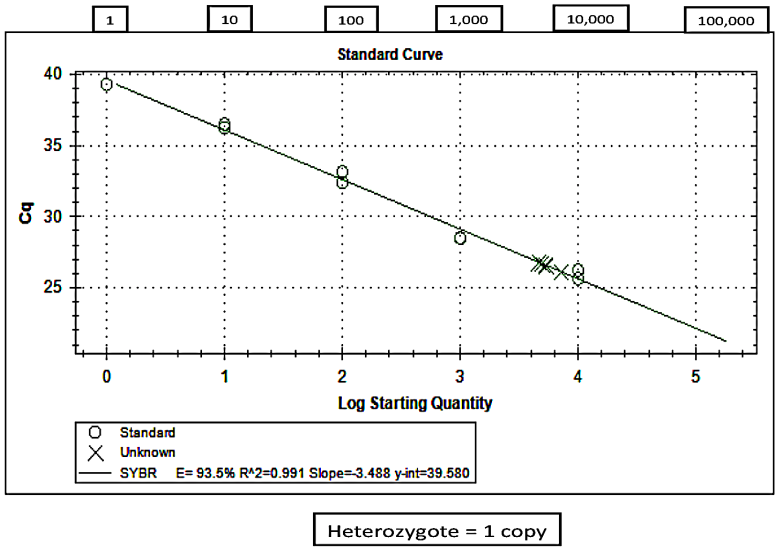

Figure 5.17 Cq values for g*SPO11* intron 1 copy number of (a) HCT116 and (b) the heterozygote 114 clones. (a) and (b) gDNA HCT116 standard curve (circles). (a) Cq values between 100,000 and 10,000 for HCT116 used at 300 ng gDNA per PCR reaction (between log 4-5) and (b) Heterozygote clone (300 ng gDNA used per PCR reaction) - Cq values between 10,000 and 1,000 (Hetero – between log 3 and 4). This result suggests that there is a log difference in the copy number of the g*SPO11* intron 1 region between HCT116 WT and the heterozygote 114 clones. Cell derived values are measured by 'X'.

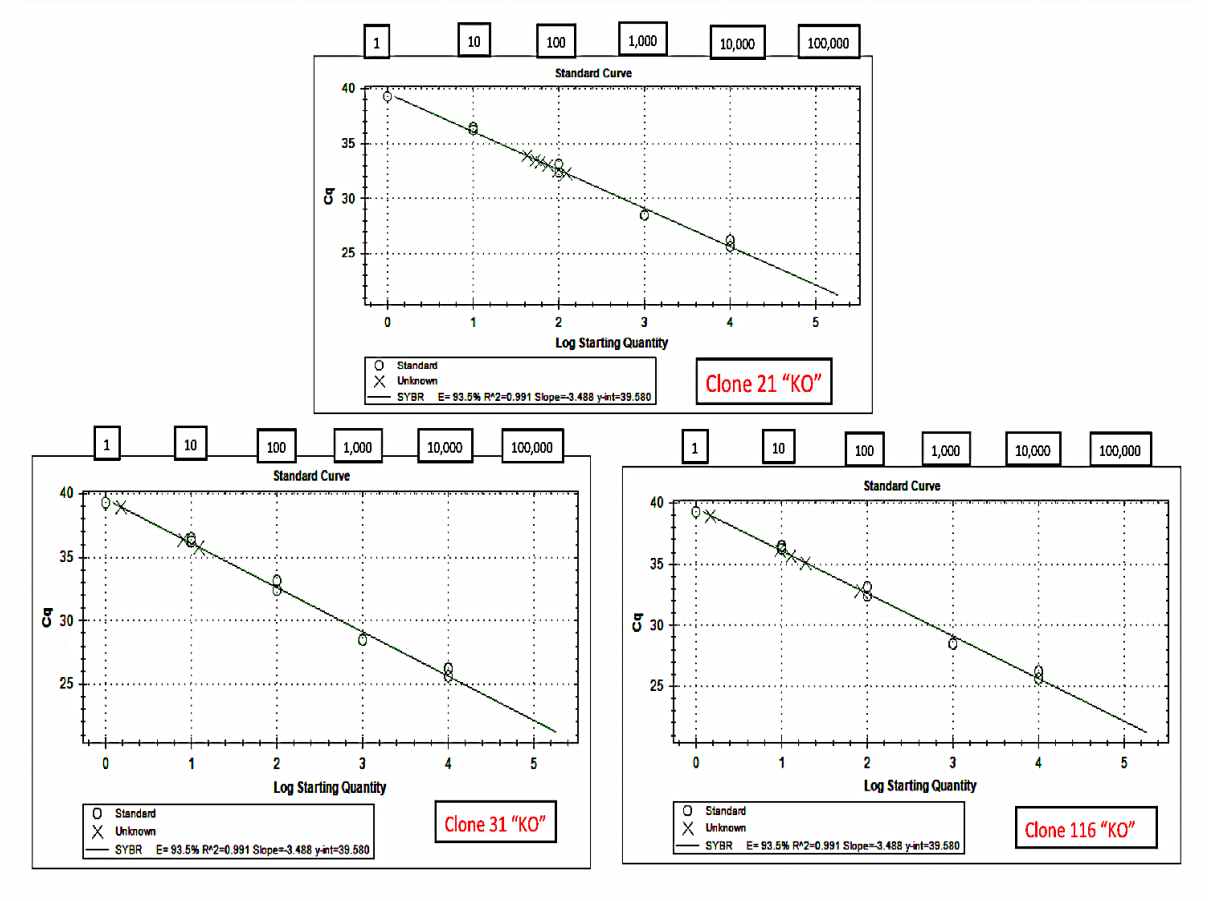

Figure 5.18 Cq values for the knockout (KO) *SPO11* cell lines. Clones KO 21, KO 31 and KO 116 gave Cq values that ranged between log 0 and 2; there is a two-log difference between the heterozygote and WT HCT116 cells and these clones. Clone derived value are measured with 'X'.

5.4 Short hairpin RNA (shRNA) depletion of SPO11

The study of *SPO11* gene function through RNA interference (RNAi) results in a significant inhibition of cell proliferation (Chapter 3). shRNA delivers short small interfering RNAs into targeted mammalian cells in a manner that is more effective when compared to other knockdown techniques (Moore *et al.,* 2010). To confirm our siRNA and our deletion observations it was opted for an inducible shRNA construct, which would target *SPO11* only in the presence of doxycyclin. HCT116 cells were transformed with viral vectors with constructs containing the transactivator, the TetOn tetracycline response element and different shRNA sequences against *SPO11*.

The different lineages were labelled "73"– targeting Exon 9, "13" – targeting Exon 10 and "93" – targeting Exon 12, depending on the *SPO11* shRNA sequence (Figure 5.19). The resultant cell lines were able to express *SPO11* shRNA in the presence of doxycycline (this was done collaboratively with Dr. Ellen Vernon)). HCT116 cells were incubated with negative control shRNA lentiviral particles or *SPO11* silencing shRNA lentiviral particles in collaboration with my colleague, Dr. Ellen Vernon; the results (Figure 5.20) show some of the cell lines obtained during the lentiviral particle transduction of HCT116 cells, as well as the selection, expansion and induction optimisation process. The cells were then treated with doxycycline in order to activate transcription of the shRNA or a scramble control. In addition, red fluorescent protein (RFP) antibody was used as a control for vector expression. Moreover, the *SPO11* mRNA level was assessed by qRT-PCR after 24 hours of doxycycline induction (Figure 5.21). Only cell lines showing significant reduction were kept and subsequent experiments were performed with these clones. *SPO11*shRNA-HCT116-93D showed a positive response.

The WCEs were prepared during doxycycline treatment and western blot carried out to ensure that successful SPO11 knockdown was achieved (Figure 5.22). As a result, significant SPO11 protein reduction was observed for HCT116 infected with *SPO11* shRNA-93 lentiviral particles in the presence of doxycycline. HCT116-*SPO11*shRNA-93 cells were plated (as described in the Methods and Materials section) for proliferation analysis as these cells showed the most significant reduction in both mRNA and protein levels.

Figure 5.23 represents the cell count for the total number of HCT116 cells induced with doxycycline (1 µg/mL) each day over a period of 7 days. The growth curves of this clone show a marked reduction in the proliferation rate under doxycycline-treated cells when compared with untreated cells. These results resemble the growth curves produced with *SPO11* siRNA-treated cells, as previously shown in Chapter 3.

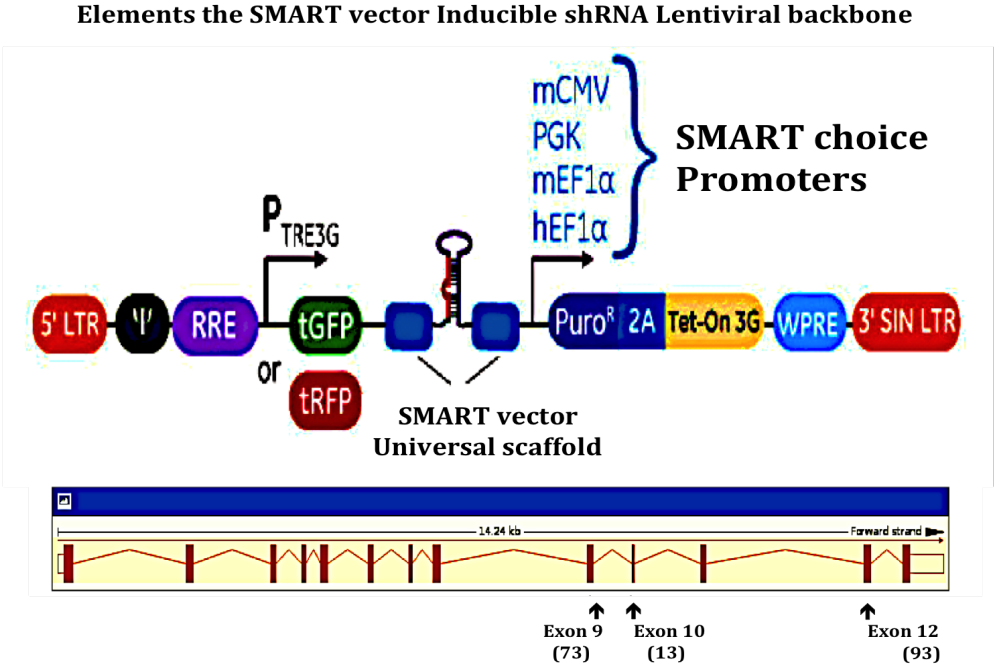

Figure 5.19 Elements of the SMART vector inducible lentiviral shRNA vector. shRNA targeting of *SPO11* with pre-made lentivirus against three separate regions in *SPO11* marked on gene map for exon 9, 10, 12. Adapted from GE healthcare (http:/dharmacon.gelifesciences.com/shrna/smartvector-inducible-lentiviral-shrna/).

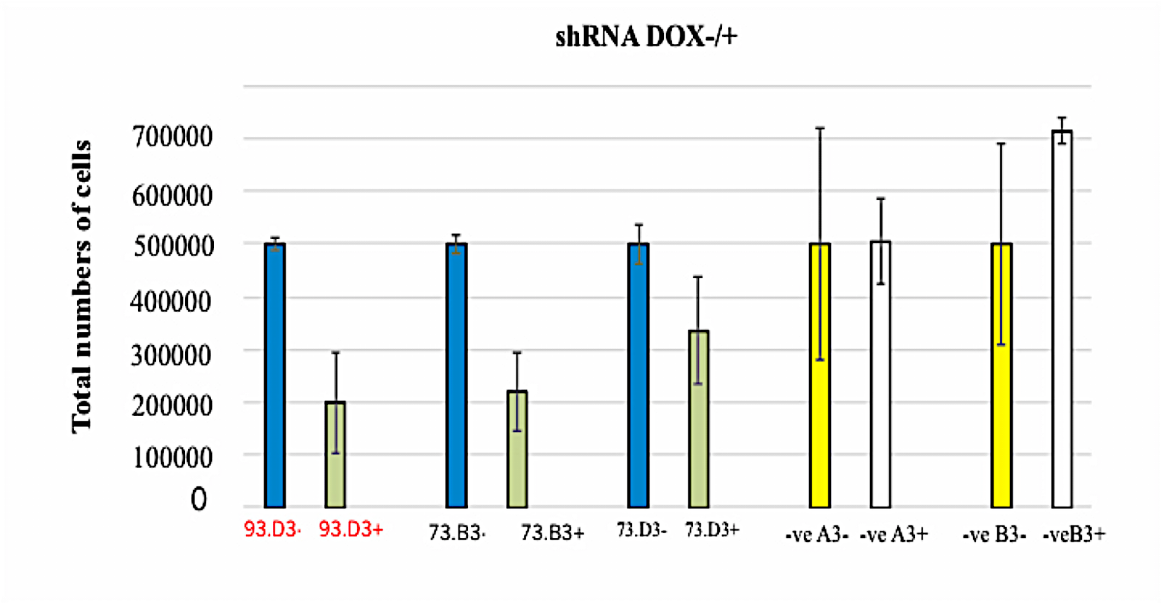

Figure 5.20 *SPO11* shRNA induction comparing total cell count relative to un-induced cells. The cell lines obtained during the selection, expansion and induction optimisation process using three different shRNA lentiviral particles (73 – targets Exon 9) – (93 – targets Exon 12) compared with negative control shRNA particles (-ve) with and without doxycycline for 72 hours. shRNA-HCT116-93D3- and shRNA-HCT116-73B3-induced cells show a marked reduction in the total number of cells when compared to their un-induced controls.

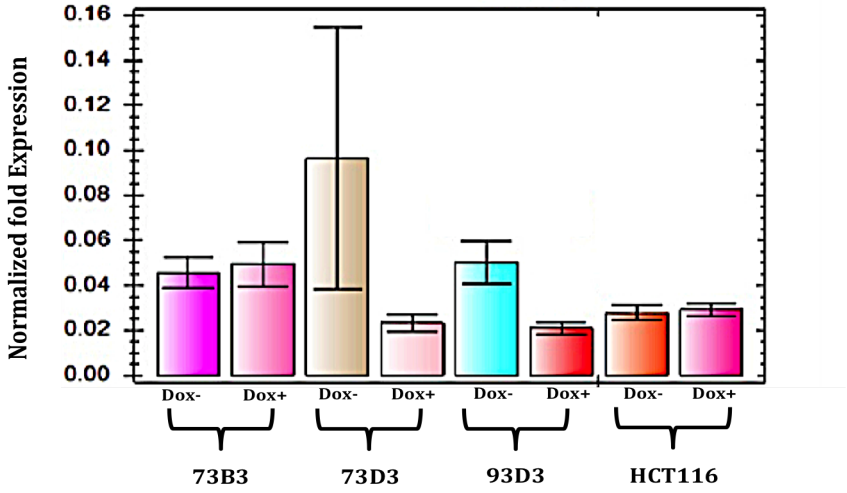

Figure 5.21 RT-qPCR analysis showing *SPO11* mRNA depletion in HCT116 using shRNA lentiviral particles. *SPO11* shRNA-HCT116 and negative control shRNA-HCT116 cell lines were established using the TRIPZ inducible lentiviral system. Different clones were obtained ("73" – targets Exon 9, "93" – targets Exon 12) and subjected to RT-qPCR. Results show *SPO11* expression after 24 hours of treatment with doxycycline (Dox). Results show a marked reduction of *SPO11* mRNA levels in shRNA-HCT116-73D3 and shRNA-HCT116-93D3 cells compared with untransfected HCT116 cells. Results are normalized to *GAPDH* and *ACTB*, and relative fold change was computed using the $\Delta\Delta Ct$ method. Error bars show the standard error of the mean.

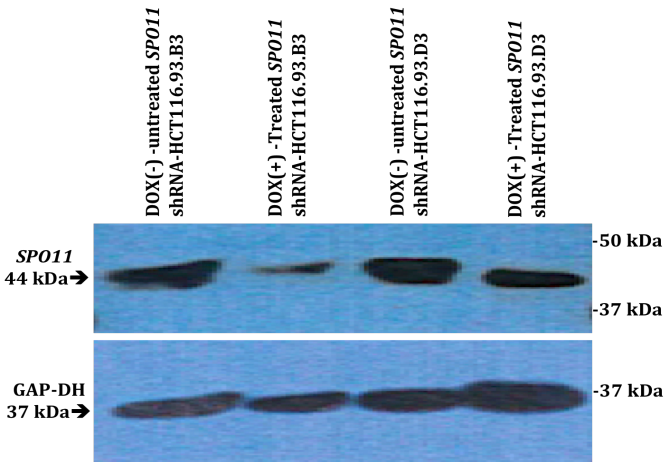

Figure 5.22 Western blot analysis showing the expression of SPO11 protein in *SPO11* shRNA targeted HCT116 cells with and without shRNA induction. *SPO11*shRNA-HCT116-93 cells were induced with doxycycline for 24 hours. Results show a marked reduction of protein levels in shRNA-HCT116-93 cells.

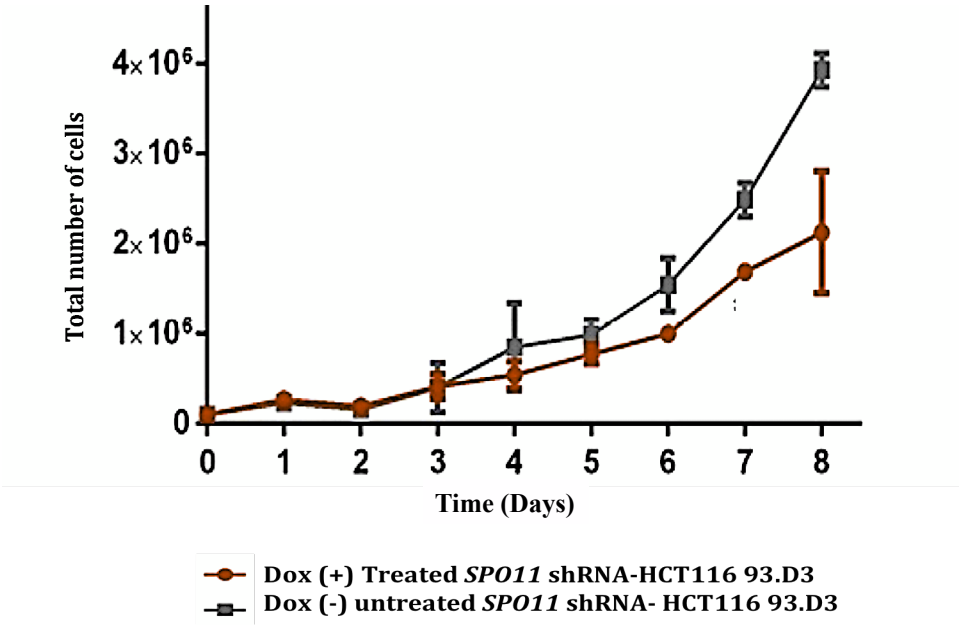

Figure 5.23 Growth curves of untreated and doxycycline-treated HCT116-SPO11shRNA 93D-cells. Analysis of the growth and proliferation of *SPO11* shRNA targeted cells in the presence and absence of doxycycline showing a reduction in cell proliferation over time. The error bars represent the standard error for the total number of cells as calculated for three repeats.

5.5 Discussion

To study the function of human *SPO11*, the CRISPR/Cas9 KO cell line HCT116-TetOn/*SPO11* was created in our laboratory (in collaborating with Dr. Ellen Vernon) and was used to investigate and analyse the cell growth and proliferation of HCT116 cells when SPO11 levels are reduced. The most encouraging results were obtained when the HCT116-TetOn cell line was transduced with CRISPR/Cas9 specifically designed to knock out exon 1 of *SPO11*, and this line showed a reduction in the growth and proliferation of cancer cells and a reduction in SPO11 protein levels. This result was consist with siRNA knockdown and confirmed that the reduction of SPO11 protein level in cancer cells may lead to inhibition of cell proliferation, as demonstrated in Chapter 3. However, a full *SPO11*-deficient cell line was never obtained as the doxycycline regulatable *SPO11* cDNA construct could not be completely switched off ('is leaky'). Low level of SPO11 protein is present in these cells even without Dox (as seen in Figure 5.13 *SPO11* KO clones in the absence of doxycycline). Due to the time constraints of this project, these cell lines could not be further manipulated to resolve this "leaky" issue but future investigation is required in order to see whether it is possible to completely switch off *SPO11* in these cells. These data again support the idea that SPO11 is essential for proliferation of cancer cells. The work in this chapter and Chapter 3 demonstrates the first preliminary evidence to suggest that *SPO11* is required for mitotic proliferation of cancer cells.

In Chapter 3 of the present study, SPO11 could be detected solely in the normal testis by western blotting for normal tissues. SPO11 is needed for different functions during meiotic cell division. *SPO11* is a mediator of interhomolog associations in *S. cerevisiae*; *spo11* mutants also reduce the length of the S-phase by 25% (Cha *et al.,* 2000). Moreover, Spo11 is responsible for initiating DSBs through Y135 residue (Bergerat *et al*., 1997); the *Spo11 Y135F* mutant does not affect S-phase but DSBs and SC are consequently not formed (Cha *et al*., 2000). This suggests that SPO11Δ siRNAs may have meiotic s-phase defects; this suggests a DSB-independent role for SPO11 in meiosis (Cha *et al.,* 2000).

The differences in survival between shRNA and CRISPR/Cas9 cells when compared to the untreated and negative controls may provide clues to other, yet uncharacterised, roles of *SPO11* and indicates that it might be essential for cancer cell survival. The *SPO11* heterozygous clone obtained during CRISPR/Cas9 targeting of HCT116 cells might have survived as the cells retained sufficient levels of SPO11. In a previous study, homozygous null mutation of *SPO11* in mice was found to be responsible for the arrested development and apoptosis of spermatocytes in the early prophase to mid-pachynema of meiosis (Smirnova *et al.,* 2006); if the same is true in cancer cells, then a full SPO11 KO might lead to apoptosis, however none was observed.

As the siRNA results obtained in Chapter 3 and CRISPR/Cas9 SPO11 targeted HCT116 cells in this chapter showed that the depletion of SPO11 affected cancer cell proliferation, shRNA was used as an inducible system in the present chapter in order to downregulate the *SPO11* gene in HCT116 cell lines. After doxycycline induction, HCT116-*SPO11* shRNA clones showed a reduction in *SPO11* mRNA and protein levels. Proliferation assays using these clones also showed a marked decrease in proliferation rates when comparing doxycycline-treated and untreated clones. Doxycycline-treated shRNA-cell lines showed lower variable knockdown efficiencies than HCT116-SPO11siRNA cells and CRISPR possibly due to the amount of shRNA per cell compared to siRNA. However, it is also possible that SPO11 depletion is a leading cause of chromosome rearrangement at the time of mitotic cell division due to incorrect replication and/or initiation of DSBs. The functional role of SPO11 in cancer cells will be discussed in more detail in the final discussion (see Chapter 7).

6. Cloning and expression of the novel cancer testis antigen *SPO11*β in *E. coli*.

6.1 Introduction

The result from Chapter 3 and 5 demonstrated that *SPO11* depletion reduced proliferation potential of cancer cells, and showed that self-renewal in cancer stem-like cells is perturbed upon *SPO11*-specific siRNA treatment. Taken together these results imply that *SPO11* is playing a role in cancer cell survival, and makes it a potentially valuable drug target. Furthermore, from the immunofluorescence work in Chapter 3, where was demonstrated that BLM and SPO11 co-localise in cancer cells, SPO11 could be acting as a topoisomerase/part of a topoisomerase complex in mitotic cells, further elevating its drug targeting potential. Previous structural work has already demonstrated that SPO11 is orthologous to the A-subunit of TopoVI DNA topoisomerase. The recent identification of a partner protein for SPO11: TopoVIB-like a protein similar in structure to the B-subunit of topoIV gives further support to our hypothesis of a "topoisomerase-like" function for SPO11 in mitotic cells. (Robert *et al.,* 2016; Vrielynck *et al.,* 2016). Topoisomerases have been conventionally used as a drug targets in cancer treatment. Specifically, DNA Topoisomerase II (Top2) is a target of many chemotherapies (Nitiss, 2009). Since Top2 is targeted by these pharmaceutical agents, the cancer cells become unable to repair their damaged DNA, and will eventually be targeted for apoptosis (Nitiss, 2009). It may be possible to target Spo11 as a form of therapy if this is the case. So, it would be interesting to determine if SPO11 and TopoVIB-like (C11orf80) co-purified in human cancer cells and have topoisomerase activity.

The aim of the work described in this chapter was to produce SPO11 protein in sufficient quantity and quality by using the Glutathion S-transferase (GST) fusion system for use in x-ray crystallography in order to determine its structure. Once the 3D structure of SPO11 was determined the hope was to identify residues on SPO11 that were important for protein recognition/function and so develop new therapeutic drugs to specifically target SPO11. Additionally, purified SPO11 was required to enable us to test the hypothesis that it could function in conjunction with C11orf80 to act as a topoisomerase (purification of c11orf80 will follow SPO11 purification) if so, then *in vitro* functional assays can be readily developed to screen for activity inhibiting small molecules.

In this chapter, it was subcloned the full length of Human *SPO11* cDNA into pGEX-2T and pGEX-6p-1 plasmids for inducible high level recombinant protein expression and purification from bacterial cell lysates. This process, however, was not trivial and involved determining the optimal conditions for maximal protein production in *E. coli*, purifying GST-tagged SPO11 from the lysate using glutathione–agarose (GA) beads, and successful removal of the GST tag. In addition, the GST-SPO11 fusion protein would be used to determine the specificity of the commercial anti-SPO11 antibody (Abcam, ab81695).

The Glutathion S-transferase (GST) fusion system is a versatile system for the expression, purification and detection of fusion proteins produced in *E. coli* (Smith, Johnson, 1988). To date fusion proteins have been successfully used throughout scientific research: in the development of vaccines, studying *in vitro* protein-protein interactions, for the production of antibodies for use in biochemical methodologies (western blots, immunoprecipitation), to further explore the structure of proteins using X-ray crystallography, and so on (Beckwith 2000). In addition *E. coli* is a particularly useful model organism for the expression of proteins because is cost effective and both prokaryotic and eukaryotic proteins can be easily expressed in large quantities (Hadders-Algra, 2008). The GST fusion system makes use of plasmid vectors that contain the coding sequence for GST upstream of a multiple cloning site where the cDNA of interest is cloned. The expression of the fusion protein is under the control of an inducible tac promoter, all pGEX vectors are also engineered with an internal lacIq gene. The lacIq gene product is a repressor protein that binds to the operator region of the *tac* promoter, preventing expression until induction by Isopropyl β-D-1-thiogalactopyranoside (IPTG), thus maintain tight control over expression of the insert, and it is this process that maintans tight control over expression of the insert. Followed by restriction sites that allow the insertion in-frame of a cloned gene (Hadders-Algra, 2008), also encode the recognition sequence for site-specific cleavage by PreScission Protease, or Thrombin recognition site between the GST domain and the multiple cloning sites. Anti-GST antibodies to these fusion tags are readily available to monitor fusion protein expression and purification.

6.2 Results

6.2.1 Subcloning of *SPO11* into a protein production vector pGEX-2T

Purifying the SPO11 protein is necessary to perform studies on its function and structure. This process was conducted by sub-cloning the full length *SPO11*β cDNA into the expression vector pGEX-2T (Figure 6.1), which contains the coding sequence for the 26 kDa glutathione S-transferase (GST) tag. The gene was released from the constructed plasmids pTRE3G::*SPO11* (Figure 6.2, 6.3) by digestion with the *Bam*HI restriction enzyme. The digested and purified pGEX-2T plasmid cut with *Bam*HI (4948 bp) was used to ligate the purified *SPO11* cDNA (1191bp) for the generation of the recombinant plasmid (Figure 6.2). The ligated plasmid pGEX-2T::*SPO11* was then transformed into competent *E. coli* cells (BL21) plated on an LB agar medium containing 100 mg/ml of ampicillin, and incubated overnight at 37°C. Random colonies were selected, and PCR reactions were performed by using internal primers for the *SPO11* gene to confirm that the colonies with the correct insertion were chosen. Colonies with a positive PCR were selected for overnight growth (Figure 6.4). The recombinant plasmid pGEX-2T::*SPO11* was digested successfully with the *Bam*HI enzyme. Analysis of the digestion on 0.8% agarose gels showed the presence of a full-length insertion of *SPO11* (1191bp). Undigested and digested pGEX-2T (4948bp) was used for comparison with the recombinant plasmids (Figure 6.5). The recombinant plasmids were confirmed with DNA sequencing to check for mutations and the correct gene orientation. Universal pGEX primers and the internal primers for *SPO11* were used for the DNA sequencing listed in Table 2.7 (see Materials and Methods).

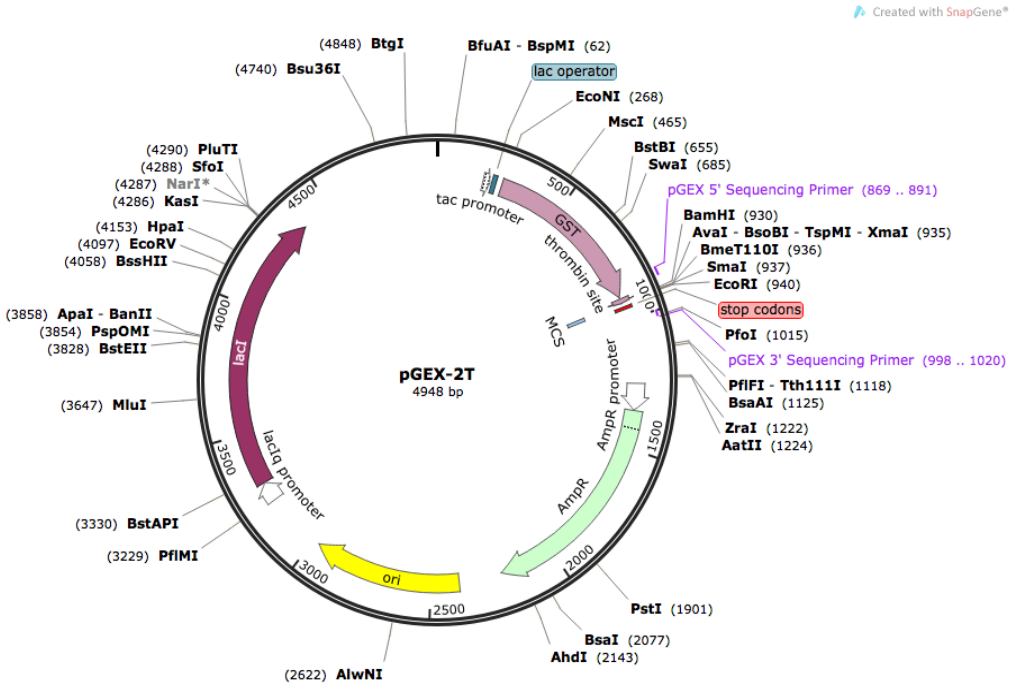

Figure 6.1 The protein expression pGEX-2T plasmid was used to sub-clone the *SPO11* cDNA. The plasmid was digested with the *Bam*HI restriction enzyme, and the cDNA was cloned into the *Bam*HI site.

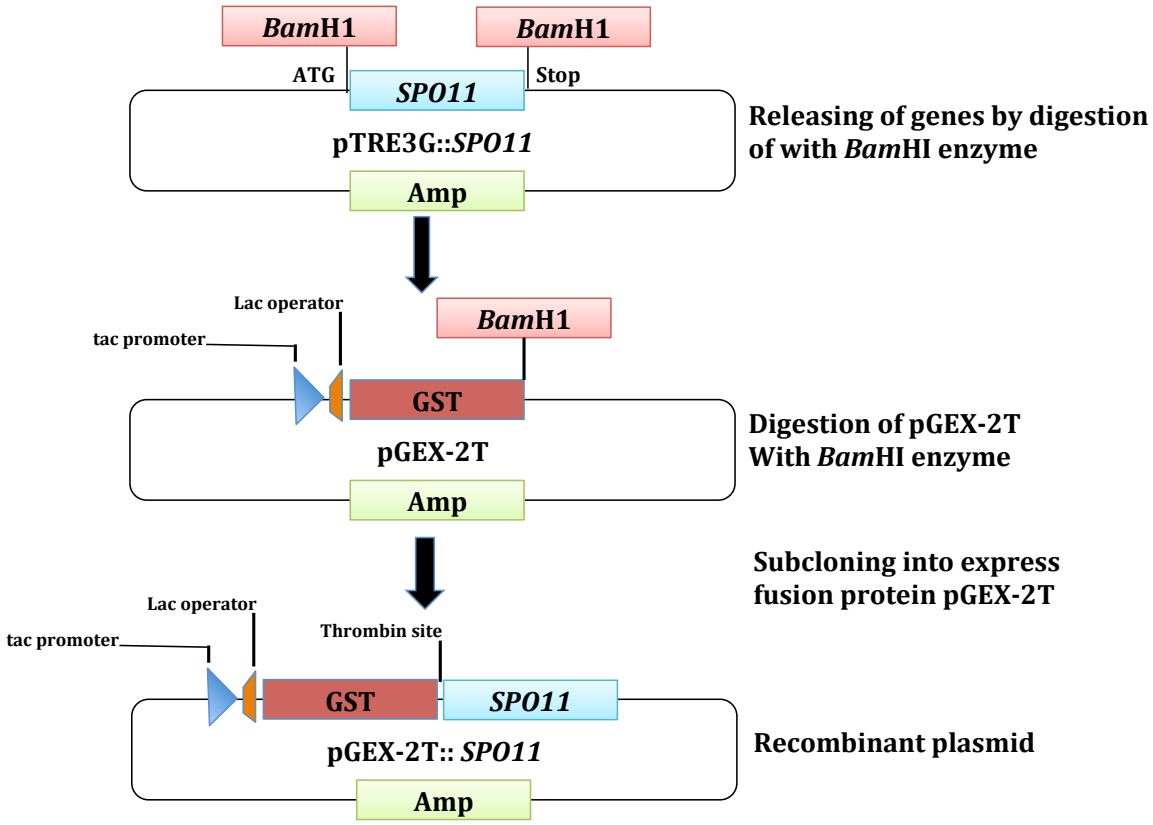

Figure 6.2 Schematic diagram of the sub-cloning strategy for the insertion of the *SPO11* cDNA into the fusion expression vector pGEX-2T. Step 1: The *SPO11* cDNA was released from the recombinant plasmids pTRE3G::*SPO11* with the use of the *Bam*HI restriction enzyme. Step 2: The pGEX-2T plasmid was digested with *Bam*H1 at the multiple cloning site (MCS) after the GST taq site. Step 3: The *SPO11* gene was cloned into pGEX-2T; the proteins have an N-terminal GST tag that aids in recombinant protein purification.

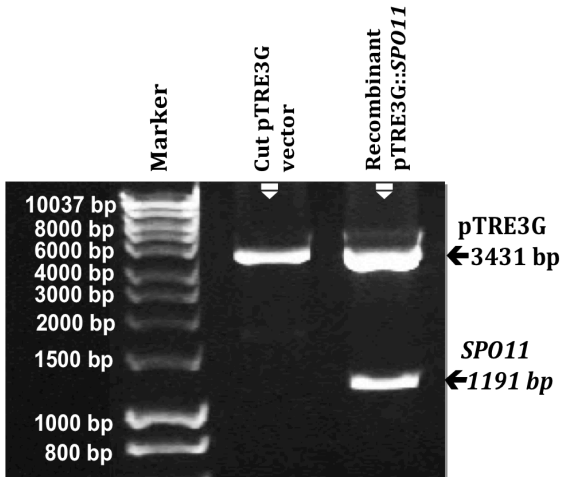

Figure 6.3 The *SPO11* cDNA was released from the plasmids pTRE3G::*SPO11* by digestion with the *Bam*HI restriction enzyme.

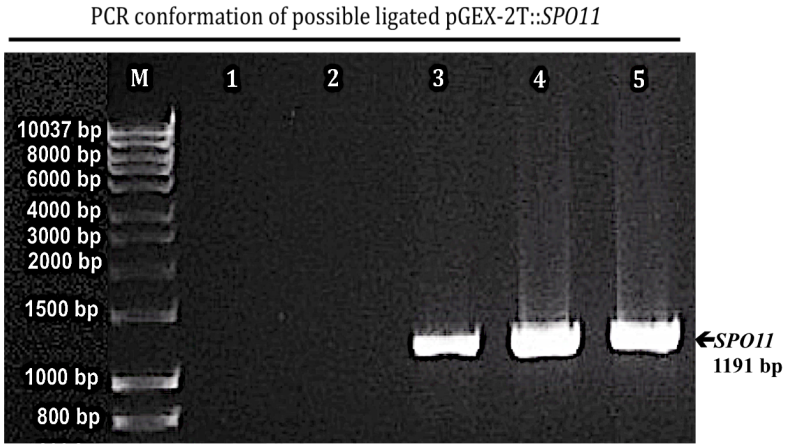

Figure 6.4 PCR profile analyses of the *SPO11* gene after being cloned into the pGEX-2T expression vector and transformed into BL21 expression *E. coli*. The gene was ligated at the *Bam*HI site with a ratio of 1:6 or 1:9 (plasmid:insert) and transformed into BL21 expression *E. coli*. Random colonies were selected, and PCR was performed to check the possibility of transformation with the use of the primer for the *SPO11* gene. PCR products were fractionated on 1% agarose gel stained with PeqGREEN DNA Day; 5 µl of HyperLadder I kb was used as a marker. Lanes 3, 4 and 5 are the colonies containing the *SPO11* cDNA.

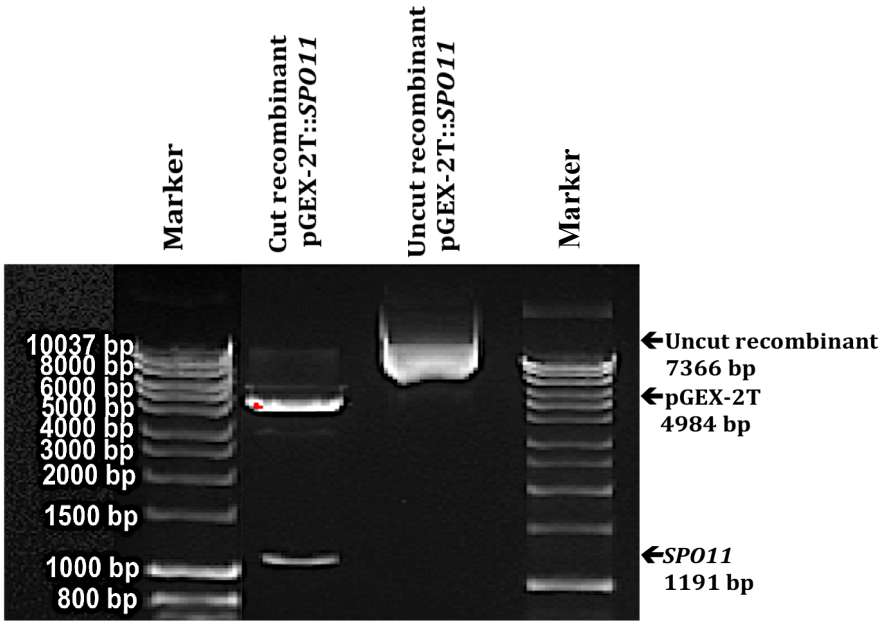

Figure 6.5 Digestion of recombinant pGEX-2T expression plasmids with the *SPO11* gene. 0.8% agarose gel stained with PeqGREEN DNA Day confirms the cloning of *SPO11* into the pGEX-2T plasmid. From left, Lane 1: digestion of recombinant pGEX-2T::*SPO11*; Lane 2: uncut recombinant pGEX-2T::*SPO11*; 5 µl of HyperLadder 1 kb was used as a marker.

6.3 Protein production

6.3.1 optimising the overexpression of *SPO11* with GST fusion proteins in *E. coli* cells

Recombinant plasmid pGEX-2T::*SPO11* was successfully transformed into *E. coli* BL21 to assess protein production. The pGEX-2T plasmid encodes a 26 kDa GST tag, which can be express under the control of the IPTG inducible *tac* promoter (Smith & Johnson, 1988). Recombination proteins were obtained from three different clones, as confirmed by DNA sequencing (Figure 6.5), and then induced in cells grown in LB media at 37°C by treatment with 100 μM IPTG for 2, 3 and 5 hours, as described in Materials and Methods (Section 2.10.1). The total cell lysates of the IPTG-induced and un-induced cells were resolved on SDS-PAGE gels. Analysis of the induced SPO11 fusion protein showed the expected size of 70 kDa, which corresponded to GST (≈26 kDa) fused to SPO11 (≈44 kDa). As positive control, an empty pGEX-2T plasmid was induced at 30°C with 100 μM IPTG for 2, 3 and 5 hours to assess the experimental conditions. The yield of fusion GST alone (≈26 kDa) and/or with fusion gene proteins showed a slight increase after 5 hours of induction with IPTG. No fusion protein was observed either with pGEX-2T alone or with the recombinant insert in the absence of IPTG. Coomassie blue stained gels were chosen to show protein production (Figure 6.6). The best inductions of the GST/SPO11 fusion protein was obtained by treatment at 30°C with 100 μM for 5 hours. Western blot analysis using an anti-GST antibody (Figure 6.7) was also performed to assess the positive induction of the recombinant plasmid. The conditions were optimised under different temperatures (30°C, 37°C).

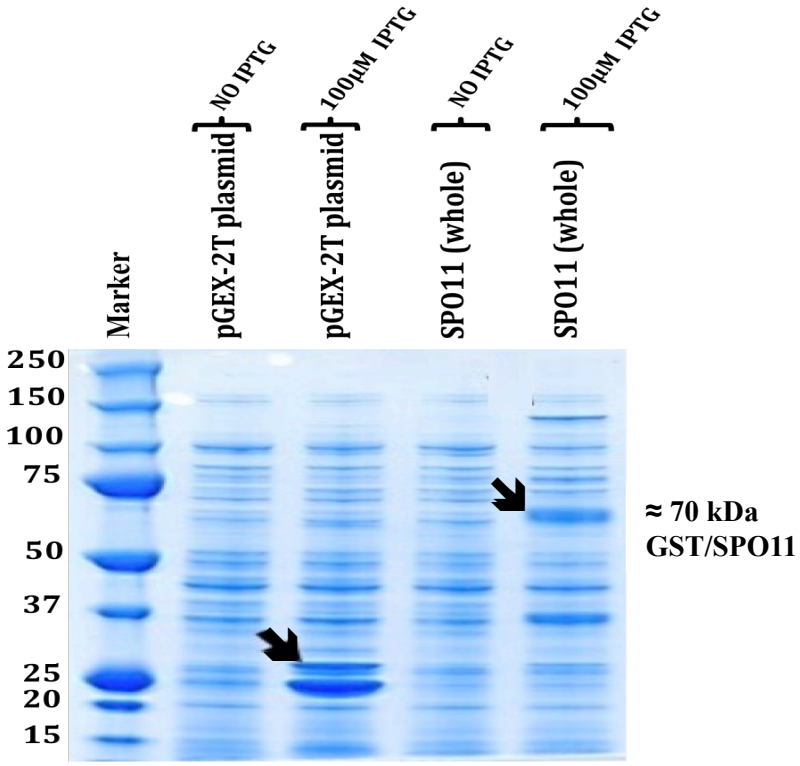

Figure 6.6 Optimised induction of GST/SPO11fusion protein in BL21 *E. coli* cells. Comassie blue stained gels show that the most optimised induction condition of the GST/SPO11 protein is induction with 100 μM IPTG at 37°C for 5 hours, arrow shows fusion protein GST/SPO11 in (≈70 kDa). Un-induced and induced pGEX-2T alone was used in the analysis and the arrow showed the GST protein in ≈26 kDa. Molecular weights are shown on the left in kDa.

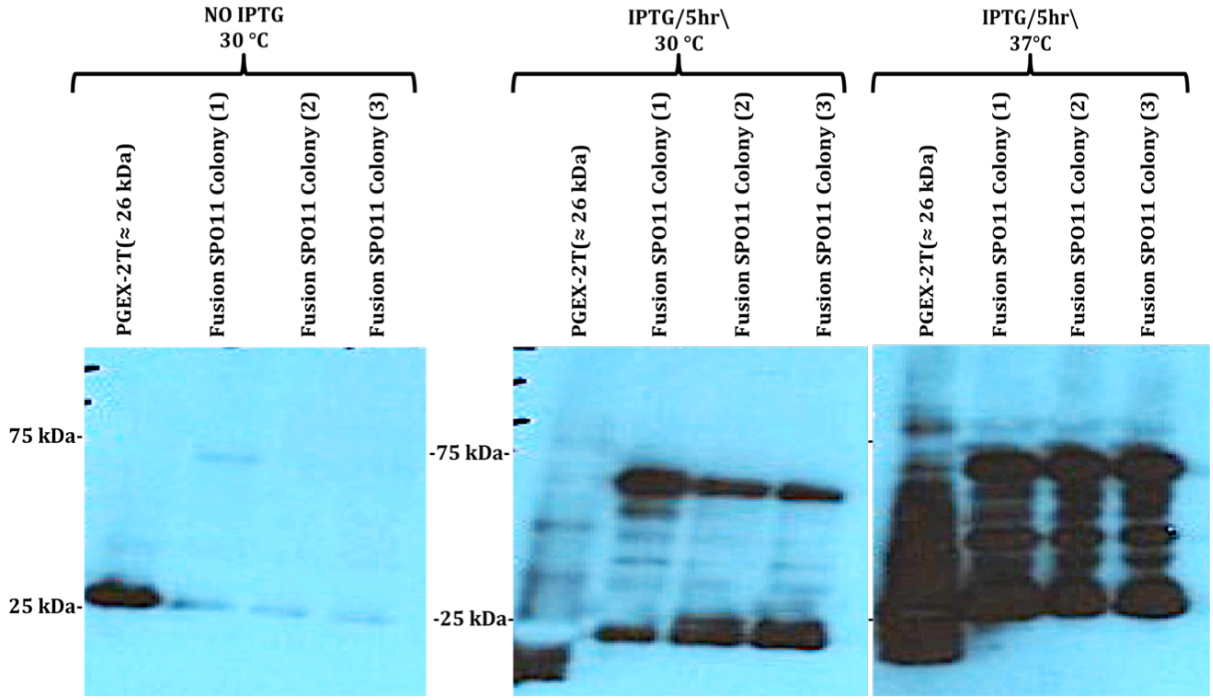

Figure 6.7 Western blot expression analysis of the induced GST/SPO11 fusion protein with the use of an anti-GST antibody. The total cell lysates for different positive clones were induced with IPTG cells and different temperature (30 °C, 37°C); the results were analysed with Westen blot using an anti-GST antibody. Analysis of the induced GST/SPO11 fusion protein showed the expected size of ≈70 kDa, which corresponded to GST(≈26 kDa) fused to SPO11 (≈44 kDa).

6.3.2 Determination the solubility of the GST/SPO11 fusion proteins

The solubility of fusion was examined under the most optimised induction condition (30°C with 100 μM IPTG for 5 hours), as described in Materials and Methods (Section 2.10.2). When both the pellet (insoluble) and the supernatants (soluble) of the induced IPTG cells were run on SDS-PAGE gels, the Coomassie blue stained gels showed a clear band that was obtained with the expected size of the induced pGEX-2T plasmid only and the GST/SPO11 fusion protein (Figure 6.8). The majority of GST/SPO11 was observed in the insoluble fractions. Therefore, before the purification steps for the GST/SPO11 fusion proteins were started, different conditions were examined to increase the solubility of the fusion proteins. These conditions included different temperatures for fusion induction, different IPTG concentrations and different times of sonication. Furthermore, the GST/SPO11 fusion protein was shown to be insoluble in the absence of denaturing detergents, so we replaced the solution in which the cells were lysed with a buffer containing different lysis buffers. In the cell lysate process, the selection of sarkosyl was an advisable choice because sarkosyl was previously examined as a type of detergent that generally stops the formation of co-aggregates when used in the process (Frankel *et al.,* 1991). It has also been suggested to maintain the fusion protein in the solution without affecting its ability to bind to affinity columns, and to facilitate the purification of insoluble proteins in high yields without affecting fusion protein functions (Park *et al.*, 2011). However, the use of 1%–2% sarkosyl with Triton X-100 at a ratio of 1:200 (sarkosyl:Triton X-100) improves the solubility of GST/SPO11. The fusion protein was also induced with a range of IPTG concentrations from 40 to 400 μM for 5 hours. The use of different IPTG induction temperatures (the figure only shows data for 30°C (Figure 6.9) revealed that decreasing the induction temperature to 30°C with 100 μM IPTG increased the amount of recovered soluble protein. However, most protein still remained in the insoluble fraction, as shown by Western blot expression analysis using an anti-GST antibody (Figure 6.10) and a rabbit anti-SPO11 antibody (Abcam, ab81695) (Figure 6.11).

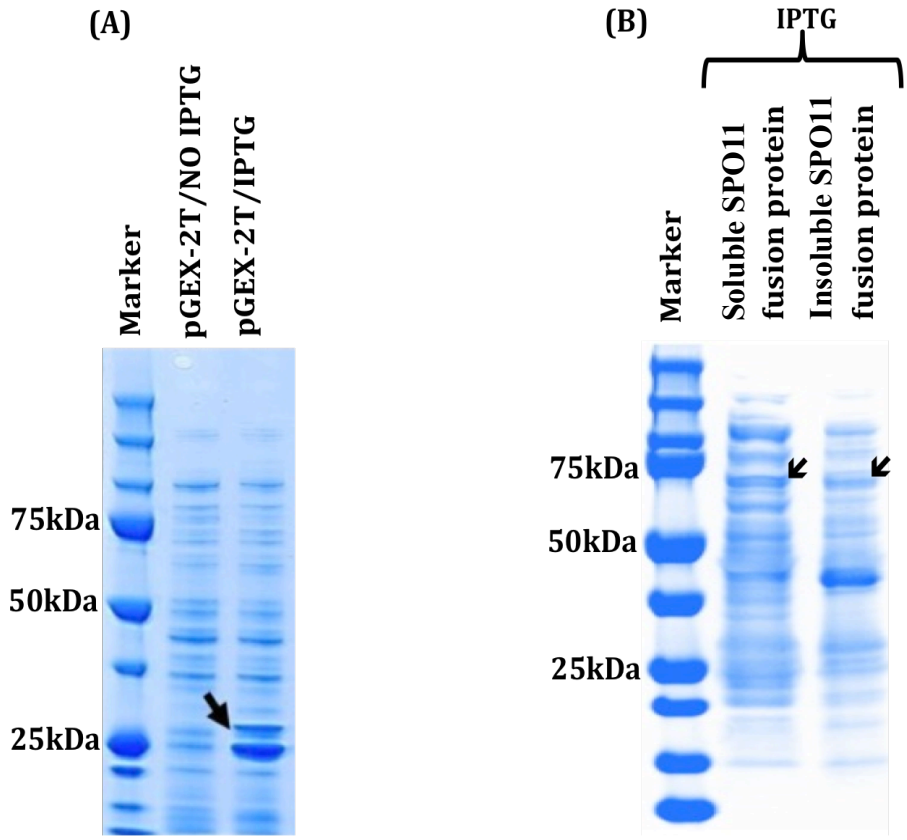

Figure 6.8 Determining the solubility of the GST/SPO11 fusion protein. Coomassie blue stained gels show the best optimised condition (30°C with 100 µM IPTG for 5 hours) when both the pellet (insoluble) and the supernatants (soluble) of the induced-IPTG cells were run on SDS-PAGE gels. (A) Un-induced and induced pGEX-2T protein alone were used to assess the induction arrow showed the GST protein in ≈26 kDa. (B) arrow showed the soluble and insoluble fusion protein GST/SPO11 in (≈70 kDa).

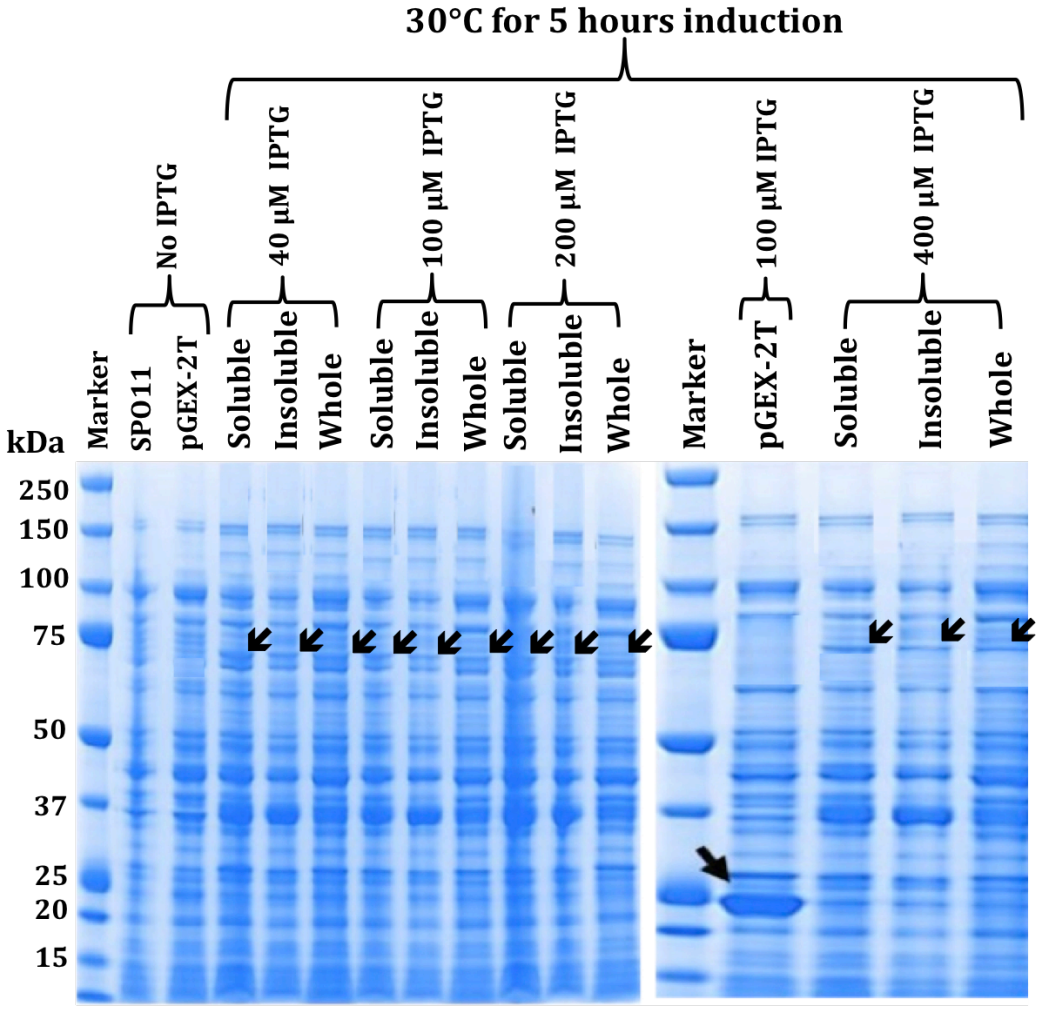

Figure. 6.9 Determining the solubility of the GST/SPO11 fusion protein with the use of different concentrations of IPTG in BL21 *E. coli* cells. Comassie blue stained gels show the induction of the fusion SPO11 protein ≈70 kDa following induction with 40, 100, 200, 400 µM IPTG at 30°C for 5 hours. Fusion GST/SPO11 shows an insoluble fraction (arrows) at all IPTG concentrations. Un-induced pGEX-2T alone or with SPO11 was used to assess the induction. Molecular weights are shown on the left in kDa.

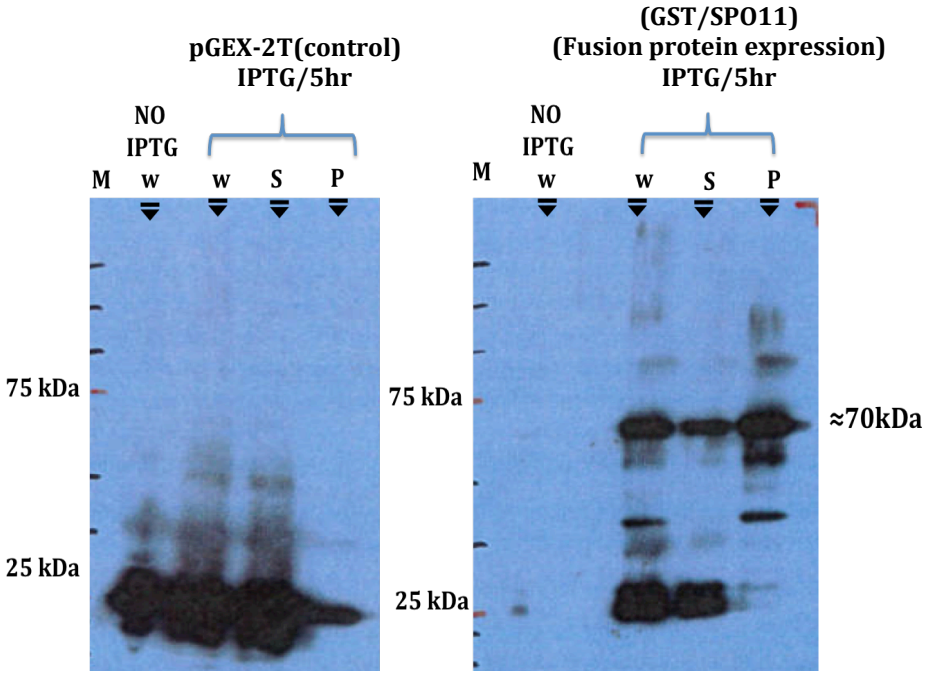

Figur 6.10 Western blot expression analysis to determine the solubility of the GST/SPO11 fusion protein with the use of an anti-GST antibody. The pellet (P=insoluble), the supernatants (S=soluble) and the whole cell lysate (W) of the induced IPTG cells were run on SDS-PAGE gels. Un-induced and induced pGEX-2T alone were used to assess the analysis (≈26 kDa). The GST/SPO11 fusion protein showed the expected size of ≈70 kDa.

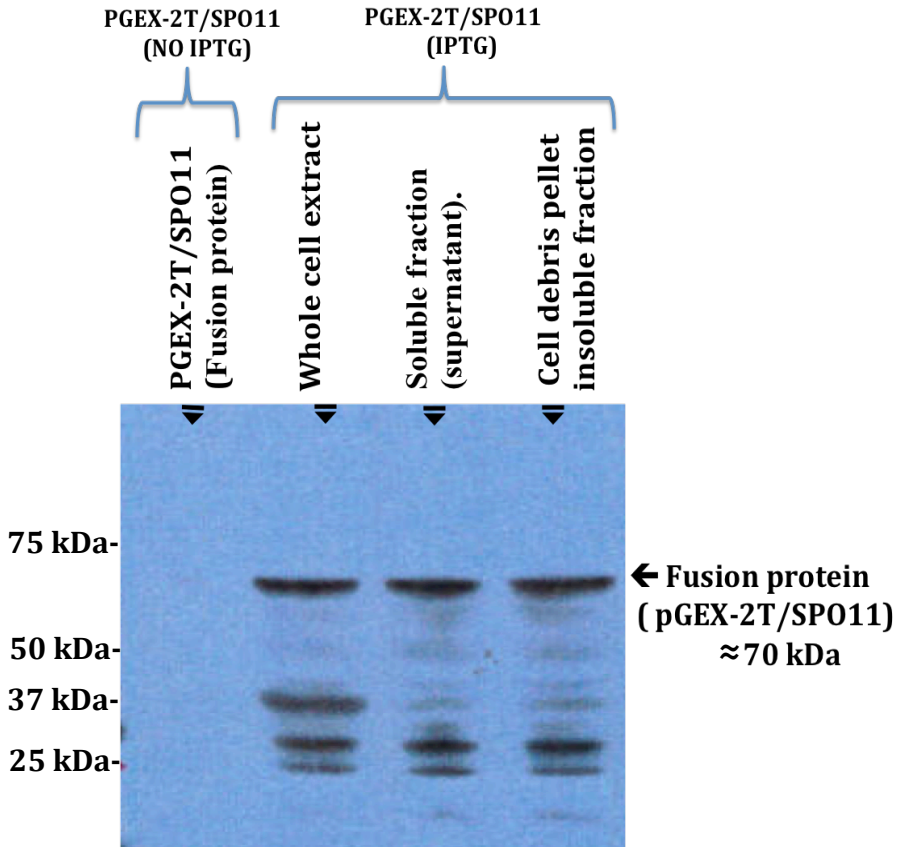

Figure 6.11 Western blot expression analysis of the induced GST/SPO11 fusion protein to determine the solubility of the SPO11 fusion protein. Western blot analysis using an anti-SPO11 antibody (Abcam, ab81695) shows the most optimised condition (30°C with 100 µM IPTG for 5 hours) when both the pellet (insoluble) and the supernatants (soluble) of the induced IPTG cells were run on SDS-PAGE gels. Uninduced pGEX- 2T/*SPO11* was used to assess the induction. The soluble and insoluble fusion GST/SPO11 protein ≈70 kDa.

6.3.3 Purification of produced fusion protein

Purification of the soluble GST/SPO11 fusion protein was performed with the use of Pierce GST spin purification kits (Thermo) and GST Spin traps (GE Healthcare), as described in Materials and Methods (Section 2.10.4). From the purification process of the GST/SPO11 fusion protein, Coomassie blue stained 4%–12% SDS-PAGE gel analysis showed that the fusion protein did not bind to the column (Figure 6.12) compared with the control pGEX-2T, which showed only a clear band with a size of ≈26 kDa. Furthermore, Western blot analysis using an anti-SPO11 antibody (Abcam, ab81695) shows the same results (Figure 6.13). Therefore, 5 mM DTT was added to the lysis buffer before extraction, as this significantly increased the binding of the GST/SPO11 fusion proteins to immobilise glutathione. Then, the GST/SPO11 protein was eluted from the resin bed by an elution buffer. The results showed that the most fusion protein GST/SPO11 coming off and was clearly detected after elution. Glutathione resins were collected after the purification process and were boiled to examine whether the fusion proteins was still bound to the resins after the elution steps. The study found that less amount of fusion protein GST/SPO11 remained associated with the column resins and did not release (Figure 6.14).

6.3.4 Thrombin cleavage of the fusion protein

Thrombin can be used to cleave any protein containing a thrombin cleavage site (see Materials and Methods, Figure 2.2); the approximate size of thrombin is ≈37 kDa. The soluble GST/SPO11 protein was purified in this experiment with the use of the optimal conditions for purification. The material used for purification was Pierce glutathione Spin columns (see Materials and Methods, Section 2.10.4). After purification, the fusion protein on the column was incubated with thrombin for cleavage and removal of the GST tag (Figure 6.15). In the next step, the quantity of thrombin required for the incubation, along with the estimated incubation time and temperature, was examined. The best temperature was 22°C, and the incubation time were from 1 to 6 hours. Furthermore, the amount of thrombin used in the reaction was 50–150 Unit/mg (one unit cleaves 100 μg protein, theoretically). 15 mg of the total GST/SPO11 fusion protein lysate was loaded onto different columns for purification and cleavage on the column, and then SDS-PAGE was used to estimate the yield, purity and extent of digestion.

The results show that the fusion protein was degraded by extensive incubation with thrombin for 6 hours; different results were obtained by increasing the amount of thrombin. The optimal condition was achieved by incubating 150 unit/mg of thrombin concentration for 2 hours and shaking it at 22°C; this condition showed bands in 44 and 37 kDa. By contrast, incubation with a thrombin concentration of 50 unit/mg showed a band of 37 kDa. Both conditions were analysed by Western blot using an anti-SPO11 antibody (Abcam, ab81695) and an anti-GST antibody (Figure 6.16). Although the thrombin cleavage was successful, most of the GST/SPO11 fusion protein remained sufficiently uncleaved. SDS-PAGE analysis using silver staining and Coomassie blue for monitoring the SPO11 protein after cleavage with thrombin showed that some of the GST/SPO11 fusion proteins passed through the first flow-through centrifugation and were released from the column after thrombin was cleaved (Figure 6.17).

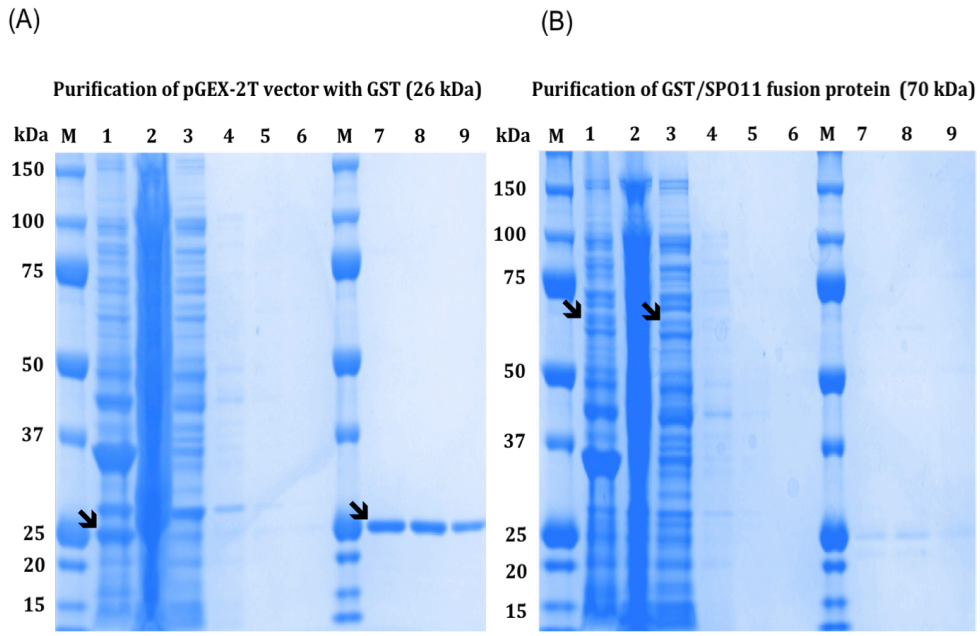

Figure 6.12 Coomassie blue stained 4%–12% SDS-PAGE gel analysis after the purification of the GST/SPO11 fusion protein. *E. coli* cells were grown in LB media at 37°C with fusion proteins containing either (A) pGEX-2T only or (B) GST/SPO11 fusion protein, and induced with 100 µM IPTG for 5 hours. The whole cell lysate was solubilised by using 2% Triton X-100 and 2% sarkosyl, and then purified by using GST thermo purification columns. From left to right; molecular weights are shown on the left in kDa; M: Protein marker: 1: Whole cell lysate of cells induced with 100 µM IPTG; 2: Soluble fraction (supernatant); 3: Flow-through fraction from the column; 4: First wash with the equilibration/wash buffer; 5: Second wash; 6: Third wash; 7: First elution buffer centrifugation; 8: Second elution buffer; 9: Third elution. (A) Arrows show a clear band of GST with a size of ≈26 kDa. (B) Arrows show that the fusion protein did not bind to the column.

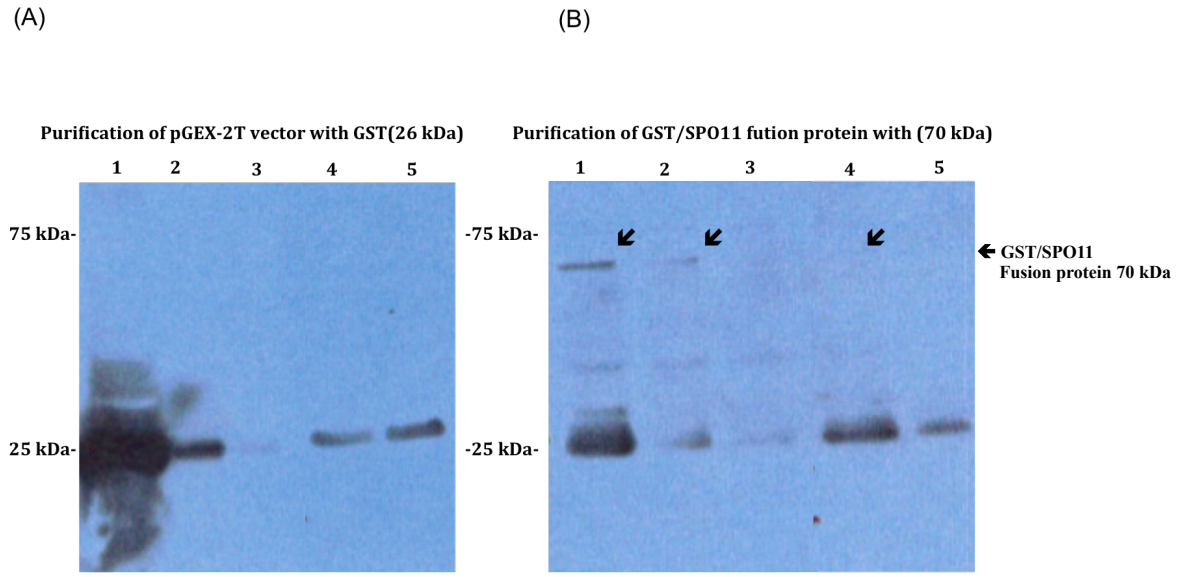

Figure 6.13 Western blot analysis after expression and purification of the fusion GST/SPO11 protein with the use of an anti-SPO11 antibody (Abcam, ab81695). *E. coli* cells were grown in LB media at 37°C with the fusion proteins containing either (A) pGEX-2T only or with (B) SPO11, and induced with 100 µM IPTG for 5 hours. The whole cell lysate was solubilised by using 2% Triton X-100 and 2% sarkosyl, and then purified by using GST thermo purification columns. From left to right, Lane 1: Soluble fraction (supernatant) of the cells induced with 100 µM IPTG; 2: Flow-through fraction from the column; 3: First wash with the equilibration/wash buffer; 4: First elution buffer centrifugation; 5: Second elution buffer. Molecular weights are shown on the left in kDa.

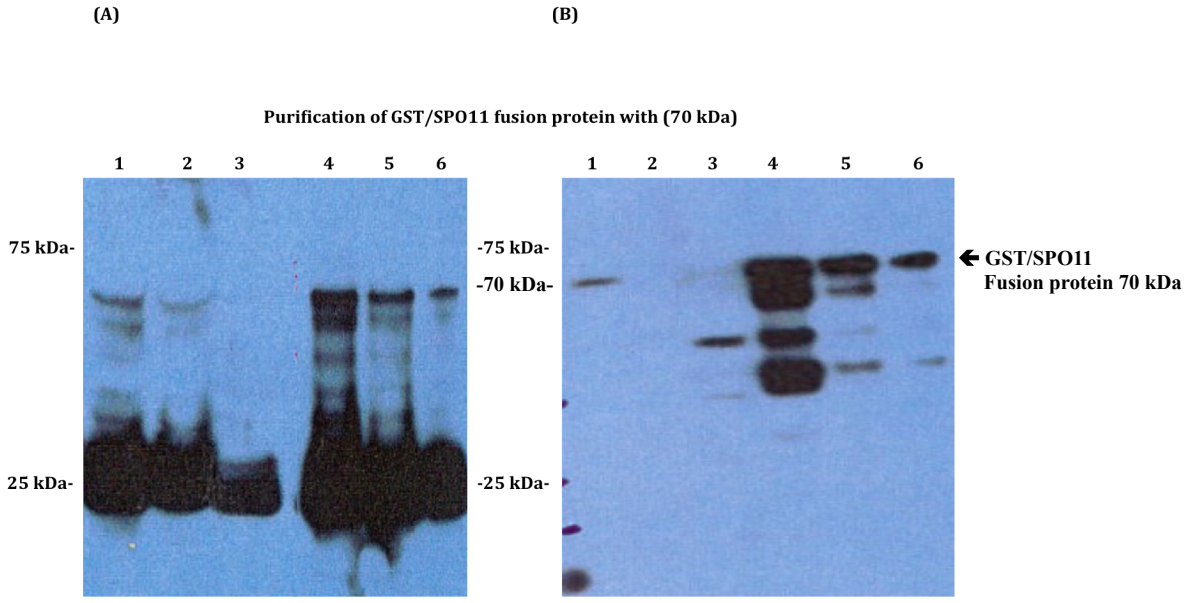

Figure 6.14 Western blot analysis after expression and purification of the fusion GST/SPO11 protein in BL21 *E. coli* cells lysed with DTT; (A) used an anti-GST antibody, and (B) used an anti-SPO11 antibody (Abcam, ab81695). DTT was added to the lysis buffer before extraction to increase the binding of the GST/SPO11 fusion protein. After sonication, the soluble materials were recovered by centrifugation, and Triton X-100 was added to a final concentration of 1%. The soluble fusion protein was then isolated from the *E. coli* cell lysates by absorption onto glutathione agarose beads in the column; purification of the soluble fusion protein of GST/SPO11 was performed by using Pierce GST spin purification, followed by elution from the column by the elution buffer and centrifugation at 700 x g for 2 minitus. From left to right, Lane 1: Soluble fraction (supernatant) of the cells induced with 100 µM IPTG; 2: Flow-through fraction from the column; 3: First wash with the equilibration/wash buffer; 4: First elution; 5: Second elution buffer, 6: Resin-bed were collected and boiled after the purification of the fusion protein; protein remained bound to the column resins. Molecular weights are shown on the left in kDa.

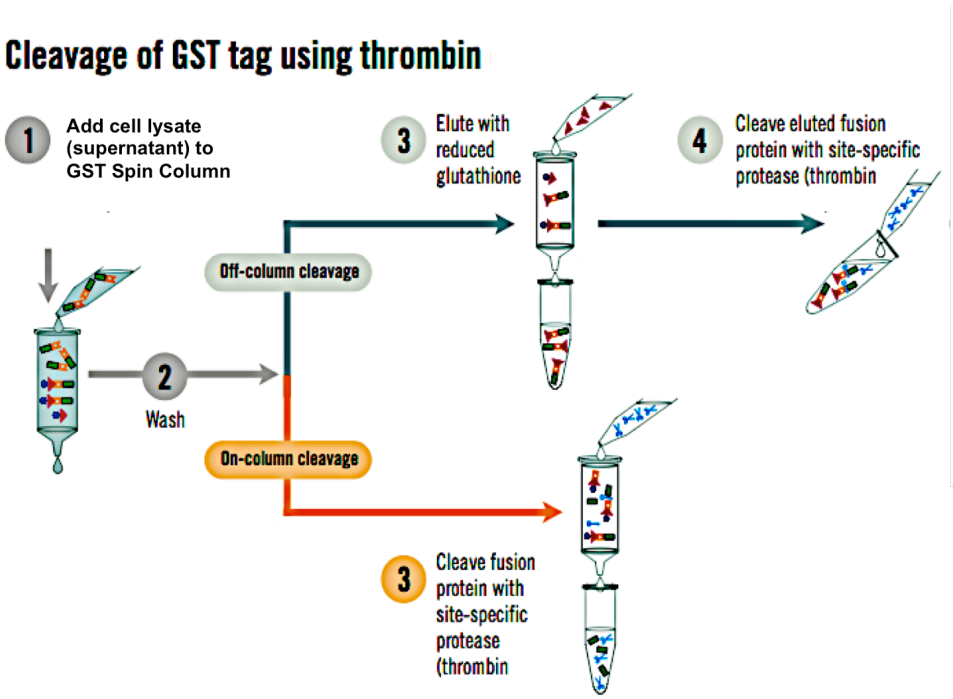

Figure 6.15. Flow chart of the affinity purification procedure and the thrombin cleavage of the GST fusion proteins. (Figures taken from the GST Gene Fusion System, Amersham Biosciences).

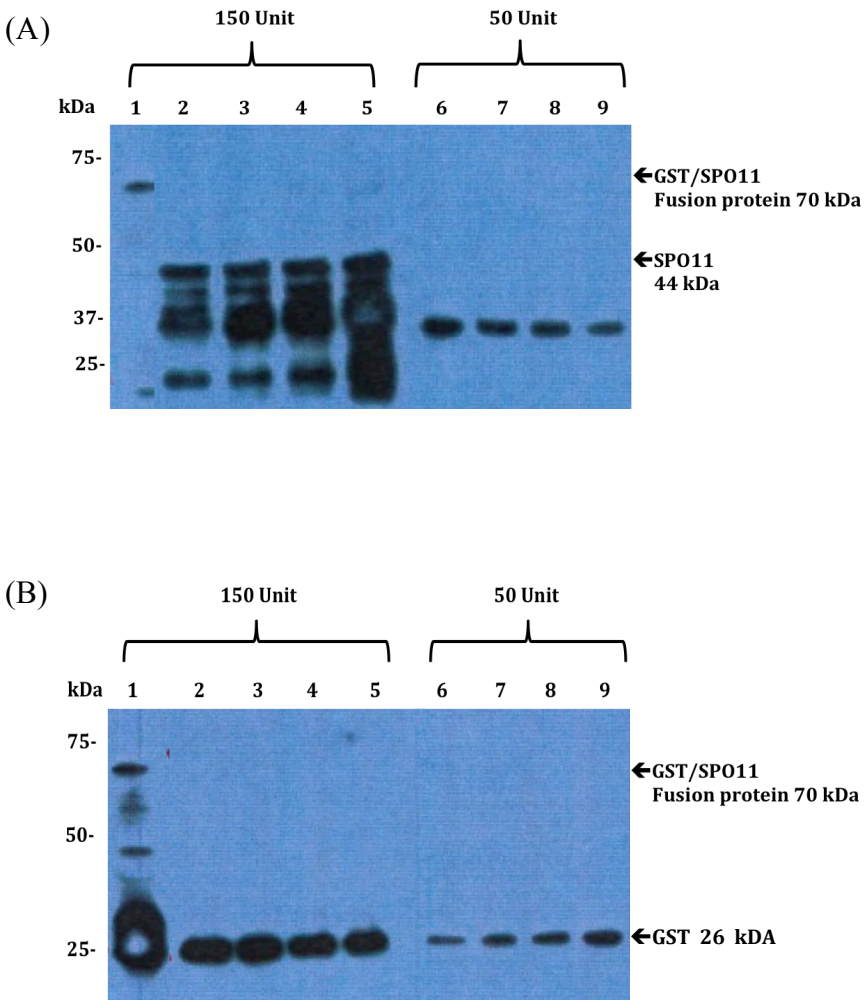

Figure 6.16 Western blot analysis to monitor the SPO11 protein after being cleaved with thrombin on a column that used (A) an anti-SPO11 antibody (Abcam, ab81695) and (B) an anti-GST antibody. Purification columns were used; they were first bound to the fusion protein and washed, and the supernatant was removed and then replaced with a mix of different units of thrombin solution (150 and 50 units) and different incubation times (1, 2, 4, 6 hours) at 22°C and then elution from each column purification then they were collected and analysed by Western blot using an anti-SPO11 antibody (Abcam, ab81695). From left to right, Lane 1: Elution of the non-cleavaged GST/SPO11 fusion protein showed that a band in 70 kDa was loaded as the control; 2: 150 units of thrombin incubated for 1 hours; 3: 150 units of thrombin incubated for 2 hours; 4: 150 units of thrombin incubated for 4 hours; 5: 150 units of thrombin incubated for 6 hours. Lane 6: 50 units of thrombin incubated for 1 hours; 7: 50 units of thrombin incubated for 2 hours; 8: 50 units of thrombin incubated for 4 hours; 9: 50 units of thrombin incubated for 6 hours. Molecular weights are shown on the left in kDa. The band with 44 kDa indicates the position of the SPO11 protein after being cleaved with thrombin, which can be identified by a comparison with the elution of the non-cleavaged protein (GST/SPO11 fusion protein) 70 kDa.

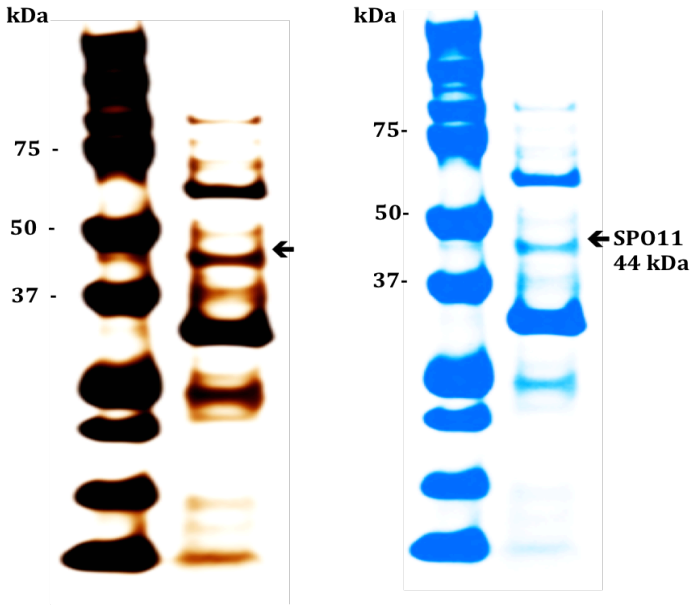

Figure 6.17 SDS-PAGE analysis using silver staining and Coomassie blue to monitor the SPO11 protein after being cleaved with thrombin. Silver staining and Coomassie blue stained 4%–12% SDS-PAGE gel analysis showed the SPO11 protein after being cleaved with thrombin and after undergoing shaking at 22°C for 2 hours. Molecular weights are shown on the left in kDa. An arrow indicates the position of the SPO11 protein after cleaved. Two bands were cut out sized (44 and 37 kDa) and sent for mass spectrometry analyses to sequence.

6.4 Sub-cloning of *SPO11* cDNA into the protein production vector pGEX-6p-1

As noted in Section 6.3.4, the results showed that multiple bands were observed at 44 kDa and 37 kDa on SDS Gel electrophoresis following thrombin cleavage when using Western blot and Coomassie blue staining. The smaller bands (37 kDa) indicated suspected cleavage of SPO11 with thrombin (non-specific cutting). Therefore, the lack of purity in the SPO11 protein after thrombin cleavage suggested that thrombin was not sufficient for cleaving the GST/SPO11 fusion protein. Consequently, the pGEX-6p-1 vector was used.

In the present study, the expression construct was prepared by inserting the *SPO11* genes into the multiple cloning sites of pGEX-6p-1, as described previously (Section 6.2.1 and Section 2.10, Materials and Methods). pGEX-6p-1 encodes the recognition sequence for site-specific cleavage between the GST domain and the multiple cloning site with PreScission Protease (Figure 6.18). As PreScission Protease has been provided with a GST tag, it can successfully be separated from the cleavage mixture concurrently with the GST part of the fusion protein. pGEX-6p-1 expression vectors allow a suitable site-specific cleavage and an instantaneous refinement in glutathione sepharose (Kaelin, *et al., 1992*). The *SPO11* genes were released from the constructed plasmids pTRE3G::*SPO11* (Figure 6.3) by digestion with the *Bam*HI restriction enzyme. The digested and purified pGEX-6p-1 plasmid with *Bam*HI (4984 bp*)* was used to ligate the purified *SPO11* cDNA (1191 bp) for generating the recombinant plasmid (Figure 6.19). The ligated plasmid pGEX-6p-1::*SPO11* was then transformed into BL21 competent cells. Plated on an LB agar medium containing 100 mg/ml of ampicillin and incubated overnight at 37°C. Random colonies were selected, and PCR reactions were performed by using the internal primers for the *SPO11* genes to confirm that the colonies with the correct insertion were chosen. Colonies with a positive PCR were selected for overnight growth. Recombinant plasmid pGEX-6p-1::*SPO11* was digested successfully with the *Bam*HI enzyme. Analysis of the digestion on 0.8% agarose gels showed the presence of a full-length insertion of *SPO11* cDNA (1191 bp). Digested pGEX-6p-1 (4984 bp) was used for comparison with the recombinant plasmids pGEX-6p-1::*SPO11* (Figure 6.20). The recombinant plasmids were confirmed by DNA sequencing to check for unwanted mutations and the correct gene orientation. Universal pGEX primers and the internal primers for *SPO11* were used for the DNA sequencing listed in Table 2.7 (see Materials and Methods).

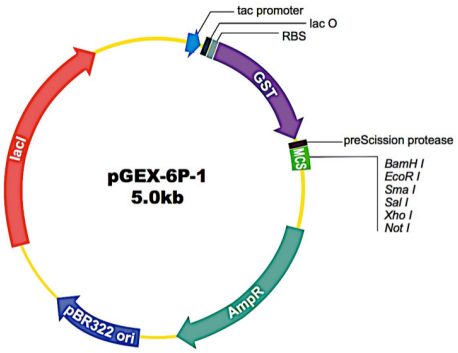

Figure 6.18 protein expression pGEX-6p-1 plasmid was used to sub-clone the *SPO11* cDNA. The plasmid was digested with *Bam*HI restriction enzyme and the gene was cloned in to the *Bam*HI site.

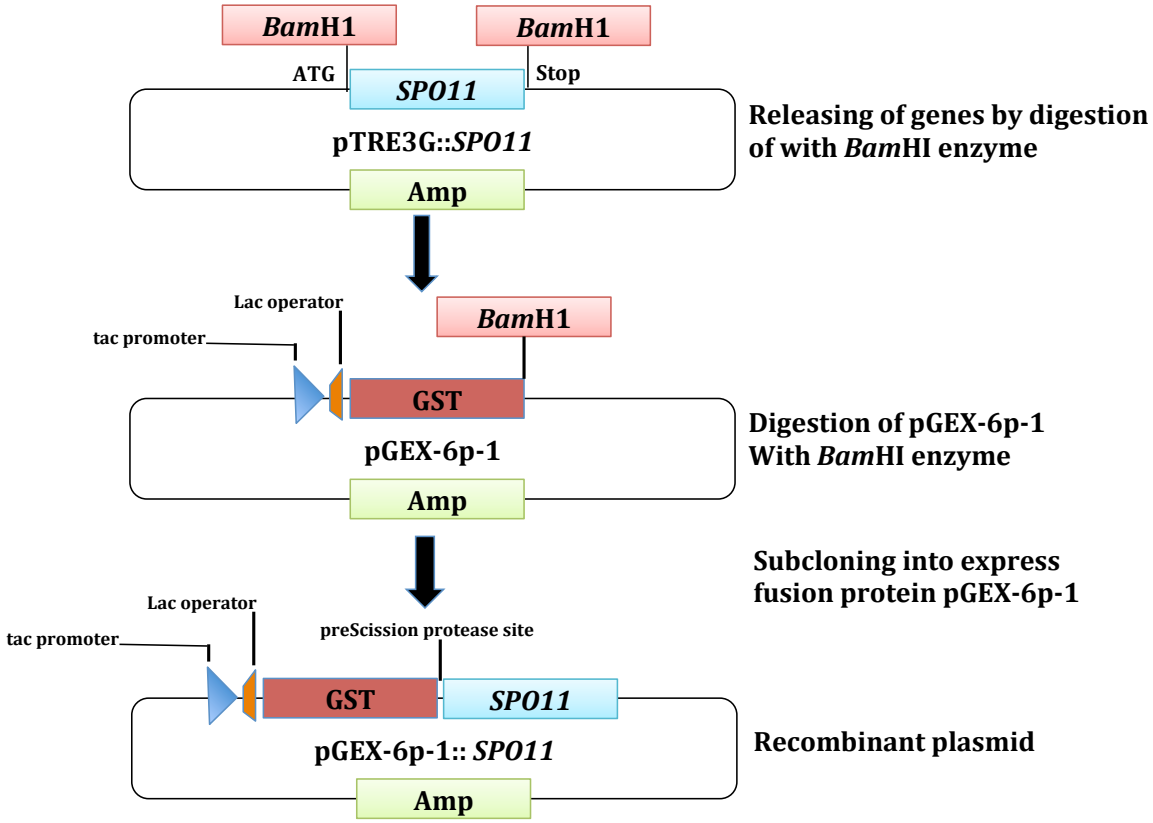

Figure 6.19 Schematic diagram of the sub-cloning strategy for the insertion of the *SPO11* gene into the fusion expression vector pGEX-6p-1. Step 1: The gene of interest was released from the recombinant plasmids pTRE3G::*SPO11* with the use of the *Bam*HI restriction enzyme. Step 2: pGEX-6p-1 plasmid was digested with *Bam*H1 at the multiple cloning site (MCS) after the GST taq site. Step 3: The *SPO11* gene was cloned into pGEX-6p-1; the proteins have an N-terminal GST tag, which aids in recombinant protein purification.

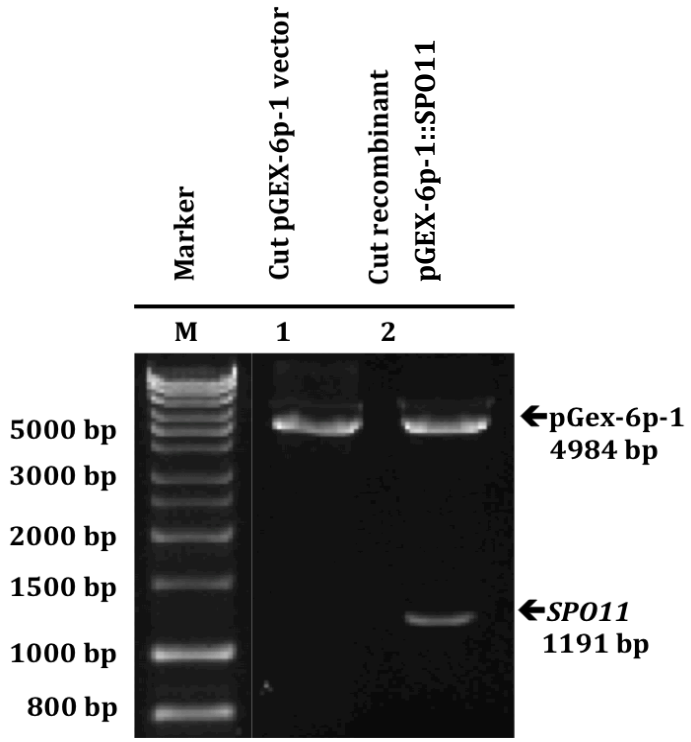

Figure 6.20 Digestion of recombinant pGEX-6p-1 expression plasmids with the *SPO11* gene. 0.8% agarose gel stained with PeqGREEN DNA Day confirms the cloning of *SPO11* into the pGEX-6p-1 plasmid. From left, Lane 1: Cut of the pGEX-6p-1 vector; Lane 2: Cut recombinant pGEX-6p-1::*SPO11*; 5 µl of HyperLadder 1 kb used as a marker.

6.4.1 optimizing the overexpression of *SPO11* with GST fusion proteins in *E. coli* cells

Recombinant plasmid pGEX-6p-1::*SPO11* was successfully transformed into *E. coli* BL21 to assess protein production. The pGEX-6p-1 plasmid contains a region encoding a 26 kDa GST tag, which can be express under the control of the IPTG-inducible tac promoter (Smith and Johnson, 1988). The production of recombination proteins was obtained from clones induced by growing cells in LB media at 37°C and treating with 100 μM IPTG for 5 hours, as described above (Sections 6.3.1 and 2.10.1, Materials and Methods). Analysis of the induced GST/SPO11 fusion protein showed the expected size of 70 kDa. To determine the solubility of the GST/SPO11 fusion proteins, the same condition described above was applied (Section 6.3.2). Both the pellet (insoluble) and the supernatants (soluble) were evaluated by using an anti-GST antibody, an anti-SPO11 antibody (Abcam, ab81695) also, Coomassie blue stained gels showed the induction in both insoluble and soluble (Figure 6.21). The results showed that the GST/SPO11 fusion protein still remained in the insoluble fraction (Figure 6.21).

6.4.2 purification of produced fusion proteins and PreScission Protease cleavage of the fusion protein

For the purified GST/SPO11 fusion protein, the same condition was applied, as described above (Section 6.3.3), and then the fusion protein was cleaved with PreScission Protease, as shown in Figure 6.22. Coomassie blue stained 4%–12% SDS-PAGE gel analysis showed that the fusion protein cleaved, and the band was in the expected size of SPO11 protein 44 kDa (Figure 6.23), as confirmed by Western blot analysis using an anti-SPO11 antibody (Abcam, ab81695); the same result was obtained after cleaved the fusion protein with PreScission (Figure 6.23).

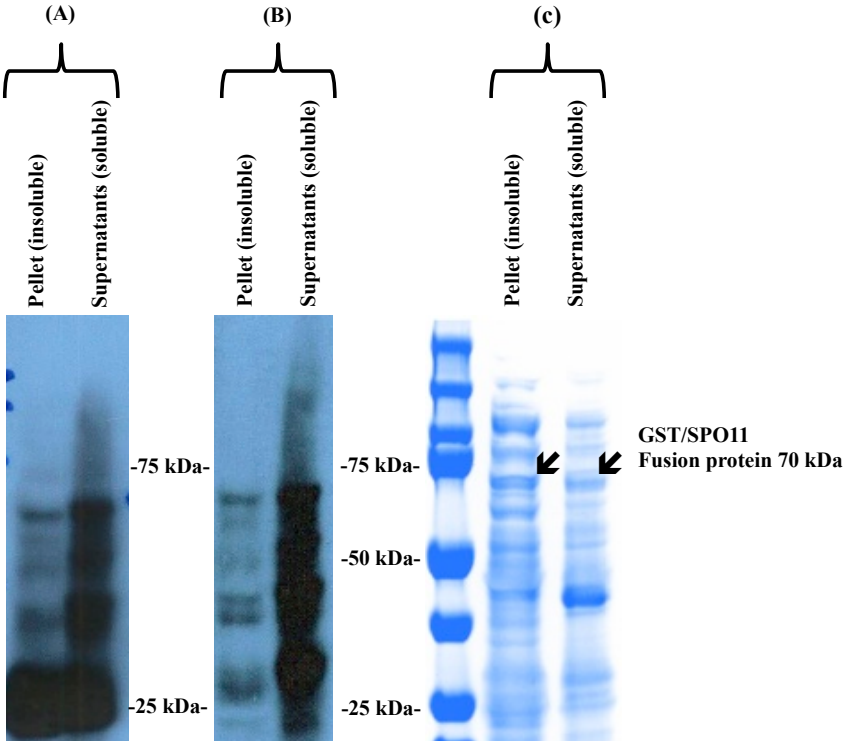

Figure 6.21 Determining the solubility of the GST/SPO11 fusion proteins. Both the pellet (insoluble) and the supernatants (soluble) showed the inductiom of the SPO11 fusion protein with 100 µM IPTG at 37°C for 5 hours. (A) Western blot expression evaluated the induction of the GST/SPO11 fusion protein with the use of an anti-GST antibody. (B) Western blot expression evaluated the induction of the GST/SPO11 fusion protein with the use of an anti-SPO11 antibody. (C) Comassie blue stained gels evaluated the induction of the GST/SPO11 protein. Arrows show equal induction in the expected size of 70 kDa in both (insoluble) and (soluble) fractions, corresponding to GST (≈26 kDa) fused to SPO11 (≈44 kDa).

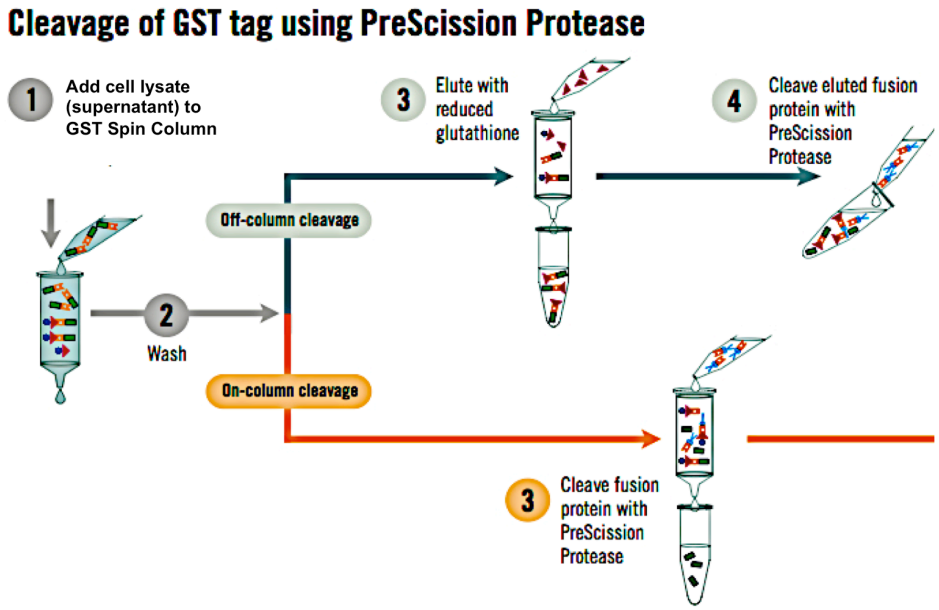

Figure 6.22. Flow chart of the affinity purification procedure and PreScission Protease cleavage of the GST fusion proteins. (Figures taken from the GST Gene Fusion System, Amersham Biosciences).

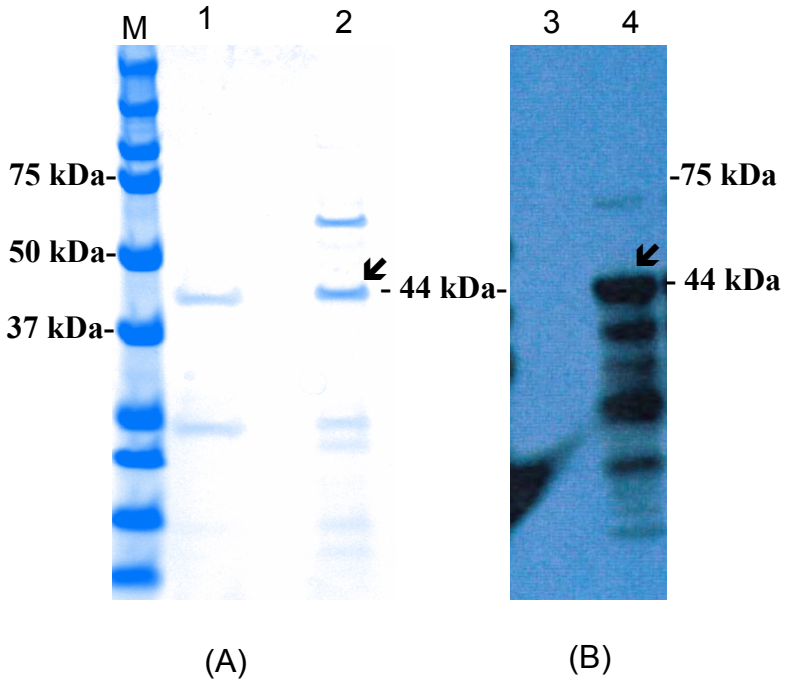

Figure 6.23 Monitoring the SPO11 protein after PreScission Protease cleavage. (A) Coomassie blue stained 4%–12% SDS-PAGE gel analysis showed that (1): PGEX-6p-1 (control) cleaved on the column with the enzyme; (2): Fusion protein (PGEX-6p-1/SPO11) cleaved on the column; an arrow indicates the SPO11 protein 44 kDa. (B) Western blot analysis used an anti-SPO11 antibody; (3): PGEX-6p-1 (control) cleaved on the column with the enzyme; (4): Fusion protein (PGEX-6p-1/SPO11) cleaved on the column; an arrow indicates the SPO11 protein 44 kDa.

6.5 Discussion

Oncogenesis is multifactorial, and emerging findings indicate cancer cells take on various germ cell-like characteristics (Mcfarlane, 2014; Feichtinger, 2014)). These germline genes are largely made up of the so-called cancer/testis (CT) genes, which are normally expressed in the testis of adult males, but become activated in cancers. CT genes have significant clinical interest because they encode cancer-specific antigens, which are novel immunotherapeutic and drug targets (Gjerstorff, 2015).

The SPO11 protein has been reported to be a CT gene and has been associated with pre-meiotic DNA replication (Koslowski, 2002). It is also a TOPOVIA-like (type IIB topoisomerase-like) protein, which acts in concert with the recently identified TOPOVIB sub-unit. Together these proteins mediate the formation of DNA double-strand breaks (DSBs) that initiate the inter-homologue meiotic recombination required for meiosis I reductional segregation (Robert, *et. al,* 2016).

The result in Chapter 3 was demonstrated that the SPO11 protein level was present in almost all cancer cell lines examined, but not present in healthy somatic tissues. This result confirms previous data demonstrating that *SPO11* is indeed a CTA, and also that *SPO11* depletion reduced proliferation potential of cancer cells (results in Chapter 3 and 5). Taken together these results support the hypothesis that SPO11 role in cancer cells, making it a potentially valuable biomarker in terms of both cancer diagnosis and prognosis. Furthermore, it believe that SPO11 is potentially acting as a topoisomerase, because co-stained cancer cells with antibodies to SPO11 and BLM showed good co-associated, together.

Recent advancement in functional and structural genomics has made high-level protein expression necessary for successful characterization of proteins. Proteins produced on a mass scale are of important use, for example, in pharmaceutical processes (e.g. high-throughput screens) as well as studying 3D protein structure in order to delineate residues important in protein function (Sury *et al.,* 1999; Stevens, *et al.,* 2000). *E. coli* is among the best studied microorganism, and has been established as a robust and cost-effective host for heterologous protein expression of many proteins (Makrides, *et al.,* 1996).

pGEX-2T and pGEX-6p-1 have been used in this study to express the SPO11 protein, Our attempt was successful to purified SPO11 in *E. coli* and the fusion protein was easily identified in western blot using commercial anti-GST HRP antibody, which should detect the SPO11 protein size because they have already cloned with the GST. The GST moiety located at the N-terminus followed by the SPO11 protein. Importantly, theses results also confirm the anti-SPO11 antibody's specifity. However, The purified SPO11 protein also was analysed by SDS-PAGE gels stained with Coomassie dye and band in expected size 44 kDa was cut in size and sent for analysed by mass spectrometry and the result confirm that contain pure SPO11 protein.

The SPO11 protein obtained after purification was not pure enough for crystal structure, but is potentially good enough to reconstitute type IIB topoisomerase activity and standard topoisomerase assay *in vitro* will provide the basis for the future development of high throughput drug screening of topoisomerase VI activity inhibition. However, our results also showed in most cases, the thrombin cleavage was inefficient and little of fusion proteins were cleaved even at high thrombin concentration (>1:50 of thrombin to substrate). This study suggests that the inefficient cleavage of fusion protein by thrombin may be due to the accessibility of the thrombin recognition site.

The work described in this chapter has focussed on the cloning and optimal expression of GST-tagged *SPO11* in order to not only validate the SPO11 antibody used in this thesis but also to obtain enough pure protein for crystal structure purposes. A topoisomerase VIB-like partner protein for SPO11 in miosis was recently identified (Robert *et al.,* 2016) Vrielynck *et al.,* 2016) it could be that *SPO11* requires topoVIBL as a partner to derive meiotic proliferation activity. These preliminary finding suggest SPO11 functions via a topoisomerase-like mechanism in cancer cells and this gene may have important applications in cancer drugs and therapeutic targets. So, it would be interesting to determine if SPO11 and topoVIBL co-purified in human cancer cells and have topoisomerase activity.

7. Summary and general discussion

Cancer is complex genetic/epigenetic disease. In most cases normal cells are transformed into cancer cells by the multi-step process of carcinogenesis. Carcinogenesis can be divided into three main steps: initiation, progression and termination. Carcinogenesis involves the accumulation of both genetic and epigenetic alterations in different genes. The three most-commonly affected gene categories are: oncogenes, tumour suppressor genes and genes involved in maintaining genomic stability (Hanahan & Weinberg 2011). In normal cells, the processes of cell growth and differentiation are tightly regulated by the proteins encoded by these genes, in order to maintain tissue homeostasis. Ultimately, a fundamental aim is to design targeted therapeutics to treat cancer without the limitation of potential adverse side effects on normal cells. Therefore, different biomarkers have been discovered that play key roles in detecting cancer and developing clinical applications (Joshi *et al*., 2016).

In terms of the latter, new human-specific antigens, known as CTAs, have gained a good deal of clinical interest, and have been identified as potential targets for immunotherapy and their corresponding genes have expression normally restricted to the testis of adult males, but become activated in cancers (Fratta, *et al.*, 2011; Whitehurst, *et al*., 2014). Moreover, CTAs have emerged to be a unique group of antigens that could potentially be important targets for antigen-specific cancer immunotherapy (Caballero & Chen, 2009; Costa *et al.,* 2007). Several studies have connected the function of CTA genes to the promotion of proliferation of different cancer cells, such as breast cancer and melanoma cells (Lajmi *et al*., 2015; Maxfield *et al.*, 2015; Wang *et al.,* 2016).

Oncogenesis is caused by a variety of factors, and recent research has demonstrated that cancer cells share some characteristics with germ cells (McFarlane, 2014; Feichtinger, 2014). Recent findings demonstrate that genes encoding factors that normally regulate meiotic chromosomes have other functions, which control oncogenic genome dynamics. For example, REC8 is a meiosis specific cohesin that could function in oncogenesis to drive changes in ploidy and reduces chromosome segregation in mitotically proliferating cells (Folco, *et al.,* 2017; Erenpreisa, *et al.,* 2009).

Another example is SYCP3, the meiotic synaptonemal complex protein, which has been shown to disrupt recombination mediated repair and drive ploidy changes in cancer cells (Hosoya, *et al.,* 2011). In addition, inter-homologue recombination regulator HOP2-MND1 has been demonstrated to be essential for oncogenic lengthening of telomeres via an inter-non-homologue break-induced replication (BIR)-mediated pathway (Cho, *et al.,* 2014).

Interestingly, SPO11 protein has been identified as a CTA (Koslowski, 2002). SPO11 has been shown to be associated with pre-meiotic DNA replication processes (Cha, *et al*., 2000). Also it's structure is highly conserved, being similar to a TOPOVIA-like (type IIB topoisomerase-like) protein that acts in concert with TOPOVIB to generate DSBs that create the inter-homologue meiotic recombination required for meiosis I reductional segregation (Robert *et. al*, 2016;Vrielynck, *et al.,* 2016).

The study propose that in cancer cells, some proteins including SPO11, SYCP3, PRDM9 and DMC1 may interrupt the mechanism that maintains genomic stability. Therefore, affecting the number of chromosomes in cells or enhancing chromosome rearrangement can be implicated of germ cell activation in cancer cells (Atanackovic *et al.*, 2011; Costa *et al*., 2007; Nielsen & Gjerstorff, 2016). Therefore, meiotic-like cell processes can be induced by up-regulation of meiotic proteins in somatic cells, leading to oncogenic genetic alterations and modification. In cancer cells, unsuitable inter-homologue recombination and inter-chromosomal recombination may occur from up-regulation of meiosis-specific proteins (Caballero & Chen, 2009). So, *SPO11* may have an important role in cancer initiation and chromosomal instability and may have meiotic-like functions in these cells leading to chromosome rearrangement or mis-segregation and plays an important role in mitotic chromosome dynamics.

Also, it has been suggested that SPO11 might have oncogenic functions separate to forming DSBs because it's expression is not limited to male germ cells (Nielsen & Gjerstorff, 2016). Janic *et al.,* (2010) studied the ectopic expression of germ-line genes in *Drosophila* tumours and concluded that the initiation and activation of these genes provides a proliferative advantage in cancer cells.

This supports the theory of soma-to-germline transformation in the carcinogenic processes, which is driven by the activation of germ-line genes, which includes CTAs (McFarlane *et al*., 2014). In this specific situation, *SPO11* might be activated in cancer cells as part of this transformation, which might contribute to their acquisition of a proliferative advantage.

Our study demonstrated the function and involvement of *SPO11* in cancer cells. Koslowski *et al.* (2002) reported that *SPO11* (CT35) is a CTA gene since its expression was detected in testis and in various cancer cells, including melanoma, lung and cervical cell lines, but not in normal tissues. In concurrence with this data this thesis showed that SPO11 protein was found to be present in the testis and also detected in all cancer cell lines tested, but not in other normal tissues, via western blot analysis. Moreover, this thesis demonstrated that the SPO11 protein was found to be required for cancer cells, where its depletion reduced the proliferative potential of cancer cells and significantly reduces the self-renewal capability of cancer stem-like cells and cancer cells. This data, taken together, suggests that cancer cells could have an obligate requirement for SPO11 to act as an oncogenic proliferative driver. Hence, this intrinsic feature could make *SPO11* a candidate therapeutic target for different cancer types. Importantly, our work validated the Abcam (ab81695) SPO11 antibody via knockdown experiments and cloning-specific GST tags, in order to confirm the identification of *SPO11* as a CTA gene.

The data presented in this thesis from western blot analysis and immunofluorescence staining indicated that the localisation of SPO11 protein in cancer cells seems to be mainly nuclear. In addition, co-staining with a BLM-specific antibody provided evidence to suggest that SPO11 could function together with BLM helicase as a topoisomerase to de-catenate segregating duplexes. BLM has been shown to play an important role in controlling homologous recombination (HR), which aims to repair DSBs and dissolve double Holliday junctions (dHJs) (Kikuchi *et al.*, 2009; Wu & Hickson, 2003). SPO11 is homologous to the topoisomerase subunit TopoVI A in archaebacteria. This protein is structurally related to the Type IIB family of eukaryotic topoisomerases, which acts in concert with the recently identified TOPOVIB subunit. Together these proteins mediate the formation of DNA (DSBs) that initiate the inter-homologue meiotic recombination required for meiosis I reductional segregation (Robert, *et. al,* 2016).

However, Rouzeau & Cordelières (2012) found that Topo IIα proteins are localised to the centromere to undertake normal decatenation during replication by BLM and PICH. As a homolog of the Topo IIB protein subunit, it is possible that the BLM protein will be able to recognise SPO11 in the same manner as the topoisomerase. It may be that in cancer cells, BLM is able to colocalize with the SPO11 protein, and use this mechanism to recruit SPO11 to the chromosomes.

Work described in this thesis demonstrates that the reduction of SPO11 protein affected the cell proliferation, which was more efficient at gene silencing methods, suggesting that SPO11 is essential for cancer cell growth. This finding is supported by the observation in this thesis that the majority of SPO11 protein depletion was seen in the floating cells, which were generated after SPO11 knockdown. Remarkably, some studies have also seen that the level or rate of tumour invasion and cell viability was also significantly reduced when depleting some CTAs, such as, XAGE1, SSX4 and GAGE in Melanoma cell lines (Caballero *et al.,* 2013). Based on the results presented in this work, the reduction of SPO11 (using *SPO11*-specific siRNAs) largely affected the size of the population of floating cells compared to attached cells.

SPO11-depleted HCT116 colonospheres did not appear to result in senescence or apoptosis as assessed by caspase-3 cleavage and β-galactosidase assays, respectively. However, when given suitable conditions for growth this can lead to the recovery of the cells from proliferation arrest. This is consistent with SPO11-depleted cells being in a quiescent-like state. The quiescent state is adopted in stem cells for the preservation of the main functional features of the cells. Cells in this state remain poised and ready to be activated, rather than being inactive or dormant (Cheung & Rando, 2013). In this thesis, a stable *SPO11* knockout colon cell line (HCT116) was created using CRISPR/Cas9 (Clustered Regularly Interspaced Short Palindromic Repeats) technique to generate null mutation of the two endogenous *SPO11* alleles. These cells were shown to have a reduced growth and proliferation rate in conjunction with a reduction in SPO11 protein levels. This result was consist with siRNA *SPO11* knockdown and confirmed that the reduction of SPO11 protein levels in cancer cells used in this thesis may lead to inhibition of cell proliferation. HCT116 cells which over-expressed *SPO11* (in a doxycycline-controlled manner) showed no significant effect on cell proliferation.

In addition, HCT116 cells were generated which expressed *SPO11* only in the presence of doxycycline. After doxycycline induction, HCT116-*SPO11* shRNA clones showed not only a reduction in *SPO11* mRNA and protein levels, but also a marked decrease in proliferation rates and elongated doubling times when comparing untreated clones and treated controls. Doxycycline-treated shRNA-cell lines showed lower knockdown efficiencies than HCT116-SPO11siRNA cells and CRISPR/Cas9 clones possibly due to the amount of shRNA per cell compared to siRNA/KO cell lines. However, it is also possible that SPO11 depletion is a leading cause of chromosome rearrangement at the time of mitotic cell division due to incorrect replication and/or initiation of DSBs.

The SPO11 protein obtained after purification was not pure enough for crystal structure determination, but is potentially good enough to use in a standard topoisomerase assay *in vitro* and will provide the basis for the future development of high throughput drug screening of topoisomerase VI activity with associated drug inhibition. These preliminary findings might suggest that SPO11 functions via a topoisomerase-like mechanism in cancer cells, and this gene may have important applications in the development of new cancer drugs. It would be interesting to determine if SPO11 and topoVIBL, the partner protein for SPO11, could be co-purified in human cancer cells and be shown to have topoisomerase activity *in vitro* using a standard topoisomerase assay employed for Archaeal TopoVI (using Archaeal TopoVI as a positive control). However, ultimately it is the study of the SPO11 crystal structure which will help to understand its physiological role as well as identify key structural amino acids and residues that can be targeted with designer drugs. This will contribute to a greater understanding of how/what proteins interact with SPO11, and to be able to specifically target SPO11 in order to limit proliferation of cancer cells.

7.1 Closing remarks

The result from this thesis has shed some light into the essential role of SPO11 protein in cancer cells making it a valuable therapeutic target for cancer. In addition, since *SPO11* is a CTA gene, it could be used for future development of new-targeted cancer drugs. Understanding the implications of *SPO11* gene and protein product as they pertain to the diagnosis and treatment of cancer will become increasingly important since the incidence of cancer and its related mortality rates are rising around the globe. *SPO11* is one of the genetic factors that contribute to the development of cancer by supporting tumour growth via abnormal meiotic cellular processes. Since *SPO11* is overexpressed in cancer cells, and is absent in normal cells, it is feasible for researchers to utilise their knowledge of this biomarker to create pharmaceutical interventions that specifically target cancer cells only for destruction leaving health cells undesirably. *SPO11* demonstrates potential as an early diagnostic tool as well as a measure of disease outcomes. It might become an important asset in tumour stratification, resulting in different therapeutic treatments for different stages/types of cancer.

The results in this thesis provide an important basis for further future investigation of the role of SPO11 into other cancer cell types, and could lead to SPO11 being identified as an important cancer biomarker. Therefore several suggestions for further investigations are proposed:

-The study of the SPO11 crystal structure will help to understand its physiological role as well as identify key amino acids involved in structure and also residues that can be targeted with designer drugs. Small inhibitors can be designed in silico and they have to be produced and tested both in vitro and in vivo.

-The crystal structure of topoisomerases is valuable tools for drug developers because this information could be utilised to determine the best structure-based designed for pharmaceuticals. This will contribute to a greater understanding of how/what proteins interact with SPO11, and to be able to specifically target SPO11 in order to limit proliferation of cancer cells. A topoispmerase VIB-like partner protein for SPO11 in meiosis was recently identified, TOPOVIBL it could be that *SPO11* requires TopoVIBL as a partner to drive mitotic proliferation activity.

TopoVIBL levels might be the limiting factors and so it could be worth studding this possibility further, this was not done as TopoVIBL was only identified as a SPO11 binding partner late in this work. So, it would be interesting to determine if SPO11 and TopoVIBL co-purified in human cancer cells and have topoisomerase activity. A topoisomerase assays for purified SPO11 and TOPOVIBL protein could be developed and used to test small molecule inhibitors in vitro. Also, carrying out co-immunoprecipitation (co-IP) using antibodies against the SPO11- interacting partners followed by western blotting to detect SPO11.

Lastly, it remains unclear whether SPO11 is directly working in tumours in situ. This is a difficult thing to discern. Aside from immunohistochemistry to assess the extent of the presence of SPO11, tumour cells could be used to directly derive tumour spheres and the role of SPO11 in their formation and maintenance could be assessed, although this provides a number of technical challenges.

So, overall, SPO11 represents a new cancer-biomarker and therapeutic targets. Gaining insight into the function of SPO11 in cancers will enable to better understand ontogenesis and design appropriate clinically relevant therapeutics to take advantage of the cancer-specific nature of SPO11 activity.

References

Aarts, M., Linardopoulos, S. & Turner, N.C. 2013. Tumour selective targeting of cell cycle kinases for cancer treatment. Current opinion in pharmacology. 13 (4). pp. 529-535.

Abramovitz, M. & Leyl &-Jones, B. 2006. A systems approach to clinical oncology: focus on breast cancer. *Proteome science.* 4 pp. 5.

Adair, S.J. & Hogan, K.T. 2009. Treatment of ovarian cancer cell lines with 5-aza-2′-deoxycytidine upregulates the expression of cancer-testis antigens and class I major histocompatibility complex-encoded molecules. *Cancer immunology, immunotherapy.* 58 (4). pp. 589-601.

Adams, S., Greeder, L., Reich, E., Shao, Y., Fosina, D., Hanson, N., Tassello, J., Singh, B., Spagnoli, G.C. & Demaria, S. 2011. Expression of cancer testis antigens in human BRCA-associated breast cancers: potential targets for immunoprevention? *Cancer immunology, immunotherapy.* 60 (7). pp. 999-1007.

Agrawal, N., Dasaradhi, P.V., Mohmmed, A., Malhotra, P., Bhatnagar, R.K. & Mukherjee, S.K. 2003. RNA interference: biology, mechanism, and applications. *Microbiology and molecular biology reviews : MMBR.* 67 (4). pp. 657-685.

Ahluwalia, M.S. & Winkler, F. 2015. Targeted and immunotherapeutic approaches in brain metastases. *American Society of Clinical Oncology educational book.American Society of Clinical Oncology.Meeting.* pp. 67-74.

Akhavan-Niaki, H. & Samadani, A.A. 2013. DNA methylation and cancer development: molecular mechanism. *Cell biochemistry and biophysics.* 67 (2). pp. 501-513.

Akhavan, D., Pourzia, A., Nourian, A., Williams, K., Nathanson, D., Babic, I., Villa, G., Tanaka, K., Nael, A., Yang, H., Dang, J., Vinters, H., Yong, W., Flagg, M., Tamanoi, F., Sasayama, T., James, C., Kornblum, H., Cloughesy, T., Cavenee, W., Bensinger, S. and Mischel, P. 2013 . De-Repression of PDGFRβ Transcription Promotes Acquired Resistance to EGFR Tyrosine Kinase Inhibitors in Glioblastoma Patients. Cancer Discovery, 3(5), pp.534-547.

Alison, M.R., Lim, S.M.L. & Nicholson, L.J. 2011. Cancer stem cells: problems for therapy? The Journal of pathology 223(2), pp. 147–61.

Almatrafi, A., Feichtinger, J., Vernon, E.G., Escobar, N.G., Wakeman, J.A., Larcombe, L.D. & McFarlane, R.J. 2014. Identification of a class of human cancer germline genes with transcriptional silencing refractory to the hypomethylating drug 5-aza-2'-deoxycytidine. *Oncoscience.* 1 (11). pp. 745-750.

Almeida, L.G., Sakabe, N.J., deOliveira, A.R., Silva, M.C., Mundstein, A.S., Cohen, T., Chen, Y.T., Chua, R., Gurung, S., Gnjatic, S., Jungbluth, A.A., Caballero, O.L., Bairoch, A., Kiesler, E., White, S.L., Simpson, A.J., Old, L.J., Camargo, A.A. & Vasconcelos, A.T. 2009. CTdatabase: a knowledge-base of high-throughput and curated data on cancer-testis antigens. *Nucleic acids research.* 37 (Database issue). pp. D816-9.

References

Aly, H.A. 2012. Cancer therapy and vaccination. *Journal of immunological methods.* 382 (1). pp. 1-23.

American Cancer Society (2017). Cancer Treatment & Survivorship Facts & Figures. [online] www.cancer.org. Available at: https://www.cancer.org/content/dam/cancer-org/research/cancer-facts-and-statistics/cancer-treatment-and-survivorship-facts-and-figures/cancer-treatment-and-survivorship-facts-and-figures-2016-2017.pdf [Accessed 29 May 2017].

Amor-GuéRet, M. 2006. Bloom syndrome, genomic instability and cancer: the SOS-like hypothesis. Cancer letters, 236, 1-12.

Anand, P., Kunnumakara, A.B., Sundaram, C., Harikumar, K.B., Tharakan, S.T., Lai, O.S., Sung, B. & Aggarwal, B.B. 2008. Cancer is a preventable disease that requires major lifestyle changes. *Pharmaceutical research.* 25 (9). pp. 2097-2116.

Apostolopoulos V. SLGS. 2015. MUC1 (CD227): a multi-tasked molecule. *Cellular and Molecular Life Sciences* vol no.72: pp no: 4475-4500.

Aravind L, Leipe DD & Koonin EV. 1998.Toprim--a conserved catalytic domain in type IA and II topoisomerases, DnaG-type primases, OLD family nucleases and RecR proteins. *Nucleic Acids Res* 26: 4205-4213.

Askew, D.S., Ashmun, R.A., Simmons, B.C. & Clevel &, J.L. 1991. Constitutive c-myc expression in an IL-3-dependent myeloid cell line suppresses cell cycle arrest and accelerates apoptosis. *Oncogene.* 6 (10). pp. 1915-1922.

Assanga, I. & Lujan, L. 2013. Cell growth curves for different cell lines and their relationship with biological activities. *International Journal of Biotechnology and Molecular Biology Research.* 4 (4). pp. 60-70.

Atanackovic, D., Luetkens, T., Kloth, B., Fuchs, G., Cao, Y., Hildebrandt, Y., Meyer, S., Bartels, K., Reinhard, H., Lajmi, N., Hegewisch-Becker, S., Schilling, G., Platzbecker, U., Kobbe, G., Schroeder, T., Bokemeyer, C. & Kroger, N. 2011. Cancer-testis antigen expression and its epigenetic modulation in acute myeloid leukemia. *American Journal of Hematology.* 86 (11). pp. 918-922.

Atcheson, C.L., DiDomenico, B., Frackman, S., Esposito, R.E. & Elder, R.T. 1987. Isolation, DNA sequence, and regulation of a meiosis-specific eukaryotic recombination gene. *Proceedings of the National Academy of Sciences of the United States of America.* 84 (22). pp. 8035-8039.

Bagci, O. & Kurtgoz, S. 2015. Amplification of Cellular Oncogenes in Solid Tumors. North *American journal of medical sciences.* 7 (8). pp. 341-346.

Bai, S., He, B. & Wilson, E.M. 2005. Melanoma antigen gene protein MAGE-11 regulates androgen receptor function by modulating the interdomain interaction. *Molecular and cellular biology.* 25 (4). pp. 1238-1257.

Barchi, M., Roig, I., Di Giacomo, M., de Rooij, D. G., Keeney, S. & Jasin, M. 2008 'ATM promotes the obligate XY crossover and both crossover control and chromosome axis integrity on autosomes', PLOS Genet., 4(5):e1000076.

Bardin, A.J. & Amon, A. 2001. Men and sin: what's the difference? *Nature Reviews Molecular Cell Biology.* 2 (11). pp. 815-826.

Barrio, M.M., Abes, R., Colombo, M., Pizzurro, G., Boix, C., Roberti, M.P., Gelize, E., Rodriguez-Zubieta, M., Mordoh, J. & Teillaud, J.L. 2012. Human macrophages and dendritic cells can equally present MART-1 antigen to CD8(+) T cells after phagocytosis of gamma-irradiated melanoma cells. *PloS one.* 7 (7). pp. e40311.

Bartlett, D.L., Liu, Z., Sathaiah, M., Ravindranathan, R., Guo, Z., He, Y. & Guo, Z.S. 2013. Oncolytic viruses as therapeutic cancer vaccines. *Molecular cancer.* 12 (1). pp. 1.

Baudat, F. & Nicolas, A. 1997. Clustering of meiotic double-strand breaks on yeast chromosome III', PNAS, 94(10):5213–18.

Baudat, F., Manova, K., Yuen, J.P., Jasin, M. & Keeney, S. 2000. Chromosome synapsis defects and sexually dimorphic meiotic progression in mice lacking Spo11. *Molecular cell.* 6 (5). pp. 989-998.

Baulande, S., Criqui, A. & Duthieuw, M. 2014. Circulating miRNAs as a new class of biomedical markers. *Medecine sciences : M/S.* 30 (3). pp. 289-296.

Beaupre, D.M. & Kurzrock, R. 1999. RAS & leukemia: from basic mechanisms to gene-directed therapy. Journal of clinical oncology : official journal of the American Society of Clinical Oncology. 17 (3). pp. 1071-1079.

Beck, B. & Blanpain, C. 2013. Unravelling cancer stem cell potential. Nature reviews. Cancer 13(10), pp. 727–38.

Beckwith, J. 2000. The all purpose gene fusion. Methods Enzymol. 326 3–7. [PubMed]

Behl, C. & Ziegler, C. 2014a. Cell Aging: Molecular Mechanisms and Implications for.

Behl, C. & Ziegler, C. 2014b. Cell Cycle: The Life Cycle of a Cell. In: *Cell Aging: Molecular Mechanisms and Implications for Disease.* Springer: pp. 9-19.

Behlke, M.A. 2006. Progress towards in vivo use of siRNAs. *Molecular therapy : the journal of the American Society of Gene Therapy.* 13 (4). pp. 644-670.Bellani, M., Boateng, K., McLeod, D. & Camerini-Otero, R. 2010. The Expression Profile of the Major Mouse SPO11 Isoforms Indicates that SPO11 Introduces Double Strand Breaks and Suggests that SPO11 Has an Additional Role in Prophase in both Spermatocytes and Oocytes. Molecular and Cellular Biology, 30(18), pp.4391-4403.

Bellani, M.A., Boateng, K.A., McLeod, D. & Camerini-Otero, R.D. 2010. The expression profile of the major mouse SPO11 isoforms indicates that SPO11beta introduces doub

strand breaks and suggests that SPO11alpha has an additional role in prophase in both spermatocytes and oocytes. *Molecular and cellular biology.* 30 (18). pp. 4391-4403.

Belpomme, D., Irigaray, P., Hardell, L., Clapp, R., Montagnier, L., Epstein, S. & Sasco, A.J. 2007. The multitude and diversity of environmental carcinogens. *Environmental research.* 105 (3). pp. 414-429.

Bergerat, A., de Massy, B., Gadelle, D., Varoutas, P.C., Nicolas, A. & Forterre, P. 1997. An atypical topoisomerase II from Archaea with implications for meiotic recombination. *Nature.* 386 (6623). pp. 414-417.

Bergerat A, Gadelle D & Forterre P. 1994, Purification of a DNA topoisomerase II from the hyperthermophilic archaeon Sulfolobus shibatae. A thermostable enzyme with both bacterial and eucaryal features. *J Biol Chem* 269: 27663-27669.

Berlin, A., Lalonde, E., Sykes, J., Zafarana, G., Chu, K.C., Ramnarine, V.R., Ishkanian, A., Sendorek, D.H., Pasic, I. & Lam, W.L. 2014. NBN gain is predictive for adverse outcome following image-guided radiotherapy for localized prostate cancer. Oncotarget. 5 (22). pp. 11081-11090.

Bhatia, N., Yang, B., Xiao, T.Z., Peters, N., Hoffmann, M.F. & Longley, B.J. 2011. Identification of novel small molecules that inhibit protein–protein interactions between MAGE and KAP-1. *Archives of Biochemistry and Biophysics.* 508 (2). pp. 217-221.

Bhuiyan, H. & Schmekel, K. 2004. Meiotic Chromosome Synapsis in Yeast Can Occur Without Spo11-Induced DNA Double-Strand Breaks. Genetics, 168(2), pp.775-783.

Bischof, O., Kim, S.-H., Irving, J., Beresten, S., Ellis, N. A. & Campisi, J. 2001. Regulation And Localization Of The Bloom Syndrome Protein In Response To Dna Damage. The Journal Of Cell Biology, 153, 367-380.

Bizard, A. & Hickson, I. 2014. The Dissolution of Double Holliday Junctions. Cold Spring Harbor Perspectives in Biology, 6(7), pp.a016477-a016477.

Blanchard, T., Srivastava, P.K. & Duan, F. 2013. Vaccines against advanced melanoma. Clinics in dermatology. 31 (2). pp. 179-190.

Blanco-Rodriguez, J. 2012. Programmed phosphorylation of histone H2AX precedes a phase of DNA double-strand break-independent synapsis in mouse meiosis. Reproduction (Cambridge, England). 144 (6). pp. 699-712.

Boateng, K.A., Bellani, M.A., Gregoretti, I.V., Pratto, F. & Camerini-Otero, R.D. 2013. Homologous pairing preceding SPO11-mediated double-strand breaks in mice. *Developmental cell.* 24 (2). pp. 196-205.

Borde, V., Goldman, A. S. & Lichten, M. 2000. Direct Coupling Between Meiotic Dna Replication And Recombination Initiation. Science, 290, 806-809.

Bornhorst, J.A. & Falke, J.J. 2000. Purification of proteins using polyhistidine affinity tags. Methods Enzymol. 326 245–254. [PMC free article] [PubMed

Brábek, J., Mierke, C.T., Rösel, D., Veselý, P. & Fabry, B. 2010. The role of the tissue microenvironment in the regulation of cancer cell motility and invasion. *Cell Communication and Signaling.* 8 (1). pp. 1.

Brasseur, F., Rimoldi, D., Lienard, D., Lethe, B., Carrel, S., Arienti, F., Suter, L., Vanwijck, R., Bourlond, A. & Humblet, Y. 1995. Expression of MAGE genes in primary and metastatic cutaneous melanoma. *International journal of cancer.* 63 (3). pp. 375-380.

Bressan, D.A., Olivares, H.A., Nelms, B.E. & Petrini, J.H. 1998. Alteration of N-terminal phosphoesterase signature motifs inactivates Saccharomyces cerevisiae Mre11. *Genetics.* 150 (2). pp. 591-600.

Bretones, G., Delgado, M.D. & León, J. 2015. Myc and cell cycle control. *Biochimica et Biophysica Acta (BBA)-Gene Regulatory Mechanisms.* 1849 (5). pp. 506-516.

Brick, K., Smagulova, F., Khil, P., Camerini-Otero, R. D. & Petukhova, G. V. 2012. Genetic recombination is directed away from functional genomic elements in mice, Nature, 485(7400):642–45.

Buard, J., Barthés, P., Grey, C. & de Massy, B. 2009 'Distinct histone modifications define initiation and repair of meiotic recombination in the mouse', EMBO J., 28(17):2616–24.

Bucher, M.H., Evdokimov, A.G. & Waugh, D.S. 2002. Differential effects of short affinity tags on the crystallization of Pyrococcus furiosus maltodextrin-binding protein. *Acta crystallographica.Section D, Biological crystallography.* 58 (Pt 3). pp. 392-397.

Bugreev, D. V., Yu, X., Egelman, E. H., & Mazin, A. V. 2007. Bloom Syndrome Helicase Stimulates RAD51 DNA Strand Exchange Activity through a Novel Mechanism Genes Dev. 213085 –3094 [PMC free article] [PubMed]

Buhler, C., Borde, V. & Lichten, M. 2007 'Mapping meiotic single-strand DNA reveals a new landscape of DNA double-strand breaks in Saccharomyces cerevisiae', PLOS Biol., 5(12):e324.

Buhler C, Gadelle D, Forterre P. 1998 Reconstitution of DNA topoisomerase VI of the thermophilic archaeon Sulfolobus shibatae from subunits separately overexpressed in Escherichia coli. *Nucleic Acids Res* 26: 5157-5162.

Buonomo, S.B., Clyne, R.K., Fuchs, J., Loidl, J., Uhlmann, F. & Nasmyth, K. 2000. Disjunction of homologous chromosomes in meiosis I depends on proteolytic cleavage of the meiotic cohesin Rec8 by separin. *Cell.* 103 (3). pp. 387-398.

Burger, M., Catto, J.W., Dalbagni, G., Grossman, H.B., Herr, H., Karakiewicz, P., Kassouf, W., Kiemeney, L.A., La Vecchia, C. & Shariat, S. 2013. Epidemiology and risk factors of urothelial bladder cancer. European urology. 63 (2). pp. 234- 241.

Butterfield, L.H. 2015. Cancer vaccines. *BMJ (Clinical research ed.).* 350 pp. h988.

Caballero, O.L. & Chen, Y.T. 2009. Cancer/testis (CT) antigens: potential targets for immunotherapy. *Cancer science.* 100 (11). pp. 2014-2021.

Caballero, O.L., Cohen, T., Gurung, S., Chua, R., Lee, P., Chen, Y.T., Jat, P. & Simpson, A.J. 2013. Effects of CT-Xp gene knock down in melanoma cell lines. *Oncotarget.* 4 (4). pp. 531-541.

Campos Perez, J., Rice, J., Escors, D., Collins, M., Paterson, A., Savelyeva, N. & Stevenson, F.K. 2013. DNA fusion vaccine designs to induce tumor-lytic CD8 T-cell attack via the immunodominant cysteine containing epitope of NY-ESO 1. *International journal of cancer.* 133 (6). pp. 1400-1407.

Cao, L., Alani, E. & Kleckner, N. 1990. A pathway for generation and processing of double-strand breaks during meiotic recombination in S. cerevisiae. *Cell.* 61 (6). pp. 1089-1101.

Cappell, K.M., Sinnott, R., Taus, P., Maxfield, K., Scarbrough, M. & Whitehurst, A.W. 2012. Multiple cancer testis antigens function to support tumor cell mitotic fidelity. *Molecular and cellular biology.* 32 (20). pp. 4131-4140.

Carelle, N., Piotto, E., Bellanger, A., Germanaud, J., Thuillier, A. & Khayat, D. 2002. Changing patient perceptions of the side effects of cancer chemotherapy. *Cancer.* 95 (1). pp. 155-163.

Carofiglio, F., Inagaki, A., de Vries, S., Wassenaar, E., Schoenmakers, S., Vermeulen, C., van Cappellen, W.A., Sleddens-Linkels, E., Grootegoed, J.A., Te Riele, H.P., de Massy, B. & Baarends, W.M. 2013. SPO11-independent DNA repair foci and their role in meiotic silencing. PLoS genetics. 9 (6). pp. e1003538.

Carroll, C. W. & Straight, A. F. 2006. Centromere Formation: From Epigenetics To Self-Assembly. Trends In Cell Biology, 16, 70-78.

Cavallo, F., De Giovanni, C., Nanni, P., Forni, G. & Lollini, P.L. 2011. 2011: the immune hallmarks of cancer. *Cancer Immunology, Immunotherapy.* 60 (3). pp. 319-326.

Celerin, M., Merino, S.T., Stone, J.E., Menzie, A.M. & Zolan, M.E. 2000. Multiple roles of Spo11 in meiotic chromosome behavior. *The EMBO journal.* 19 (11). pp. 2739-2750.

Cervantes, M. D., Farah, J. A. & Smith, G. R. 2000. Meiotic Dna Breaks Associated With Recombination In S. Pombe. Molecular Cell, 5, 883-888.

Cesare, A.J. & Reddel, R.R. 2010. Alternative lengthening of telomeres: models, mechanisms and implications. *Nature reviews.Genetics.* 11 (5). pp. 319-330.

Cha, R.S., Weiner, B.M., Keeney, S., Dekker, J. & Kleckner, N. 2000. Progression of meiotic DNA replication is modulated by interchromosomal interaction proteins, negatively by Spo11p and positively by Rec8p. *Genes & development.* 14 (4). pp. 493-503.

Chaffer, C.L. & Weinberg, R.A. 2011. A perspective on cancer cell metastasis. *Science.* 331 (6024). pp. 1559-1564.

Chaganti, R. S., Schonberg, S. & German J. 1974. A Manyfold Increase in Sister Chromatid Exchanges in Bloom's Syndrome Lymphocytes. Proc. Natl. Acad. Sci. U.S.A., 71, 4508–4512

Chaganti, R. S., Schonberg, S. & German, J. 1974. Proc. Natl. Acad. Sci. U.S. A., 714508 – 4512.

Champoux, J. J. 2001. DNA Topoisomerases: Structure, Function, and Mechanism. Annu. Rev. Biochem., 70, 369–413.

Chan, K. L., North, P. S. & Hickson, I. D. 2007. BLM is required for faithful chromosome segregation and its localization defines a class of ultrafine anaphase bridges. EMBO J., 26, 3397–3409.

Chang, M., Bellaoui, M., Zhang, C., Desai, R., Morozov, P., Delgado-Cruzata, L., Rothstein, R., Freyer, G. A., Boone, C. & Brown, G. W. 2005. *RMI1/NCE4*, a suppressor of genome instability, encodes a member of the RecQ helicase/Topo III complex. EMBO J., 24, 2024–2033.

Cheema, Z., Hari-Gupta, Y., Kita, G., Farrar, D., Seddon, I., Corr, J. & Klenova, E. 2014. Expression of the cancer testis antigen BORIS correlates with prostate cancer. The Prostate. 74 (2). pp. 164-176.

Cheever, M.A., Allison, J.P., Ferris, A.S., Finn, O.J., Hastings, B.M., Hecht, T.T., Mellman, I., Prindiville, S.A., Viner, J.L., Weiner, L.M. & Matrisian, L.M. 2009. The prioritization of cancer antigens: a national cancer institute pilot project for the acceleration of translational research. *Clinical cancer research : an official journal of the American Association for Cancer Research.* 15 (17). pp. 5323-5337.

Chen, Y.J., Dominguez-Brauer, C., Wang, Z., Asara, J.M., Costa, R.H., Tyner, A.L., Lau, L.F. & Raychaudhuri, P. 2009. A conserved phosphorylation site within the forkhead domain of FoxM1B is required for its activation by cyclin-CDK1. *The Journal of biological chemistry.* 284 (44). pp. 30695-30707.

Chen, Y.T. 2014. Detection of cancer/testis antigens as a diagnostic tool in routine pathology practice. *Oncoimmunology.* 3 pp. e28132.

Chen, Y.T., Chadburn, A., Lee, P., Hsu, M., Ritter, E., Chiu, A., Gnjatic, S., Pfreundschuh, M., Knowles, D.M. & Old, L.J. 2010. Expression of cancer testis antigen CT45 in classical Hodgkin lymphoma and other B-cell lymphomas. *Proceedings of the National Academy of Sciences of the United States of America.* 107 (7). pp. 3093-3098.

Chen, Y.T., Scanlan, M.J., Sahin, U., Tureci, O., Gure, A.O., Tsang, S., Williamson, B., Stockert, E., Pfreundschuh, M. & Old, L.J. 1997. A testicular antigen aberrantly expressed in human cancers detected by autologous antibody screening. *Proceedings of the National Academy of Sciences of the United States of America.* 94 (5). pp. 1914-1918.

Chen, Y.T., Venditti, C.A., Theiler, G., Stevenson, B.J., Iseli, C., Gure, A.O., Jongeneel, C.V., Old, L.J. & Simpson, A.J. 2005. Identification of CT46/HORMAD1, an immunogenic cancer/testis antigen encoding a putative meiosis-related protein. *Cancer immunity.* 5 pp. 9.

Chen, Z., Yang, H. & Pavletich, N.P. 2008. Mechanism of homologous recombination from the RecA-ssDNA/dsDNA structures. *Nature.* 453 (7194). pp. 489-484.

Cheng, Y.H., Wong, E.W. & Cheng, C.Y. 2011. Cancer/testis (CT) antigens, carcinogenesis and spermatogenesis. *Spermatogenesis.* 1 (3). pp. 209-220.

Cheok, C. F., Bachrati, C. Z., Chan, K. L., Ralf, C., Wu, L. & Hickson, I. D. 2005. Biochem. Soc. Trans., 331456 –1459.

Cheson, B.D. & Leonard, J.P. 2008. Monoclonal antibody therapy for B-cell non-Hodgkin's lymphoma. *New England Journal of Medicine.* 359 (6). pp. 613-626.

Chicheportiche, A., Bernardino-Sgherri, J., de Massy, B. & Dutrillaux, B. 2007. Characterization of Spo11-dependent and independent phospho-H2AX foci during meiotic prophase I in the male mouse. *Journal of cell science.* 120 (Pt 10). pp. 1733-1742.

Cho, N.W., Dilley, R.L., Lampson, M.A. & Greenberg, R.A. 2014. Interchromosomal homology searches drive directional ALT telomere movement and synapsis. *Cell.* 159 (1). pp. 108-121.

Chomez, P., De Backer, O., Bertrand, M., De Plaen, E., Boon, T. & Lucas, S. 2001. An overview of the MAGE gene family with the identification of all human members of the family. *Cancer research.* 61 (14). pp. 5544-5551.

Choudhury, J.D., Kumar, S., Mayank, V., Mehta, J. & Bardalai, D. 2012. A review on apoptosis & its different pathway. *International Journal of Biological and Pharmaceutical Research.* 3 pp. 848-861.

Clevers, H. 2011. The cancer stem cell: premises, promises and challenges. Nature medicine 17(3), pp. 313–9.

Clift, D. & Marston, A. 2011. The role of shugoshin in meiotic chromosome segregation. *Cytogenetic and genome research.* 133 (2-4). pp. 234-242.

Cohen, C.J., Gartner, J.J., Horovitz-Fried, M., Shamalov, K., Trebska-McGowan, K., Bliskovsky, V.V., Parkhurst, M.R., Ankri, C., Prickett, T.D. & Crystal, J.S. 2015. Isolation of neoantigen-specific T cells from tumor and peripheral lymphocytes. *The Journal of clinical investigation.* 125 (10). pp. 3981-3991.

Cole, F., Kauppi, L., Lange, J., Roig, I., Wang, R., Keeney, S. & Jasin, M. 2012. Homeostatic control of recombination is implemented progressively in mouse meiosis. *Nature cell biology.* 14 (4). pp. 424-430.

Cole, F., Keeney, S. & Jasin, M. 2010. Evolutionary conservation of meiotic DSB proteins: more than just Spo11. *Genes & development.* 24 (12). pp. 1201-1207.

Cole, F., Keeney, S. & Jasin, M. 2010, Comprehensive, fine-scale dissection of homologous recombination outcomes at a hot spot in mouse meiosis', Mol Cell., 39(5):700–10.

Collins, C., Rommens, J.M., Kowbel, D., Godfrey, T., Tanner, M., Hwang, S.I., Polikoff, D., Nonet, G., Cochran, J., Myambo, K., Jay, K.E., Froula, J., Cloutier, T., Kuo, W.L., Yaswen, P., Dairkee, S., Giovanola, J., Hutchinson, G.B., Isola, J., Kallioniemi, O.P.,

Palazzolo, M., Martin, C., Ericsson, C., Pinkel, D., Albertson, D., Li, W.B. & Gray, J.W. 1998. Positional cloning of ZNF217 and NABC1: genes amplified at 20q13.2 and overexpressed in breast carcinoma. *Proceedings of the National Academy of Sciences of the United States of America.* 95 (15). pp. 8703-8708.

Corbett, K. D. & Berger, J. M. 2003. Structure of the topoisomerase VI-B subunit: implications for type II topoisomerase mechanism and evolution. *The EMBO Journal,* 22**,** 151-163.

Corbett, K.D., Benedetti, P. & Berger, J.M. 2007. Holoenzyme assembly and ATP-mediated conformational dynamics of topoisomerase VI. *Nature structural & molecular biology.* 14 (7). pp. 611-619.

Costa, F.F., Le Blanc, K. & Brodin, B. 2007. Concise review: cancer/testis antigens, stem cells, and cancer. *Stem cells (Dayton, Ohio).* 25 (3). pp. 707-711.

Costa, Y., Speed, R., Ollinger, R., Alsheimer, M., Semple, C.A., Gautier, P., Maratou, K., Novak, I., Hoog, C., Benavente, R. & Cooke, H.J. 2005. Two novel proteins recruited by synaptonemal complex protein 1 (SYCP1) are at the centre of meiosis. *Journal of cell science.* 118 (Pt 12). pp. 2755-2762.

Criscitiello, C. 2012. Tumor-associated antigens in breast cancer. *Breast care (Basel, Switzerland).* 7 (4). pp. 262-266.

Croce, C.M. 2008. Oncogenes and cancer. New England journal of medicine. 358 (5). pp. 502-511.

Cromie, G.A. & Smith, G.R. 2007. Branching out: meiotic recombination and its regulation. *Trends in cell biology.* 17 (9). pp. 448-455.

Cronwright, G., Le Blanc, K., Gotherstrom, C., Darcy, P., Ehnman, M. & Brodin, B. 2005. Cancer/testis antigen expression in human mesenchymal stem cells: down-regulation of SSX impairs cell migration and matrix metalloproteinase 2 expression. *Cancer research.* 65 (6). pp. 2207-2215.

Dang, C.V., Resar, L.M., Emison, E., Kim, S., Li, Q., Prescott, J.E., Wonsey, D. & Zeller, K. 1999. Function of the c-Myc oncogenic transcription factor. *Experimental cell research.* 253 (1). pp. 63-77.

Dash, P. 1994. Apoptosis; Basic Medical Sciences, St. *George's, University of London.*

Davies, H., Bignell, G.R., Cox, C., Stephens, P., Edkins, S., Clegg, S., Teague, J., Woffendin, H., Garnett, M.J. & Bottomley, W. 2002. Mutations of the BRAF gene in human cancer. Nature. 417 (6892). pp. 949-954.

De Backer, O., Arden, K.C., Boretti, M., Vantomme, V., De Smet, C., Czekay, S., Viars, C.S., De Plaen, E., Brasseur, F., Chomez, P., Van den Eynde, B., Boon, T. & van der Bruggen, P. 1999. Characterization of the GAGE genes that are expressed in various human cancers and in normal testis. Cancer research. 59 (13). pp. 3157-3165.

De Smet, C. & Loriot, A. 2010. DNA hypomethylation in cancer: epigenetic scars of a neoplastic journey. *Epigenetics.* 5 (3). pp. 206-213.

De Vries, F.A., de Boer, E., van den Bosch, M., Baarends, W.M., Ooms, M., Yuan, L., Liu, J.G., van Zeeland, A.A., Heyting, C. & Pastink, A. 2005. Mouse Sycp1 functions in synaptonemal complex assembly, meiotic recombination, and XY body formation. Genes & development. 19 (11). pp. 1376-1389.

DE, E., VAN DEN, B., Knuth, A. & BOONT, T. 1991. A gene encoding an antigen recognized by cytolytic T lymphocytes on a human melanoma.

Debnath, J., Baehrecke, E.H. & Kroemer, G. 2005. Does autophagy contribute to cell death? *Autophagy.* 1 (2). pp. 66-74.

Deltcheva, E., K. Chylinski, C.M. Sharma, K. Gonzales, Y. Chao, Z.A. Pirzada, M.R. Eckert, J. Vogel, & E. Charpentier. 2011. CRISPR RNA maturation by trans-encoded small RNA and host factor RNase III. Nature 471:602-607.

Dernburg, A.F., McDonald, K., Moulder, G., Barstead, R., Dresser, M. & Villeneuve, A.M. 1998. Meiotic recombination in C. elegans initiates by a conserved mechanism and is dispensable for homologous chromosome synapsis. *Cell.* 94 (3). pp. 387-398.

Di Fagagna, F.d., Reaper, P.M., Clay-Farrace, L., Fiegler, H., Carr, P., von Zglinicki, T., Saretzki, G., Carter, N.P. & Jackson, S.P. 2003. A DNA damage checkpoint response in telomere-initiated senescence. Nature. 426 (6963). pp. 194-198.

Doll, E., Molnar, M., Hiraoka, Y. & Kohli, J. 2005, Characterization of rec15, an early meiotic recombination gene in Schizosaccharomyces pombe', Curr Genet., 48(5):323–33.

Doyle, J.M., Gao, J., Wang, J., Yang, M. & Potts, P.R. 2010. MAGE-RING protein complexes comprise a family of E3 ubiquitin ligases. Molecular cell. 39 (6). pp. 963-974.

Eichler, A.F. & Plotkin, S.R. 2008. Brain metastases. *Current treatment options in neurology.* 10 (4). pp. 308-314.

Elmore, S. 2007. Apoptosis: a review of programmed cell death. *Toxicologic pathology.* 35 (4). pp. 495-516.

Eneriz, E., Garate, L., Cordeu, L., Cervantes, F., Prosper, F., Heiniger, A. and Torres, A. 2007. Epigenetic regulation of human cancer/testis antigen gene, HAGE, in chronic myeloid leukemia. Haematologica, 92(2), pp.153-162.

Erenpreisa J, Cragg MS, Salmina K, Hausmann M, Scherthan H. The role of meiotic cohesin REC8 in chromosome segregation in g irradiation-induced endoploy ploid tumour cells. Exp Cell Res. 2009;315(15):2593-2603.

Esposito, M.S. & Esposito, R.E. 1969. The genetic control of sporulation in Saccharomyces. I. The isolation of temperature-sensitive sporulation-deficient mutants. *Genetics.* 61 (1). pp. 79-89.

Esteller, M. & Herman, J.G. 2002. Cancer as an epigenetic disease: DNA methylation and chromatin alterations in human tumours. *The Journal of pathology.* 196 (1). pp. 1-7.

Ewen, M.E. 1994. The cell cycle and the retinoblastoma protein family. *Cancer and metastasis reviews.* 13 (1). pp. 45-66.

Feichtinger, J., Aldeailej, I., Anderson, R., Almutairi, M., Almatrafi, A., Alsiwiehri, N., Griffiths, K., Stuart, N., Wakeman, J.A., Larcombe, L. & McFarlane, R.J. 2012. Meta-analysis of clinical data using human meiotic genes identifies a novel cohort of highly restricted cancer-specific marker genes. *Oncotarget.* 3 (8). pp. 843-853.

Feichtinger, J., Larcombe, L. & McFarlane, R.J. 2014. Meta-analysis of expression of l (3) mbt tumor-associated germline genes supports the model that a soma-to-germline transition is a hallmark of human cancers. *International journal of cancer.* 134 (10). pp. 2359-2365.

Feinberg, A.P. & Vogelstein, B. 1983. Hypomethylation distinguishes genes of some human cancers from their normal counterparts. *Nature.* 301 (5895). pp. 89-92.

Ferguson, L.R., Chen, H., Collins, A.R., Connell, M., Damia, G., Dasgupta, S., Malhotra, M., Meeker, A.K., Amedei, A. & Amin, A. 2015. Genomic instability in human cancer: Molecular insights and opportunities for therapeutic attack and prevention through diet and nutrition. Seminars in cancer biology. Elsevier: pp. S5.

Ferlay, J., Soerjomataram, I., Dikshit, R., Eser, S., Mathers, C., Rebelo, M., Parkin, D.M., Forman, D. & Bray, F. 2015. Cancer incidence and mortality worldwide: sources, methods and major patterns in GLOBOCAN 2012. International journal of cancer. 136 (5). pp. E359-E386.

Finn, R.S., Aleshin, A. & Slamon, D.J. 2016. Targeting the cyclin-dependent kinases (CDK) 4/6 in estrogen receptor-positive breast cancers. *Breast Cancer Research.* 18 (1). pp. 1.

Fire, A., Xu, S., Montgomery, M.K., Kostas, S.A., Driver, S.E. & Mello, C.C. 1998. Potent and specific genetic interference by double-stranded RNA in Caenorhabditis elegans. *Nature.* 391 (6669). pp. 806-811.

Folco HD, Chalamcharla VR, Sugiyama T, Thillainadesan G, Zofall M, Balachandran V, Dhakshnamoorthy J, Mizuguchi T, Grewal SI. Untimely expression of gametogenic genes in vegetative cells causes uniparent disomy. Nature. 2017;543(7643):126-130.

Formigli, L., Papucci, L., Tani, A., Schiavone, N., Tempestini, A., Orlandini, G.E., Capaccioli, S. & Orlandini, S.Z. 2000. Aponecrosis: morphological and biochemical exploration of a syncretic process of cell death sharing apoptosis and necrosis. *Journal of cellular physiology.* 182 (1). pp. 41-49.

Franceschini, D., Franzese, C., Navarria, P., Ascolese, A.M., De Rose, F., Del Vecchio, M., Santoro, A. & Scorsetti, M. 2016. Radiotherapy and immunotherapy: Can this combination change the prognosis of patients with melanoma brain metastases? *Cancer treatment reviews.* 50 pp. 1-8.

Fratta, E., Coral, S., Covre, A., Parisi, G., Colizzi, F., Danielli, R., Nicolay, H.J., Sigalotti, L. & Maio, M. 2011. The biology of cancer testis antigens: putative function, regulation and therapeutic potential. *Molecular oncology.* 5 (2). pp. 164-182.

Fraune, J., Schramm, S., Alsheimer, M. & Benavente, R. 2012. The mammalian synaptonemal complex: protein components, assembly and role in meiotic recombination. *Experimental cell research.* 318 (12). pp. 1340-1346.

Freitas, M., Malheiros, S., Stavale, J.N., Biassi, T.P., Zamuner, F.T., de Souza Begnami, M., Soares, F.A. & Vettore, A.L. 2013. Expression of cancer/testis antigens is correlated with improved survival in glioblastoma. *Oncotarget.* 4 (4). pp. 636-646.

Fridman, W., Pagès, F., Sautès-Fridman, C. and Galon, J. 2012. The immune contexture in human tumours: impact on clinical outcome. Nature Reviews Cancer, 12(4), pp.298-306.

Fridman, W.H., Remark, R., Goc, J., Giraldo, N.A., Becht, E., Hammond, S.A., Damotte, D., Dieu-Nosjean, M.C. & Sautes-Fridman, C. 2014. The immune microenvironment: a major player in human cancers. *International archives of allergy and immunology.* 164 (1). pp. 13-26.

Fu, C., Zhao, H., Wang, Y., Cai, H., Xiao, Y., Zeng, Y. & Chen, H. 2016. Tumor-associated antigens: Tn antigen, sTn antigen, and T antigen. *HLA.*

Fukuda, T., Pratto, F., Schimenti, J.C., Turner, J.M., Camerini-Otero, R.D. & Hoog, C. 2012. Phosphorylation of chromosome core components may serve as axis marks for the status of chromosomal events during mammalian meiosis. *PLoS genetics.* 8 (2). pp. e1002485.

Gadelle D, Filee J, Buhler C. 2003 Phylogenomics of type II DNA topoisomerases. *Bioessays* 25: 232-242.

Gaillard, H., García-Muse, T. & Aguilera, A. 2015. Replication stress and cancer. Nature Reviews Cancer, 15(5), pp.276-289.

Garcia-Cruz, R., Roig, I. & Caldes, M.G. 2009. Maternal origin of the human aneuploidies. Are homolog synapsis and recombination to blame? Notes (learned) from the underbelly. *Genome dynamics.* 5 pp. 128-136.

Gaugler, B., Van den Eynde, B., van der Bruggen, P., Romero, P., Gaforio, J.J., De Plaen, E., Lethe, B., Brasseur, F. & Boon, T. 1994. Human gene MAGE-3 codes for an antigen recognized on a melanoma by autologous cytolytic T lymphocytes. The Journal of experimental medicine. 179 (3). pp. 921-930.

Geary, S., Cambareri, A., Sincock, P., Fitter, S. and Ashman, L. 2001. Differential tissue expression of epitopes of the tetraspanin CD151 recognised by monoclonal antibodies. Tissue Antigens, 58(3), pp.141-153.

Gedye, C., Quirk, J., Browning, J., Svobodova, S., John, T., Sluka, P., Dunbar, P.R., Corbeil, D., Cebon, J. & Davis, I.D. 2009. Cancer/testis antigens can be immunological targets in clonogenic CD133+ melanoma cells. *Cancer immunology, immunotherapy : CII.* 58 (10). pp. 1635-1646.

Geleta, B., Makonnen, E. & Abay, S.M. 2016. Cyclic Dependent Kinase (CDK): Role in Cancer Pathogenesis and as Drug Target in Cancer Therapeutics. *Journal of Cancer Science & Therapy.* 8 (6). pp. 160-167.

German, J 1995. Bloom's syndrome. *Dermatol. Clin*., 13, 7-18.

German, J. 1993. Bloom syndrome: a mendelian prototype of somatic mutational disease.

Gerton, J.L. & Hawley, R.S. 2005. Homologous chromosome interactions in meiosis: diversity amidst conservation. *Nature Reviews Genetics.* 6 (6). pp. 477-487.

Ghafouri-Fard, S. & Modarressi, M.H. 2012. Expression of cancer-testis genes in brain tumors: implications for cancer immunotherapy. *Immunotherapy.* 4 (1). pp. 59-75.

Giacinti, C. & Giordano, A. 2006. RB and cell cycle progression. *Oncogene.* 25 (38). pp. 5220-5227.

GILL, J., ELLIS, B., BOGUSLAWSKI, S. & TANG, P. 1996. Direct Western blot detection of HA epitope-tagged proteins using Anti-HA-peroxidase. *Biochemica.* 1 pp. 41-43.

Girard, F., Strausfeld, U., Fernandez, A. & Lamb, N.J. 1991. Cyclin A is required for the onset of DNA replication in mammalian fibroblasts. *Cell.* 67 (6). pp. 1169-1179.

Gjerstorff, M.F., Andersen, M.H. & Ditzel, H.J. 2015. Oncogenic cancer/testis antigens: prime candidates for immunotherapy. *Oncotarget.* 6 (18). pp. 15772-15787.

Gossen, M. & Bujard, H. 1992. Tight control of gene expression in mammalian cells by tetracycline-responsive promoters. *Proceedings of the National Academy of Sciences of the United States of America.* 89 (12). pp. 5547-5551.

Graille, M., Cladiere, L., Durand, D., Lecointe, F., Gadelle, D., Quevillon-Cheruel, S., Vachette, P., Forterre, P. & van Tilbeurgh, H. 2008. Crystal structure of an intact type II DNA topoisomerase: insights into DNA transfer mechanisms. *Structure (London, England : 1993).* 16 (3). pp. 360-370.

Gratz, S.J., A.M. Cummings, J.N. Nguyen, D.C. Hamm, L.K. Donohue, M.M. Harrison, J. Wildonger, & K.M. O'Connor-Giles. 2013. Genome engineering of Drosophila with the CRISPR RNA-guided Cas9 nuclease. Genetics 194:1029-1035

Gray, S., Allison, R. M., Garcia, V., Goldman, A. S. & Neale, M. J. 2013, Positive regulation of meiotic DNA double-strand break formation by activation of the DNA damage checkpoint kinase Mec1(ATR)', Open Biol., 3(7):130019.

Grey, C., Barthes, P., Chauveau-Le Friec, G., Langa, F., Baudat, F. & de Massy, B. 2011. Mouse PRDM9 DNA-binding specificity determines sites of histone H3 lysine 4 trimethylation for initiation of meiotic recombination. *PLoS biology.* 9 (10). pp. e1001176.

Grizzi, F., Mirandola, L., Qehajaj, D., Cobos, E., Figueroa, J.A. & Chiriva-Internati, M. 2015. Cancer-testis antigens and immunotherapy in the light of cancer complexity. *International reviews of immunology.* 34 (2). pp. 143-153.

Gros, A., Robbins, P.F., Yao, X., Li, Y.F., Turcotte, S., Tran, E., Wunderlich, J.R., Mixon, A., Farid, S. & Dudley, M.E. 2014. PD-1 identifies the patient-specific CD8 tumor-reactive repertoire infiltrating human tumors. *The Journal of clinical investigation.* 124 (5). pp. 2246-2259.

Guadagno, T.M. & Newport, J.W. 1996. Cdk2 kinase is required for entry into mitosis as a positive regulator of Cdc2–cyclin B kinase activity. *Cell.* 84 (1). pp. 73-82.

Guillon, H., Baudat, F., Grey, C., Liskay, R.M. & De Massy, B. 2005. Crossover and noncrossover pathways in mouse meiosis. *Molecular cell.* 20 (4). pp. 563-573.

Hamer, G., Wang, H., Bolcun-Filas, E., Cooke, H.J., Benavente, R. & Hoog, C. 2008. Progression of meiotic recombination requires structural maturation of the central element of the synaptonemal complex. *Journal of cell science.* 121 (Pt 15). pp. 2445-2451.

Hanahan, D. & Weinberg, R.A. 2000. The hallmarks of cancer. Cell. 100 (1). pp. 57- 70.

Hanahan, D. & Weinberg, R.A. 2011. Hallmarks of cancer: the next generation. *Cell.* 144 (5). pp. 646-674.

Handel, M.A. & Schimenti, J.C. 2010a. Genetics of mammalian meiosis: regulation, dynamics and impact on fertility. *Nature reviews.Genetics.* 11 (2). pp. 124-136.

Hannon, G.J. 2002. RNA interference. *Nature.* 418 (6894). pp. 244-251.

Hardwick, J.M. & Soane, L. 2013. Multiple functions of BCL-2 family proteins. *Cold Spring Harbor perspectives in biology.* 5 (2). pp. 10.1101/cshperspect.a008722.

Harley, C.B., Futcher, A.B. & Greider, C.W. 1990. Telomeres shorten during ageing of human fibroblasts.

Harper, L., Golubovskaya, I. & Cande, W.Z. 2004. A bouquet of chromosomes. *Journal of cell science.* 117 (Pt 18). pp. 4025-4032.

Harris, S.L. & Levine, A.J. 2005. The p53 pathway: positive and negative feedback loops. *Oncogene.* 24 (17). pp. 2899-2908.

Harris, T.J. & Drake, C.G. 2013. Primer on tumor immunology and cancer immunotherapy. *Journal for immunotherapy of cancer.* 1 (1). pp. 1.

Hartung F, Angelis KJ, Meister A, Schubert I, Melzer M, Puchta H. An archaebacterial topoisomerase homolog not present in other eukaryotes is indispensable for cell proliferation of plants. Curr Biol. 2002; 12(20):1787-1791.

Hartung F, Wurz-Wildersinn R, Fuchs J, et al. 2007. The catalytically active tyrosine residues of both SPO11-1 and SPO11-2 are required for meiotic double-strand break induction in Arabidopsis. *Plant Cell* 19: 3090-3099.

Hartung, F. & Puchta, H. 2000.Molecular characterisation of two paralogous SPO11 homologues in Ara-bidopsis thaliana', Nucleic Acids Res., 28(7):1548–54.

Hartwell, L.H. & Kastan, M.B. 1994. Cell cycle control and cancer. *Science.* 266 (5192). pp. 1821.

Hatakeyama, M. & Weinberg, R.A. 1995. The role of RB in cell cycle control. In: *Progress in cell cycle research.* Springer: pp. 9-19.

Hatzimichael, E. & Crook, T. 2013. Cancer epigenetics: new therapies and new challenges. *Journal of drug delivery.* 2013 pp. 529312.

Henderson, K.A. & Keeney, S. 2004. Tying synaptonemal complex initiation to the formation and programmed repair of DNA double-strand breaks. *Proceedings of the National Academy of Sciences of the United States of America.* 101 (13). pp. 4519-4524.

Henderson, K.A. & Keeney, S. 2005. Synaptonemal complex formation: where does it start? *BioEssays : news and reviews in molecular, cellular and developmental biology.* 27 (10). pp. 995-998.

Henson, J.D., Neumann, A.A., Yeager, T.R. & Reddel, R.R. 2002. Alternative lengthening of telomeres in mammalian cells. *Oncogene.* 21 (4).

Herceg, Z. & Wang, Z.Q. 2001. Functions of poly(ADP-ribose) polymerase (PARP) in DNA repair, genomic integrity and cell death. *Mutation research.* 477 (1-2). pp. 97-110.

Heyer, W.D., Ehmsen, K.T. & Liu, J. 2010. Regulation of homologous recombination in eukaryotes. *Annual Review of Genetics.* 44 pp. 113-139.

Hiasa, H., DiGate, R. J. & Marians K. J. 1994. Decatenating activity of Escherichia coli DNA gyrase and topoisomerase I and III during oriC and pBR322 DNA replication in vitro. *J. Biol. Chemi.*, 269, 2093-2099.

Hickson, I. D. 2003. Nat. Rev. Cancer, 3169 –178.

Hickson, I. D. 2003. RecQ helicases: caretakers of the genome. Nat. Rev. Cancer, 3, 169–178.

Hirohashi, Y., Torigoe, T., Tsukahara, T., Kanaseki, T., Kochin, V. & Sato, N. 2016. Immune responses to human cancer stem-like cells/cancer-initiating cells. *Cancer science.* 107 (1). pp. 12-17.

Hoffman, B. & Liebermann, D. 2008. Apoptotic signaling by c-MYC. *Oncogene.* 27 (50). pp. 6462-6472.

Hofmann, O., Caballero, O.L., Stevenson, B.J., Chen, Y.T., Cohen, T., Chua, R., Maher, C.A., Panji, S., Schaefer, U., Kruger, A., Lehvaslaiho, M., Carninci, P., Hayashizaki, Y., Jongeneel, C.V., Simpson, A.J., Old, L.J. & Hide, W. 2008. Genome-wide analysis of cancer/testis gene expression. *Proceedings of the National Academy of Sciences of the United States of America.* 105 (51). pp. 20422-20427.

Hohenauer, T. & Moore, A.W. 2012. The Prdm family: expanding roles in stem cells and development. *Development (Cambridge, England).* 139 (13). pp. 2267-2282.

Holland, A. J. & Cleveland, D. W. 2009. Boveri Revisited: Chromosomal Instability, Aneuploidy And Tumorigenesis. Nature Reviews Molecular Cell Biology, 10, 478-487.

Hosoya, N., Okajima, M., Kinomura, A., Fujii, Y., Hiyama, T., Sun, J., Tashiro, S. & Miyagawa, K. 2011. Synaptonemal complex protein SYCP3 impairs mitotic recombination by interfering with BRCA2. *EMBO reports.* 13 (1). pp. 44-51.

Hu, Y. & Smyth, G.K. 2009. ELDA: extreme limiting dilution analysis for comparing depleted and enriched populations in stem cell and other assays. *Journal of immunological methods.* 347 (1-2). pp. 70-78.

Hudolin, T., Juretic, A., Spagnoli, G.C., Pasini, J., Bandic, D., Heberer, M., Kosicek, M. & Cacic, M. 2006. Immunohistochemical expression of tumor antigens MAGE-A1, MAGE-A3/4, and NY-ESO-1 in cancerous and benign prostatic tissue. *The Prostate.* 66 (1). pp. 13-18.

Hunder, N.N., Wallen, H., Cao, J., Hendricks, D.W., Reilly, J.Z., Rodmyre, R., Jungbluth, A., Gnjatic, S., Thompson, J.A. & Yee, C. 2008. Treatment of metastatic melanoma with autologous CD4+ T cells against NY-ESO-1. *The New England journal of medicine.* 358 (25). pp. 2698-2703.

Hung, M.C. & Link, W. 2011. Protein localization in disease and therapy. *Journal of cell science.* 124 (Pt 20). pp. 3381-3392.

Hunter, N. 2007. Meiotic recombination. In: *Molecular genetics of recombination.* Springer: pp. 381-442.

Hunter, N. 2015. Meiotic Recombination: The Essence of Heredity. *Cold Spring Harbor perspectives in biology.* 7 (12). pp. 10.1101/cshperspect.a016618.

Ibrahim, A.E., Arends, M.J., Silva, A.L., Wyllie, A.H., Greger, L., Ito, Y., Vowler, S.L., Huang, T.H., Tavare, S., Murrell, A. & Brenton, J.D. 2011. Sequential DNA methylation changes are associated with DNMT3B overexpression in colorectal neoplastic progression. *Gut.* 60 (4). pp. 499-508.

Iclozan, C. & Gabrilovich, D.I. 2012. Recent advances in immunotherapy of lung cancer. *Journal of Lung Cancer.* 11 (1). pp. 1-11.

Inagaki, A., Schoenmakers, S. & Baarends, W.M. 2010. DNA double strand break repair, chromosome synapsis and transcriptional silencing in meiosis. *Epigenetics.* 5 (4). pp. 255-266.

Ishiguro, K., Kim, J., Fujiyama-Nakamura, S., Kato, S. & Watanabe, Y. 2011. A new meiosis-specific cohesin complex implicated in the cohesin code for homologous pairing. EMBO reports. 12 (3). pp. 267-275.

Ivanov, E.L., Korolev, V.G. & Fabre, F. 1992. XRS2, a DNA repair gene of Saccharomyces cerevisiae, is needed for meiotic recombination. *Genetics.* 132 (3). pp. 651-664.

Jackson, S.P. & Bartek, J. 2009. The DNA-damage response in human biology and disease. *Nature.* 461 (7267). pp. 1071-1078.

Jagadish, N., Parashar, D., Gupta, N., Agarwal, S., Sharma, A., Fatima, R., Suri, V., Kumar, R., Gupta, A. & Lohiya, N.K. 2016. A novel cancer testis antigen target a-kinase anchor protein (AKAP4) for the early diagnosis and immunotherapy of colon cancer. OncoImmunology. 5 (2). pp. e1078965.

Janic, A., Mendizabal, L., Llamazares, S., Rossell, D. & Gonzalez, C. 2010. Ectopic expression of germline genes drives malignant brain tumor growth in Drosophila. *Science (New York, N.Y.).* 330 (6012). pp. 1824-1827.

Jayashree, B.S., Nigam, S., Pai, A., Patel, H.K., Reddy, N.D., Kumar, N. & Rao, C.M. 2015. Targets in anticancer research--A review. *Indian journal of experimental biology.* 53 (8). pp. 489-507.

Jayshree, A., Jayashree, S. and Thangaraju, N. 2016. Chlorella vulgaris and Chlamydomonas reinhardtii: Effective Antioxidant, Antibacterial and Anticancer Mediators. Indian Journal of Pharmaceutical Sciences, 78(5).

Jemal, A., Bray, F., Center, M.M., Ferlay, J., Ward, E. & Forman, D. 2011. Global cancer statistics. *CA: a cancer journal for clinicians.* 61 (2). pp. 69-90.

Jinek, M., K. Chylinski, I. Fonfara, M. Hauer, J.A. Doudna, and E. Charpentier. 2012. A programmable dual-RNA-guided DNA endonuclease in adaptive bacterial immunity. Science 337:816-821.

Johnson, F. B., Lombard, D. B., Neff, N. F., Mastrangelo, M. A., Dewolf, W., Ellis, N. A., Marciniak, R. A., Yin, Y., Jaenisch, R. & Guarente L. 2000. Association of the Bloom Syndrome Protein with Topoisomerase IIIα in Somatic and Meiotic Cells. Cancer Res., 60, 1162–1167.

June, C.H., Riddell, S.R. & Schumacher, T.N. 2015. Adoptive cellular therapy: a race to the finish line. *Science translational medicine.* 7 (280). pp. 280ps7.

Jungbluth, A.A., Antonescu, C.R., Busam, K.J., Iversen, K., Kolb, D., Coplan, K., Chen, Y.T., Stockert, E., Ladanyi, M. & Old, L.J. 2001. Monophasic and biphasic synovial sarcomas abundantly express cancer/testis antigen NY-ESO-1 but not MAGE-A1 or CT7. *International Journal of Cancer.* 94 (2). pp. 252-256.

Jungbluth, A.A., Ely, S., DiLiberto, M., Niesvizky, R., Williamson, B., Frosina, D., Chen, Y.T., Bhardwaj, N., Chen-Kiang, S., Old, L.J. & Cho, H.J. 2005. The cancer-testis

antigens CT7 (MAGE-C1) and MAGE-A3/6 are commonly expressed in multiple myeloma and correlate with plasma-cell proliferation. *Blood.* 106 (1). pp. 167-174.

Kalejs, M. & Erenpreisa, J. 2005. Cancer/testis antigens and gametogenesis: a review and" brain-storming" session. *Cancer cell international.* 5 (1). pp. 1.

Kalejs, M., Ivanov, A., Plakhins, G., Cragg, M.S., Emzinsh, D., Illidge, T.M. & Erenpreisa, J. 2006. Upregulation of meiosis-specific genes in lymphoma cell lines following genotoxic insult and induction of mitotic catastrophe. *BMC cancer.* 6 pp. 6.

Kalos, M., Levine, B.L., Porter, D.L., Katz, S., Grupp, S.A., Bagg, A. & June, C.H. 2011. T cells with chimeric antigen receptors have potent antitumor effects and can establish memory in patients with advanced leukemia. *Science translational medicine.* 3 (95). pp. 95ra73.

Kamath-Loeb, A., Loeb, L. & Fry, M. 2012. The Werner Syndrome Protein Is Distinguished from the Bloom Syndrome Protein by Its Capacity to Tightly Bind Diverse DNA Structures. PLoS ONE, 7(1), p.e30189.

Kandoth, C., McLellan, M.D., Vandin, F., Ye, K., Niu, B., Lu, C., Xie, M., Zhang, Q., McMichael, J.F. & Wyczalkowski, M.A. 2013. Mutational landscape and significance across 12 major cancer types. Nature. 502 (7471). pp. 333-339.

Kanwar, S.S., Yu, Y., Nautiyal, J., Patel, B.B. & Majumdar, A.P.N. 2010. The Wnt/beta-catenin pathway regulates growth and maintenance of colonospheres. Molecular cancer 9, p. 212.

Kapust, R. & Waugh, D. 1999. Escherichia colimaltose-binding protein is uncommonly effective at promoting the solubility of polypeptides to which it is fused. *Protein Science*, 8(8), pp.1668-1674.

Karch, J., Kwong, J.Q., Burr, A.R., Sargent, M.A., Elrod, J.W., Peixoto, P.M., Martinez-Caballero, S., Osinska, H., Cheng, E.H., Robbins, J., Kinnally, K.W. & Molkentin, J.D. 2013. Bax and Bak function as the outer membrane component of the mitochondrial permeability pore in regulating necrotic cell death in mice. *eLife.* 2 pp. e00772.

Karlseder, J., Broccoli, D., Dai, Y., Hardy, S. & de Lange, T. 1999. p53- and ATM-dependent apoptosis induced by telomeres lacking TRF2. *Science (New York, N.Y.).* 283 (5406). pp. 1321-1325.

Karow, J. K., Constantinou, A., Li, J. L., West, S. C. & Hickson, I. D. 2000. Proc. Natl. Acad. Sci. U. S. A., 976504 –6508.

Karpanen, T. & Olweus, J. 2015. T-cell receptor gene therapy--ready to go viral? *Molecular oncology.* 9 (10). pp. 2019-2042.

Kasibhatla, S. & Tseng, B. 2003. Why target apoptosis in cancer treatment? *Molecular cancer therapeutics.* 2 (6). pp. 573-580.

Kau, T.R., Way, J.C. & Silver, P.A. 2004. Nuclear transport and cancer: from mechanism to intervention. *Nature reviews.Cancer.* 4 (2). pp. 106-117.

Kauppi, L., Barchi, M., Baudat, F., Romanienko, P.J., Keeney, S. & Jasin, M. 2011. Distinct properties of the XY pseudoautosomal region crucial for male meiosis. *Science (New York, N.Y.).* 331 (6019). pp. 916-920.

Kaur, S., Momi, N., Chakraborty, S., Wagner, D.G., Horn, A.J., Lele, S.M., Theodorescu, D. & Batra, S.K. 2014. Altered expression of transmembrane mucins, MUC1 and MUC4, in bladder cancer: pathological implications in diagnosis. *PloS one.* 9 (3). pp. e92742.

Kawabata, M., Kawabata, T. & Nishibori, M. 2005. Role of recA/RAD51 family proteins in mammals. *Acta Medica Okayama.* 59 (1). pp. 1-9.

Keeney S GC, Kleckner N.1997. Meiosis-specific DNA double-strand breaks are catalyzed by Spo11, a member of a widely conserved protein family. *Cell* vol no. 88: pp no: 375-384.

Keeney S, Lange J & Mohibullah N. 2014 Self-organization of meiotic recombination initiation: general principles and molecular pathways. *Annu Rev Genet* 48: 187-214.

Keeney S. 2001. Mechanism and control of meiotic recombination initiation. *Curr Top Dev Biol* 52: 1-53.

KEENEY, S. & NEALE, M. 2006. Initiation of meiotic recombination by formation of DNA double-strand breaks: mechanism and regulation. Portland Press Limited.

Keeney, S. & Neale, M.J. 2006. Initiation of meiotic recombination by formation of DNA double-strand breaks: mechanism and regulation. *Biochemical Society transactions.* 34 (Pt 4). pp. 523-525.

KEENEY, S. 2001. Mechanism and control of meiotic recombination initiation. Current topics in developmental biology, 52, 1-53.

Keeney, S. 2001. Mechanism and control of meiotic recombination initiation. *Current topics in developmental biology.* 52 pp. 1-53.

Keeney, S. 2007. Spo11 and the formation of DNA double-strand breaks in meiosis. In: *Recombination and meiosis.* Springer: pp. 81-123.

Keeney, S., Baudat, F., Angeles, M., Zhou, Z.H., Copeland, N.G., Jenkins, N.A., Manova, K. & Jasin, M. 1999. A mouse homolog of the Saccharomyces cerevisiae meiotic recombination DNA transesterase Spo11p. *Genomics.* 61 (2). pp. 170-182.

KEENEY, S., GIROUX, C. N. & KLECKNER, N. 1997. Meiosis-specific DNA double-strand breaks are catalyzed by Spo11, a member of a widely conserved protein family. Cell, 88, 375-384.

Keeney, S., Giroux, C.N. & Kleckner, N. 1997. Meiosis-specific DNA double-strand breaks are catalyzed by Spo11, a member of a widely conserved protein family. *Cell.* 88 (3). pp. 375-384.

Kelland, K. 2014, Archaeologists discover earliest example of human with cancer, Reuters, London.

Kiessling, A., Wehner, R., Fussel, S., Bachmann, M., Wirth, M.P. & Schmitz, M. 2012. Tumor-associated antigens for specific immunotherapy of prostate cancer. *Cancers.* 4 (1). pp. 193-217.

Kiessling, F., Fokong, S., Koczera, P., Lederle, W. and Lammers, T. 2012. Ultrasound Microbubbles for Molecular Diagnosis, Therapy, and Theranostics. Journal of Nuclear Medicine, 53(3), pp.345-348.

Kikuchi, K., Abdel-Aziz, H.I., Taniguchi, Y., Yamazoe, M., Takeda, S. & Hirota, K. 2009. Bloom DNA helicase facilitates homologous recombination between diverged homologous sequences. *The Journal of biological chemistry.* 284 (39). pp. 26360-26367.

Kim, K. and Roberts, C. 2016. Targeting EZH2 in cancer. Nature Medicine, 22(2), pp.128-134.

Kim, R., Kulkarni, P. & Hannenhalli, S. 2013. Derepression of Cancer/testis antigens in cancer is associated with distinct patterns of DNA hypomethylation. *BMC cancer.* 13 pp. 144-2407-13-144.

Kim, S. 2015. New and emerging factors in tumorigenesis: an overview. Cancer management and research. 7 pp. 225.

Kim, Y., Park, H., Park, D., Lee, Y.S., Choe, J., Hahn, J.H., Lee, H., Kim, Y.M. & Jeoung, D. 2010. Cancer/testis antigen CAGE exerts negative regulation on p53 expression through HDAC2 and confers resistance to anti-cancer drugs. The Journal of biological chemistry. 285 (34). pp. 25957-25968.

Kisiel, J.B., Limburg, P.J. & Boardman, L.A. 2016. Colonic Polyps and Colorectal Cancer. Practical Gastroenterology and Hepatology Board Review Toolkit. pp. 349.

Kittler, R., Putz, G., Pelletier, L., Poser, I., Heninger, A.K., Drechsel, D., Fischer, S., Konstantinova, I., Habermann, B., Grabner, H., Yaspo, M.L., Himmelbauer, H., Korn, B., Neugebauer, K., Pisabarro, M.T. & Buchholz, F. 2004. An endoribonuclease-prepared siRNA screen in human cells identifies genes essential for cell division. *Nature.* 432 (7020). pp. 1036-1040.

Kleckner, N. 1996. Meiosis: how could it work? *Proceedings of the National Academy of Sciences of the United States of America.* 93 (16). pp. 8167-8174.

Klein, U., Esposito, G., Baudat, F., Keeney, S. & Jasin, M. 2002. Mice deficient for the type II topoisomerase-like DNA transesterase Spo11 show normal immunoglobulin somatic hypermutation and class switching. *European journal of immunology.* 32 (2). pp. 316-321.

Klenova, E.M., Morse, H.C.,3rd, Ohlsson, R. & Lobanenkov, V.V. 2002. The novel BORIS + CTCF gene family is uniquely involved in the epigenetics of normal biology and cancer. *Seminars in cancer biology.* 12 (5). pp. 399-414.

Kochenderfer, J.N., Dudley, M.E., Feldman, S.A., Wilson, W.H., Spaner, D.E., Maric, I., Stetler-Stevenson, M., Phan, G.Q., Hughes, M.S., Sherry, R.M., Yang, J.C., Kammula, U.S., Devillier, L., Carpenter, R., Nathan, D.A., Morgan, R.A., Laurencot, C. & Rosenberg, S.A. 2012. B-cell depletion and remissions of malignancy along with cytokine-associated toxicity in a clinical trial of anti-CD19 chimeric-antigen-receptor-transduced T cells. *Blood.* 119 (12). pp. 2709-2720.

Koslowski, M., Tureci, O., Bell, C., Krause, P., Lehr, H.A., Brunner, J., Seitz, G., Nestle, F.O., Huber, C. & Sahin, U. 2002. Multiple splice variants of lactate dehydrogenase C selectively expressed in human cancer. *Cancer research.* 62 (22). pp. 6750-6755.

Kouzarides, T. 2007. Chromatin Modifications and Their Function. Cell, 128(4), pp.693-705.

Kozlowska, A., Mackiewicz, J. & Mackiewicz, A. 2013. Therapeutic gene modified cell based cancer vaccines. *Gene.* 525 (2). pp. 200-207.

Kramer, G., Kudlicki, W., McCarthy, D., Tsalkova, T., Simmons, D. & Hardesty, B. 1999. N-terminal and C-terminal modifications affect folding, release from the ribosomes and stability of in vitro synthesized proteins. *The international journal of biochemistry & cell biology.* 31 (1). pp. 231-241.

Krishnadas, D., Shapiro, T. and Lucas, K. 2012. Complete Remission Following Decitabine/Dendritic Cell Vaccine for Relapsed Neuroblastoma. PEDIATRICS, 131(1), pp.e336-e341.

Krishnadas, D.K., Bai, F. & Lucas, K. 2013. Cancer testis antigen and immunotherapy. ImmunoTargets and Therapy. 2 pp. 11-19.

Kronja & TL Orr-Weaver. 2011 Translational regulation of the cell cycle: when, where, how and why? *Philos Trans R Soc Lond B Biol Sci.* vol. 366: pp.3638-3652.

Kuhn, E. M. & Therman, E. 1986. Cancer Genet. Cytogenet, 221 –18.

Kumar, R., Bourbon, H. M. & de Massy, B. 2010.Functional conservation of Mei4 for meiotic DNA double-strand break formation from yeasts to mice, Genes Dev., 24(12):1266–80.

Kung, A.L., Rebel, V.I., Bronson, R.T., Ch'ng, L.E., Sieff, C.A., Livingston, D.M. & Yao, T.P. 2000. Gene dose-dependent control of hematopoiesis and hematologic tumor suppression by CBP. *Genes & development.* 14 (3). pp. 272-277.

Kuo, K., Chou, T., Hsu, H., Chen, W. & Wang, L. 2012a. Prognostic significance of NBS1 and Snail expression in esophageal squamous cell carcinoma. Annals of surgical oncology. 19 (3). pp. 549-557.

Kuo, Y., Lin, Y., Chen, H., Wang, Y., Chiou, Y., Lin, H., Pan, H., Wu, C., Su, S. & Hsu, C. 2012b. SEPT12 mutations cause male infertility with defective sperm annulus. Human mutation. 33 (4). pp. 710-719.

Kurashige, T., Noguchi, Y., Saika, T., Ono, T., Nagata, Y., Jungbluth, A., Ritter, G., Chen, Y.T., Stockert, E., Tsushima, T., Kumon, H., Old, L.J. & Nakayama, E. 2001. Ny-ESO-1 expression and immunogenicity associated with transitional cell carcinoma: correlation with tumor grade. *Cancer research.* 61 (12). pp. 4671-4674.

Kurzbauer, M. T., Uanschou, C., Chen, D. & Schlögelhofer, P. 2012, The recombinases DMC1 and RAD51 are functionally and spatially separated during meiosis in Arabidopsis', Plant Cell, 24(5):2058– 70.

LaBaer, J., Garrett, M.D., Stevenson, L.F., Slingerland, J.M., Sandhu, C., Chou, H.S., Fattaey, A. & Harlow, E. 1997. New functional activities for the p21 family of CDK inhibitors. *Genes & development.* 11 (7). pp. 847-862.

Lai, J.P., Robbins, P.F., Raffeld, M., Aung, P.P., Tsokos, M., Rosenberg, S.A., Miettinen, M.M. & Lee, C.C. 2012. NY-ESO-1 expression in synovial sarcoma and other mesenchymal tumors: significance for NY-ESO-1-based targeted therapy and differential diagnosis. *Modern pathology : an official journal of the United States and Canadian Academy of Pathology, Inc.* 25 (6). pp. 854-858.

Lajmi, N., Luetkens, T., Yousef, S., Templin, J., Cao, Y., Hildebrandt, Y., Bartels, K., Kröger, N. & Atanackovic, D. 2015. Cancer-testis antigen MAGEC2 promotes proliferation and resistance to apoptosis in Multiple Myeloma. *British journal of haematology.* 171 (5). pp. 752-762.

Lake, C. M., Nielsen, R. J., Guo, F., Unruh, J. R., Slaughter, B. D. and Hawley, R. S. 2015. Vilya, a component of the recombination nodule, is required for meiotic double-strand break formation in Drosophila. eLife, 4:e08287.

Lam, I. & Keeney, S. 2014. Mechanism and regulation of meiotic recombination initiation. *Cold Spring Harbor perspectives in biology.* 7 (1). pp. a016634.

Lange, J., Pan, J., Cole, F., Thelen, M.P., Jasin, M. & Keeney, S. 2011. ATM controls meiotic double-strand-break formation. *Nature.* 479 (7372). pp. 237-240.

Langer, R. & Vacanti, J. 2016. Advances in tissue engineering. Journal of pediatric surgery. 51 (1). pp. 8-12.

Larsson, L. 2011. Oncogene-and tumor suppressor gene-mediated suppression of cellular senescence. *Seminars in cancer biology.* Elsevier: pp. 367.

Lawrence, M.S., Stojanov, P., Mermel, C.H., Robinson, J.T., Garraway, L.A., Golub, T.R., Meyerson, M., Gabriel, S.B., Lander, E.S. & Getz, G. 2014. Discovery and saturation analysis of cancer genes across 21 tumour types. Nature. 505 (7484). pp. 495-501.

Lee, B. & Amon, A. 2001. Meiosis: how to create a specialized cell cycle. *Current opinion in cell biology.* 13 (6). pp. 770-777.

Lee, J. & Hirano, T. 2011. RAD21L, a novel cohesin subunit implicated in linking homologous chromosomes in mammalian meiosis. The Journal of cell biology. 192 (2). pp. 263-276.

Levine, A.J., Puzio-Kuter, A.M., Chan, C.S. & Hainaut, P. 2016. The Role of the p53 Protein in Stem-Cell Biology and Epigenetic Regulation. Cold Spring Harbor perspectives in medicine.

Li, R., Pang, X.Q., Chen, W.C., Li, L., Tian, W.Y. & Zhang, X.G. 2012. Gastric cancer cell lines AGS before and after CD40 signal activating. *Molecular biology reports.*

Lin Y & Smith GR. 1994, Transient, meiosis-induced expression of the rec6 and rec12 genes of Schizosaccharomyces pombe. *Genetics* 136: 769-779.

Lindsey, S.F., Byrnes, D.M., Eller, M.S., Rosa, A.M., Dabas, N., Escandon, J. & Grichnik, J.M. 2013. Potential role of meiosis proteins in melanoma chromosomal instability. *Journal of skin cancer.* 2013 pp. 190109.

Lisby, M., Barlow, J.H., Burgess, R.C. & Rothstein, R. 2004. Choreography of the DNA damage response: spatiotemporal relationships among checkpoint and repair proteins. *Cell.* 118 (6). pp. 699-713.

Litvinov, I.V., Cordeiro, B., Huang, Y., Zargham, H., Pehr, K., Dore, M.A., Gilbert, M., Zhou, Y., Kupper, T.S. & Sasseville, D. 2014. Ectopic expression of cancer-testis antigens in cutaneous T-cell lymphoma patients. *Clinical cancer research : an official journal of the American Association for Cancer Research.* 20 (14). pp. 3799-3808.

Liu, J.G., Yuan, L., Brundell, E., Bjorkroth, B., Daneholt, B. & Hoog, C. 1996. Localization of the N-terminus of SCP1 to the central element of the synaptonemal complex and evidence for direct interactions between the N-termini of SCP1 molecules organized head-to-head. *Experimental cell research.* 226 (1). pp. 11-19.

Liu, L.F. 1989. DNA topoisomerase poisons as antitumor drugs. *Annual Review of Biochemistry.* 58 (1). pp. 351-375.

Liu, Y. & West, S. C. 2008. More complexity to the Bloom's syndrome complex. Genes. Dev., 22, 2737–2742.

Loew, R., Heinz, N., Hampf, M., Bujard, H. & Gossen, M. 2010. Improved Tet-responsive promoters with minimized background expression. *BMC biotechnology.* 10 pp. 81-6750-10-81.

Loidl, J. 2013. The hidden talents of SPO11. *Developmental cell.* 24 (2). pp. 123-124.

Longhese, M.P., Guerini, I., Baldo, V. & Clerici, M. 2008. Surveillance mechanisms monitoring chromosome breaks during mitosis and meiosis. *DNA repair.* 7 (4). pp. 545-557.

Loriot, A., Boon, T. & De Smet, C. 2003. Five new human cancer-germline genes identified among 12 genes expressed in spermatogonia. *International journal of cancer.* 105 (3). pp. 371-376.

Luborsky, J. 2001. Tumour antigens recognised by antibodies. *eLS.*

References

Lupinacci, R., Andraus, W., De Paiva Haddad, L., Carneiro D′Albuquerque, L. and Herman, P. 2013. Simultaneous laparoscopic resection of primary colorectal cancer and associated liver metastases: a systematic review. Techniques in Coloproctology, 18(2), pp.129-135.

Lupinacci, R.M., Menegaux, F. & Tresallet, C. 2013. Hepatocellular carcinoma, from monitoring to treatment. *Soins; la revue de reference infirmiere.* (780) (780). pp. 35-37.

Lutz, W., Leon, J. & Eilers, M. 2002. Contributions of Myc to tumorigenesis. *Biochimica Et Biophysica Acta (BBA)-Reviews on Cancer.* 1602 (1). pp. 61-71.

Lutz, W.K. 2002. Differences in individual susceptibility to toxic effects of chemicals determine the dose-response relationship and consequences of setting exposure standards. *Toxicology letters.* 126 (3). pp. 155-158.

Ma, Y., Jin, J., Dong, C., Cheng, E.C., Lin, H., Huang, Y. & Qiu, C. 2010. High-efficiency siRNA-based gene knockdown in human embryonic stem cells. *RNA (New York, N.Y.).* 16 (12). pp. 2564-2569.

Macaluso, M., Montanari, M., Cinti, C. & Giordano, A. 2005. Modulation of cell cycle components by epigenetic and genetic events. *Seminars in oncology.* Elsevier: pp. 452.

Macheret, M. & Halazonetis, T.D. 2015. DNA replication stress as a hallmark of cancer. *Annual Review of Pathology: Mechanisms of Disease.* 10 pp. 425-448.

MacQueen, A.J. & Hochwagen, A. 2011. Checkpoint mechanisms: the puppet masters of meiotic prophase. *Trends in cell biology.* 21 (7). pp. 393-400.

Magee, J. a, Piskounova, E. & Morrison, S.J. 2012. Cancer stem cells: impact, heterogeneity, and uncertainty. Cancer cell 21(3), pp. 283–96.

Mali, P., L. Yang, K.M. Esvelt, J. Aach, M. Guell, J.E. DiCarlo, J.E. Norville, & G.M. Church. 2013. RNA-guided human genome engineering via Cas9. Science 339:823-826.

Malik, S.B., Ramesh, M.A., Hulstrand, A.M. & Logsdon, J.M.,Jr 2007. Protist homologs of the meiotic Spo11 gene and topoisomerase VI reveal an evolutionary history of gene duplication and lineage-specific loss. *Molecular biology and evolution.* 24 (12). pp. 2827-2841.

Maluszek, M. 2015. Multifunctionality of MDM2 protein and its role in genomic instability of cancer cells. Postepy biochemii. 61 (1). pp. 42-51.

Mankouri, H. W. & Hickson, I. D. 2007. The RecQ helicase–topoisomerase III–Rmi1 complex: a DNA structure-specific ‘dissolvasome’? Trends Biochem. Sci., 32, 538–546.

Mansouri, K., Mostafie, A., Rezazadeh, D., Shahlaei, M. & Modarressi, M.H. 2016. New function of TSGA10 gene in angiogenesis and tumor metastasis: a response to a challengeable paradox. Human molecular genetics. 25 (2). pp. 233-244.

Marais, A., Ji, Z., Child, E.S., Krause, E., Mann, D.J. & Sharrocks, A.D. 2010. Cell cycle-dependent regulation of the forkhead transcription factor FOXK2 by CDK.cyclin complexes. *The Journal of biological chemistry.* 285 (46). pp. 35728-35739.

Marcar, L., Maclaine, N.J., Hupp, T.R. & Meek, D.W. 2010b. Mage-A cancer/testis antigens inhibit p53 function by blocking its interaction with chromatin. Cancer research. 70 (24). pp. 10362-10370.

Mariaule, G. & Belmont, P. 2014. Cyclin-dependent kinase inhibitors as marketed anticancer drugs: where are we now? A short survey. *Molecules.* 19 (9). pp. 14366-14382.

Marques-Torrejon, M.A., Porlan, E., Banito, A., Gomez-Ibarlucea, E., Lopez-Contreras, A.J., Fernandez-Capetillo, O., Vidal, A., Gil, J., Torres, J. & Farinas, I. 2013. Cyclin-dependent kinase inhibitor p21 controls adult neural stem cell expansion by regulating Sox2 gene expression. *Cell stem cell.* 12 (1). pp. 88-100.

Marraffini, L.A. & E.J. Sontheimer. 2010. CRISPR interference: RNA-directed adaptive immunity in bacteria and archaea. Nat. Rev. Genet. 11:181-190.

Marston, A.L. & Amon, A. 2004. Meiosis: cell-cycle controls shuffle & deal. *Nature Reviews Molecular Cell Biology.* 5 (12). pp. 983-997.

Martin-Moreno, J.M., Soerjomataram, I. & Magnusson, G. 2008. Cancer causes and prevention: a condensed appraisal in Europe in 2008. European journal of cancer. 44 (10). pp. 1390-1403.

Martini, E., et al. 2011. Genome-wide analysis of heterodu-plex DNA in mismatch repair–deficient yeast cells reveals novel properties of meiotic recombination pathways', PLOS Genet., 7(9):e1002305.

Maxfield, K.E., Taus, P.J., Corcoran, K., Wooten, J., Macion, J., Zhou, Y., Borromeo, M., Kollipara, R.K., Yan, J. & Xie, Y. 2015. Comprehensive functional characterization of cancer-testis antigens defines obligate participation in multiple hallmarks of cancer. *Nature communications.* 6.

McFarlane, R.J., Feichtinger, J. & Larcombe, L. 2014. Cancer germline gene activation: friend or foe? *Cell Cycle.* 13 (14). pp. 2151-2152.

McFarlane, R.J., Feichtinger, J. & Larcombe, L. 2015. Germline/meiotic genes in cancer: new dimensions. *Cell cycle (Georgetown, Tex.).* 14 (6). pp. 791-792.

McIlwain, D.R., Berger, T. & Mak, T.W. 2013. Caspase functions in cell death and disease. *Cold Spring Harbor perspectives in biology.* 5 (4). pp. a008656.

McKee, B. D., Yan, R. & Tsai, J. H. 2012. 'Meiosis in male Drosophila', Spermatogenesis, 2(3):167–84.

McKim, K.S. & Hayashi-Hagihara, A. 1998. mei-W68 in Drosophila melanogaster encodes a Spo11 homolog: evidence that the mechanism for initiating meiotic recombination is conserved. *Genes & development.* 12 (18). pp. 2932-2942.

McKinnon, P.J. 2009. DNA repair deficiency and neurological disease. *Nature Reviews Neuroscience.* 10 (2). pp. 100-112.

McMahill, M.S., Sham, C.W. & Bishop, D.K. 2007. Synthesis-dependent strand annealing in meiosis. *PLoS biology.* 5 (11). pp. e299.

Meacham, C.E. & Morrison, S.J. 2013. Tumour heterogeneity and cancer cell plasticity. Nature 501(7467), pp. 328–37.

Meek, D.W. & Marcar, L. 2012. MAGE-A antigens as targets in tumour therapy. *Cancer letters.* 324 (2). pp. 126-132.

Meetei, A. R., Sechi, S., Wallisch, M., Yang, D., Young, M. K., Joenje, H., Hoatlin, M. E., & Wang, W. 2003, A multiprotein nuclear complex connects Fanconi anemia and Bloom syndrome.Mol. Cell. Biol. 233417 –3426 [PMC free article] [PubMed]

Mellman, I., Coukos, G. & Dranoff, G. 2011a. Cancer immunotherapy comes of age. *Nature.* 480 (7378). pp. 480-489.

Meneely, P.M. & Bloom, J.C. 2013. SMG-ly knocking out gene expression in specific cells: an educational primer for use with "a novel strategy for cell-autonomous gene knockdown in caenorhabditis elegans defines a cell-specific function for the G-protein subunit GOA-1". *Genetics.* 195 (4). pp. 1201-1207.

Merino, S.T., Cummings, W.J., Acharya, S.N. & Zolan, M.E. 2000. Replication-dependent early meiotic requirement for Spo11 and Rad50. *Proceedings of the National Academy of Sciences of the United States of America.* 97 (19). pp. 10477-10482.

Meuwissen, R.L., Offenberg, H.H., Dietrich, A.J., Riesewijk, A., van Iersel, M. & Heyting, C. 1992. A coiled-coil related protein specific for synapsed regions of meiotic prophase chromosomes. *The EMBO journal.* 11 (13). pp. 5091-5100.

Meyer, N. & Penn, L.Z. 2008. Reflecting on 25 years with MYC. *Nature Reviews Cancer.* 8 (12). pp. 976-990.

Mian, I.S., Bradwell, A.R. & Olson, A.J. 1991. Structure, function and properties of antibody binding sites. *Journal of Molecular Biology.* 217 (1). pp. 133-151.

Mirandola, L., J Cannon, M., Cobos, E., Bernardini, G., Jenkins, M.R., Kast, W.M. & Chiriva-Internati, M. 2011. Cancer testis antigens: novel biomarkers and targetable proteins for ovarian cancer. *International reviews of immunology.* 30 (2-3). pp. 127-137.

Mirkovic J HB, Roncarati P, Demoulin S. 2015. Carcinogenic HPV infection in the cervical squamo-columnar junction. *The Journal of pathology* vol no. 236: pp no: 265-271.

Molina, N.B., Minvielle, M.C. & Basualdo, J.A. 2004. Células RK13: Influencia de la concentración de suero fetal bovino en el tiempo de duplicación. *Acta bioquím.clín.latinoam.* 38 (4). pp. 477-480.

Moller, H., Flatt, G. & Moran, A. 2011. High cancer mortality rates in the elderly in the UK. Cancer Epidemiology. 35 (5). pp. 407-412.

Moore, C.B., Guthrie, E.H., Huang, M.T. & Taxman, D.J. 2010. Short hairpin RNA (shRNA): design, delivery, and assessment of gene knockdown. *Methods in molecular biology (Clifton, N.J.).* 629 pp. 141-158.

Morgan, R.A., Dudley, M.E., Wunderlich, J.R., Hughes, M.S., Yang, J.C., Sherry, R.M., Royal, R.E., Topalian, S.L., Kammula, U.S., Restifo, N.P., Zheng, Z., Nahvi, A., de Vries, C.R., Rogers-Freezer, L.J., Mavroukakis, S.A. & Rosenberg, S.A. 2006. Cancer regression in patients after transfer of genetically engineered lymphocytes. *Science (New York, N.Y.).* 314 (5796). pp. 126-129.

Morlacchi, S., Sciandra, F., Bigotti, M.G., Bozzi, M., Hubner, W., Galtieri, A., Giardina, B. & Brancaccio, A. 2012. Insertion of a myc-tag within alpha-dystroglycan domains improves its biochemical and microscopic detection. *BMC biochemistry.* 13 pp. 14-2091-13-14.

Morris, L.G. & Chan, T.A. 2015. Therapeutic targeting of tumor suppressor genes. Cancer. 121 (9). pp. 1357-1368.

Mullen, J. R., Nallaseth, F. S., Lan, Y. Q., Slagle, C. E. & Brill, S. J. 2005. Yeast Rmi1/Nce4 Controls Genome Stability as a Subunit of the Sgs1-Top3 Complex. Mol. Cell. Biol., 25,4476–4487.

Munkley, J. 2016. The role of sialyl-Tn in cancer. *International journal of molecular sciences.* 17 (3). pp. 275.

Murakami, H. & Keeney, S. 2008. Regulating The Formation Of Dna Double-Strand Breaks In Meiosis. Genes & Development, 22, 286-292.

Murakami, H. and Keeney, S. 2014. Temporospatial coordination of meiotic DNA replication and recombination via DDK recruitment to replisomes, Cell, 158(4):861–73.

Nakajima, T., Kiyohara, E., Wada, H., Yamauchi, T., Itai, T. & Kaneda, Y. 2013. *A Novel Therapy for Melanoma and Prostate Cancer Using a Non-Replicating Sendai Virus Particle (HVJ-E).* INTECH Open Access Publisher.

Nardiello, T., Jungbluth, A.A., Mei, A., Diliberto, M., Huang, X., Dabrowski, A., Andrade, V.C., Wasserstrum, R., Ely, S., Niesvizky, R., Pearse, R., Coleman, M., Jayabalan, D.S., Bhardwaj, N., Old, L.J., Chen-Kiang, S. & Cho, H.J. 2011. MAGE-A inhibits apoptosis in proliferating myeloma cells through repression of Bax and maintenance of survivin. Clinical cancer research : an official journal of the American Association for Cancer Research. 17 (13). pp. 4309-4319.

Neale, M. J. 2010. PRDM9 points the zinc finger at meiotic recombination hotspots, Genome Biol., 11(2):104.

Neale, M.J. & Keeney, S. 2006. Clarifying the mechanics of DNA strand exchange in meiotic recombination. *Nature.* 442 (7099). pp. 153-158.

Neale, M.J., Pan, J. & Keeney, S. 2005. Endonucleolytic processing of covalent protein-linked DNA double-strand breaks. *Nature.* 436 (7053). pp. 1053-1057.

Negri Jr, W.J., Phillips, J.M. & Cree, C. 2016. Review-SI 2016; 2016: e00120 ft. Science. 2016.

Negrini, S., Gorgoulis, V.G. & Halazonetis, T.D. 2010. Genomic instability an evolving hallmark of cancer. *Nature reviews Molecular cell biology.* 11 (3). pp. 220-228.

Nelson, P.T., Zhang, P.J., Spagnoli, G.C., Tomaszewski, J.E., Pasha, T.L., Frosina, D., Caballero, O.L., Simpson, A.J., Old, L.J. & Jungbluth, A.A. 2007. Cancer/testis (CT) antigens are expressed in fetal ovary. Cancer immunity. 7 pp. 1.

Nichols, M. D., Deangelis, K., Keck, J. L. & Berger, J. M. 1999. Structure and function of an archaeal topoisomerase VI subunit with homology to the meiotic recombination factor Spo11. The EMBO Journal, 18, 6177-6188.

Nichols, M. D., Deangelis, K., Keck, J. L. & Berger, J. M. 1999. Structure And Function Of An Archaeal Topoisomerase Vi Subunit With Homology To The Meiotic Recombination Factor Spo11. The Embo Journal, 18, 6177-6188.

Nielsen, A.Y. & Gjerstorff, M.F. 2016. Ectopic Expression of Testis Germ Cell Proteins in Cancer and Its Potential Role in Genomic Instability. *International journal of molecular sciences.* 17 (6). pp. 10.3390/ijms17060890.

Nishikawa, H., Maeda, Y., Ishida, T., Gnjatic, S., Sato, E., Mori, F., Sugiyama, D., Ito, A., Fukumori, Y., Utsunomiya, A., Inagaki, H., Old, L.J., Ueda, R. & Sakaguchi, S. 2012. Cancer/testis antigens are novel targets of immunotherapy for adult T-cell leukemia/lymphoma. *Blood.* 119 (13). pp. 3097-3104.

Nitiss, J.L. 2009. Targeting DNA topoisomerase II in cancer chemotherapy. *Nature reviews.Cancer.* 9 (5). pp. 338-350.

Nojima, H. 1997. Cell cycle checkpoints, chromosome stability and the progression of cancer. *Human cell.* 10 (4). pp. 221-230.

Norbury, C.J. & Hickson, I.D. 2001. Cellular responses to DNA damage. *Annual Review of Pharmacology and Toxicology.* 41 (1). pp. 367-401.

Nurse, P. 1990. Universal control mechanism regulating onset of M-phase. *Nature.* 344 (6266). pp. 503-508.

O'Brien, C. a, Pollett, A., Gallinger, S. & Dick, J.E. 2007. A human colon cancer cell capable of initiating tumour growth in immunodeficient mice. Nature 445(7123), pp. 106–10.

Odajima, J., Wills, Z.P., Ndassa, Y.M., Terunuma, M., Kretschmannova, K., Deeb, T.Z., Geng, Y., Gawrzak, S., Quadros, I.M., Newman, J., Das, M., Jecrois, M.E., Yu, Q., Li, N., Bienvenu, F., Moss, S.J., Greenberg, M.E., Marto, J.A. & Sicinski, P. 2011. Cyclin E

constrains Cdk5 activity to regulate synaptic plasticity and memory formation. *Developmental cell.* 21 (4). pp. 655-668.

Odunsi, K., Jungbluth, A.A., Stockert, E., Qian, F., Gnjatic, S., Tammela, J., Intengan, M., Beck, A., Keitz, B., Santiago, D., Williamson, B., Scanlan, M.J., Ritter, G., Chen, Y.T., Driscoll, D., Sood, A., Lele, S. & Old, L.J. 2003. NY-ESO-1 and LAGE-1 cancer-testis antigens are potential targets for immunotherapy in epithelial ovarian cancer. *Cancer research.* 63 (18). pp. 6076-6083.

Öllinger, R., Childs, A.J., Burgess, H.M., Speed, R.M., Lundegaard, P.R., Reynolds, N., Gray, N.K., Cooke, H.J. & Adams, I.R. 2008. Deletion of the pluripotency- associated Tex19. 1 gene causes activation of endogenous retroviruses and defective spermatogenesis in mice. PLoS Genet. 4 (9). pp. e1000199.

Ollinger, R., Reichmann, J. & Adams, I.R. 2010. Meiosis and retrotransposon silencing during germ cell development in mice. *Differentiation; research in biological diversity.* 79 (3). pp. 147-158.

Olsen, E., Duvic, M., Frankel, A., Kim, Y., Martin, A., Vonderheid, E., Jegasothy, B., Wood, G., Gordon, M., Heald, P., Oseroff, A., Pinter-Brown, L., Bowen, G., Kuzel, T., Fivenson, D., Foss, F., Glode, M., Molina, A., Knobler, E., Stewart, S., Cooper, K., Stevens, S., Craig, F., Reuben, J., Bacha, P. & Nichols, J. 2001. Pivotal phase III trial of two dose levels of denileukin diftitox for the treatment of cutaneous T-cell lymphoma. *Journal of clinical oncology : official journal of the American Society of Clinical Oncology.* 19 (2). pp. 376-388.

Oum, J.H., Seong, C., Kwon, Y., Ji, J.H., Sid, A., Ramakrishnan, S., Ira, G., Malkova, A., Sung, P., Lee, S.E. & Shim, E.Y. 2011. RSC facilitates Rad59-dependent homologous recombination between sister chromatids by promoting cohesin loading at DNA double-strand breaks. *Molecular and cellular biology.* 31 (19). pp. 3924-3937.

Owens, J.B., Mathews, J., Davy, P., Stoytchev, I., Moisyadi, S. & Allsopp, R. 2013. Effective Targeted Gene Knockdown in Mammalian Cells Using the piggyBac Transposase-based Delivery System. *Molecular therapy.Nucleic acids.* 2 pp. e137.

Page, J., Berrios, S., Rufas, J.S., Parra, M.T., Suja, J.A., Heyting, C. & Fernandez-Donoso, R. 2003. The pairing of X and Y chromosomes during meiotic prophase in the marsupial species Thylamys elegans is maintained by a dense plate developed from their axial elements. *Journal of cell science.* 116 (Pt 3). pp. 551-560.

Page, S.L. & Hawley, R.S. 2004. The genetics and molecular biology of the synaptonemal complex. *Annu.Rev.Cell Dev.Biol.* 20 pp. 525-558.

Paques, F. & Haber, J.E. 1999. Multiple pathways of recombination induced by double-strand breaks in Saccharomyces cerevisiae. *Microbiology and molecular biology reviews : MMBR.* 63 (2). pp. 349-404.

Pardoll, D. 2003. Does the immune system see tumors as foreign or self? *Annual Review of Immunology.* 21 (1). pp. 807-839.

Park, C.S., Shen, Y., Suppipat, K., Tomolonis, J., Puppi, M., Mistretta, T., Ma, L., Green, M. & Lacorazza, D. 2016. KLF4 promotes self-renewal by repressing DYRK2-mediated degradation of c-Myc in leukemic stem cells: development of targeted therapy. Cancer research. 76 (14 Supplement). pp. 3334-3334.

Parka, L.S., Hernandez-Ramirez, R.U., Silverberg, M.J., Crothers, K.A. & Dubrow, R. 2016. Prevalence of non-HIV cancer risk factors in persons living with HIV/AIDS. AIDS. 30 (2). pp. 273-291.

Patel, J.H., Du, Y., Ard, P.G., Phillips, C., Carella, B., Chen, C.J., Rakowski, C., Chatterjee, C., Lieberman, P.M., Lane, W.S., Blobel, G.A. & McMahon, S.B. 2004. The c-MYC oncoprotein is a substrate of the acetyltransferases hGCN5/PCAF and TIP60. *Molecular and cellular biology.* 24 (24). pp. 10826-10834.

Pecina A, Smith KN, Mezard C. 2002, Targeted stimulation of meiotic recombination. *Cell* 111: 173-184.

Pellestor, F., Anahory, T., Lefort, G., Puechberty, J., Liehr, T., Hedon, B. & Sarda, P. 2011. Complex chromosomal rearrangements: origin and meiotic behavior. *Human reproduction update.* 17 (4). pp. 476-494.

Petukhova, G.V., Pezza, R.J., Vanevski, F., Ploquin, M., Masson, J. & Camerini-Otero, R.D. 2005. The Hop2 and Mnd1 proteins act in concert with Rad51 and Dmc1 in meiotic recombination. *Nature structural & molecular biology.* 12 (5). pp. 449-453.

Petukhova, G.V., Romanienko, P.J. & Camerini-Otero, R.D. 2003. The Hop2 protein has a direct role in promoting interhomolog interactions during mouse meiosis. *Developmental cell.* 5 (6). pp. 927-936.

Peyressatre, M., Prevel, C., Pellerano, M. & Morris, M.C. 2015. Targeting cyclin-dependent kinases in human cancers: from small molecules to Peptide inhibitors. *Cancers.* 7 (1). pp. 179-237.

Pfau, S.J. & Amon, A. 2012. Chromosomal instability and aneuploidy in cancer: from yeast to man. EMBO reports. 13 (6). pp. 515-527.

Pierce, B. A. 2012. Genetics: A conceptual approach, Macmillan.

Piotti, K.C., Scognamiglio, T., Chiu, R. & Chen, Y.T. 2013. Expression of cancer/testis (CT) antigens in squamous cell carcinoma of the head and neck: evaluation as markers of squamous dysplasia. *Pathology, research and practice.* 209 (11). pp. 721-726.

Pippa, R., Espinosa, L., Gundem, G., Garcia-Escudero, R., Dominguez, A., Orlando, S., Gallastegui, E., Saiz, C., Besson, A., Pujol, M.J., Lopez-Bigas, N., Paramio, J.M., Bigas, A. & Bachs, O. 2012. p27Kip1 represses transcription by direct interaction with p130/E2F4 at the promoters of target genes. *Oncogene.* 31 (38). pp. 4207-4220.

Plank, J., Wu, J. & Hsieh, T. 2006. Topoisomerase III and Bloom's helicase can resolve a mobile double Holliday junction substrate through convergent branch migration. Proceedings of the National Academy of Sciences, 103(30), pp.11118-11123.

Pollack, S.M., Jungbluth, A.A., Hoch, B.L., Farrar, E.A., Bleakley, M., Schneider, D.J., Loggers, E.T., Rodler, E., Eary, J.F. & Conrad III, E.U. 2012. NY-ESO-1 is a ubiquitous immunotherapeutic target antigen for patients with myxoid/round cell liposarcoma. *Cancer.* 118 (18). pp. 4564-4570.

Pommier, Y., Schwartz, R.E., Zwelling, L.A. & Kohn, K.W. 1985. Effects of DNA intercalating agents on topoisomerase II induced DNA strand cleavage in isolated mammalian cell nuclei. *Biochemistry.* 24 (23). pp. 6406-6410.

Porter, D.L., Levine, B.L., Kalos, M., Bagg, A. & June, C.H. 2011. Chimeric antigen receptor–modified T cells in chronic lymphoid leukemia. *New England Journal of Medicine.* 365 (8). pp. 725-733.

Prabhu, V.V., Hong, B., Allen, J.E., Zhang, S., Lulla, A.R., Dicker, D.T. & El-Deiry, W.S. 2016. Small-Molecule Prodigiosin Restores p53 Tumor Suppressor Activity in Chemoresistant Colorectal Cancer Stem Cells via c-Jun-Mediated DeltaNp73 Inhibition and p73 Activation. Cancer research. 76 (7). pp. 1989-1999.

Prieler, S., Penkner, A., Borde, V. & Klein, F. 2005a. The control of Spo11's interaction with meiotic recombination hotspots. *Genes & development.* 19 (2). pp. 255-269.

Prieler, S., Penkner, A., Borde, V. & Klein, F. 2005b. The control of Spo11's interaction with meiotic recombination hotspots. *Genes & development.* 19 (2). pp. 255-269.

Pylayeva-Gupta, Y., Grabocka, E. & Bar-Sagi, D. 2011. RAS oncogenes: weaving a tumorigenic web. *Nature Reviews Cancer.* 11 (11). pp. 761-774.

Qi, D. and Cobrinik, D. 2016. MDM2 but not MDM4 promotes retinoblastoma cell proliferation through p53-independent regulation of MYCN translation. Oncogene, 36(13), pp.1760-1769.

Qiao, H., Chen, J.K., Reynolds, A., Hoog, C., Paddy, M. & Hunter, N. 2012. Interplay between synaptonemal complex, homologous recombination, and centromeres during mammalian meiosis. *PLoS genetics.* 8 (6). pp. e1002790.

Rajagopalan, K., Mooney, S.M., Parekh, N., Getzenberg, R.H. & Kulkarni, P. 2011. A majority of the cancer/testis antigens are intrinsically disordered proteins. *Journal of cellular biochemistry.* 112 (11). pp. 3256-3267.

Raynard, S., Bussen, W. & Sung P. 2006. A Double Holliday Junction Dissolvasome Comprising BLM, Topoisomerase IIIα, and BLAP75. J. Biol. Chem., 281, 13861–13864.

Ren, B., Wei, X., Zou, G., He, J., Xu, G., Xu, F., Huang, Y., Zhu, H., Li, Y. & Ma, G. 2016. Cancer testis antigen SPAG9 is a promising marker for the diagnosis and treatment of lung cancer. Oncology reports. 35 (5). pp. 2599-2605.

Renkvist, N., Castelli, C., Robbins, P.F. & Parmiani, G. 2001. A listing of human tumor antigens recognized by T cells. *Cancer Immunology, Immunotherapy.* 50 (1). pp. 3-15.

Ribeiro, J., Abby, E., Livera, G. & Martini, E. 2015. RPA homologs and ssDNA processing during meiotic recombination, Chromosoma. 125:265–76.

Ricci-Vitiani, L., Lombardi, D.G., Pilozzi, E., Biffoni, M., Todaro, M., Peschle, C. & De Maria, R. 2007. Identification and expansion of human colon-cancer- initiating cells. Nature 445(7123), pp. 111–5.

Richardson, C., Moynahan, M.E. & Jasin, M. 1998. Double-strand break repair by interchromosomal recombination: suppression of chromosomal translocations. *Genes & development.* 12 (24). pp. 3831-3842.

Rivera, E. & Gomez, H. 2010. Chemotherapy resistance in metastatic breast cancer: the evolving role of ixabepilone. *Breast cancer research : BCR.* 12 Suppl 2 pp. S2.

Robbins, P.F., Morgan, R.A., Feldman, S.A., Yang, J.C., Sherry, R.M., Dudley, M.E., Wunderlich, J.R., Nahvi, A.V., Helman, L.J., Mackall, C.L., Kammula, U.S., Hughes, M.S., Restifo, N.P., Raffeld, M., Lee, C.C., Levy, C.L., Li, Y.F., El-Gamil, M., Schwarz, S.L., Laurencot, C. & Rosenberg, S.A. 2011. Tumor regression in patients with metastatic synovial cell sarcoma and melanoma using genetically engineered lymphocytes reactive with NY-ESO-1. *Journal of clinical oncology : official journal of the American Society of Clinical Oncology.* 29 (7). pp. 917-924.

Robert T, Vrielynck N, Mézard C, de Massy B, Grenlon M. A new light on the meiotic DSB catalytic complex. Semin Cell Dev Biol. 2016; 54:165-176.

Robert, T., Nore, A., Brun, C., Maffre, C., Crimi, B., Bourbon, H. & de Massy, B. 2016. The TopoVIB-Like Protein Family Is Required for Meiotic DNA Double-Strand Break Formation. Obstetrical & Gynecological Survey, 71(6), pp.350-351.

Robert, T., Nore, A., Brun, C., Maffre, C., Crimi, B., Bourbon, H.M. & de Massy, B. 2016. The TopoVIB-Like protein family is required for meiotic DNA double-strand break formation. *Science (New York, N.Y.).* 351 (6276). pp. 943-949.

Rodenhuis, S. 1992. Ras and Human Tumors. Seminars in cancer biology. 3 (4). pp. 241-247.

Roman-Gomez, J., Jimenez-Velasco, A., Agirre, X., Castillejo, J.A., Navarro, G., San Jose-Eneriz, E., Garate, L., Cordeu, L., Cervantes, F., Prosper, F., Heiniger, A. & Torres, A. 2007. Epigenetic regulation of human cancer/testis antigen gene, HAGE, in chronic myeloid leukemia. *Haematologica.* 92 (2). pp. 153-162.

Romanienko, P. & Camerini-Otero, R. 2000. The Mouse Spo11 Gene Is Required for Meiotic Chromosome Synapsis. Molecular Cell, 6(5),

Romanienko, P.J. & Camerini-Otero, R.D. 1999. Cloning, characterization, and localization of mouse and human SPO11. *Genomics.* 61 (2). pp. 156-169.

Romanienko, P.J. & Camerini-Otero, R.D. 2000a. The mouse Spo11 gene is required for meiotic chromosome synapsis. *Molecular cell.* 6 (5). pp. 975-987.

Rosa, A.M., Dabas, N., Byrnes, D.M., Eller, M.S. & Grichnik, J.M. 2012. Germ cell proteins in melanoma: prognosis, diagnosis, treatment, and theories on expression. *Journal of skin cancer.* 2012 pp. 621968.

Rosenberg, S.A. 1997. Cancer vaccines based on the identification of genes encoding cancer regression antigens. *Immunology today.* 18 (4). pp. 175-182.

Ross, M.T., Grafham, D.V., Coffey, A.J., Scherer, S., McLay, K., Muzny, D., Platzer, M., Howell, G.R., Burrows, C. & Bird, C.P. 2005. The DNA sequence of the human X chromosome. *Nature.* 434 (7031). pp. 325-337.

Rousseaux, S., Debernardi, A., Jacquiau, B., Vitte, A.L., Vesin, A., Nagy-Mignotte, H., Moro-Sibilot, D., Brichon, P.Y., Lantuejoul, S., Hainaut, P., Laffaire, J., de Reynies, A., Beer, D.G., Timsit, J.F., Brambilla, C., Brambilla, E. & Khochbin, S. 2013. Ectopic activation of germline and placental genes identifies aggressive metastasis-prone lung cancers. *Science translational medicine.* 5 (186). pp. 186ra66.

Rousseaux, S., Wang, J. & Khochbin, S. 2013. Cancer hallmarks sustained by ectopic activations of placenta/male germline genes. *Cell cycle (Georgetown, Tex.).* 12 (15). pp. 2331-2332.

Rouzeau, S., Cordelières, F. P., Buhagiar-Labarchède, G., Hurbain, I., Onclercq-Delic, R., Gemble, S., Magnaghi-Jaulin, L., Jaulin, C. & Amor-Guéret, M. 2012. Bloom's Syndrome And Pich Helicases Cooperate With Topoisomerase Iiα In Centromere Disjunction Before Anaphase. Plos One, 7, E33905.

Roy, S., K Narang, B., K Rastogi, S. & K Rawal, R. 2015. A novel multiple tyrosine- kinase targeted agent to explore the future perspectives of anti-angiogenic therapy for the treatment of multiple solid tumors: cabozantinib. Anti-Cancer Agents in Medicinal Chemistry (Formerly Current Medicinal Chemistry-Anti- Cancer Agents). 15 (1). pp. 37-47.

Ruddon, R.W. 2007. *Cancer biology.* Oxford University Press.

Rutz, S. & Scheffold, A. 2004. Towards in vivo application of RNA interference - new toys, old problems. *Arthritis research & therapy.* 6 (2). pp. 78-85.

Sahin, U., Türeci, Ö & Pfreundschuh, M. 1997. Serological identification of human tumor antigens. Current opinion in immunology. 9 (5). pp. 709-716.

Salmaninejad, A., Zamani, M.R., Pourvahedi, M., Golchehre, Z., Bereshneh, A.H. & Rezaei, N. 2016. Cancer/Testis Antigens: Expression, Regulation, Tumor Invasion, and Use in Immunotherapy of Cancers. Immunological investigations. pp. 1-22.

Sammut, S.J., Feichtinger, J., Stuart, N., Wakeman, J.A., Larcombe, L. & McFarlane, R.J. 2014. A novel cohort of cancer-testis biomarker genes revealed through meta-analysis of clinical data sets. Oncoscience. 1 (5). pp. 349-359.

San Filippo, J., Sung, P. & Klein, H. 2008. Mechanism of eukaryotic homologous recombination. *Annu.Rev.Biochem.* 77 pp. 229-257.

Sandal, T. 2002. Molecular aspects of the mammalian cell cycle and cancer. *The oncologist.* 7 (1). pp. 73-81.

Sartori, A.A., Lukas, C., Coates, J., Mistrik, M., Fu, S., Bartek, J., Baer, R., Lukas, J. & Jackson, S.P. 2007. Human CtIP promotes DNA end resection. *Nature.* 450 (7169). pp. 509-514.

Sathyanarayanan, V. & Neelapu, S.S. 2015. Cancer immunotherapy: Strategies for personalization and combinatorial approaches. *Molecular oncology.* 9 (10). pp. 2043-2053.

Sattler, M., Reddy, M.M., Hasina, R., Gangadhar, T. & Salgia, R. 2011. The role of the c-Met pathway in lung cancer and the potential for targeted therapy. *Therapeutic advances in medical oncology.* 3 (4). pp. 171-184.

Sawant, P., Kshar, A., Byakodi, R. & Paranjpe, A. 2014. Immunofluorescence in Oral Mucosal Diseases–A Review. *Oral Surgery, Oral Medicine, Oral Radiology.* 2 (1). pp. 6-10.

Scanlan, M.J., Gure, A.O., Jungbluth, A.A., Old, L.J. & Chen, Y.T. 2002. Cancer/testis antigens: an expanding family of targets for cancer immunotherapy. *Immunological reviews.* 188 pp. 22-32.

Scanlan, M.J., Simpson, A.J. & Old, L.J. 2004. The cancer/testis genes: review, standardization, and commentary. *Cancer immunity.* 4 pp. 1.

Schramm, S., Fraune, J., Naumann, R., Hernandez-Hernandez, A., Hoog, C., Cooke, H.J., Alsheimer, M. & Benavente, R. 2011. A novel mouse synaptonemal complex protein is essential for loading of central element proteins, recombination, and fertility. *PLoS genetics.* 7 (5). pp. e1002088.

Schwacha, A. & Kleckner, N. 1994. Identification of joint molecules that form frequently between homologs but rarely between sister chromatids during yeast meiosis. *Cell.* 76 (1). pp. 51-63.

Schwarzenbach, H., Eichelser, C., Steinbach, B., Tadewaldt, J., Pantel, K., Lobanenkov, V. & Loukinov, D. 2014. Differential regulation of MAGE-A1 promoter activity by BORIS and Sp1, both interacting with the TATA binding protein. BMC cancer. 14 (1). pp. 1.

Seipel, K., Marques, M.T., Bozzini, M.A., Meinken, C., Mueller, B.U. & Pabst, T. 2016. Inactivation of the p53-KLF4-CEBPA Axis in Acute Myeloid Leukemia. Clinical cancer research : an official journal of the American Association for Cancer Research. 22 (3). pp. 746-756.

Seki, M., Nakagawa, T., Seki, T., Kato, G., Tada, S., Takahashi, Y., Yoshimura, A., Kobayashi, T., Aoki, A., Otsuki, M., Habermann, F., Tanabe, H., Ishii, Y. and Enomoto, T. 2006. Bloom Helicase and DNA Topoisomerase III Are Involved in the Dissolution of Sister Chromatids. Molecular and Cellular Biology, 26(16), pp.6299-6307.

Shang, B., Gao, A., Pan, Y., Zhang, G., Tu, J., Zhou, Y., Yang, P., Cao, Z., Wei, Q. & Ding, Y. 2014. CT45A1 acts as a new proto-oncogene to trigger tumorigenesis and cancer metastasis. *Cell death & disease.* 5 (6). pp. e1285.

Shannon, M., Richardson, L., Christian, A., Handel, M.A. & Thelen, M.P. 1999. Differential gene expression of mammalian SPO11/TOP6A homologs during meiosis. *FEBS letters.* 462 (3). pp. 329-334.

Sharma, P., Shen, Y., Wen, S., Bajorin, D.F., Reuter, V.E., Old, L.J. & Jungbluth, A.A. 2006. Cancer-testis antigens: expression and correlation with survival in human urothelial carcinoma. *Clinical cancer research : an official journal of the American Association for Cancer Research.* 12 (18). pp. 5442-5447.

Sharma, S., Javadekar, S., Pandey, M., Srivastava, M., Kumari, R. & Raghavan, S. 2015. Homology and enzymatic requirements of microhomology-dependent alternative end joining. Cell death & disease. 6 (3). pp. e1697.

Sharma, S., Kelly, T.K. & Jones, P.A. 2010. Epigenetics in cancer. Carcinogenesis. 31 (1). pp. 27-36.

Sharma, S., Lee, D., Li, B., Quinlan, M., Takahashi, F., Maheswaran, S., McDermott, U., Azizian, N., Zou, L., Fischbach, M., Wong, K., Brandstetter, K., Wittner, B., Ramaswamy, S., Classon, M. and Settleman, J. 2010. A Chromatin-Mediated Reversible Drug-Tolerant State in Cancer Cell Subpopulations. Cell, 141(1), pp.69-80.

Sherr, C.J. 1996. Cancer cell cycles. *Science (New York, N.Y.).* 274 (5293). pp. 1672-1677.

Shigeno, K., Yoshida, H., Pan, L., Luo, J.M., Fujisawa, S., Naito, K., Nakamura, S., Shinjo, K., Takeshita, A., Ohno, R. & Ohnishi, K. 2004. Disease-related potential of mutations in transcriptional cofactors CREB-binding protein and p300 in leukemias. *Cancer letters.* 213 (1). pp. 11-20.

Siderakis, M. & Tarsounas, M. 2007. Telomere regulation and function during meiosis. *Chromosome Research.* 15 (5). pp. 667-679.

Siegel, R., Miller, K. and Jemal, A. 2016. Cancer statistics, 2016. CA: A Cancer Journal for Clinicians, 66(1), pp.7-30.

Siegel, R., Naishadham, D. & Jemal, A. 2012. Cancer statistics, 2012. *CA: a cancer journal for clinicians.* 62 (1). pp. 10-29.

Siegel, R., Naishadham, D. & Jemal, A. 2013. Cancer statistics, 2013. CA: a cancer journal for clinicians. 63 (1). pp. 11-30.

Simpson, A.J., Caballero, O.L., Jungbluth, A., Chen, Y.T. & Old, L.J. 2005. Cancer/testis antigens, gametogenesis and cancer. *Nature reviews.Cancer.* 5 (8). pp. 615-625.

Singh, A.M. & Dalton, S. 2014. Cell Cycle Regulation of Pluripotent Stem Cells. *Stem Cells: From Basic Research to Therapy, Volume 1: Basic Stem Cell Biology, Tissue Formation during Development, and Model Organisms.* pp. 3.

Singh, A.P., Chauhan, S.C., Bafna, S., Johansson, S.L., Smith, L.M., Moniaux, N., Lin, M.F. & Batra, S.K. 2006. Aberrant expression of transmembrane mucins, MUC1 and MUC4, in human prostate carcinomas. *The Prostate.* 66 (4). pp. 421-429.

Sliwkowski, M.X. & Mellman, I. 2013. Antibody therapeutics in cancer. *Science (New York, N.Y.).* 341 (6151). pp. 1192-1198.

Slotkin, E., de Stanchina, E., Cartegni, L., Ladanyi, M. & Spraggon, L. 2016. Abstract B26: Therapeutic targeting of sarcomas driven by EWSR1 fusion oncogenes by modulation of the fusion oncogene pre-mRNA. Cancer research. 76 (5 Supplement). pp. B26-B26.

Smith, D. & Johnson, K. 1988. Single-step purification of polypeptides expressed in Escherichia coli as fusions with glutathione S-transferase. Gene, 67(1), pp.31-40.

Smith, D.B. 2000. Generating fusions to glutathione S-transferase for protein studies. Methods Enzymol. 326 254–270. [PubMed]

Solit, D.B., Garraway, L.A., Pratilas, C.A., Sawai, A., Getz, G., Basso, A., Ye, Q., Lobo, J.M., She, Y. & Osman, I. 2006. BRAF mutation predicts sensitivity to MEK inhibition. Nature. 439 (7074). pp. 358-362.

Song, M. & Giovannucci, E.L. 2015. Cancer risk: many factors contribute. Science (New York, N.Y.). 347 (6223). pp. 728-729.

Sonnenschein, C. & Soto, A.M. 2013. The aging of the 2000 and 2011 Hallmarks of Cancer reviews: a critique. *Journal of Biosciences.* 38 (3). pp. 651-663.

Sonoda, E., Sasaki, M.S., Morrison, C., Yamaguchi-Iwai, Y., Takata, M.& Takeda, S. 1999. Sister Chromatid Exchanges Are Mediated by Homologous Recombination in Vertebrate Cells. Mol. Cell. Biol., 19, 5166–5169.

Sorensen, C.S. & Syljuasen, R.G. 2012. Safeguarding genome integrity: the checkpoint kinases ATR, CHK1 and WEE1 restrain CDK activity during normal DNA replication. *Nucleic acids research.* 40 (2). pp. 477-486.

Souhami, R.L. & Tobias, J.S. 2005. Cancer and its management. 5th ed. Blackwell Pub: Malden, Mass.

Sperandio, S., de Belle, I. & Bredesen, D.E. 2000. An alternative, nonapoptotic form of programmed cell death. *Proceedings of the National Academy of Sciences of the United States of America.* 97 (26). pp. 14376-14381.

Spinks, C.A. 2000. Broad-specificity immunoassay of low molecular weight food contaminants: new paths to Utopia! *Trends in Food Science & Technology.* 11 (6). pp. 210-217.

Sprink, T & Hartung, F. 2014. The Splicing Fate of Plant SPO11 Genes. Frontiers in Plant Science, 5.

Stange, D.E. & Clevers, H. 2013. Concise review: the yin and yang of intestinal (cancer) stem cells and their progenitors. Stem cells 31(11), pp. 2287–95.

Stevens, R.C. 2000. Design of high-throughput methods of protein production for structural biology. Struct. Fold. Des. 8 R177–R185. [PubMed

Stevenson, B.J., Iseli, C., Panji, S., Zahn-Zabal, M., Hide, W., Old, L.J., Simpson, A.J. & Jongeneel, C.V. 2007. Rapid evolution of cancer/testis genes on the X chromosome. Bmc Genomics. 8 (1). pp. 1.

Storlazzi, A., Tesse, S., Gargano, S., James, F., Kleckner, N. & Zickler, D. 2003. Meiotic double-strand breaks at the interface of chromosome movement, chromosome remodeling, and reductional division. *Genes & development.* 17 (21). pp. 2675-2687.

Story, E. & Johnston, D. 2016. Multiple Metastatic Somatic Tissue Ganglioneuroma from a Primary Adrenal Ganglioneuro blastoma in a Pediatric Patient. Cancer Res Oncol. 2 (005).

Stratton, M.R., Campbell, P.J. & Futreal, P.A. 2009a. The cancer genome. Nature. 458 (7239). pp. 719-724.

Stratton, M.R., Campbell, P.J. & Futreal, P.A. 2009b. The cancer genome. Nature. 458 (7239). pp. 719-724.

Sukach, a. N. & Ivanov, E.N. 2007. Formation of spherical colonies as a property of stem cells. Cell and Tissue Biology 1(6), pp. 476–481.

Sulek, J., Goliadze, E., Zhou, S., Manjili, M.H., Toor, A. & Guruli, G. 2016. The Expression of Cancer/Testis Antigens in Kidney and Bladder Malignancies. Archives of Medicine.

Sumiyoshi, T., Sato, K., Yamamoto, H., Iwasaki, Y.W., Siomi, H. & Siomi, M.C. 2016. Loss of l(3)mbt leads to acquisition of the ping-pong cycle in Drosophila ovarian somatic cells. *Genes & development.* 30 (14). pp. 1617-1622.

Sung, P. & Klein, H. 2006. Nat. Rev. Mol. Cell Biol., 7739 –79. Wu, L., & Hickson, I. D. 2003. The Bloom's syndrome helicase suppresses crossing over during homologous recombination.Nature 426870 –874 [PubMed]

Surget, S., Khoury, M.P. & Bourdon, J. 2014. Uncovering the role of p53 splice variants in human malignancy: a clinical perspective. Onco Targets Ther. 7 pp. 57-68.

Suri, A. 2006. Cancer testis antigens–their importance in immunotherapy and in the early detection of cancer. *Expert opinion on biological therapy.* 6 (4). pp. 379-389.

Suri, A., Jagadish, N., Saini, S. & Gupta, N. 2015. Targeting cancer testis antigens for biomarkers and immunotherapy in colorectal cancer: Current status and challenges. *World journal of gastrointestinal oncology.* 7 (12). pp. 492-502.

Suryadinata, R., Sadowski, M. & Sarcevic, B. 2010. Control of cell cycle progression by phosphorylation of cyclin-dependent kinase (CDK) substrates. *Bioscience reports.* 30 (4). pp. 243-255.

Suski, C. & Marians, K. J. 2008. Resolution of Converging Replication Forks by RecQ and Topoisomerase III. Mol. Cell., 30, 779–789.

Szostak, J. W., Orr-Weaver, T. L., Rothstein, R. J. & Stahl, F. W.1983.'The double-strand-break repair model for recombination', Cell, 33(1):25–35.

Tanner, M.M., Tirkkonen, M., Kallioniemi, A., Collins, C., Stokke, T., Karhu, R., Kowbel, D., Shadravan, F., Hintz, M. & Kuo, W.L. 1994. Increased copy number at 20q13 in breast cancer: defining the critical region and exclusion of candidate genes. *Cancer research.* 54 (16). pp. 4257-4260.

Tarnowski, M., Czerewaty, M., Deskur, A., Safranow, K., Marlicz, W., Urasińska, E., Ratajczak, M.Z. & Starzyńska, T. 2016. Expression of Cancer Testis Antigens in Colorectal Cancer: New Prognostic and Therapeutic Implications. Disease markers. 2016.

Taswell, C. 1987. Limiting dilution assays for the separation, characterization, and quantitation of biologically active particles and their clonal progeny. *Cell separation: methods and selected applications.* 4 (6). pp. 109-145.

Taubert, H. 2004. Detection of disseminated tumor cells in peripheral blood of patients with breast cancer: correlation to nodal status and occurrence of metastases. Gynecologic Oncology, 92(1), pp.256-261.

Taubert, S., Gorrini, C., Frank, S.R., Parisi, T., Fuchs, M., Chan, H.M., Livingston, D.M. & Amati, B. 2004. E2F-dependent histone acetylation and recruitment of the Tip60 acetyltransferase complex to chromatin in late G1. *Molecular and cellular biology.* 24 (10). pp. 4546-4556.

Tauchi, H. 2000. Positional cloning and functional analysis of the gene responsible for Nijmegen breakage syndrome, NBS1. Journal of radiation research. 41 (1). pp. 9-17.

Teodoro, A.J., Oliveira, F.L., Martins, N.B., Maia Gde, A., Martucci, R.B. & Borojevic, R. 2012. Effect of lycopene on cell viability and cell cycle progression in human cancer cell lines. *Cancer cell international.* 12 (1). pp. 36-2867-12-36.

Terpe, K. 2003. Overview of tag protein fusions: from molecular and biochemical fundamentals to commercial systems. *Applied Microbiology and Biotechnology.* 60 (5). pp. 523-533.

Theurillat, J.P., Ingold, F., Frei, C., Zippelius, A., Varga, Z., Seifert, B., Chen, Y.T., Jager, D., Knuth, A. & Moch, H. 2007. NY-ESO-1 protein expression in primary breast carcinoma and metastases: correlation with CD8+ T-cell and CD79a+ plasmacytic/B-cell infiltration. *International journal of cancer.* 120 (11). pp. 2411-2417.

Thoma, C.R., Toso, A., Meraldi, P. & Krek, W. 2011. Mechanisms of aneuploidy and its suppression by tumour suppressor proteins. *Swiss medical weekly.* 141 pp. w13170.

Timmerman, D., Testa, A., Bourne, T., Ferrazzi, E., Ameye, L., Konstantinovic, M., Van Calster, B., Collins, W., Vergote, I., Van Huffel, S. and Valentin, L. 2005. Logistic Regression Model to Distinguish Between the Benign and Malignant Adnexal Mass Before Surgery: A Multicenter Study by the International Ovarian Tumor Analysis Group. Journal of Clinical Oncology, 23(34), pp.8794-8801.

Tomasetti, C., Vogelstein, B. & Parmigiani, G. 2013. Half or more of the somatic mutations in cancers of self-renewing tissues originate prior to tumor initiation. Proceedings of the National Academy of Sciences of the United States of America. 110 (6). pp. 1999-2004.

Tong, W.G., Chen, R., Plunkett, W., Siegel, D., Sinha, R., Harvey, R.D., Badros, A.Z., Popplewell, L., Coutre, S., Fox, J.A., Mahadocon, K., Chen, T., Kegley, P., Hoch, U. & Wierda, W.G. 2010. Phase I and pharmacologic study of SNS-032, a potent and selective Cdk2, 7, and 9 inhibitor, in patients with advanced chronic lymphocytic leukemia and multiple myeloma. *Journal of clinical oncology : official journal of the American Society of Clinical Oncology.* 28 (18). pp. 3015-3022.

Torre, L., Bray, F., Siegel, R., Ferlay, J., Lortet-Tieulent, J. and Jemal, A. 2015. Global cancer statistics, 2012. CA: A Cancer Journal for Clinicians, 65(2), pp.87-108.

Tran, E., Turcotte, S., Gros, A., Robbins, P.F., Lu, Y.C., Dudley, M.E., Wunderlich, J.R., Somerville, R.P., Hogan, K., Hinrichs, C.S., Parkhurst, M.R., Yang, J.C. & Rosenberg, S.A. 2014. Cancer immunotherapy based on mutation-specific CD4+ T cells in a patient with epithelial cancer. *Science (New York, N.Y.).* 344 (6184). pp. 641-645.

Trego, K.S., Groesser, T., Davalos, A.R., Parplys, A.C., Zhao, W., Nelson, M.R., Hlaing, A., Shih, B., Rydberg, B. & Pluth, J.M. 2016. Non-catalytic Roles for XPG with BRCA1 and BRCA2 in Homologous Recombination and Genome Stability. Molecular cell. 61 (4). pp. 535-546.

Tsai, C. J., Mets, D. G., Albrecht, M. R., Nix, P., Chan, A. & Meyer, B. J. 2008, Meiotic crossover number and distribution are regulated by a dosage compensation protein that resembles a condensin subunit'. Genes Dev. 22(2):194–211.

Tsai, J.H. & McKee, B.D. 2011. Homologous pairing and the role of pairing centers in meiosis. *Journal of cell science.* 124 (Pt 12). pp. 1955-1963.

Tureci, O., Sahin, U., Zwick, C., Koslowski, M., Seitz, G. & Pfreundschuh, M. 1998. Identification of a meiosis-specific protein as a member of the class of cancer/testis antigens. *Proceedings of the National Academy of Sciences of the United States of America.* 95 (9). pp. 5211-5216.

Tykvart, J., Navratil, V., Sedlak, F., Corey, E., Colombatti, M., Fracasso, G., Koukolik, F., Barinka, C., Sacha, P. & Konvalinka, J. 2014. Comparative analysis of monoclonal antibodies against prostate-specific membrane antigen (PSMA). *The Prostate.* 74 (16). pp. 1674-1690.

Tzifi, F., Economopoulou, C., Gourgiotis, D., Ardavanis, A., Papageorgiou, S. & Scorilas, A. 2012. The Role of BCL2 Family of Apoptosis Regulator Proteins in Acute and Chronic Leukemias. *Advances in hematology.* 2012 pp. 524308.

Urlinger, S., Baron, U., Thellmann, M., Hasan, M.T., Bujard, H. & Hillen, W. 2000. Exploring the sequence space for tetracycline-dependent transcriptional activators: novel mutations yield expanded range and sensitivity. *Proceedings of the National Academy of Sciences of the United States of America.* 97 (14). pp. 7963-7968.

Valmori, D., Souleimanian, N.E., Tosello, V., Bhardwaj, N., Adams, S., O'Neill, D., Pavlick, A., Escalon, J.B., Cruz, C.M., Angiulli, A., Angiulli, F., Mears, G., Vogel, S.M., Pan, L., Jungbluth, A.A., Hoffmann, E.W., Venhaus, R., Ritter, G., Old, L.J. & Ayyoub, M. 2007. Vaccination with NY-ESO-1 protein and CpG in Montanide induces integrated antibody/Th1 responses and CD8 T cells through cross-priming. *Proceedings of the National Academy of Sciences of the United States of America.* 104 (21). pp. 8947-8952.

Van Cutsem, E., Köhne, C., Hitre, E., Zaluski, J., Chang Chien, C., Makhson, A., D'Haens, G., Pintér, T., Lim, R. & Bodoky, G. 2009. Cetuximab and chemotherapy as initial treatment for metastatic colorectal cancer. *New England Journal of Medicine.* 360 (14). pp. 1408-1417.

Van Duin, M., Broyl, A., de Knegt, Y., Goldschmidt, H., Richardson, P.G., Hop, W.C., van der Holt, B., Joseph-Pietras, D., Mulligan, G., Neuwirth, R., Sahota, S.S. & Sonneveld, P. 2011. Cancer testis antigens in newly diagnosed and relapse multiple myeloma: prognostic markers and potential targets for immunotherapy. *Haematologica.* 96 (11). pp. 1662-1669.

Vander Bruggen, P. & Traversari, C. 1991. A gene encoding an antigen recognized by cytolytic T lymphocytes on a human melanoma. Science. 254 (5038). pp. 1643.

Vander Heiden, M.G., Cantley, L.C. & Thompson, C.B. 2009. Understanding the Warburg effect: the metabolic requirements of cell proliferation. *Science (New York, N.Y.).* 324 (5930). pp. 1029-1033.

Vatolin, S., Abdullaev, Z., Pack, S.D., Flanagan, P.T., Custer, M., Loukinov, D.I., Pugacheva, E., Hong, J.A., Morse, H.,3rd, Schrump, D.S., Risinger, J.I., Barrett, J.C. & Lobanenkov, V.V. 2005. Conditional expression of the CTCF-paralogous transcriptional factor BORIS in normal cells results in demethylation and derepression of MAGE-A1 and reactivation of other cancer-testis genes. Cancer research. 65 (17). pp. 7751-7762.

Velazquez, E.F., Jungbluth, A.A., Yancovitz, M., Gnjatic, S., Adams, S., O'Neill, D., Zavilevich, K., Albukh, T., Christos, P., Mazumdar, M., Pavlick, A., Polsky, D., Shapiro, R., Berman, R., Spira, J., Busam, K., Osman, I. & Bhardwaj, N. 2007. Expression of the cancer/testis antigen NY-ESO-1 in primary and metastatic malignant melanoma (MM)--correlation with prognostic factors. *Cancer immunity.* 7 pp. 11.

Verdecchia, A., De Angelis, G. & Capocaccia, R. 2002. Estimation and projections of cancer prevalence from cancer registry data. *Statistics in medicine.* 21 (22). pp. 3511-3526.

Vermeulen, K., Van Bockstaele, D.R. & Berneman, Z.N. 2003. The cell cycle: a review of regulation, deregulation and therapeutic targets in cancer. *Cell proliferation.* 36 (3). pp. 131-149.

Vigna, E., Cavalieri, S., Ailles, L., Geuna, M., Loew, R., Bujard, H. & Naldini, L. 2002. Robust and efficient regulation of transgene expression in vivo by improved tetracycline-dependent lentiviral vectors. *Molecular therapy : the journal of the American Society of Gene Therapy.* 5 (3). pp. 252-261.

Vogel, C.L., Cobleigh, M.A., Tripathy, D., Gutheil, J.C., Harris, L.N., Fehrenbacher, L., Slamon, D.J., Murphy, M., Novotny, W.F., Burchmore, M., Shak, S., Stewart, S.J. & Press, M. 2002. Efficacy and safety of trastuzumab as a single agent in first-line treatment of HER2-overexpressing metastatic breast cancer. *Journal of clinical oncology : official journal of the American Society of Clinical Oncology.* 20 (3). pp. 719-726.

Vogelstein, B. & Kinzler, K.W. 2004. Cancer genes and the pathways they control. *Nature medicine.* 10 (8). pp. 789-799.

Vogelstein, B., Papadopoulos, N., Velculescu, V.E., Zhou, S., Diaz, L.A.,Jr & Kinzler, K.W. 2013. Cancer genome landscapes. Science (New York, N.Y.). 339 (6127). pp. 1546-1558.

Vogt, P.K. 2012. Retroviral oncogenes: a historical primer. *Nature reviews.Cancer.* 12 (9). pp. 639-648.

Vos, J., Stiggelbout, A., Oosterwijk, J., Gomez-Garcia, E., Menko, F., Collee, J., van Asperen, C. and Tibben, A. 2011. A counselee-oriented perspective on risk communication in genetic counseling: Explaining the inaccuracy of the counselees' risk perception shortly after BRCA1/2 test result disclosure. Genetics in Medicine, 13(9), pp.800-811.

Vos, L.J., Famulski, J.K. & Chan, G.K. 2011. hZwint-1 bridges the inner and outer kinetochore: identification of the kinetochore localization domain and the hZw10-interaction domain. *The Biochemical journal.* 436 (1). pp. 157-168.

Vrielynck, N., Chambon, A., Vezon, D., Pereira, L., Chelysheva, L., De Muyt, A., Mezard, C., Mayer, C. & Grelon, M. 2016. A DNA topoisomerase VI-like complex initiates meiotic recombination. *Science (New York, N.Y.).* 351 (6276). pp. 939-943.

Waldman, T., Lengauer, C., Kinzler, K.W. & Vogelstein, B. 1996. Uncoupling of S phase and mitosis induced by anticancer agents in cells lacking p21. *Nature.* 381 (6584). pp. 713-716.

Wang, C., Gu, Y., Zhang, K., Xie, K., Zhu, M., Dai, N., Jiang, Y., Guo, X., Liu, M. & Dai, J. 2016. Systematic identification of genes with a cancer-testis expression pattern in 19 cancer types. *Nature communications.* 7.

Wang, H., Mannava, S., Grachtchouk, V., Zhuang, D., Soengas, M., Gudkov, A., Prochownik, E. & Nikiforov, M. 2008. c-Myc depletion inhibits proliferation of human tumor cells at various stages of the cell cycle. *Oncogene.* 27 (13). pp. 1905-1915.

Wang, J. C. 2002. Cellular roles of DNA topoisomerases: a molecular perspective. Nat. Rev. Mol. Cell Biol., 3, 430–440.

Wang, S.C. & Hung, M.C. 2005. Cytoplasmic/nuclear shuttling and tumor progression. *Annals of the New York Academy of Sciences.* 1059 pp. 11-15.

Wang, W., Singh, S., Zeng, D.L., King, K. & Nema, S. 2007a. Antibody structure, instability, and formulation. *Journal of pharmaceutical sciences.* 96 (1). pp. 1-26.

Wang, Z., Zhu, Y., Ding, S., He, F., Beier, R.C., Li, J., Jiang, H., Feng, C., Wan, Y., Zhang, S., Kai, Z., Yang, X. & Shen, J. 2007b. Development of a monoclonal antibody-based broad-specificity ELISA for fluoroquinolone antibiotics in foods and molecular modeling studies of cross-reactive compounds. *Analytical Chemistry.* 79 (12). pp. 4471-4483.

Ward, A., Hopkins, J., Mckay, M., Murray, S. & Jordan, P.W. 2016. Genetic Interactions Between the Meiosis-Specific Cohesin Components, STAG3, REC8, and RAD21L. G3 (Bethesda, Md.). 6 (6). pp. 1713-1724.

Washio, M., Mori, M., Mikami, K., Miki, T., Watanabe, Y., Nakao, M., Kubo, T., Suzuki, K., Ozasa, K., Wakai, K. & Tamakoshi, A. 2016. Risk Factors for Upper and Lower Urinary Tract Cancer Death in a Japanese Population: Findings from the Japan Collaborative Cohort Study for Evaluation of Cancer Risk (JACC Study). Asian Pacific journal of cancer prevention : APJCP. 17 (7). pp. 3545- 3549.

Weinberg, R. 2013. *The biology of cancer.* Garland science.

Weinberg, R.A. 1995. The retinoblastoma protein and cell cycle control. *Cell.* 81 (3). pp. 323-330.

Weiner, L.M., Surana, R. & Wang, S. 2010. Monoclonal antibodies: versatile platforms for cancer immunotherapy. *Nature reviews.Immunology.* 10 (5). pp. 317-327.

Weiser, T.S., Guo, Z.S., Ohnmacht, G.A., Parkhurst, M.L., Tong-On, P., Marincola, F.M., Fischette, M.R., Yu, X., Chen, G.A., Hong, J.A., Stewart, J.H., Nguyen, D.M., Rosenberg, S.A. & Schrump, D.S. 2001. Sequential 5-Aza-2 deoxycytidine-depsipeptide FR901228 treatment induces apoptosis preferentially in cancer cells and facilitates their recognition by cytolytic T lymphocytes specific for NY-ESO-1. *Journal of immunotherapy (Hagerstown, Md.: 1997).* 24 (2). pp. 151-161.

Wen, J., Li, H., Tao, W., Savoldo, B., Foglesong, J., King, L., Zu, Y. and Chang, C. 2014. High throughput quantitative reverse transcription PCR assays revealing over-expression of cancer testis antigen genes in multiple myeloma stem cell-like side population cells. British Journal of Haematology, 166(5), pp.711-719.

Weon, J.L. & Potts, P.R. 2015. The MAGE protein family and cancer. Current opinion in cell biology. 37 pp. 1-8.

Whilding, L.M. & Maher, J. 2015. CAR T-cell immunotherapy: The path from the by-road to the freeway? *Molecular oncology.* 9 (10). pp. 1994-2018.

Whitehurst, A.W. 2014. Cause and consequence of cancer/testis antigen activation in cancer. *Annual Review of Pharmacology and Toxicology.* 54 pp. 251-272.

Wilkinson, M.F. & Shyu, A.B. 2001. Multifunctional regulatory proteins that control gene expression in both the nucleus and the cytoplasm. *BioEssays : news and reviews in molecular, cellular and developmental biology.* 23 (9). pp. 775-787.

Williams, G.H. & Stoeber, K. 2012. The cell cycle and cancer. *The Journal of pathology.* 226 (2). pp. 352-364.

Wodarz, D. & Zauber, A.G. 2015. Cancer: Risk factors and random chances. Nature. 517 (7536). pp. 563-564.

Wu, C. & Bekaii-Saab, T. 2012. CpG Island Methylation, Microsatellite Instability, and BRAF Mutations and Their Clinical Application in the Treatment of Colon Cancer. *Chemotherapy research and practice.* 2012 pp. 359041.

Wu, L. & Hickson, I.D. 2003. The Bloom's syndrome helicase suppresses crossing over during homologous recombination. *Nature.* 426 (6968). pp. 870-874.

Wu, L., Bachrati, C. Z., Ou, J., Xu, C., Yin, J., Chang, M., Wang, W., Li, L., Brown, G. W. & Hickson I. D. 2006. BLAP75/RMI1 promotes the BLM-dependent dissolution of homologous recombination intermediates. Proc. Natl. Acad. Sci. U.S.A., 103, 4068–4073

Wu, L., Davies, S. L., North, P. S., Goulaouic, H., Riou, J. F., Turley, H., Gatter, K. C. & Hickson, I. D. 2000. The Bloom's Syndrome Gene Product Interacts with Topoisomerase III. J. Biol. Chem., 275, 9636–9644.

Wu, Y., Li, Y. and Lin, Y. 2002. Expression of MAGE-12 in lung cancer. Lung Cancer, 35(1), p.95.

Wyllie, A.H., Kerr, J.R. & Currie, A. 1980. Cell death: the significance of apoptosis. *International review of cytology.* 68 pp. 251-306.

Xu, D., Guo, R., Sobeck, A., Bachrati, C. Z., Yang, J., Enomoto, T., Brown, G. W., Hoatlin, M. E., Hickson, I. D. & Wang, W. 2008. RMI, a new OB-fold complex essential for Bloom syndrome protein to maintain genome stability. Genes. Dev., 22, 2843–2855.

Xu, H., Shan, J., Jurukovski, V., Yuan, L., Li, J. & Tian, K. 2007. TSP50 encodes a testis-specific protease and is negatively regulated by p53. *Cancer research.* 67 (3). pp. 1239-1245.

Yanagida, M. 2005. Basic mechanism of eukaryotic chromosome segregation. Philosophical Transactions of the Royal Society of London B: Biological Sciences, 360, 609-621.

Yamada, T. & Ohta, K. 2013. Initiation of meiotic recombination in chromatin structure. *Journal of Biochemistry.* 154 (2). pp. 107-114.

Yanagida M. 2005. Basic Mechanism of Eukaryotic Chromosome Segregation. Philosophical Transaction of The Royal Socity of London B: Biological Sciences, 360, 609-621.

Yan, J., Jiang, J., Lim, C.A., Wu, Q., Ng, H.H. & Chin, K.C. 2007. BLIMP1 regulates cell growth through repression of p53 transcription. *Proceedings of the National Academy of Sciences of the United States of America.* 104 (6). pp. 1841-1846.

Yang, P., Huo, Z., Liao, H. & Zhou, Q. 2015. Cancer/testis antigens trigger epithelial-mesenchymal transition and genesis of cancer stem-like cells. Current pharmaceutical design. 21 (10). pp. 1292-1300.

Yang, Z. & Sweedler, J.V. 2014. Application of capillary electrophoresis for the early diagnosis of cancer. *Analytical and bioanalytical chemistry.* 406 (17). pp. 4013-4031.

Yao, T., Oh, S.P., Fuchs, M., Zhou, N., Ch'ng, L., Newsome, D., Bronson, R.T., Li, E., Livingston, D.M. & Eckner, R. 1998. Gene dosage–dependent embryonic development and proliferation defects in mice lacking the transcriptional integrator p300. *Cell.* 93 (3). pp. 361-372.

Yap, C., Peterson, A.L., Castellani, G., Sedivy, J.M. & Neretti, N. 2011. Kinetic profiling of the c-Myc transcriptome and bioinformatic analysis of repressed gene promoters. *Cell Cycle.* 10 (13). pp. 2184-2196.

Yawata, T., Nakai, E., Park, K.C., Chihara, T., Kumazawa, A., Toyonaga, S., Masahira, T., Nakabayashi, H., Kaji, T. & Shimizu, K. 2010. Enhanced expression of cancer testis antigen genes in glioma stem cells. Molecular carcinogenesis. 49 (6). pp. 532-544.

Yeh, H., Lin, S., Wu, Y., Chan, N. & Chi, P. 2017. Functional Characterization of the Meiosis-Specific DNA Double-Strand Break Inducing Factor SPO-11 from C. elegans. Scientific Reports, 7(1).

Yin, J., Sobeck, A., Xu, C., Meetei, A. R., Hoatlin, M., Li, L. & Wang, W. 2005. BLAP75, an essential component of Bloom's syndrome protein complexes that maintain genome integrity. EMBO J., 24,1465–1476.

Yoshida, K. & Miki, Y. 2004. Role of BRCA1 and BRCA2 as regulators of DNA repair, transcription, and cell cycle in response to DNA damage. Cancer science. 95 (11). pp. 866-871.

Zakharyevich, K., Ma, Y., Tang, S., Hwang, P. Y., Boiteux, S. and Hunter, N. 2010.Temporally and biochemically distinct activities of Exo1 during meiosis: double-strand break resection and resolution of double Holliday junctions. Mol Cell., 40(6):1001–15.

Zendman, A.J., Ruiter, D.J. & Van Muijen, G.N. 2003. Cancer/testis-associated genes: identification, expression profile, and putative function. *Journal of cellular physiology.* 194 (3). pp. 272-288.

Zhang, J., Gao, Y., Yu, M., Wu, H., Ai, Z., Wu, Y., Liu, H., Du, J., Guo, Z. & Zhang, Y. 2015a. Retinoic acid induces embryonic stem cell differentiation by altering both encoding RNA and microRNA expression. PloS one. 10 (7). pp. e0132566.

Zhong, Y., Guan, K., Guo, S., Zhou, C., Wang, D., Ma, W., Zhang, Y., Li, C. & Zhang, S. 2010. Spheres derived from the human SK-RC-42 renal cell carcinoma cell line are enriched in cancer stem cells. Cancer letters 299(2), pp. 150–60.

Zhou, L., Bao, Y.L., Zhang, Y., Wu, Y., Yu, C.L., Huang, Y.X., Sun, Y., Zheng, L.H. & Li, Y.X. 2010. Knockdown of TSP50 inhibits cell proliferation and induces apoptosis in P19 cells. *IUBMB life.* 62 (11). pp. 825-832.

Zickler, D. & Kleckner, N. 1998. The leptotene-zygotene transition of meiosis. *Annual Review of Genetics.* 32 (1). pp. 619-697.

Zickler, D. & Kleckner, N. 1999. Meiotic chromosomes: integrating structure and function. *Annual Review of Genetics.* 33 pp. 603-754.

Zickler, D. & Kleckner, N. 2015. Recombination, Pairing, and Synapsis of Homologs during Meiosis. *Cold Spring Harbor perspectives in biology.* 7 (6). pp. 10.1101/cshperspect.a016626.

Zickler, D. 2006. From early homologue recognition to synaptonemal complex formation. *Chromosoma.* 115 (3). pp. 158-174.

Ziegler, C. & Behl, C. 2014. Cell aging: molecular mechanisms and implications for disease.